Pathogenesis of Retinoic Acid-induced Developmental Ocular Defects Studied Using Mouse Models

LAU, Wing Sze Josephine

A Thesis Submitted in Partial Fulfilment
of the Requirements for the Degree of
Doctor of Philosophy
in
Ophthalmology and Visual Sciences

April 2009

Thesis / Assessment Committee

Professor YAM, Hin Fai (Chair)

Professor PANG, Chi Pui (Thesis Supervisor)

Professor SHUM, Sau Wan (Thesis Co-supervisor)

Professor WANG, Chi Chiu (Committee member)

Professor CHAN Siu Yuen, (External Examiner)

ACKNOWLEDGEMENTS

I would like to express my deepest and most sincere gratitude to my supervisor, Prof. C.P. Pang. His knowledge and logical way of thinking have been of great value to my project and have been an inspiration to me. His understanding, encouragement and guidance have provided me with great enthusiasm for this thesis.

I am immensely grateful to my co-supervisor, Prof. Alisa Shum, who introduced me to the field of retinoid in embryonic development. It is my real pleasure to be able to work in her laboratory over these past 3 years. I must thank her for her excellent advice, thoughtful guidance and constructive comments with regard to my project as well as my life. Her research attitude, keen determination and enthusiasm have demonstrated clearly to me the meaning of a famous quote "patience, persistence and perspiration make an unbeatable combination for success".

My heartfelt thanks should go to Drs Gary Yam and Ronald Wang for their continuous support and suggestions throughout my study period.

This Ph.D. work could not be completed without generous help from Miss HL Choi, Ms Jenny Hou and Ms Corinna Au. They showed me how to conduct excellent research and to achieve high quality result. Sincere gratitude should also go to Drs Siu-wai Choi and Wai-chi Kwong for their expert advice on English writing and statistical analysis respectively.

Special thanks are due to Ms HL Choi and Ms Rachel Kwok for their technical support in microtome processing. I am also grateful to Mr Leo Lee for his kind help in performing real time RT-PCR. Without their help, I would not have been able to complete my project.

Continuous support was received from my labmates, Mr Kia Chia, Miss Rachel Kwok, Mr Leo Lee and Mr Alan Leung. As my companions during my study period, we often shared laughter, and they supported me without fail in my toughest moments. I owe them a great deal.

I must extend my thanks and utmost appreciation to my fiancé, my parents, my brother, and sister-in-law for being by my side through all my struggles and successes during this study period. I could never have reached this milestone without their believing in me and giving me all the love and emotional support I could ever need.

Learning to be a faithful person is the most important accomplishment during these three years. Thank you my Lord.

TABLE OF CONTENT

Chapter 2: General Materials and Methods

Chapter 3: Time, Dose and Strain Responses to RA-induced Ocular Defects

LIST OF FIGURES

LIST OF FIGURES

LIST OF FIGURES

LIST OF FIGURES

LIST OF GRAPHS

LIST OF GRAPHS

LIST OF GRAPHS

LIST OF GRAPHS

LIST OF TABLES

LIST OF TABLES

LIST OF TABLES

LIST OF TABLES

LIST OF TABLES

ABBREVIATIONS

bp	Base pairs
BCIP	5-Bromo-4-Chloro-3'-Indolyphosphate p-Toluidine
CRABP	Cellular retinoic acid binding protein
CRBP	Cellular retinol binding protein
DIG	Digoxigenin
DMEM	Dulbecco's Modified Eagle's Medium
DEPC	Diethylene pyrocarbonate
E	Embryonic day
HPLC	High pressure liquid chromatography
HPLC/MS	High pressure liquid chromatography/mass spectrometry
ICR	Institute of Cancer Research
NBP	Nitro-blue tetrazolium chloride
P	Postnatal
PB	Phosphate buffer
PBLT	Phosphate buffer saline containing levamisole and triton-X100
PBS	Phosphate buffered saline
PBSL	Phosphate buffered saline containing levamisole
PBT	Phosphate buffered saline containing 1% Tween-20
PCR	Polymerase china reaction
RA	All-*trans* retinoic acid
RALDH	Retinaldehyde dehydrogenase
RAR	Retinoic acid receptors
RARE	Retinoic acid response element
RBP	Retinol binding protein
RPE	Retinal pigment epithelium
rpm	Revolutions per minute
RT-PCR	Reverse transcription polymerase chain reaction
RXR	Retinoid X receptors
VAD	Vitamin A deficiency
X-gal	5-bromo-4-chloro-3-idolyl-β-galactopyranoside

ABSTRACT

Vitamin A (retinol) and its most active metabolite, all-*trans* retinoic acid (RA) is essential for vision in the adult and for eye development in the embryo. It is well documented that in humans, excess intake or deficiency of vitamin A or RA is associated with congenital ocular defects such as microphthalmia. However, the underlying mechanism remains unclear. The aim of this study is to examine the pathogenic mechanism of RA-induced developmental ocular defects.

To determine if there are strain differences in the susceptibility to RA-induced ocular defects, two mouse strains were used. They are C57BL/6J (C57), mice that spontaneously develop ocular defects and ICR mice, which are not prone to developing ocular defects. Detailed time and dose response studies were conducted and eye defects were examined in near-term fetuses. C57 fetuses were found to be significantly more susceptible to RA-induced anophthalmia / microphthalmia than ICR fetuses.

Since the teratogenic effect of RA is highly developmental stage-dependent, it is possible that there is a difference in the developmental stage between these 2 mouse strains at the time of RA injection. Indeed, it was found that the developmental stage of ICR embryos was approximately 6 hours ahead of C57 embryos. However, the role that this factor plays in the differential strain susceptibility to RA can be excluded since C57 fetuses were still 3 times more susceptible to developing anophthalmia / microphthalmia than ICR fetuses that were subject to RA treatment at equivalent developmental stages. Comparison of

susceptibility to RA-induced anophthalmia / microphthalmia was also made among heterozygous fetuses obtained from reciprocal matings between C57 and ICR male and female mice, and those in homozygous ICR and C57 fetuses. Results showed that the C57 strain has conferred both genetic predisposition and maternal effects in increasing the embryo's susceptibility to RA-induced ocular defects.

In addition, detailed morphological and histological studies were conducted to determine if RA treatment caused early embryonic changes with strain difference. When compared with ICR embryos, C57 embryos exhibited more pronounced responses to RA, including developmental retardation, underdevelopment of the anterior neural plate and absence of or smaller optic pit / optic vesicle formation. However, RA treatment did not cause abnormal apoptosis in the early stages in both strains.

Since the type of RA-induced ocular defects mimic those that developed in *Raldh2* null mutant embryos, the effect of RA treatment on the expression of RA synthesizing enzymes, *Raldh2* and *Raldh3*, and the RA-inducible gene *Cyp26a1*, as well as some early eye development genes were examined. Exogenously administered RA reduced the mRNA expression levels of *Raldh2*, *Raldh3* and *Cyp26a1* in the head region, with C57 embryos showing a greater reduction than ICR embryos.

As exogenously administered RA suppressed the expression of the RA synthesizing enzymes, further investigation on whether this would lead to deficiency in endogenous RA concentrations was conducted. Results showed that exogenously

administered RA significantly reduced the endogenous RA level in the head region with C57 embryos showing a greater reduction than ICR embryos.

Taken together, results of this thesis suggest that there is a strain difference in susceptibility to RA-induced ocular defects in which exogenously applied RA suppresses the expression of RA synthesizing enzymes and leads to endogenous RA deficiency. This finding may shed light on understanding why both excess and deficiency of RA can lead to similar types of ocular defects.

撮要

維生素 A(視黃醇)和其最活躍的代謝物視黃酸對成人及胚胎的眼部發育是必不可少的。跟據案例，人類攝入過量或不足維生素 A(或視黃酸)與先天性眼部缺陷相關，例如先天性小眼症。不過，潛在的病理機制仍不清楚。本研究的目的是探索視黃酸引發眼部缺陷的發病機制。

為確認不同品系小鼠對視黃酸誘發的眼部缺陷是否有著不同的敏感度，實驗使用兩個不同品系的小鼠。第一種是 C57BL/6J (C57)小鼠，此品系小鼠的胚胎較容易具自發性的眼部缺陷。另一品系是 ICR 小鼠，其胚胎一般不易於發生眼部缺陷。我們對快出生的胎兒進行了詳細的時間和劑量反應研究，並對眼睛的缺陷進行檢查。結果發現，C57 小鼠胎兒比 ICR 小鼠的胎兒更容易產生視黃酸誘發的先天性無眼症或小眼症。

由於視黃酸的致畸作用與胚胎的發育階段高度相關，上述現象可能是因為在視黃酸注射時，兩種品系的小鼠正處於不同的發育階段。結果發現，ICR 胚胎的發育階段比起 C57 胚胎大約提前 6 個小時。不過，該因素對視黃酸敏感性所起的作用仍可被排除，這是因為在同等的發育階段的情況下，C57 小鼠比起 ICR 小鼠更容易發生先天性無眼症或小眼症，且前者發生率是後者的三倍。對於相互間交配的 C57 和 ICR 雜合子胎兒與那些在純合子的 ICR 和 C57 胎兒對視黃酸誘發先天性小眼症的敏感度進行比較。結果表明，C57 品系因有遺傳傾向和產婦的影響，所以較易患有視黃酸誘發的先天性無眼症或小眼症。

除此之外，我使用深入的形態學組織學檢查以確定視黃酸是否引起與品系相關的早期胚胎變化。當與 ICR 相比，C57 品系對視黃酸有較明顯的反應，包括發育遲緩、缺乏或規模較小的視神經坑/視囊泡的形成和欠缺前神經板。不過，兩種品系的小鼠早期階段胚胎對視黃酸注射皆沒有發生不正常的細胞凋亡。

由於視黃酸所引導的眼部缺陷與 *Raldh2*(最早出現的視黃酸合成酶)null mutant 胚胎所產生的眼部缺陷很相似。因而我們研究了視黃酸對視黃酸合成酶(如 *Raldh2*和 *Raldh3*)和視黃酸誘導基因(如 *Cyp26a1*)以及早期眼部發育基因表達水平的影響。結果發現注射外源性視黃酸使 *Raldh2*，*Raldh3* 和 *Cyp26a1* mRNA 在頭部區域的表達水平下調，其中 C57 胚胎表現出更大的敏感性。

因注射外源視黃酸會造成視黃酸合成酶和視黃酸誘導基因下調，所以我們進一步調查這些基因的下調會否有導致胚胎的內源視黃酸耗竭。結果表明，注射外源視黃酸的確造成胚胎的內源視黃酸耗竭，其中 C57 胚胎對外源性視黃酸表現出更大的致畸敏感性。

綜合以上所述，不同品系對視黃酸引致的眼部缺陷有不同的敏感性。其中注射外源視黃酸會引起視黃酸合成酶水平下調，從而導致胚胎的內源視黃酸不足。該研究揭示了因視黃酸過剩或不足所導致眼部缺陷可能的致病機制。

CHAPTER 1

General Introduction

1.1 OCULAR DEVELOPMENT

The eye is an extension of the central nervous system. It is an exquisitely complex structure that is capable of gathering a wealth of information in the form of refracted light. It is perfectly constructed for providing high visual acuity and colour vision as well as the ability to judge the relative distance of objects in space and to track moving objects. Eye morphogenesis originates from primordial tissues derived from a number of sources, including the wall of the diencephalon, the overlying surface ectoderm and migratory neural crest cells (O'Rahilly, 1975; Bron et al., 1997; Wright, 1997). The eye develops over several weeks during the early embryonic period and the key developmental processes are described as follow and summarized in Table 1-1.

1.1.1 Specification of the eye field and optic vesicle morphogenesis

During gastrulation, the developing eye is a single eye field (or eye anlage), which is a population of cells in the central region of the anterior neural plate that gives rise to the primordial eye (Li et al., 1997; Mathers et al., 1997) (Figure 1-1 A). By outpouching in the inner surface of the anterior neural fold on either side of the midline, two small optic pits appear in the neuroepithelium (Figure 1-1 B). By the time the cranial neural tube fuses, the optic pits become optic vesicles by lateral evaginations of the newly developed forebrain (prosencephalon) (Figure 1-1 C). These optic vesicles each extend laterally towards the overlying non-neural surface ectoderm which will eventually become the lens and cornea. Mesenchyme between the optic vesicle and the surface ectoderm is displaced as the two tissues come into close physical contact (Kaufman, 1992; Kaufman, 1999; Chow and Lang,

Table 1-1 **Comparison of timing of key events in eye development between human and mouse**

Human gestation	Mouse gestation - Embryonic day (E) - Postnatal day (P)	Major events in oculogenesis
3rd week	E8.5	- Optic pit forms
4th week	E9	- Optic vesicle grows - Lens placode forms
5th week	E11.5	- Optic cup grows - Lens vesicle develops
early 6th week	E12.5	- Optic fissure closes
late 6th week	E13.5	- Retinal neurogenesis begins - Ganglion cells born
7th week	E14.5	- Anterior chamber forms between lens and cornea - Lens fibres grow and elongate
8th week	E16.5	- Optic nerve developed
8th month	P11	- Retinal neurogenesis completed

2001).

1.1.2 Growth, patterning and closure of the optic cup

Shortly after contact of optic vesicle and overlying surface ectoderm is made, there is simultaneous thickening of the two layers in contact (Figure 1-1 C). The neuroectodermal thickening in the lateral wall of the optic vesicle is destined to become the neural retina. The corresponding surface ectodermal thickening becomes the lens placode (Pei and Rhodin, 1970). This is a critical period in eye development during which induction signals exchange between the optic vesicles and the surface ectoderm (Hyer et al., 1998; Hyer et al., 2003). At the same time, a process of invagination of the distal neuroepithelium gives rise to a bi-layered optic cup (Figure 1-1 D). The inner layer of the optic cup (facing the lens) forms the presumptive neural retina, while the outer later of the optic cup gives rise to the presumptive retinal pigment epithelium (RPE). At the ventral surface of the optic cup, the process of invagination forms a groove, the optic fissure, that runs continuously from the ventral-most region of the neural retina and along the ventral aspect of the optic stalk to the junction with the diencephalon. Prior to its closures, the optic fissure allows the entry of blood vessels within the eye and an exit route for projecting axons (Bron et al., 1997). The optic fissure closes at 6^{th} week of human gestation [embryonic day (E) 12.5 in the mouse].

1.1.3 Anterior segment (cornea, ciliary body and iris)

Development of the anterior segment relies on interactions between these neural crest-derived mesenchyme and cells derived from the neuroepithelium of the

optic cup and from the surface ectoderm (Figure 1-1 D & E).

Formation of the cornea is the result of a series of inductive events in eye formation, with the lens vesicle interacting with the overlying surface ectoderm (Figure 1-1 D). This highly coordinated, multi-steps process results in the transformation of a typical surface ectoderm to a transparent, multi-layered structure with a complex extracellular matrix and cellular contributions from several sources (Figure 1-1 E) (Hay, 1979).

The ciliary body and iris are derived from the distal tips of the optic cup, which is mainly composed of neuroectodermal elements, at the point where the inner and outer optic cup layers meet (Figure 1-1 D) (Beebe, 1986). Further layering of mesenchyme will contribute to the formation of ciliary stroma and muscle. Continuous differentiation of the neuroectodermal component of the iris will later form the sphincter, dilator, and iris epithelial cells. At the same time, the circulatory supply of primitive lens will partially fuse with the mesenchyme to form the pupillary membrane (Bron et al., 1997; Gregory-Evans, 2000; Chow and Lang, 2001).

1.1.4 Lens development

While the optic cup is developing from the forebrain, a similar change is taking place in the surface ectoderm opposite to the open lips of the developing optic cup. At first, cells of the surface ectoderm thicken to form a structure known as the lens placode (Figure 1-1 C). Rapid growth of this region results in the invagination of the surface cells to form a lens vesicle, which ultimately separates from the

surface to form a hollow spherical vesicle, which is initially composed of a single cell layer surrounded by the basal lamina (Figure 1-1 D). The vesicle expands, developing a central cavity with an anterior wall of cells forming the anterior lens epithelium and a posterior wall formed by the primary lens fibres that elongate and fill up the vesicle cavity (Figure 1-1 E). The nuclei of the lens fibres disappear by the 7th week of human gestation and become increasingly transparent. Later on, secondary fibre cells differentiate from proliferating epithelial cells in the equatorial zone at the margin of the lens epithelium. After birth and throughout life, new fibres continue to be added at a slower rate (Francis et al., 1999; McAvoy et al., 1999).

1.1.5 Development of retinal neurons and optic nerve

As a consequence of invagination by the optic vesicle to form the optic cup, a double layer of neuroectoderm is formed; the outer layer is melanin-synthesizing retinal pigment epithelium (RPE) and the inner layer becomes the multilayered neural retina (Figure 1 D). This process, termed as neurogenesis, begins at the end of the 6th week of human gestation (E12.5 in mouse) which eventually generates the mature retinal infrastructure.

Multipotent retinal progenital cells of the neural retina give rise to Müller glial cells and six distinct types of retinal neurons. They are the cone and rod photoreceptor cells, the bipolar, amacrine and horizontal cells of the inner nuclear layer, and the ganglion cells, which project axons along the optic nerve. The photoreceptor cells express the photo-pigment opsin genes, which bind the chromophore, 11-cis retinal (metabolites of vitamin A), and provide photosensitivity to the retina. The characteristic laminated structure of the mature retina develops by

the 8th month of human gestation and in mouse neurogenesis, it is only completed by P (postnatal) 11 (Figure 1-1 F).

The non-neuronal RPE forms an epithelial monolayer structure adjacent to the photoreceptor cells. Ganglion cells project their axons into the optic stalk and promote the optic stalk neuroepithelium to develop into glial cells. The optic stalk gradually transforms into optic nerve by the 8th week of human gestation (E16.5 in mouse) (Figure 1-1 F).

1.2 CONGENITAL OCULAR DEFECTS

Defects present at birth that affect the eyes or vision are termed as congenital ocular defects. They are one of the most common causes of blindness in children and a significant cause of blindness worldwide. There are about 1.4 million blind children in the world, among which 17% are due to congenital eye defects (Johnson et al., 2003). Congenital eye defects can impair vision or even cause blindness. Some conditions are immediately apparent in the infant, while others may not be detected until later in life. The majority of congenital eye defects have complex uncharacterised causes. Known reasons for congenital ocular defects, although identified in the minority of cases only, include genetic causes, environmental factors and intrauterine infections (World Health Organization, 2000).

The most common structural ocular defect at birth is congenital cataract with an incidence rate of about 3 in 10,000 live births. This defect accounts for 10% cases of childhood blindness (Rahi and Dezateux, 2001; Francis and Moore, 2004). Other common defects include anophthalmia, microphthalmia and coloboma.

Failure of specification of the eye field and optic vesicle morphogenesis can lead to the absence of eye formation, anophthalmia, which may be unilateral or bilateral. The incidence rate is around 0.3 in 10,000 live births (Stoll et al., 1992; Warburg, 1993; Stoll et al., 1997). Anophthalmia may be primary, when there is no evagination of the neural tube to form the optic vesicles, or secondary, when the entire anterior end of the neural tube is malformed. A third category, consecutive or degenerative anophthalmia was applied to cases where optic vesicles have degenerated and disappeared subsequent to formation (Mann, 1953). Very often, anophthalmia is accompanied by other severe cranio-cerebral congenital defects (Stoll et al., 1997).

Disruption of growth, patterning and closure of the optic cup can lead to microphthalmia and / or coloboma. Microphthalmia can be unilateral or bilateral. The eye may be very small with other ocular defects or it may appear to be normal, but miniature in size. It may be associated with other congenital anomalies such as Trisomy 13. Severe microphthalmia, often accompanied by other ocular defects (Stoll et al., 1997), is a common cause of childhood blindness. Epidemiological studies estimate incidence rates of around 1.8 in 10,000 live births (Stoll et al., 1992; Warburg, 1993; Stoll et al., 1997). It was estimated that about 3.2% to 11.2% of blind children have microphthalmia (Fraunfelder et al., 1985; Traboulsi, 1999).

Coloboma is caused by incomplete closure of the fissure of the optic cup and results in the persistence of a fissure in the globe. It can affect every part of the globe traversed by the fissure from the iris to the optic nerve (Onwochei et al., 2000). The estimated incidence rate is around 0.7 in 10,000 live births (Stoll et al., 1992;

Warburg, 1993; Stoll et al., 1997). It represents a significant cause of congenital poor vision while in some cases, it can be asymptomatic and only visible with ophthalmic instrumentation (Gregory-Evans, 2000). It is frequently seen in association with other developmental ocular defects such as microphthalmia and anophthalmia (Hornby et al., 2000a; Gregory-Evans et al., 2004; Chang et al., 2006). Since anophthalmia and microphthalmia are the most severe types of congenital ocular defects that could very likely lead to total blindness in infancy (Hornby et al., 2000b), therefore in this thesis, focus is placed on the pathogenesis of these two phenotypes.

1.2.1 Genetic causes

The precise pathogenesis of anophthalmia and microphthalmia remains unknown. Many epidemiological studies have shown that both heritable and environmental factors cause anophthalmia and microphthalmia (Bardakjian et al., 2007). In general, the heritable factors include chromosomal aberration and monogenic mutation, and representative examples are summarized in Tables 1-2 and 1-3 respectively.

1.2.2 Intrauterine infections

Intrauterine infections affecting the developing neural tube during the first few weeks of gestation may cause anophthalmia or microphthalmia. Examples are Rubella (O'Neill, 1998; Busby et al., 2005), Cytomegalovirus (McCarthy et al., 1980; Tsutsui et al., 1993), Varicella-zoster virus (Fujita et al., 2004; Palano et al., 2005), toxoplasmosis (O'Neill, 1998) and Herpes simplex virus (Chalhub et al., 1977; Hutto

Table 1-2 Chromosomal abnormalities associated with anophthalmia/microphthalmia.

Chromosomal Abnormalities	Other Features	References
Trisomy 9 moasic syndrome	Congenital heart defects, prenatal growth deficiency, learning difficulties.	(Tarani et al., 1994; Arnold et al., 1995)
Trisomy 13 (Patau syndrome)	Holoprosencephaly, moderate microcephaly, coloboma, retinal dysplasia, cyclopia, cleft lip/palate, cardiac defects, genital abnormalities.	(Cogan and Kuwabara, 1964; Magni et al., 1991)
Trisomy 18 (Edwards syndrome)	Polyhydramnios, single umbilical artery, small placenta, low foetal activity, learning difficulties, hypertonicity, hypoplasia of skeletal muscle, subcutaneous, adipose tissue, prominent occipital bone, low-set malformed auricles, micrognathia, cardiac defects.	(Calderone et al., 1983)
Triploidy syndrome	Large placenta with hydatidiform changes, growth deficiency, syndactyly, congenital heart defects, brain anomalies, holoprosencephaly.	(Fulton et al., 1977; Ginsberg et al., 1981)

Information were extracted from Bardakjian et al., (2007).

Table 1-3 Ocular phenotypes associated with monogenic mutations linked to anophthalmia/microphthalmia.

Gene	Locus (Inheritance)	Major Human Ocular Phenotypes	References
Sox2	3q26.3-q27 (Autosomal Dominant)	Anophthalmia/microphthalmia	(Fantes et al., 2003; Hagstrom et al., 2005; Ragge et al., 2005)
Pax6	11p13 (Autosomal Dominant)	Aniridia, Peters anomaly, autosomal dominant keratopathy, foveal hypoplasia, optic nerve malformations, anophthalmia	(Glaser et al., 1994)
Otx2	14q22 (Autosomal Dominant)	Anophthalmia/microphthalmia, retinal dysplasia, optic nerve malformations	(Henderson et al., 2007; Ragge et al., 2005)
Rax	18q21.3 (Autosomal Recessive)	Anophthalmia/microphthalmia	(Voronina et al., 2004)
Chx10	14q24.3 (Autosomal Recessive)	Microphthalmia	(Bar-Yosef et al., 2004; Ferda et al., 2000)
Foxe3	1p32	Anterior segment dysgenesis, congenital primary aphakia	(Valleix et al., 2006)

et al., 1987). A woman can have such an infection and not be aware of it because these infections can produce few or no symptoms in adults. However, most of these intrauterine infections are preventable if women of child-bearing age undergo regular detailed body check well before planning to have baby.

1.2.3 Environmental factors

Teratogenic exposures are those that can cause an embryo or fetus to develop abnormally. Several factors determine whether an agent is teratogenic, including gestational timing of the exposure, as well as the dose, route and nature of the agent itself. The most critical period in embryonic ocular development is during the early 2^{nd} to 5^{th} week of human gestation. Numerous substances are well-documented as ocular teratogens and those representative ones that cause anophthalmia or microphthalmia are summarized in Table 1-4.

Maternal hyperthermia (Smith et al., 1978; Shiota, 1982), diabetes (Gale, 1991; Heilig et al., 2003; James et al., 2007) and alcoholism (Clarren and Smith, 1978; Stromland, 1985) during early pregnancy have been proven to be teratogenic in causing anophthalmia or microphthalmia in experimental animals and humans. On the other hand, both excess and deficiency of vitamin A (retinol) and retinoids can lead to a similar spectrum of congenital defects including anophthalmia and microphthalmia (for reference, please refer to Table 1-4). However, the underlying pathogenic mechanism of causing these similar ocular defects in both extreme situations is still far from clear. Among all these environmental factors, vitamin A deficiency (VAD) is the most common teratogen affecting developing countries (World Health Organization, 2000).

Table 1-4 Teratogenic agents that cause anophthalmia/microphthalmia.

Teratogens	References
Radiation	(Dekaban, 1968)
Maternal metabolic imbalance	
♦ Hyperthermia	(Smith et al., 1978; Shiota, 1982)
♦ Diabetes	(Gale, 1991; Heilig et al., 2003; James et al., 2007)
♦ Alcoholism	(Clarren and Smith, 1978; Stromland, 1985)
Thalidomide	(Gilkes and Strode, 1963)
Valproic acid	(Kuriyama et al., 1988; McMahon and Braddock, 2001)
Vitamin A	
♦ Excess	(Rothman et al., 1995; Hornby et al., 2003)
♦ Deficiency	(Hale, 1933, 1935; Sarma, 1959; Padmanabhan et al., 1981; Hornby et al., 2003; Smets et al., 2006)
Retinoic acid	
♦ Excess	(Benke, 1984; De La Cruz et al., 1984; Lammer et al., 1985; Hansen and Pearl, 1985; Sulik et al., 1995)
♦ Deficiency	(Grondona et al., 1996; Dickman et al., 1997; Mic et al., 2004; Halilagic et al., 2007)

1.3 VITAMIN A

Vitamin A, that is retinol, is a lipid-soluble vitamin. It is essential for the function and survival of adult vertebrates because of its crucial role in many essential biological processes such as vision, immunity, reproduction, growth, development and control of cellular proliferation and differentiation (De Luca, 1991; De Luca et al., 1995; Chambon, 1996; Mark et al., 2006). It is even more critical for embryonic development because VAD occurring during gestation results in a wide spectrum of congenital defects as mentioned in section 1.2.3. The term retinoids refer to the metabolic derivatives of vitamin A and its synthetic analogues. Provitamin A is the dietary source of retinol and is supplied as carotenoids (mainly β-carotene) in vegetables and preformed retinyl esters in animal meat (Blomhoff, 1994). Vitamin A is stored as retinyl esters, mainly in the liver, but also in the lung and bone marrow.

Cells receive retinol from the bloodstream where it is bound to retinol binding protein (RBP) (Napoli et al., 1991). Within cells that respond to retinoic acid (RA), the bioactive metabolites of vitamin A, safeguards exist to control retinol levels in the form of cellular retinol binding proteins (CRBP I and CRBP II) and cellular RA binding proteins (CRABP I and CRABP II) that buffer free retinoid concentrations in the cytoplasm (Napoli et al., 1991). In the cytoplasm, retinol is first converted to retinal or retinaldehyde, which forms the light-sensitive chromophore bound to opsin, by alcohol or retinol dehydrogenases (Lamb and Pugh, Jr., 2004). It is then converted to RA by retinaldehyde dehydrogenases (RALDH) (Duester, 1996) for regulating gene transcription. RA is then further degraded to inactive compounds by the action of a cytochrome P450 enzyme called CYP26

(Napoli, 1999). RA acts at the level of the nucleus to activate specific retinoic acid responsive genes by binding to nuclear receptors which are members of a large family that include, among many others, steroid and thyroid hormone receptors (Mangelsdorf et al., 1995). The RA receptors fall into two classes, RAR and RXR. Each class comprises three different isotypes (α, β and γ). They function either as homodimers or as heterodimers (Mangelsdorf and Evans, 1995) and these dimers then bind to a specific sequence of base pairs in the upstream promoter region known as the retinoic acid response element (RARE) of the RA target genes. There are over 500 proteins found in every organ of the body which can be regulated by RA (Gudas, 1994; McCaffery and Dräger, 2000; Balmer and Blomhoff, 2002; Williams et al., 2004), demonstrating that RA itself is a very important signaling molecule.

1.3.1 The role of retinoids in adult

The importance of retinoids in biological processes has been extensively studied since the identification of VAD in the First World War. Emerging evidence show that VAD is associated with night blindness (Perisse and Polacchi, 1980; World Health Organization, 2000), skin diseases (McLaren, 1966; Klein-Szanto et al., 1980) and dysfunctions of immune (Smith et al., 1987; Bowman et al., 1990; Semba et al., 1993), skeletal (Harris et al., 1978) and nervous systems (Rahman et al., 1996). Moreover, VAD has also shown to be related to tumorigenesis (Sun and Lotan, 2002; Fields et al., 2007). On the other hand, excess intake of vitamin A also causes adverse effects on various systems such as the skin (Silverman et al., 1987), eye (Marcus et al., 1985), liver (Nollevaux et al., 2006), skeletal (Binkley and Krueger, 2000; Lips, 2003) and central nervous systems (O'Donnell, 2004).

Other than having vitamin A from dietary intake or food supplementation, people can also take in high doses of synthetic retinoids as therapeutics for treating skin problems such as severe cystic acne. These drugs are isotretinoin (Roaccutane®) and tretinoin (Retin A®) which can be administered orally or topically. However, it is well-documented that intake of synthetic retinoids creates various types of side effects including depression (Bruno et al., 1984; Hanson and Leachman, 2001) and a broad spectrum of congenital birth defects such as ocular malformations (Lammer et al., 1985; Rosa et al., 1986). Hence, the World Health Organization has recommended that daily consumption of retinol should not exceed 800 μg for pregnant women (World Health Organization, 1998b).

Retinoids have long been known to play crucial roles in vision. Night blindness or impaired dark adaptation, as one of the first identified symptoms observed in VAD in humans, was found as far back as in the ancient Egyptian medical documentation. Retinaldehyde serves as chromophore for all known visual pigments. Particularly, the 11-*cis* isomer of retinaldehyde binds to G-protein coupled receptors called opsin, to form both the rod and cone visual pigments. Light isomerizes the bound 11-*cis* retinal to the all-*trans* form, initiating excitation of the photoreceptor cell. Following isomerization and release from the opsin, all-*trans* retinal is reduced to all-*trans* retinol and travels back to the retinal pigment epithelium to be "recharged". Finally, it is oxidized to 11-*cis* retinal before traveling back to the rod outer segment where it can again be conjugated to an opsin to form a new, functional visual pigment (rhodopsin). With the lack of raw materials to synthesize rhodopsin, one will have difficulty with proper vision in the dark.

Mild VAD may result in changes in the conjunctiva called Bitot's spots (Darby et al., 1960; Sommer et al., 1981). Severe or prolonged VAD causes a condition called xeropthalmia (dry eyes), characterized by changes in the cells of the cornea that ultimately result in corneal ulcers, scarring, and blindness (Oomen, 1974; Sommer, 1990; Sommer, 1998).

1.3.2 The role of RA in embryonic development

Apart from its indispensable importance in providing vision, retinoids are also essential for many processes of embryonic development. The most potent and biologically active form of retinoids, all-*trans* RA has been extensively studied in the field of developmental biology for over 30 years. It has been well-documented that RA is present in most of the embryonic tissues (McCaffery and Dräger, 1994; Horton and Maden, 1995; Schweigert et al., 2002). The wide spectrum of functions of endogenous RA in embryonic development includes differentiation, proliferation, apoptosis and morphogenesis (McCaffery and Dräger, 2000; Germain et al., 2006; Mark et al., 2006).

As aforementioned, RA acts upon the RARE to regulate the expression of a panel of target genes in which more than 500 genes may be involved (Balmer and Blomhoff, 2002; Williams et al., 2004). Those that are of conspicuous importance in early development include *Bmp, Wnt, Hox, Fgf* and *Shh.* If the temporal and spatial distributions of embryonic endogenous RA are altered at a time when these early acting genes should be switched on, numerous malformations can be resulted due to silencing or over-transcription of the genes concerned.

Other than spatiotemporal regulation of endogenous RA synthesis, retinoid signalling regulated by RARs is also important for embryogenesis. As mentioned earlier in section 1.3, RAR functions by directly interacting with DNA regulatory sequences leading to modulation of gene transcription. The generation of mice carrying single or double mutations in *RARα, RARβ* and *RARγ* proved that they control retinoid signalling since the resulted phenotypes, including ocular defects, are similar to those observed in VAD (Mark et al., 2006). Studies on the temporal and spatial expressions of RAR review that as early as E6.5, i.e. the egg cylinder stage, *RARα* mRNA is detected ubiquitously in both embryonic and extraembryonic tissues whereas *RARγ* mRNA is detected in embryonic but not extraembryonic tissues. However, there is lack of mRNA expression of *RARβ*. At E7.5, *RARα* and *RARγ* mRNA is still detected in both embryonic and extraembryonic tissues, while *RARβ* mRNA begins to be observed in the presumptive hindbrain. At 1 day later, the *RARβ* mRNA expresses uniquely in the hindbrain region whereas the other 2 isoforms express ubiquitously in the embryo (Ruberte et al., 1991; Ang and Duester, 1997).

Although RARs broadly express in the embryo of all stages, it is reported that in early gastrula, the RARs in the rostral embryonic tissue must function as repressors which is probably to prevent premature activation of target genes that determine posterior cell fate (Niederreither and Dolle, 2008). Hence, any alteration in bioavailability of endogenous RA will have effect on RA-responsive genes by improper activation of RARs, which normally function as transcriptional repressors in the anterior region.

One of the embryonic tissues that is profoundly sensitive to the

availability of endogenous RA is the developing hindbrain. It was found that after RA administration to mouse embryos, the hindbrain Hox genes such as *Hox-2.9* and *Krox-20* (Murphy and Hill, 1991; Morriss-Kay et al., 1991) were all induced in an anterior direction and then regressed, leaving behind an altered expression pattern that eventually resulted in disrupted rhombomere arrangement or segmentation. Thus instead of the normal rhombomeric sequence of 1, 2, 3, 4, 5, 6 and 7, RA administration causes rhombomere 2 and 3 to transform into 4 and 5 respectively, producing the sequence of 1, 4, 5, 4, 5, 6 and 7 (Marshall et al., 1992). On the other hand, the converse situation of RA deprivation is also highlighted in the developing hindbrain. In RA-deficient quail and rat embryos, the posterior part of the hindbrain is either missing or fails to form rhombomere boundaries, resulting in missing or altered structure of pons and medulla (Maden et al., 1996).

Since RA plays an important role in many biological processes, maternal deficiency of vitamin A at different gestational stages have been reported to cause a variety of congenital birth defects, low birth weight and even fetal death (World Health Organization, 1998a). While VAD remains a public health concern throughout the developing countries, using high doses of vitamin A as supplementation for alleviating the problem remains controversial, partly because excess intake of vitamin A during pregnancy is also profoundly dangerous to the developing embryo (Rothman et al., 1995). The types of congenital malformations resulted from deficiency or excess of vitamin A are comparable, which include microcephaly, microphthalmia or anophthalmia, and malformations of the heart (Wilson et al., 1953; Sarma, 1959; Geelen, 1979; Yasuda et al., 1986; Rothman et al., 1995). Moreover, depletion of endogenous RA or excess intake of RA during

embryonic development causes various malformations in different developing organs such as craniofacial and nervous system abnormalities, ocular defects, cardiovascular anomalies and limb dysmorphology (Lammer et al., 1985; Rosa et al., 1986; Yasuda et al., 1986; Coberly et al., 1996; Niederreither et al., 1999; Niederreither et al., 2000; Mic et al., 2002; Dupe et al., 2003; Mic et al., 2004b; Ribes et al., 2006). In fact, there is indication that the nature and spectrum of RA-induced malformations depend on the dose and the developmental stages at the time of exposure (Soprano and Soprano, 1995; Holson et al., 1999; Collins and Mao, 1999). Maternal exposure to RA in early gestation period results in abnormalities of the central nervous system while exposure to RA in late gestation causes limb and renal abnormalities (Yasuda et al., 1986; Alles and Sulik, 1989; Alles and Sulik, 1992; Tse et al., 2005).

Several pathogenic mechanisms have been proposed to explain congenital defects of various developing organs caused by RA exposure. Retinoids decrease the adhesion of neural crest cells to substrate and their ability to migrate (Smith-Thomas et al., 1987; Moro Balbas et al., 1993; Li et al., 2001). It was reported that RA-induced malformation of the eye in mouse fetuses was mediated via altering the migratory pathway of cranial neural crest cells (Ozeki and Shirai, 1998). Moreover, exposure to RA has been reported to inhibit cell proliferation of many cell types which eventually led to malformation of the developing organ concerned. For example, RA has been shown to be crucial in embryonic cardiovascular development by controlling the proliferation rate of endothelial cells and modulating the remodelling of capillary plexuses (Lai et al., 2003; Bohnsack et al., 2004).

Apart from altered proliferation rate, exogenous RA can induce cell death

in developing organs, which in turn leads to reduction in cell number and results in malformed structures (Kochhar et al., 1993; Shum et al., 1999). Insufficiency of progenitor cells may probably lead to hypoplasia or agenesis of the developing organ. In the case of embryonic caudal development, exposure to RA has been shown to induce caudal regression and excessive cell death was found in the tail bud mesenchyme (Shum et al., 1999).

As mentioned earlier in section 1.3, the pleiotropic effect of RA is either mediated by RAR/RXR dimers bound to RARE-containing genes, and is directly affected by the availability of endogenous RA, or through less direct mechanisms such as changes of mRNA stability or protein turnover. When the embryonic endogenous RA distribution is spatially or temporally incorrect, both deficiency and excess of RA can lead to numerous congenital defects. For instance, it is well known that high doses of RA can cause truncation of the frontonasal and maxillary processes and thus produce bilateral clefting of the lip and palate (Rosa et al., 1986; Abbott et al., 1989; Emmanouil-Nikoloussi et al., 2000). It was found that exposure to a high dose of RA resulted in inhibition of *Shh* and *Patched* expressions while *Fgf8* was not affected in the craniofacial primordia, and abolishment of the polarizing activity of these tissues (Helms et al., 1997). On the other hand, it was reported that in *Raldh2* null mutant embryos, *Fgf8* and its associated transcription factors almost completely failed to be activated in the facial ectoderm (Ribes et al., 2006).

The eye is highly susceptible to retinoid excess or deficiency early in its formation (Luo et al., 2006). Interestingly, the types of ocular defects resulted from

maternal RA exposure are similar to those resulted from embryonic depletion of endogenous RA, for example, microphthalmia (Sulik et al., 1995; Ozeki and Shirai, 1998; Niederreither et al., 2002; Ribes et al., 2006). The accuracy of spatiotemporal distribution of endogenous RA depends on the interplay between RA-synthesizing and degrading enzymes, i.e. RALDH and CYP26 respectively. In the mouse developing eyes, RA synthesizing genes, namely, *Raldh1*, *Raldh2* and *Raldh3* are expressed in non-overlapping domains First, *Raldh2* is transiently expressed in optic vesicles (Wagner et al., 2000; Mic et al., 2004a). From E9.5 onwards, *Raldh1* and *Raldh3* are mainly detected in the dorsal and ventral fields of the retina respectively (McCaffery et al., 1999; Li et al., 2000; Mic et al., 2000; Suzuki et al., 2000). These expression domains are separated by a stripe expressing the RA-degrading enzymes *Cyp26a1* and *Cyp26c1* (Fujii et al., 1997; Sakai et al., 2004). This unique arrangement of RA-regulatory enzymes generates three zonal distributions of different concentrations of endogenous RA along the dorsoventral axis, which suggests that endogenous RA plays essential roles in controlling embryonic eye development. Moreover, the locus of *Cyp26a1* has been shown to have two RARE, R1 and R2 (Loudig et al., 2005). Hence *Cyp26a1* expression level is inducible by the endogenous RA level. *Raldh2*, which is the key and earliest expressed *Raldh* gene in the embryo, is required for optic cup formation as there was no eye formation in *Raldh2* null mutant embryos. *Raldh2* is also essential for setting the correct expression of *Raldh3* at later stages in the developing eye (Mic et al., 2004a; Halilagic et al., 2007). Other than deprivation of RA synthesis, exogenously applied RA can also lead to failure in eye formation (Sulik et al., 1995). However, so far, there is no proposed mechanism that can explain why both deficiency and excess of RA can generate similar ocular defects in the embryo.

1.4 DIFFERENTIAL SUSCEPTIBILITY TO RA TERATOGENICITY IN ANIMAL MODELS

Various animal models have been widely employed to examine the teratogenic effects of retinoids. They include pig (Hale, 1933; Hale, 1935), hamster (Williams et al., 1984; Colon-Teicher et al., 1996), rat (Padmanabhan et al., 1981; Holson et al., 1999), mouse (Ozeki and Shirai, 1998; Enwright, III and Grainger, 2000) and chick (Golz et al., 2004; Maden et al., 2007). Identification of factors associated with species or strain differences in response to RA deficiency or excess can provide important clues regarding the underlying mechanism of how RA deficiency or excess cause similar birth defects. Results from animal models may provide insights into understanding individual variability in human susceptibility to RA-induced teratogenesis.

For instance, Collin et al. (2006) reported that there was differential susceptibility to RA-induced forelimb ectrodactyly in C57BL/6N (C57) mouse strain over SWV mouse strain (Collins et al., 2006) and this is consistent with all previously tested teratogenic agents (Scott et al., 1990; Lee et al., 2004). This strain-specific susceptibility towards RA-induced limb dysmorphology is not accountable by differences in developmental stages or pharmacokinetics at the whole embryo level. The underlying mechanism for such strain differences remain to be elucidated.

Moreover, the same embryonic cell populations of different strains also exhibit differential sensitivity to teratogens. It has been illustrated by Chen et al.

(2000) that there was a reduction in ganglioside GM1 content and faster lateral mobility of membrane lipids in C57 (a mouse strain sensitive to ethanol) neural crest cells than in ICR (a mouse strain less sensitive to ethanol) neural crest cells both under control conditions and ethanol treatment, suggesting that it could account for such inter-strain differential response to ethanol-induced malformations.

Other than differential cellular responses during the course of teratogenic insult, different maternal factors and genetic predispositions can attribute to differential strain sensitivity to teratogens. In a study on the effect of acute prenatal ethanol administration, susceptible C57 strain and resistant Short-Sleep mouse strain were used in a reciprocal crosses design. It was found that hybrid litters carried by C57 mothers had a higher rate of ethanol-induced malformations than similarly treated hybrid litters of Short-sleep mothers, suggesting that maternal or genetic factors could account for such differential fetal susceptibility to ethanol-induced malformations (Gilliam et al., 1997).

1.5 STRATEGY OF THE THESIS

It is well-known that in humans, both excess intake and deficiency of vitamin A or RA during pregnancy are associated with ocular malformations such as microphthalmia. However, the underlying pathogenic mechanism remains unclear. The aim of this thesis is therefore to study the pathogenesis of RA-induced developmental ocular defects by using mouse models.

To achieve this, I have employed two mouse stains as the animal model. They are C57 mice that spontaneously develop ocular defects (Smith et al., 1994)

and ICR mice, which are not prone to develop ocular defects (Sulik et al., 1995). First, in ***Chapter 3***, I have conducted detailed time and dose response studies by injecting pregnant mice with various dosages of RA at different gestational days. Eye defects were examined in near-term fetuses. By comparing the frequency of anophthalmia (total absence of eyes), and microphthalmia (small eyes), the most severe types of ocular defects, C57 fetuses were found to be significantly more susceptible to RA-induced ocular defects than ICR fetuses.

After establishing the mouse models with differential strain response to RA-induced ocular defects, I have proposed and worked on 3 hypotheses that might contribute to the differential strain susceptibility to RA-induced ocular defects.

First Hypothesis

Since the teratogenic effect of RA is developmental stage-dependent, it is possible that there is a difference in the developmental stage between these 2 mouse strains at the time of RA injection. Hence, in ***Chapter 3***, I have compared the somite stage, which is a general growth parameter, of ICR and C57 embryos at different time points from E8 to E9.5.

Second Hypothesis

As mentioned in section 1.4, maternal factors and genetic predispositions can attribute to differential strain responses to RA. Hence, in ***Chapter 3***, I have compared the frequency of RA-induced ocular defects in heterozygous fetuses obtained from reciprocal matings between C57 and ICR mice with those in homozygous ICR and C57 fetuses.

Third Hypothesis

Since the types of spontaneous eye defects developed in C57 mice mimic those caused by excess or deficiency of RA, I speculated that differences in RA-associated mechanisms may be involved in differential strain response to RA-induced ocular defects. First, in ***Chapter 4***, I have conducted detailed morphological and histological studies to determine early embryonic changes after RA treatment. Then in ***Chapter 5***, I have compared early molecular changes in the embryo after RA treatment, particularly focussing on genes involved in RA synthesis and metabolism, and also genes involved in early eye development.

It has been shown that exogenously applied RA could cause prolonged down-regulation of the RA synthesizing enzymes (Niederreither et al., 1997; Dobbs-McAuliffe et al., 2004). Hence, it is possible that the teratogenic insult will cause deficiency of RA, which in turn affects RA-dependent processes involved in early eye development, thus leading to ocular malformations. To examine this possibility, in ***Chapter 6***, I have measured the RA concentrations in the embryo after RA treatment.

Finally, in ***Chapter 7***, results of this study were concluded and future perspectives were discussed.

CHAPTER 2

General Materials and Methods

2.1 PREPARATION OF ALL-*TRANS* RA

To prepare a stock solution of *all-trans* retinoic acid (RA) (*Sigma*) at final concentration of 3.33 mg/ml, 50 mg of *all-trans* RA was dissolved in 1.5ml of absolute alcohol. It was vortexed for 3 hours and then suspended in peanut oil (*Sigma*) to a final volume of 15 ml. To prevent photo-oxidation, RA was kept in a tube wrapped with aluminum foil throughout the process. Different concentrations of RA suspension were prepared for dose response study by further dilution with peanut oil so that similar volume of suspension was injected intraperitoneally into the mice. Preparation of lower dose of RA solution for injection was prepared freshly on the same day as the stock RA solution prepared. This working RA solution was then aliquot into small portion in tubes wrapped with aluminum foil, kept at 4°C and used within 2 weeks. The aliquot of working RA solution in a single tube was used for only 2 days so as to minimize the chances of being photo-degraded when withdrawing oil for injection.

2.2 MOUSE MAINTENANCE AND MATING METHOD

Outbred ICR (Institute of Cancer Research) and inbred C57BL/6J (C57) mice were kept in a 12:12 hours light-dark cycle with the dark period starting from 11 p.m. to 11 a.m.. A male mouse was paired up with one female mouse for 2 hours from 9 a.m. to 11 a.m. At 11 a.m., the female mice were checked for the presence of a copulation plug as the indicator for successful mating. Ten o'clock in the morning was considered as embryonic day (E) 0.

2.3 EMBRYO DISSECTION

Pregnant mouse at the appropriate gestational day was sacrificed by cervical dislocation. The abdominal wall was cut open and the uterus was removed. Embryos were dissected out in ice-cold phosphate buffered saline (PBS) and freed from the decidual tissues, extra-embryonic membranes, yolk sac and amnion under a stereomicroscope (SV40, *Zeiss*). External embryonic morphology was examined and subsequently embryos were fixed for further histological and molecular analyses. For embryos collected for *in situ* hybridization, holes were punched in the brain regions and heart tubes to prevent non-specific staining caused by trapping of solution. For embryos prepared for whole mount *in situ* hybridization or *in situ* end-labeling, they were fixed in freshly-prepared 4% paraformaldehyde (*Sigma*) in PBS at 4°C overnight. For haematoxylin and eosin staining, embryos were fixed in Bouin fixing solution (*BDH*) at room temperature for 1 to 2 days. For near-term fetuses, the head was first cut out, washed with PBS and then immersed in Bouin fixing solution for 7 days. Tissues were then further trimmed to periocular region and fixed in Bouin fixing solution again for another 2 weeks. Tissues were then washed in 70% ethanol for 1 day before processing by an automatic processing machine as described in section 2.4.1.

2.4 PREPARATION OF PARAFFIN SECTIONS

2.4.1 Dehydration and embedding

For embryos at early embryonic stages, they were washed and dehydrated by passing through a series of ethanol in ascending concentrations (50, 70, 87, 95

and 100%). In each dehydration step, the alcohol solution was changed twice at 20-minute interval. After dehydration, samples were cleared in a mixture of absolute ethanol and Histoclear (*National Diagnostics*) (1:1 vol/vol) for 30 minutes and then were completely cleared in Histoclear for 30 minutes with 2 changes. Wax infiltration was done by transferring the embryo to molted wax (fibrowax, *BDH*) in glass embedding mould at 60°C for 1 to 2 hours. After orienting the embryo to the desired cutting plan, the wax was left at room temperature to solidify. The wax block was kept in room temperature until use.

For the fetal heads of near-term fetuses, all the dehydration, clearing and wax infiltration processes were done by using an automatic processing machine (Pathcentre, *Shandon*). The fetal tissues were passed through a series of ascending concentrations of ethanol (70, 80 and 95%) at 2-hour intervals and finally dehydrated 3 times in absolute ethanol at 2-hour intervals. Tissues were then cleared in xylene twice for 1.5 hours in each step. After clearing, tissues were infiltrated with paraffin for 6 hours with 4 changes of wax.

2.4.2 Microtome sectioning

The wax block was trimmed and mounted onto embedding cassette, and then properly held in the microtome *(Leica)*. A ribbon of paraffin sections of 6 μm in thickness was obtained and spread out by water in a water bath set at 40°C. The sections were then placed onto microscopic slides that had been coated with 3-triethoxysilylpropylamine (TESPA, *Sigma*) in serial manner. Sections were dried completely and kept in desiccators at room temperature until use.

2.4.3 Haematoxylin and eosin staining

The sections on slides were dewaxed in three changes of xylene at 15-minute interval and then rehydrated by passing through a series of ethanol in descending concentrations (100, 95, 80 and 70%). The sections were then washed under running tap water for 5 minutes and stained with Harris's Haematoxylin for 5 minutes. After washing in running tap water, the sections were quickly dipped in acid alcohol for 8 seconds for color differentiation. It was then oxidized in alkaline Scott tap water for 5 minutes to further enhance the blue color. After washing in running tap water for 5 minutes, they were stained in eosin for 10 minutes and quickly dehydrated by passing through a series of ethanol in ascending concentrations and ended with three changes of absolute alcohol. The sections were then cleared in three changes of xylene for 15 minutes in each step and then mounted with permount (*Fisher Scientific*) for histological examination by light microscopy.

2.5 PREPARATION OF PLASMID DNA

2.5.1 Bacterial transformation

Plasmid DNA was added to 50 µl of competent cells (DH5α competent cells, *Gibco*), mixed and then put on ice for 30 minutes. The mixture was heat shock at 42°C for exactly 2 minutes and immediately chilled on ice for 1 minute. Two hundred milliliter of LB broth with 80 µl/ml ampicillin (*Roche*) was added to the mixture and incubated at 37°C for 1 hour with gentle shaking. Different volumes of mixture (ranging from 10 µl to 300 µl) were spreaded evenly on the agar plates

containing 80 µl/ml ampicillin. The plate was then incubated at 37°C overnight. A single bacterial colony was selected and put into 10 ml LB broth with ampicillin and incubated at 37°C for 15 hours under vigorous shaking. After overnight incubation, 500 µl of cell suspension was mixed with 250 µl of 50% glycerol (*Roche*). The mixture was immediately frozen in liquid nitrogen and stored at -80°C.

2.5.2 Plasmid DNA extraction

Bacteria with insertion of desired DNA plasmid grown in 10 ml of LB broth supplemented with ampicillin was harvested by centrifugation (Mistral 2000, *MSE*) at 3,000 rpm for 15 minutes at room temperature. By using the Rapid Plasmid Miniprep System (*Marligen Biosciences*), the cell pellet was resuspended in 250 µl of Cell Suspension Buffer [50 mM Tris-HCl (pH8.0), 10 mM EDTA, 20 mg/ml RNase A] and vortex until homogenous. The cells were lysed by the addition of 250 µl of Cell Lysis Solution (200 mM NaOH, 1% SDS), mixed gently and incubated in room temperature for 5 minutes. Neutralization Buffer at a volume of 350 µl was added and mixed immediately by inverting the tube until the solution was homogenous. The protein debris was removed by centrifugation (Centrifuge 5415C, *Eppendorf*) at 12,000 g for 10 minutes at room temperature. The supernatant was collected and loaded onto the spin cartridge inside a 2 ml wash tube and then centrifuged at 12,000 g for 1 minute. The flow-through was discarded and the spin cartridge-containing wash tube was washed with 700 µl of Wash Buffer [containing 200 mM NaCl, 10 mM EDTA, 50 mM Tris-HCl (pH 8.0), 80% ethanol] and then was centrifuged at 12,000 g for 1 minute. The flow-through was discarded and the spin-cartridge-containing tube was re-centrifuged again to remove residual wash buffer. Warm RNase-free autoclaved water at a volume of 70 µl was added to the

center of the spin cartridge and incubated for 2 minutes. The plasmid DNA was harvested by centrifugation at 12,000 g for 2 minutes and stored at -20°C until use.

2.6 PREPARATION OF RIBROPROBES

Ribroprobes labeled with digoxigenin (DIG) were synthesized from *in vitro* reverse transcription on the linearized plasmid DNA.

2.6.1 Linearization of plasmid DNA

The plasmid DNA was linearized by cutting at the restriction sites as mentioned in the materials and methods section of the relevant chapter.

The reaction mixture was as follow:

Plasmid DNA	X
Restriction enzyme	20 units
10X reaction buffer	5 µl
RNase-free autoclaved water	make up to a final volume of 50 µl

X = volume equal to 5 µg of plasmid DNA

The enzymatic linearization reaction was performed by incubating the mixture at 37°C at 700 rpm for 2 hours (Thermomixer 5436, *Eppendorf*). The sample was then extracted with phenol:chloroform:isoamyl alcohol (25:24:1). After centrifugation (14,000 g for 10 minutes at 4°C), the upper aqueous layer was harvested and mixed well with equal volume of isopropanol (*BDH*) at 4°C for DNA precipitation. The mixture was centrifuged immediately at 14,000 g at 4°C for 10 minutes. The pellet of linearized plasmid DNA was then washed with 700 µl of 70%

ethanol and dried under vacuum (DNA Speed Vac, *Savant*) for 3 minutes. The pellet was resuspended in 20 µl of autoclaved water and stored at -20°C.

2.6.2 *In vitro* transcription

The reaction mixture was as follow:

10X DIG RNA labeling nucleotides mix	2 µl
10X Transcription buffer	2 µl
RNasin ribonuclease inhibitor	1 µl
RNA polymerase	1 µl
Linearized DNA plasmid (1 µg/µl)	X
Diethylpyrocarbonate (DEPC)-treated water	Make up to a final volume of 20 µl

The reaction mixture was then incubated for 2 hours at 37°C with gentle shaking. Afterwards, 2 µl of reaction mixture was mixed with DNA sample loading dye (*Promega*) and subjected to 1% agarose gel electrophoresis. The gel was then stained with ethidium bromide (0.5 µg/ml) and visualized under ultraviolet illumination to estimate the molecular size, quantity and quality of the synthesized ribroprobe. Removal of the DNA template in the reaction mixture was done by addition of 20 U RNase-free DNase (*Roche*) at 37°C for 15 minutes with gentle shaking. The ribroprobe was then precipitated by addition of 100 µl of TE buffer [10 mM Tris-HCl (pH 7.4), 0.1 mM EDTA], 10 µl of 4M LiCl and 300 µl of ice-chilled absolute alcohol and kept at -20°C for 2 hours. The pellet of ribroprobe was obtained by centrifugation at 14,000 g at 4°C for 15 minutes. The pellet was washed with 70% ethanol and dried under vacuum. It was then dissolved in 70 µl of DEPC-treated water and the optical density of the ribroprobe at 260nm was

measured by spectrophotometry (GeneQuant, *Pharmacia Biotech*) to quantify its final concentration.

2.6.3 Spot test

To verify whether the ribroprobe had been successfully labeled with DIG-conjugated nucleotides, spot test was performed. One microlitre of ribroprobes under test was diluted in 5 µl of 5X SSC and then denatured by boiling for 5 minutes followed by quick chilling on ice for 1 minute. One microliter of boiled mixture was spotted onto the hybridization transfer membrane (Hybond-N, *Amersham*) and dried at room temperature for 5 minutes. The membrane was crosslinked under ultraviolet light (UK Crosslinker, *Stratagene*) for 2 minutes. Afterwards, the membrane was soaked in 2X SSC followed by washing twice in PBT (PBS with 0.1% Tween-20, *Sigma*) for 5 minutes each. The membrane was then incubated with alkaline phosphatase-conjugated anti-digoxigenin antibody (1:5000 vol/vol in PBT, *Roche*) for 30 minutes. Membrane was washed with PBT, followed by washing twice in NTMT [100 mM NaCl, 100 mM Tris-HCl (pH 9.5), 50 mM $MgCl_2$, 0.1% Tween-20] for 5 minutes each. The signal was then visualized by developing in 4.5 µl of nitro-blue tetrazolium chloride (NBT, *Roche*) (75 mg/ml stock in 70% N,N-dimethyl formamide) and 3.5 µl of 5-Bromo-4-Chloro-3'-Indolyphosphate p-Toluidine (BCIP, *Roche*) (50 mg/ml stock in N,N-dimethyl formamide) per ml of NTMT at room temperature in dark for 30 minutes. The dot developed into a dark blue spot indicate a positive result.

2.7 WHOLE MOUNT *IN SITU* HYBRIDIZATION

2.7.1 Collection and preparation of mouse embryos

Timed pregnant mice were sacrificed by cervical dislocation and embryos were immediately dissected out in ice-cold DEPC-treated PBS. To prevent contamination by RNase, all solutions used for *in situ* hybridization were treated with DEPC, except the steps after application of RNase. Embryos were fixed in freshly prepared 4% paraformaldehyde in PBS at 4°C overnight with gentle shaking. The fixed embryos were washed in PBT for 15 minutes with two changes and then dehydrated in a series of methanol (*BDH*) in ascending concentrations (25, 50 and 75%) and 2 final changes of absolute methanol at 15-minute intervals. To prevent degradation of RNA, all washing and dehydration processes are carried out at 4°C. After complete dehydration, embryos were kept at -20°C until use.

2.7.2 Pre-hybridization and hybridization

Embryos were rehydrated through a series of methanol in descending concentrations (75, 50 and 25% in PBT) for 15 minutes each. Embryos were washed in PBT twice and then bleached in 6% of hydrogen peroxide (*Sigma*) in PBT for 1 to 1.5 hours at room temperature. Embryos were washed with PBT for 3 times and then treated with proteinase K (10 μg/ml in PBT) *(Roche)*. The optimal duration of enzymatic digestion was dependent on the stage of embryos, i.e. embryos at E8, E8.5, E9 and E9.5 for 3, 5, 8, 10 minutes respectively. Enzymatic digestion was stopped by addition of glycine (2 mg/ml in PBT) (*BDH*). After washing for 15 minutes in PBT, they were re-fixed in freshly-prepared 4% paraformaldehyde with

0.2% glutaldehyde in PBT for 20 minutes. After washing with PBT, embryos were incubated in 1 ml of freshly-prepared pre-hybridization buffer [50% de-ionized formamide, 5X SSC (pH 4.5), 50 μg/ml yeast tRNA, 50 μg/ml heparin, 1% SDS] at room temperature for 10 minutes. Afterwards, fresh pre-hybridization buffer was changed and embryos were then incubated at 70°C for 90 minutes. Embryos were then placed in hybridization buffer (1 ml pre-hybridization buffer with 1 μg ribroprobes) at 70°C overnight with gentle shaking.

2.7.3 Post-hybridization washing and antibody incubation

After hybridization, embryos were washed twice in solution 1 [50% formamide (Sigma), 5X SSC (pH 4.5), 1% SDS] for 30 minutes in each step at 70°C. Embryos were then washed once in a solution containing equal volumes of solution 1 and solution 2 [0.5 M NaCl, 10 mM Tris-HCl (pH 7.5), 0.1% Tween-20] at 70°C for 15 minutes. Embryos were then washed in solution 2 at room temperature 3 times for 15 minutes in each step. The non-specific unbound ribroprobes were digested by 100 μg/ml of RNase A (*Roche*) in solution 2 at 37°C with gentle shaking. Reaction was stopped by removal of enzyme-containing solution 2 and washed again in solution 2 for another 15 minutes. Embryos were then washed twice in solution 3 [50% formamide, 2X SSC (pH 4.5)] at 65°C for 30 minutes followed by 3 changes of TBST [0.14 M NaCl, 2.7 mM KCl, 25 mM Tris-HCl (pH7.5), 0.1% Tween-20] for 10 minutes at room temperature. Embryos were then incubated with 10% heat-treated sheep serum (heat-treated at 56°C for 30 minutes) (*Jackson Immuno*) in TBST for 90 minutes to block non-specific binding.

Pre-absorbed antibody was obtained by suspension of 3 mg of

acetone-dried embryo powder in 0.5 ml TBST followed by heat treating at 70°C for 30 minutes. After heat inactivation, the mixture was then incubated with 5 µl of heat-treated sheep serum and 1 µl of alkaline phosphatase-conjugated anti-digoxigenin antibody (*Roche*) at 4°C for 5 hours with gentle shaking. The supernatant with pre-absorbed antibody was harvested by centrifugation at 14,000 g for 15 minutes at 4°C and diluted to 2 ml with 1% heat-treated sheep serum in TBST. After blocking in 10% sheep serum, embryos were incubated in diluted pre-absorbed antibody at 4°C overnight with gentle shaking.

2.7.4 Post antibody washing and signal detection

After antibody binding, embryos were washed in TBST for 5 times with 1 hour each and left in TBST at room temperature overnight. Embryos were then transferred to glass vial covered with aluminum foil and washed in NTMT for 3 times with 15 minutes each and then incubated in NBT/BCIP in NTMT (refer to Section 2.6.3) at room temperature for 2 hours for signal development. After reaching the optimal color, embryos were washed twice in PBT and then twice in PBS for 30 minutes in each step. Embryos were post-fixed in 4% paraformaldehyde in PBS at 4°C overnight. Embryos were then washed twice in PBS, followed by passing through a series of glycerol in ascending concentrations in autoclaved water (50%, 75% and 100%). Images were then captured by digital camera (DFC 480, *Leica*) fitted onto stereomicroscope (MZ16, *Leica*).

2.8 REAL-TIME QUANTITATIVE REVERSE TRANSCRIPTION-POLYMERASE CHAIN REACTION (RT-PCR)

2.8.1 Collection and storage of embryos

Samples were dissected in DEPC-treated ice-cold PBS. To allow full penetration of the reagent into the tissue, the embryonic tissue was put into RNA*later* RNA Stabilization Reagent (*Qiagen*) in 10-fold volume immediately after dissection and kept at 4°C overnight. The tissue was then stored at -20°C until use.

2.8.2 Total RNA extraction

The RNeasy Mini Kit (*Qiagen*) was used to extract total RNA according to the manufacturer's instructions. First, the RNA*later* RNA Stabilization Reagent was pipetted off. The tissue was lysed in 600 µl of Buffer RLT (provided in the kit), added with 1% β-mercaptoethanol (*BDH*), by passing through a 25 gauge needle fitted onto a one ml syringe several times. Six hundred µl of 70% ethanol was added and then mixed with the lysate by pipetting up and down. The lysate/ethanol mixture was added to the RNeasy mini column (provided in the kit) and centrifuged at 13,000 rpm for 30 seconds and the flow-through was discarded. Seven hundred µl of Buffer RW1 (provided in the kit) was pipetted into the RNeasy column and then centrifuged at 13,000 rpm for 30 seconds and the flow-through was discarded. Five hundred µl of Buffer RPE (provided in the kit) was then added into the column and centrifuged at 13,000 rpm for 30 seconds. This procedure was repeated. The flow-through was discarded and centrifuged at 13,000 rpm for 1 minute to eliminate any leftover Buffer RPE. The RNeasy column was transferred to a new 1.5 ml microfuge tube. Fifty µl of RNase-free water was added directly onto the RNeasy silica-gel membrane to elute the RNA. After allowing to stand for 2 minutes, the microfuge tube with the column was centrifuged at 13,000 rpm for 1 minute, which

would elute the RNA in the flow-through. Total RNA concentrations were measured by spectrophotometry at a wavelength of 260 nm.

2.8.3 Reverse transcription

Total RNA extracted was subjected to first-strand cDNA synthesis by using the High Capacity cDNA Reverse Transcription Kit (*Applied Biosystems*). To synthesize 10 µl of cDNA solution, the following reagents were mixed together, 500 ng of total RNA, 1 µl of 10X Reverse Transcription Buffer, 0.4 µl of 100 mM dNTP, 1 µl of 10x Reverse Transcription random primers, 0.5 µl MultiScribe™ Reverse Transcriptase (50 U/µl) and 0.5 µl of RNase Inhibitor (20 U/µl). DEPC-treated water was added to the reaction mixture to make up a final volume to 10 µl. Reverse transcription was performed in a thermal cycler (icycler, *BioRad*) at 25°C for 10 minutes, followed by 37°C for 120 minutes and then 85°C for 5 seconds. The cDNA synthesized was kept at 4°C if used within one week, or at -20°C for longer term of storage.

2.8.4 Polymerase chain reaction

The cDNA synthesized was subjected to quantitative polymerase chain reaction (PCR) using ABI 7500 Fast Real-Time PCR system (*Applied Biosystems*). Various sets of primers specific for different genes were used. PCR amplification was performed in a reaction mixture containing 2 µl of cDNA, 1 µl each of 10 pmol/µl forward and reverse primers, 10 µl of 2X iQ™ SYBR® Green Supermix (*Bio-Rad*) which was made up with DEPC-treated water to a final volume of 20 µl. Each sample was amplified and performed in triplicate.

For each PCR, a no-template sample was included to serve as the negative control, and a set of cDNA standards (refer to Section 2.8.5) of known quantity was added and performed in duplicate for quantifying the amount of the target gene.

To initiate amplification, PCR conditions started at 95°C for 10 minutes to activate the iTaq® DNA polymerase (*Bio-Rad*) present in the PCR Master Mix. This was followed by 40 cycles comprising of denaturation at 95°C for 15 seconds and annealing/extension at 55°C for 1 minute. The quantity of the target gene was analyzed by ABI Prism®7000 SDS Software (*Applied Biosystems*).

2.8.5 Preparation of cDNA standards

The cDNA standards were generated by PCR amplification of serially diluted cDNA plasmids of *β-actin*, or the target gene of known concentrations. The cDNA plasmid was prepared as described in Section 2.5.2 and quantified by spectrophotometry at 260 nm. The cDNA plasmid was adjusted to 20 ng/µl with DEPC-treated water. Finally, 10-fold serial dilutions were made-up to obtain a set of standards ranging from 0.02 g to 2 ng.

CHAPTER 3

Time and Dose Responses to RA-induced Ocular Defects

3.1 INTRODUCTION

RA is essential for eye development. Either too much or too little of RA can inhibit eye formation (Shenefelt, 1972; Hyatt et al., 1996; Avantaggiato et al., 1996; Dickman et al., 1997). However, the underlying mechanism is poorly understood.

As a powerful teratogen, RA displays teratogenic effects in strain-, time- and dose-dependent manners.

3.1.1 Strain response to RA

Interspecies differences to teratogenicity can be the result of a differing in pharmacokinetic processes that determine the crucial dose-time relationships in the embryo (Nau, 1986). Moreover, it has been well documented that among different mouse strains, there are differential teratogenic responses towards teratogens. For example, differential susceptibility to RA administration was found in C57 strain in which it was more susceptible to embryolethality, induction of cardiovascular defects and forelimb ectrodactyly than SWV strain, whereas the latter strain was more susceptible to the induction of agenesis of ear, thymus and tail as well as cleft palate (Collins et al., 2006).

Several lines of evidence show that C57 strain, of which the rate of spontaneous occurrence of eye defect is about 10%, is more prone to teratogen-induced eye defects, particularly, microphthalmia (Smith et al., 1994). This pigmented mouse strain therefore has been widely employed as an animal

model in the study of ocular teratogenicity since 1960's (Cook and Sulik, 1986). On the other hand, there are evidences which show that ICR strain is resistant to RA-induced ocular malformations (Sulik et al., 1995).

Experiments using mouse strains that have different responses to teratogens can provide information about genetic predisposition and relative maternal contribution to teratogenesis. This can be achieved by using a reciprocal intercrossing design, which can help to differentiate the influence of maternal and fetal genotypes. Male and female mice are mated either with the same strain or reciprocally with a different strain to result in 4 types of fetuses: two homozygous and two heterozygous. In theory, the heterozygous fetuses resulting from reciprocal crosses have similar genetic composition but developed in different maternal environments. Thus, if these two types of heterozygous fetuses show differences in teratogenic response, it may suggest that maternal factors do influence the response.

In fact, maternal effects are known to exist (Gilliam and Irtenkauf, 1990; Gilliam et al., 1997). Reciprocal crosses between susceptible C57 mice and resistant Long-Sleep mice (Gilliam and Irtenkauf, 1990) suggest that subject to ethanol exposure, C57 strain provides a susceptible maternal environment to the teratogenic effect whereas the maternal environment of Long-Sleep mice confers dominance towards resistance to ethanol teratogenesis. Several sources of variation could account for the maternal effects played by certain mouse strain, such as differences in the origin of the sex chromosome, the cytoplasmic contribution of each parent to the gamete, the maternal uterine environment and genomic imprinting (Carlier et al., 1992).

Other than maternal factors, differences in the developmental stage on the same gestational day has been reported to occur in different mouse strains (Thiel et al., 1993). This can be one of the possible factors contributing to strain differences in susceptibility to RA. Hence, it is essential to ascertain the exact phase of development when results of short-term teratogenic exposure, i.e. single dose, are interpreted.

3.1.2 Time response to RA

In mammalian embryonic development, there are 3 definite phases which are pre-implantation, embryonic and fetal periods. The time from conception to implantation is regarded as the "all or none" period, because insults to the embryo will likely result in death of the conceptus and miscarriage (or resorption), or else, it will survive without malformations (Stromland et al., 1991). At this stage, the embryo is undifferentiated. Repair and recovery processes are possible through multiplication of the pluripotent cells to replace those which have been lost. Exposure of embryos to teratogens during pre-implantation stage usually does not cause congenital malformations, unless the agent persists in the body beyond this period (Stromland et al., 1991).

In the embryonic period, organogenesis occurs and this is the period of maximum sensitivity to RA teratogenicity, since not only are tissues differentiating rapidly but damage to them becomes irreversible. Exposure to RA during this period has the greatest likelihood of causing structural malformations. It has been suggested that RA induced changes in the expression of *Hox* genes which initiate posteriorization (Simeone et al., 1995). Moreover, excessive cell death was detected

in the developing cranial region after RA administration (Geelen et al., 1980; Sulik et al., 1988).

Since RA is capable of affecting many organ systems, the pattern of defects produced depends on which systems are undergoing differentiation at the time of teratogenic insult. Embryos exposed to RA during gastrulation and organogenesis elicit a wide spectrum of defects, including limb malformation, body axis transformation, exencephaly, eye defect, craniofacial malformation and caudal regression (Geelen et al., 1980; Rothman et al., 1995; Ross et al., 2000).

Embryonic exposure to RA is highly time-dependent. It has been reported that administration of RA at about mid-late streak stage induced loss of morphological and molecular markers of the forebrain (Simeone et al., 1995), while administration at 2-4 hours later, i.e. about late streak stage, caused an ordered repatterning of the hindbrain (Avantaggiato et al., 1996). With regard to eye development, it has been suggested that the critical period for RA-induced severe eye defects in the mouse is in E7 (Sulik et al., 1995; Ozeki and Shirai, 1998; Ozeki et al., 1999). However, in these studies, pregnant mice were obtained from overnight mating. Hence, the precise time of mating was unknown and thus the exact developmental stage at which the embryo was subjected to RA insult could not be determined.

The fetal phase is the period when most organs and systems have already formed and they are undergoing growth and functional maturation. Fetuses are less susceptible to RA toxicity in this period than those in early phase. RA affects fetal

growth (e.g. intrauterine growth retardation), the size of a specific organ or the function of the organ, rather than causing gross structural malformations. Reduced weight of the cerebellum was reported when RA was administered to embryos at late gestational stages (Holson et al., 1997b). Moreover, it has been reported that when prenatal embryos were exposed to low doses of RA, there were behavioral changes and difficulty in learning in the newborn offspring (Hutchings et al., 1973; Adams, 1993; Holson et al., 1997a).

3.1.3 Dose response to RA

Other than the time of administration, the dosage and the route of administration of teratogens are also critical for initiation of abnormal embryogenesis (Wilson, 1973). According to the Wilson's 6 principles, susceptibility to teratogenesis varies with the nature of the teratogen itself, the route and the degree of maternal exposure, the rate of placental transfer and systemic absorption and the composition of the maternal and embryonic/fetal genotypes. Placenta serves as a barrier that isolates the embryo from the maternal side as well as a selective filtration site for removing toxic materials from the maternal side. Shenefelt (1972) has reported that, in hamster, the morphogenesis of various types of malformations induced by RA was dose-dependent. Moreover, it has also been reported that topical administration of RA did not alter maternal plasma retinoid levels while administration of the same dose intraperitoneally or orally did alter plasma retinoid levels (Nau, 1993).

Owing to its short half-life and fast metabolism, RA is difficult to retain inside the body and its metabolites can readily be eliminated. Previous report has

shown that maximum concentration of RA in embryonic tissues was attained 3 hours after administration, and that tissue RA level returned to pre-treatment level within 8 hours, indicating that the effect of RA administration lasted only for a very short period of time (Satre and Kochhar, 1989).

3.2 EXPERIMENTAL DESIGN

As mentioned in section 1.3, it is well-known that in humans, both excess intake and deficiency of vitamin A or RA during early pregnancy are associated with ocular malformations. However, to date, the underlying pathogenic mechanism of how these opposite conditions in retinoid homeostasis can cause similar types of ocular malformations remains unclear. The aim of this thesis is therefore to study the pathogenesis of RA-induced developmental eye defects by using mouse models. To achieve this, first, I have set up mouse models by employing two mouse strains. They are C57 strain that spontaneously develops ocular defects (Smith et al., 1994; Sulik et al., 1995) and ICR strain, which is not prone to develop ocular defects (Sulik et al., 1995).

As mentioned in section 3.1.2, other studies showed that only 2 – 4 hours difference in the time of RA administration could result in totally distinct spectrum of defects (Simeone et al., 1995; Avantaggiato et al., 1996). Moreover, a critical window for RA-induced ocular malformations could not be precisely established from results of previous studies due to overnight mating (Sulik et al., 1995; Ozeki and Shirai, 1998; Ozeki et al., 1999). To this end, I have first established a precise stage-specific study to determine RA teratogenicity in causing eye malformations. Taking into account results of previous reports (Rutledge et al., 1994; Sulik et al., 1995; Ozeki and Shirai, 1998; Ozeki et al., 1999) which showed the different effective dosages of RA in causing ocular malformations, I have conducted a detailed dose-dependent response study. Strain differences in susceptibility to RA-induced ocular defects can then be obtained by comparing the frequency of

ocular defects in near-term fetuses of these 2 strains. Since ICR is an albino strain, it may impose difficulty in determining the eye size by gross morphological examination and thus lead to underestimation of the frequency of microphthalmia. Hence, to better distinguish the type and severity of ocular malformations obtained in different groups, detailed histological examination has been conducted.

As mentioned in section 3.1.1, differential strain susceptibility to RA-induced ocular defects can be due to differences in the developmental stage when exposed to RA. To investigate this possibility, the developmental stage of the embryo was assessed by counting the somite number, which is a general parameter for embryonic growth (van Maele-Fabry et al., 1992). In general, each somite takes about 2 hours to develop and this may help to estimate the extent of difference in the developmental stage (in terms of hours) between embryos of the two mouse strains. If differences in the developmental stage do exist among these 2 strains, it is essential to determine if such discrepancy also exists at the time of maternal RA injection. To do this, morphological staging of pre-somitic embryos were recorded according to the detailed descriptions in Downs and Davies (1993). Comparison of strain differences in susceptibility to RA was then conducted between embryos of the two mouse strains at equivalent developmental stages at the time of RA injection.

Genetic predisposition and maternal effects can also account for strain differences in susceptibility to RA. To this end, the frequencies of ocular malformations in fetuses of different genotypes and in different maternal environments were compared. Two groups of heterozygous fetuses with similar

genetic compositions but developed under different maternal environments were obtained by reciprocal matings between male and female mice of C57 and ICR strains. They were compared with homozygous C57 and ICR fetuses.

Experimental Design

To establish a minimal dose and a critical window for RA-induced ocular defects, dose and time responses studies were performed.

To compare the ocular malformations caused by RA treatment on ICR and C57 fetuses, detailed microscopic analyses on H&E stained sections were performed.

To study if there was any difference in the developmental stage between ICR and C57 strains, counting of somite number and staging of embryos at presomitic stages were conducted.

To study genetic predisposition and maternal effects, the frequency of ocular and non-ocular defects of fetuses from 4 types of crossing, C57♂ x ICR♀, ICR♂ x C57♀, ICR♂ x ICR♀ and C57♂ x C57♀, was counted.

3.3 MATERIALS AND METHODS

3.3.1 Strain, time and dose responses to RA

Preparation of RA was the same as described in section 2.1. To determine the stage specificity of the effect of RA and dose response on eye development, a single dose of RA at different concentrations (25, 12.5 and 6.25 mg/kg) was injected intraperitoneally into time-mated pregnant mice at E7, E7.25, E7.5. Mice without injection served as the control (CON). In our laboratory, no evidence of teratogenicity imposed by peanut oil was found as control embryos/fetuses receiving maternal intraperitoneal oil injection were morphologically normal. In fact, the final volume of alcohol in the oil suspension of 25, 12.5 and 6.25 mg/kg are 0.025, 0.0125 and 0.00625 ml/kg respectively. It is well-documented that the minimum teratogenic dose of alcohol via twice intraperitoneally injection is 3.75ml/kg (Cook and Sulik, 1988) and therefore the alcohol in oil suspension used in this study was 1000 times less than this teratogenic alcohol dosage. Pregnant mice were sacrificed at E18.5 by cervical dislocation. The numbers of implantation and resorption sites were recorded. Viable fetuses were harvested and examined under a stereomicroscope for gross morphological abnormalities.

Gross morphological examination was performed as an initial step to analyze the severity of RA teratogenicity in inducing ocular malformations. Detailed microscopic analyses to identify various types of ocular malformations were performed on haematoxylin and eosin stained sections as described in section 2.4.3. Fetal heads which fixed in Bouin fixative solution were first cut vertically to the coronal suture as well as transversely to the temporomandibular joint and then

subjected to serial dehydration in automatic processing machine. Serial sections cut in coronal plane were cut and laid on TESPA-coated slides.

To find out if there was any difference in the developmental stage between these 2 mouse strains, the somite number was counted. To further identify if there was any difference in their developmental stages at the time of maternal RA injection, morphological staging of embryos at pre-somitic stages was recorded according to the detailed descriptions in Downs and Davies (1993).

3.3.2 Genetic predisposition and maternal effects

To determine whether the mouse strain's genotype would predispose embryos to RA-induced ocular defects and to find out if maternal effects would further exacerbate the teratogenicity of RA, reciprocal crossing between male and female mice of C57 and ICR strains were conducted to produce fetuses with similar genetic compositions but under the effect of different maternal factors. Together with C57 and ICR homozygous fetuses, all 4 groups of fetuses were subject to maternal RA administration. Gross morphological and histological examinations on ocular malformations of these fetuses were performed and the frequency of ocular malformations was compared.

3.3.3 Statistical analysis

Intra- and inter-group comparisons on the resorption rate were conducted by one-way ANOVA followed by Bonferroni test and Independent sample *t* test respectively. Differences in the somite number of embryos of the 2 mouse strains

were tested by Independent sample *t* test. The distribution of embryos at different pre-somitic stages was analyzed by *chi*-square test. The frequency of defects observed by gross morphological and histological examinations was analyzed by *chi*-square test. The genotype dominance of strain and maternal effects were assessed by testing the frequency of ocular defects in each genotype of homozygous and heterozygous fetuses with logistic regression. All statistical analyses were carried out using SPSS software (*SPSS*), with statistical significance level set at $p < 0.05$.

3.4 RESULTS

At different gestational day (E7, E7.25 and E7.5), various dosages of RA (6.25, 12.5 and 25 mg/kg) were intraperitoneally injected into ICR and C57 pregnant mice. For simplicity of description, in the following, 6.25, 12.5 and 25 mg/kg of RA were referred as low, medium and high doses respectively. The overall resorption rate in ICR and C57 conceptuses were summarized in Tables 3-1 and 3-2 respectively. Other than causing lethality, RA treatment also resulted in different ocular and non-ocular abnormalities in both ICR and C57 fetuses. Results were summarized in Tables 3-3 and 3-4 respectively.

3.4.1 Maternal RA administration caused resorption

Maternal administration of RA led to an increase in resorption in ICR conceptuses. Results and statistical analyses were summarized in Tables 3-1 and 3-5 respectively and presented in Graph 3-1. In the ICR strain, it was found that RA treatment at E7 resulted in an increase in resorption rate in low dose (25%, $p = 0.07$), medium dose (77%, $p < 0.001$), high dose (98%, $p < 0.001$) when compared with the control (CON) group (3%). Medium dose of RA treatment at E7.25 resulted in significant increase in resorption rate when compared with RA treatment with the same dose at E7 ($p < 0.001$). At E7.5, medium and high doses of RA resulted in 100% resorption whereas low dose led to 84% resorption.

Table 3-1 Time and dose responses to RA-induced resorption in ICR fetuses.

ICR										
Time of injection	**CON**	**E7**			**E7.25**			**E7.5**		
Dosages of RA		**Low**	**Medium**	**High**	**Low**	**Medium**	**High**	**Low**	**Medium**	**High**
No of litters	5	10	11	9	8	8	6	8	7	7
No. of implantations	65	142	137	134	106	110	77	115	94	97
No. of live fetuses	63	106	31	2	69	11	0	19	0	0
No. of resorptions	2	36	106	132	37	99	77	95	94	97
Resorption rate (% ± SE)	3 ± 1.8	25 ± 7.4	77 ± 3.9	98 ± 2	35 ± 4	90 ± 0.7	100	84 ± 8.1	100	100

Table 3-2 **Time and dose responses to RA-induced resorption in C57 fetuses.**

C57										
Time of injection	**CON**	**E7**			**E7.25**			**E7.5**		
Dosages of RA		**Low**	**Medium**	**High**	**Low**	**Medium**	**High**	**Low**	**Medium**	**High**
No of litters	6	10	5	6	12	7	6	14	5	5
No. of implantations	40	67	40	44	85	51	42	104	32	33
No. of live fetuses	36	30	2	0	22	0	0	27	0	0
No. of resorptions	4	37	38	44	63	51	42	77	32	33
Resorption rate (% ± SE)	10 ± 4.8	55 ± 3.8	95 ± 4.4	100	74 ± 7.5	100	100	72 ± 7.3	100	100

Table 3-3 Time and dose responses to RA-induced ocular and non-ocular defects in ICR fetuses.

ICR										
Time of injection	**CON**	**E7**			**E7.25**			**E7.5**		
Dosages of RA		**Low**	**Medium**	**High**	**Low**	**Medium**	**High**	**Low**	**Medium**	**High**
No. of live fetuses examined	**63**	**106**	**31**	**2**	**69**	**11**	**0**	**19**	**0**	**0**
No. of fetuses with malformations ^	5 (8%)	73 (69%)	25 (81%)	2 (100%)	46 (67%)	9 (82%)	N/A	17 (89%)	N/A	N/A
No. of fetuses with ocular defects ^	5 (8%)	55 (52%)	19 (61%)	2 (100%)	43 (62%)	9 (82%)		17 (89%)		
Total no. of malformed eyes @	5 (4%)	90 (42%)	37 (60%)	4 (100%)	53 (38%)	14 (64%)		23 (61%)		
Ocular defects										
No. of anophthalmia @	0 (0%)	39 (18%)	19 (31%)	4 (100%)	26 (19%)	12 (55%)	N/A	5 (13%)	N/A	N/A
No. of microphthalmia@	2 (2%)	28 (13%)	7 (11%)	0 (0%)	24 (17%)	2 (9%)		1 (3%)		
Total no. of anophthalmia and microphthalmia @	2 (2%)	67 (32%)	26 (42%)	4 (100%)	50 (36%)	14 (64%)		6 (16%)		
No. of exophthalmia @	0 (0%)	4 (2%)	0 (0%)	0 (0%)	3 (2%)	1 (5%)		5 (13%)		
No. of eyes without eyelid @	0 (0%)	16 (8%)	10 (16%)	1 (25%)	20 (14%)	0 (0%)		13 (34%)		
No. of eyes with no or small lens @	2 (2%)	29 (14%)	7 (11%)	0 (0%)	24 (17%)	1 (5%)		1 (3%)		
No. of eyes with other minor ocular defects @	5 (4%)	48 (23%)	18 (29%)	0 (0%)	27 (20%)	2 (9%)		9 (24%)		
Non-ocular defects										
No. of fetuses with exencephaly ^	0 (0%)	19 (18%)	10 (32%)	1 (50%)	23 (33%)	1 (11%)	N/A	12 (63%)	N/A	N/A
No. of fetuses with cleft palate ^	0 (0%)	18 (17%)	9 (29%)	1 (50%)	6 (9%)	4 (44%)		2 (11%)		

^ Percentage represented captioned defect over the total number of fetuses examined.

@ Percentage represented captioned defect over the total number of fetal eyes examined.

N/A Not applicable

Table 3-4 **Time and dose responses to RA-induced ocular and non-ocular defects in C57 fetuses.**

C57										
Time of injection	**CON**	**E7**			**E7.25**			**E7.5**		
Dosages of RA		**Low**	**Medium**	**High**	**Low**	**Medium**	**High**	**Low**	**Medium**	**High**
No. of live fetuses examined	**36**	**30**	**2**	**0**	**22**	**0**	**0**	**27**	**0**	**0**
No. of fetuses with malformations ^	8 (22%)	25 (83%)	2 (100%)	N/A	22 (100%)	N/A	N/A	27 (100%)	NA	NA
No. of fetuses with ocular defects ^	8 (22%)	24 (80%)	2 (100%)		22 (100%)			27 (100%)		
Total no. of malformed eyes @	9 (13%)	45 (75%)	4 (100%)		43 (98%)			54 (100%)		
Ocular defects										
No. of anophthalmia @	1 (1%)	16 (27%)	0 (0%)	N/A	35 (80%)	N/A	N/A	53 (98%)	N/A	N/A
No. of microphthalmia@	7 (10%)	21 (35%)	3 (75%)		8 (18%)			1 (2%)		
Total no. of anophthalmia and microphthalmia @	8 (11%)	37 (62%)	3 (75%)		43 (98%)			54 (100%)		
No. of exophthalmia @	0 (0%)	0 (0%)	0 (0%)		1 (2%)			0 (0%)		
No. of eyes without eyelid @	0 (0%)	0 (0%)	0 (0%)		1 (2%)			0 (0%)		
No. of eyes with no or small lens @	7 (10%)	21 (35%)	2 (50%)		8 (18%)			1 (2%)		
No. of eyes with other minor ocular defects @	1 (1%)	15 (25%)	2 (50%)		3 (7%)			1 (2%)		
Non-ocular defects										
No. of fetuses with exencephaly ^	0 (0%)	0 (0%)	0 (0%)	N/A	0 (0%)	N/A	N/A	8 (30%)	NA	NA
No. of fetuses with cleft palate ^	0 (0%)	6 (20%)	2 (100%)		5 (23%)			6 (22%)		

^ Percentage represented captioned defect over the total number of fetuses examined.

@ Percentage represented captioned defect over the total number of fetal eyes examined.

N/A Not applicable

Table 3-5 Statistical analysis on time and dose responses to RA-induced resorption in ICR fetuses.

ICR					
Time response					
***p*-value**	**CON vs E7**	**CON vs E7.25**	**CON vs E7.5**	**E7 vs E7.25**	**E7.25 vs E7.5**
Low dose	0.070	0.035*	< 0.001*	1	< 0.001*
Medium dose	< 0.001*	< 0.001*	< 0.001*	0.077	0.370
High dose	< 0.001*	< 0.001*	< 0.001*	1	1
Dose response					
***p*-value**	**CON vs Low dose**	**CON vs Medium dose**	**CON vs High dose**	**Low dose vs Medium dose**	**Medium dose vs High dose**
E7	0.070	< 0.001*	< 0.001*	< 0.001*	0.027*
E7.25	< 0.001*	< 0.001*	< 0.001*	< 0.001*	0.306
E7.5	< 0.001*	< 0.001*	< 0.001*	0.155	1

* statistical significant

Low dose of RA administration at E7.25 only slightly increased the resorption rate to 35% in comparison to 25% at E7. However, when low dose of RA was applied 6 hours later, i.e. E7.5, the resorption rate was significantly increased to 84% when compared with same dose at E7.25 ($p > 0.001$). Medium dose of RA administration at E7 resulted in 77% resorption rate, whereas at E7.25, a slight increase in resorption rate was found (90%). High dose of RA administration at all gestational days led to 100% resorption.

In C57 conceptuses, maternal RA administration also resulted in statistically significant increase in resorption rate. Results and statistical analyses

were summarized in Tables 3-2 and 3-6 respectively and presented in Graph 3-2. When compared with the CON group (10%), significant increase in resorption rate was found in conceptuses treated with low dose (55%, $p = 0.002$), medium dose (95%, $p < 0.001$) and high dose (100%, $p < 0.001$) of RA at E7. When low dose of RA was applied 6 and 12 hours later, i.e. E7.25 and E7.5 respectively, 74% and 72% of conceptuses respectively were resorbed, although the increase was not statistically significant. Moreover, administration of medium and high doses of RA resulted at nearly all fetal resorption in all gestational days examined.

Table 3-6 Statistical analysis on time and dose responses to RA-induced resorption in C57 fetuses.

C57					
Time response					
***p*-value**	**CON vs E7**	**CON vs E7.25**	**CON vs E7.5**	**E7 vs E7.25**	**E7.25 vs E7.5**
Low dose	0.002*	< 0.001*	< 0.001*	0.364	1
Medium dose	< 0.001*	< 0.001*	< 0.001*	1	1
High dose	< 0.001*	< 0.001*	< 0.001*	1	1
Dose response					
***p*-value**	**CON vs Low dose**	**CON vs Medium dose**	**CON vs High dose**	**Low dose vs Medium dose**	**Medium dose vs High dose**
E7	< 0.001*	< 0.001*	< 0.001*	< 0.001*	1
E7.25	< 0.001*	< 0.001*	< 0.001*	0.029*	1
E7.5	< 0.001*	< 0.001*	< 0.001*	0.080	1

* statistical significant

The dose and time responses to RA-induced resorption were compared between ICR and C57 conceptuses to determine if there were any strain differences.

Results of statistical analyses were summarized in Tables 3-7 and presented in Graphs 3-3 and 3-4 respectively. It was found that C57 conceptuses were significantly more prone to be resorbed when administered with low ($p < 0.001$) and medium ($p = 0.016$) doses of RA at E7 in comparison to ICR conceptuses. Moreover, C57 conceptuses receiving low and medium doses of RA treatment at E7.25 were significantly more prone to be resorbed ($p < 0.001$ and $p = 0.040$ respectively) in comparing with ICR conceptuses. At E7.5, over 70% of both ICR and C57 conceptuses were resorbed when treated with low dose of RA. At high dose of RA treatment, almost all ICR and C57 conceptuses were resorbed.

Table 3-7 Statistical analysis of strain difference in time and dose response to RA-induced resorption.

ICR vs C57			
***p*-value**	**Low dose**	**Medium dose**	**High dose**
E7	< 0.001*	0.016*	0.435
E7.25	< 0.001*	0.040*	N/A
E7.5	0.311	N/A	N/A

* statistical significant

N/A not applicable when comparison was made on zero-valued data

Resulted showed that C57 strain was significantly more prone to be resorbed when subject to low dose of RA at E7 ($p = 0.001$) as well as E7.25 ($p < 0.001$) (Graph 3-4). Moreover, resulted showed that RA administration at E7.5 (even with low dose) caused very high resorption rate in both strains. Medium dose of RA applied at E7 and E7.25 in C57 conceptuses resulted in significantly higher resorption rates ($p < 0.016$ and $p < 0.040$ respectively) than that in ICR conceptuses showing that C57 conceptuses were more prone to RA teratogenicity. High dose of

RA resulted in almost total resorption in all gestational day examined.

3.4.2 Maternal RA administration resulted in ocular defects.

Various types of abnormalities were resulted after RA treatment. Since medium and high doses of RA treatment resulted in high fetolethality, therefore, to simplify the comparison in the following sections, only low dose of RA treatment were chosen for comparison.

3.4.2.1 Total number of malformed eyes

One of the important issues in this chapter was to find out if there were any strain-, time- and dose-responses in RA-induced ocular malformation. Ocular malformations determined by gross morphological examination of fetal eyes can be categorized into various types such as anophthalmia (no eye, Figure 3-1 D), microphthalmia (Figure 3-1 C), eye without eyelid (Figure 3-1B) as well as exophthalmia (Figure 3-1 E). Since ICR is an albino strain, it may impose difficulty in determining the eye size by gross morphological examination and thus lead to underestimation of the frequency of ocular defects. Histological examination was therefore performed to overcome this difficulty. Moreover, histological examinations could further identify other ocular defects caused by RA treatment such as microphakia (small lens, Figure 3-2 B), aphakia (no lens, Figure 3-2 C), faulty separation between cornea and lens (Figure 3-2 F) and rupture in posterior lens capsule (Figure 3-2 G). To have an overview on the wide spectrum of RA-induced ocular defects, comparison was first conducted on "total malformed eyes". The frequency and statistical analyses are as follow.

In ICR fetuses, 4% of fetal eyes spontaneously developed malformations in the CON group (Tables 3-3 and 3-8 and Graph 3-5). Low dose of RA administration at E7 significantly increased the frequency of malformed eyes (42%, $p < 0.001$) when compared with the CON group. There was further increase in the frequency of eyes with malformations when RA was administered at E7.5 (61%).

Table 3-8 Statistical analysis on the frequency of total number of malformed eyes in ICR and C57 fetuses treated with low dose of RA at different gestational days.

Total no of malformed eyes induced by low dose of RA					
Intra-comparison in ICR					
Time of injection	CON vs E7	CON vs E7.25	CON vs E7.5	E7 vs E7.25	E7.25 vs E7.5
***p*-value**	< 0.001*	< 0.001*	< 0.001*	0.452	0.015*
Intra-comparison in C57					
Time of injection	CON vs E7	CON vs E7.25	CON vs E7.5	E7 vs E7.25	E7.25 vs E7.5
***p*-value**	< 0.001*	< 0.001*	< 0.001*	0.002*	0.265
Inter-comparisons between ICR and C57					
Time of injection	CON	E7	E7.25	E7.5	
***p*-value**	0.024*	< 0.001*	< 0.001*	< 0.001*	

* statistically significant

In C57 fetuses, 13% of fetal eyes had spontaneous malformations (Figures 3-4 and 3-8 and Graph 3-5). Low dose of RA administration at E7 significantly increased the frequency of malformed eyes (75%, $p < 0.001$) when compared with the CON group. When RA was administered at E7.25 and E7.5, there was further significant increase in the frequency of eyes with malformations to 98% and 100%

respectively.

In comparing the frequency of total number of malformed eyes between the two strains, C57 fetuses exhibited significantly higher frequency than ICR fetuses after exposure to low dose of RA at all gestational days examined (Table 3-8).

3.4.2.2 Anophthalmia and microphthalmia

3.4.2.2.1 Anophthalmia

This is the most severe type of ocular defects in mouse as well as in human. A histological section of a normal eye is shown in Figure 3-2 A for reference. In anophthalmia, there is no eye rudiment inside the eye socket (Figure 3-2 D).

In examining the eyes of ICR fetuses, it was found that administration of low dose of RA at E7 resulted in 18% anophthalmia which was significantly ($p < 0.001$) different from the CON group (Tables 3-3 and 3-9 and Graph 3-6). However, RA treatment at E7.25 and E7.5 resulted in similar frequency of anophthalmia.

Table 3-9 Statistical analysis on the frequency of anophthalmia in ICR and C57 fetuses treated with low dose of RA at different gestational days.

Anophthalmia induced by low dose of RA					
Intra-comparison in ICR					
Time of injection	CON vs E7	CON vs E7.25	CON vs E7.5	E7 vs E7.25	E7.25 vs E7.5
***p*-value**	< 0.001*	< 0.001*	< 0.001*	0.917	0.415
Intra-comparison in C57					
Time of injection	CON vs E7	CON vs E7.25	CON vs E7.5	E7 vs E7.25	E7.25 vs E7.5
***p*-value**	< 0.001*	< 0.001*	< 0.001*	< 0.001*	0.002*
Inter-comparisons between ICR and C57					
Time of injection	CON	E7	E7.25	E7.5	
***p*-value**	0.185	0.159	< 0.001*	< 0.001*	

* statistically significant

In the CON group of C57 fetuses, it was found that 1% of the examined fetal eyes spontaneously developed anophthalmia (Table 3-4 and Graph 3-6). Low dose of RA treatment resulted in significant increase in the frequency of anophthalmia at all gestational days examined (Table 3-9). RA applied at E7 resulted in 27% ($p < 0.001$) of anophthalmia when compared with the CON group. Further significant increase was resulted when RA was administered at later stages i.e. at E7.25 (80%, $p < 0.001$) and E7.5 (98%, $p = 0.002$).

Regarding differential strain susceptibility to RA, result showed that there was a strain-specific response to RA-induced anophthalmia (Table 3-9). At E7.25, the frequency in C57 was 80% which was about 4 fold increase in comparison to

ICR. Moreover, the frequency of anophthalmia in C57 resulted from RA administration at E7.5 was over 7 fold than that in ICR.

3.4.2.2.2 Microphthalmia

Other than anophthalmia, microphthalmia is another kind of severe type of ocular defect (Figures 3-2 B and C). The size of the whole eye decreases and is usually associated with no or small lens. In ICR fetuses, low dose of RA treatment at E7 resulted in significant increase in the frequency of microphthalmia when compared with the CON group (Tables 3-3 and 3-10 and Graph 3-7, $p < 0.001$). However, low dose of RA applied at E.7.5 resulted in 3% of microphthalmia and this was probably because the majority of ocular defects identified in this group were eyes without eyelid or with other minor ocular defect.

Table 3-10 Statistical analysis on the frequency of microphthalmia in ICR and C57 fetuses treated with low dose of RA at different gestational days.

Microphthalmia induced by low dose of RA					
Intra-comparison in ICR					
Time of injection	CON vs E7	CON vs E7.25	CON vs E7.5	E7 vs E7.25	E7.25 vs E7.5
***p*-value**	< 0.001*	< 0.001*	0.674	0.282	0.021*
Intra-comparison in C57					
Time of injection	CON vs E7	CON vs E7.25	CON vs E7.5	E7 vs E7.25	E7.25 vs E7.5
***p*-value**	< 0.001*	0.188	0.073	0.059	0.005*
Inter-comparisons between ICR and C57					
Time of injection	CON	E7	E7.25	E7.5	
***p*-value**	0.008*	< 0.001*	0.410	0.801	

* statistically significant

In the CON group of C57 fetuses, it was found that 10% of the examined fetal eyes spontaneously developed microphthalmia (Table 3-4). Low dose of RA treatment at E7 resulted in significant increase in the frequency of microphthalmia when compared with the CON group (35%, $p < 0.001$). However, administration of RA at later gestational days i.e. at E7.25 and E7.5 resulted in decrease in frequency of microphthalmia. This was due to the fact that instead of developing microphthalmia, the fetuses developed anophthalmia, such that at E7.5, the frequency of anophthalmia was as high as 98%.

When comparing the strain difference in susceptibility to RA, it was found that significant difference can be found at E7 only (Table 3-10, $p < 0.001$). This is apparently opposite to what we can observe in analyzing the strain difference in

susceptibility of anophthalmia (Table 3-9). Microphthalmia seemed to be the major ocular defect resulted from exposure to RA at earlier gestational day while anophthalmia was the major ocular defect when exposed at later gestational days.

3.4.2.2.3 Anophthalmia and microphthalmia

As either anophthalmia or microphthalmia resulted in blindness, therefore I have counted the total frequency of anophthalmia together with microphthalmia to show the severity of vision loss resulted in fetuses.

In ICR fetuses, low dose of RA treatment at E7 resulted in significant increase in total frequency of anophthalmia and microphthalmia (32%, $p < 0.001$) when compared with the CON group (Tables 3-3 and 3-11 and Graph 3-8). However, there was no further increase in such frequency when RA was applied at later gestational days.

Table 3-11 Statistical analysis on the total frequency of anophthalmia and microphthalmia in ICR and C57 fetuses treated with low dose of RA at different gestational days.

Anophthalmia and microphthalmia induced by low dose of RA					
Intra-comparison in ICR					
Time of injection	CON vs E7	CON vs E7.25	CON vs E7.5	E7 vs E7.25	E7.25 vs E7.5
***p*-value**	< 0.001*	< 0.001*	< 0.001*	0.370	0.017*
Intra-comparison in C57					
Time of injection	CON vs E7	CON vs E7.25	CON vs E7.5	E7 vs E7.25	E7.25 vs E7.5
***p*-value**	< 0.001*	< 0.001*	< 0.001*	< 0.001*	0.265
Inter-comparisons between ICR and C57					
Time of injection	CON	E7	E7.25	E7.5	
***p*-value**	0.003*	< 0.001*	< 0.001*	< 0.001*	

* statistically significant

C57 fetuses spontaneously developed anophthalmia as well as microphthalmia (11%) and the result was tabulated in Tables 3-4 and 3-11. In comparison with the CON group, there was significant increase in the total frequency of anophthalmia and microphthalmia when low dose of RA was applied at E7 (62%, $p < 0.001$). Moreover, administration of RA at later gestational days further significantly increased the total frequency such that treatment of RA at E7.5 resulted in 100% of fetal eyes having classified as anophthalmia (98%) or microphthalmia (2%).

In comparing the total frequency of anophthalmia and microphthalmia between the two strains, C57 fetuses exhibited significantly higher frequency than ICR fetuses after exposure to low dose of RA at all gestational days examined (Table

3-11). The total frequencies were 2-fold, 3-fold and 6-fold higher in C57 fetuses than in ICR fetuses when RA was administered at E7, E7.25 and E7.5 respectively. These results suggested that C57 fetuses were more prone to develop severe type of eye defects when exposed to low dose of RA during early gestational days.

3.4.2.3 Exophthalmia

Excess vitamin A and RA can induce congenital exophthalmia (Geelen, 1979) and it is classified as bulging of the eyeball anteriorly out of the orbit (Figure 3-1 E).

In ICR fetuses, no exophthalmia were found in the CON group (Table 3-3). When low dose of RA was administered at later gestational day, i.e. at E7.5, ICR fetuses resulted in significantly higher frequency of exophthalmia when compared with that at E7.25 (Table 3-12).

Table 3-12 Statistical analysis on the frequency of exophthalmia in ICR and C57 fetuses treated with low dose of RA at different gestational days.

Exophthalmia induced by low dose of RA					
Intra-comparison in ICR					
Time of injection	CON vs E7	CON vs E7.25	CON vs E7.5	E7 vs E7.25	E7.25 vs E7.5
***p*-value**	0.121	0.096	< 0.001*	0.851	0.004*
Intra-comparison in C57					
Time of injection	CON vs E7	CON vs E7.25	CON vs E7.5	E7 vs E7.25	E7.25 vs E7.5
***p*-value**	N/A	0.199	N/A	0.241	0.265
Inter-comparisons between ICR and C57					
Time of injection	CON	E7	E7.25	E7.5	
***p*-value**	N/A	0.284	0.969	0.006*	

* statistically significant

N/A not applicable when comparison was made on zero-valued data valued data

In C57 fetuses, exophthalmia seemed to be a rare phenotype caused by RA treatment at all gestational days examined. Only 1% of the fetal eye developed exophthalmia after exposure to low dose of RA at E7.25 (Tables 3-4 and 3-12).

In comparing the frequency of exophthalmia between the two strains, ICR fetuses exhibited significantly higher frequency than C57 fetuses after exposure to low dose of RA at E7.5 (Table 3-12).

3.4.2.4 Eyes without eyelids

The eyelids of fetuses were closed at birth (Figure 3-1 A). Eyes without

eyelids are usually associated with exencephaly (Ross et al., 2005).

In ICR fetuses, low dose of RA administration significantly resulted in eyes with no eyelid (Tables 3-3 and 3-13, Graph 3-10). When RA was applied at later gestational days, there was an increase in the frequency of eyes with no eyelid from 8% at E7 to 34% at E7.5.

Table 3-13 Statistical analysis on the frequency of eyes without eyelid in ICR and C57 fetuses treated with low dose of RA at different gestational days.

Eyes without eyelid induced by low dose of RA					
Intra-comparison in ICR					
Time of injection	CON vs E7	CON vs E7.25	CON vs E7.5	E7 vs E7.25	E7.25 vs E7.5
***p*-value**	0.002*	< 0.001*	< 0.001*	0.370	0.006*
Intra-comparison in C57					
Time of injection	CON vs E7	CON vs E7.25	CON vs E7.5	E7 vs E7.25	E7.25 vs E7.5
***p*-value**	N/A	0.199	N/A	0.245	0.265
Inter-comparisons between ICR and C57					
Time of injection	CON	E7	E7.25	E7.5	
***p*-value**	N/A	0.028*	0.027*	< 0.001*	

* statistically significant

N/A not applicable when comparison was made on zero-valued data valued data

RA administration did not affect the development of eyelid in C57 fetuses as only 1% of fetal eyes without eyelid were found after RA treatment at E7.25 (Graph 3-10). Hence, ICR fetuses exhibited greater sensitivity to RA-induced eyes without eyelid than C57 fetuses at all 3 gestational days of RA administration.

3.4.2.5 Eyes with no or small lens

Other than abovementioned ocular defects, microphthalmia were often associated with macroscopic defects of the lens, namely, aphakia (no lens, Figure 3-2 C) and microphakia (small lens, Figure 3-2 B).

To summarize the overall frequency of fetuses with lens defect, I have grouped together the frequency of eyes with no lens and small lens for comparison. In ICR fetuses, low dose of RA treatment at E7 resulted in a frequency of 14% of fetal eyes with lens defects, which was significantly higher than the CON group ($p <$ 0.001) (Tables 3-3 and 3-14 and Graph 3-11). Similar frequency was obtained when low dose of RA was applied at E7.25.

Table 3-14 Statistical analysis on the frequency of eyes with no or small lens in ICR and C57 fetuses treated with low dose of RA at different gestational days.

Eyes with no or small lens induced by low dose of RA					
Intra-comparison in ICR					
Time of injection	CON vs E7	CON vs E7.25	CON vs E7.5	E7 vs E7.25	E7.25 vs E7.5
***p*-value**	< 0.001*	< 0.001*	0.674	0.344	0.021*
Intra-comparison in C57					
Time of injection	CON vs E7	CON vs E7.25	CON vs E7.5	E7 vs E7.25	E7.25 vs E7.5
***p*-value**	< 0.001*	0.188	0.073	0.059	0.005*
Inter-comparisons between ICR and C57					
Time of injection	CON	E7	E7.25	E7.5	
***p*-value**	0.008*	< 0.001*	0.905	0.801	

* statistically significant

In C57 fetuses, 10% of fetal eyes developed lens defects in the CON group (Tables 3-4 and 3-14). Low dose of RA at E7 significantly induced eyes with no or small lens in 35% of fetal eyes when compared with the control group ($p < 0.001$) (Tables 3-4 and 3-14 and Graph 3-11). RA treatment applied at E7.25 could not further enhance the frequency of fetal eyes with lens defect. As 98% of the fetal eyes became anophthalmic in C57 strain after RA treatment at E7.5, only 2% of fetal eyes developed lens defects was recorded.

Comparison of the increase in frequency of fetal eyes with lens defects in the ICR and C57 fetuses administered with RA at E7 showed that C57 fetuses were significantly more prone to develop lens defects (Table 3-14).

3.4.2.6 Eyes with other minor ocular defects

Some minor ocular defects could be found in histologically examination of the fetal eyes. For example, corneal stalk attached to the lens (Figure 3-2 E), rupture of lens capsule (Figure 3-2 G), and undifferentiated mesenchyme present in the vitreous cavity (Figure 3-2 H). These defects could be associated with microphthalmia or present alone.

In ICR fetuses, low dose of RA treatment at E7 significantly induced minor ocular defects in 23% of fetal eyes when compared with the CON group ($p < 0.001$) (Tables 3-3 and 3-15 and Graph 3-12). RA treatment applied at later gestational day could not further enhance the frequency of minor ocular defects.

Table 3-15 Statistical analysis on the frequency of eyes with other minor defects in ICR and C57 fetuses treated with low dose of RA at different gestational days.

Eyes with other minor defects induced by low dose of RA					
Intra-comparison in ICR					
Time of injection	CON vs E7	CON vs E7.25	CON vs E7.5	E7 vs E7.25	E7.25 vs E7.5
***p*-value**	< 0.001*	< 0.001*	< 0.001*	0.493	0.577
Intra-comparison in C57					
Time of injection	CON vs E7	CON vs E7.25	CON vs E7.5	E7 vs E7.25	E7.25 vs E7.5
***p*-value**	< 0.001*	0.012*	0.837	0.015*	0.217
Inter-comparisons between ICR and C57					
Time of injection	CON	E7	E7.25	E7.5	
***p*-value**	0.308	0.702	0.047*	0.035*	

* statistically significant

In C57 fetuses, result showed that low dose of RA treatment at E7 significantly increased the frequency of minor ocular defects when compared with the CON group (25%, $p < 0.001$) (Table 3-15 and Graph 3-12). Since after RA treatment at E7.25 and E7.5 over 80% and 98% respectively of C57 fetal eyes were in fact anophthalmia, therefore, the frequency of minor ocular defects observed in these groups were both significantly lower than that in RA treatment at E7. Because of this fact, it is not surprising that comparison of the frequency of minor ocular defects in ICR and C57 fetuses receiving RA treatment at E7.25 and E7.5 resulted in significant difference as most of the C57 fetal eyes developed into anophthalmia (Table 3-15).

3.4.3 Maternal RA administration resulted in non-ocular defects

3.4.3.1 Exencephaly

ICR fetuses did not spontaneously developed exencephaly without RA treatment. However, there was significant increase in the frequency of exencephaly after low dose of RA treatment at E7 (18%, $p < 0.001$) as illustrated in Tables 3-3 and 3-16, Graph 3-13 and Figure 3-1 B. When low dose of RA was applied at E7.25, the frequency was significantly higher than that resulted from injection at E7 (33%, $p = 0.019$). Application of RA at later stage (E7.5) led to further significant increase in the frequency of exencephaly (63%, $p = 0.02$).

Table 3-16 Statistical analysis on the frequency of exencephaly in ICR and C57 fetuses treated with low dose of RA at different gestational days.

Exencephaly induced by low dose of RA					
Intra-comparison in ICR					
Time of injection	CON vs E7	CON vs E7.25	CON vs E7.5	E7 vs E7.25	E7.25 vs E7.5
***p*-value**	< 0.001*	< 0.001*	< 0.001*	0.019*	0.020*
Intra-comparison in C57					
Time of injection	CON vs E7	CON vs E7.25	CON vs E7.5	E7 vs E7.25	E7.25 vs E7.5
***p*-value**	N/A	N/A	< 0.001*	N/A	0.020*
Inter-comparisons between ICR and C57					
Time of injection	CON	E7	E7.25	E7.5	
***p*-value**	N/A	0.012*	0.002*	0.010*	

* statistically significant

N/A not applicable when comparison was made on zero-valued data valued data

In C57 fetuses, after low dose and medium doses of RA insult, no exencephaly could be observed (Table 3-4). However, when low dose of RA was injected at E7.5, 30% of fetuses developed exencephaly which was significantly higher than that at E7.25 ($p = 0.02$).

Concerning strain difference in the frequency of exencephaly, it was found that ICR was significantly more prone to develop this defect than C57 when low dose of RA administered at E7, E7.25 and E7.5 (Table 3-16).

3.4.3.2 Cleft palate

Other than exencephaly, there are other types of congenital malformations commonly found in RA teratogenicity study. Cleft palate is one of them and the frequency of this defect was summarized in Tables 3-3 and 3-17 and Graph 3-14. In ICR, while no fetus developed cleft palate in the control group, application of low dose of RA at E7 resulted in a frequency of 17% of cleft palate ($p < 0.001$). Application of RA at later gestational days, E7.25 and E7.5 could not further increase the malformation frequency.

Table 3-17 Statistical analysis on the frequency of cleft palate in ICR and C57 fetuses treated with low dose of RA at different gestational days.

Cleft palate induced by low dose of RA					
Intra-comparison in ICR					
Time of injection	CON vs E7	CON vs E7.25	CON vs E7.5	E7 vs E7.25	E7.25 vs E7.5
***p*-value**	< 0.001*	0.017*	0.009*	0.119	0.806
Intra-comparison in C57					
Time of injection	CON vs E7	CON vs E7.25	CON vs E7.5	E7 vs E7.25	E7.25 vs E7.5
***p*-value**	0.005*	0.003*	0.003*	0.812	0.966
Inter-comparisons between ICR and C57					
Time of injection	CON	E7	E7.25	E7.5	
***p*-value**	N/A	0.702	0.079	0.327	

* statistically significant

N/A not applicable when comparison was made on zero-valued data valued data

In C57, cleft palate was also not observed in the fetus of the CON group. After low dose of RA injection at E7, 20% of fetuses exhibited cleft palate (Tables 3-4 and 3-17). However, there was no further increase in the frequency of cleft palate when RA was administered at later gestational days, i.e. E7.25 and E7.5.

In comparing ICR and C57 fetuses, there was no strain difference in RA-induced cleft palate (Table 3-17).

3.4.4 Comparison of developmental stages of ICR and C57 embryos during early period of organogenesis

As mentioned in section 3.2, differential strain susceptibility to RA-induced ocular defects could be due to difference in developmental stages of the embryos when they were exposed to RA. To determine if this factor did exist the somite number (illustrated in Figure 3-3) of embryos of the two strains at different gestational days was counted and the result was summarized in Tables 3-18 and 3-19 and Graphs 3-15 and 3-16.

Result showed that in both strains, there was linear increase in somite number from E8 to E9.5. However, when embryos of the two strains were compared at the same gestational day (Table 3-18 and Graph 3-15), the somite number of ICR embryos was statistically significantly greater than that of C57 embryos. This indicates that ICR embryos are developmentally more advance than C57 embryos.

Furthermore, when the somite number of embryos of the two strains at different gestational days was compared, it was found that there was no significant difference between ICR embryos at the gestational day that was 6 hours behind that of C57 embryos (Table 3-19 and Graph 3-16). Hence showing that ICR embryos are developmentally 6 hours ahead of C57 embryos during early period of organogenesis (around E8-E9.5)

Table 3-18 Comparison of somite number of ICR and C57 embryos at the same gestational day.

Mouse strain (CON)	ICR	C57	ICR	C57	ICR	C57	ICR	C57	ICR	C57
Gestational day	E8		E8.25		E8.5		E9		E9.5	
No. of litters	7	4	8	5	6	10	6	9	5	9
No. of implantations	92	25	109	33	84	59	83	60	69	55
No. of resorptions	2	2	4	3	2	5	2	6	3	6
% of resorption	2.0	7.8	3.5	8.2	2.3	8.7	2.3	9.9	4.0	10.3
No. of viable embryos	90	23	105	30	82	54	81	54	66	49
Somite no. (± SE)	4.73 ± 0.21	2.52 ± 0.19	8.94 ± 0.12	4.47 ± 0.21	12.63 ± 0.91	8.81 ± 0.36	19.51 ± 0.21	16.2 ± 0.38	23.89 ± 0.18	21.88 ± 0.39
p-value	0.03*		< 0.001*		< 0.001*		< 0.001*		< 0001*	

* Statistically significant when C57 was compared with ICR at the same gestational day

Table 3-19 Comparison of somite number of ICR and C57 embryos with 6 hour difference in gestational age.

Mouse strain (CON)	ICR	C57	ICR	C57	ICR	C57	ICR	C57	ICR	C57
Gestational day	E8 – 6hr (E7.75)	E8	E8.25 – 6hr (E8)	E8.25	E8.5 – 6hr (E8.25)	E8.5	E9 – 6hr (E8.75)	E9	E9.5 – 6hr (E9.25)	E9.5
No. of litters	7	4	7	5	8	10	6	9	6	9
No. of implantations	97	25	92	33	109	59	76	60	77	55
No. of resorptions	2	2	2	3	4	5	0	6	1	6
% of resorption	2.0	7.8	2.0	8.2	3.5	8.7	0.0	9.9	1.5	10.3
No. of viable embryos	95	23	90	30	105	54	76	54	76	49
Somite no. (± SE)	2.42 ± 0.17	2.52 ± 0.1	4.73 ± 0.21	4.47 ± 0.21	8.94 ± 0.12	8.81 ± 0.36	16.70 ± 0.21	16.2 ± 0.38	21.91 ± 0.19	21.88 ± 0.39
p-value	0.778		0.549		0.674		0.223		0.945	

3.4.5 Comparison of developmental stages of ICR and C57 embryos at the time of receiving maternal RA treatment

As mentioned in section 3.4.4, ICR embryos develop 6 hours ahead of C57 embryos during the early period of organogenesis, it is very likely that this difference in developmental stage may also exist during the time of RA treatment. To this end, C57 embryos at E7.25 and ICR embryos at E7.0 were harvested and detailed morphological staging of embryos was conducted according to Downs et al. (1993). Results were summarized in Table 3-20 and Graph 3-17. Morphology of embryos at different pre-somatic stages was shown in Figure 3-4.

Four developmental stages were identified in ICR embryos at E7, namely, pre-streak, early streak, mid-streak and late streak. About 90% of the embryos were found at early and mid-streak stages. In fact, similar pattern of distribution of developmental stages was also found in C57 embryos at E7.25. Statistical analyses by using chi-square test showed that there was no significant difference in developmental stages of C57 embryos at E7.25 and ICR embryos at E7, suggesting that ICR embryos was developmentally 6 hours ahead of C57 embryos when they were maternally administered with RA at the same gestational day.

Table 3-20 Statistical analysis on the distribution of pre-somitic embryos.

Mouse strain (CON)	C57	ICR	*p*-value
No. of litters	15	12	
No. of embryos examined	96	159	
Pre-somitic stages:			
Pre-streak (%)	3 (3%)	9 (6%)	1.000
Early streak (%)	42 (44%)	81 (51%)	0.520
Mid streak (%)	45 (47%)	61 (38%)	0.512
Late streak (%)	6 (6%)	8 (5%)	0.630

3.4.6 Comparison at equivalent developmental stages

After identifying the equivalent developmental stage of ICR and C57 embryos during early period of organogenesis and at the time of RA administration, strain susceptibility to RA teratogenicity should be determined by comparing C57 embryos exposed to RA injection at E7.25 and ICR embryos at E7.

The result of statistical analysis on the total frequency of anophthalmia and microphthalmia was shown in Table 3-21. Result showed that the total frequency of anophthalmia and microphthalmia in C57 fetal eyes following RA treatment was 3 fold higher than that of ICR fetuses. This indicated that factors other than difference in developmental stage must exist to account for the significant strain difference in susceptibility to develop the most severe type of ocular defects after RA treatment. For all subsequent studies, comparison was made between ICR embryos exposed to maternal administration of RA at E7 with C57 embryos at E7.25.

Table 3-21 Statistical analysis on the frequency of ocular and non-ocular defects in ICR and C57 fetuses treated with low dose of RA at equivalent developmental stage.

MOUSE STRAIN (CON)	ICR	C57	*p*-value
Dosage of RA	Low dose		
Time of RA injection	E7	E7.25	
Frequency of anophthalmia @	18%	80%	< 0.001*
Frequency of microphthalmia @	13%	18%	0.388
Total frequency of anophthalmia and microphthalmia @	32%	98%	< 0.001*
Frequency of exophthalmia @	2%	2%	0.866
Frequency of eyes without eyelid @	8%	2%	0.201
Frequency of eyes with no or small lens @	14%	18%	0.440
Frequency of eyes with other minor ocular defects @	23%	7%	0.017*
Frequency of exencephaly ^	18%	0%	0.031*
Frequency of cleft palate ^	17%	23%	0.523

@ Percentage represented captioned defect over the total number of fetal eyes examined

^ Percentage represented captioned defect over the total number of fetuses examined.

* Statistically significant with C57 compared with ICR

3.4.7 Genotypic dominance and maternal effects

To study if any genotypic dominance and/or maternal effects of C57 strain might contribute to the increased susceptibility to RA induced ocular defects, fetuses with different genetic compositions and under different maternal effects were produced from mating between C57♂ x ICR♀, ICR♂ x C57♀, ICR♂ x ICR♀ and C57♂ x C57♀. Fetuses were subjected to maternal administration with low dose of RA (6.25 mg/kg) at E7.25.

The frequency of different types of defects in the 4 groups of fetuses was summarized in Table 3-22 and presented in Graphs 3-18, 3-19 and 3-20.

3.4.7.1 Total frequency of anophthalmia and microphthalmia

Since the main objective of this study was to find out whether genetic and/or maternal factors in C57 strain could account for the increased susceptibility to RA-induced ocular defects, particularly the severe type of eye defects, I have therefore used total frequency of anophthalmia and microphthalmia as the parameter for comparison. Results showed that in the CON group, the spontaneous rate of developing anophthalmia or microphthalmia in heterozygous fetuses was very low (C57♂ x ICR♀ = 1% and ICR♂ x C57♀ = 3%) when compared with C57 homozygous fetuses (11%) (Graph 3-18). However, when low dose of RA was administered, the total frequency of anophthalmia or microphthalmia in heterozygous fetuses obtained from mating of ICR♂ x C57♀ was 73%, which was about 2 fold increase when compared with ICR homozygous fetuses. In heterozygous fetuses obtained from mating of C57♂ x ICR♀, the total frequency of

Table 3-22 Incidence of ocular and non-ocular defects in fetuses of different genotypes treated with low dose of RA at E7.25.

Treatment group	CON				Low dose of RA administered at E7.25			
Genotype of fetuses	ICR♂ x ICR♀	C57♂ x ICR♀	ICR♂ x C57♀	C57♂ x C57♀	ICR♂ x ICR♀	C57♂ x ICR♀	ICR♂ x C57♀	C57♂ x C57♀
No of litters	5	8	9	6	8	12	8	12
No. of implantations	65	86	41	40	106	146	44	85
No. of live fetuses	63	83	38	36	69	124	24	22
No. of resorptions	2	3	3	4	37	22	20	63
Resorption rate (%)	3 ± 1.8	3 ± 1.8	9 ± 4.8	10 ± 4.8	35 ± 4.0	14 ± 3.4	41 ± 10.1	74 ± 7.5
No. of fetuses with malformations ^	5 (8%)	3 (4%)	5 (13%)	8 (22%)	46 (67%)	109 (88%)	21 (88%)	22 (100%)
No. of fetuses with ocular defects ^	5 (8%)	3 (4%)	5 (13%)	8 (22%)	43 (62%)	106 (85%)	21 (88%)	22 (100%)
Total no. of malformed eyes @	5 (4%)	3 (2%)	6 (8%)	9 (13%)	53 (38%)	181 (73%)	39 (81%)	44 (100%)
Ocular defects								
No. of anophthalmia @	0 (0%) Bi: 0 Uni: 0 L uni: 0 R uni: 0	0 (0%) Bi: 0 Uni: 0 L uni: 0 R uni: 0	0 (0%) Bi: 0 Uni: 0 L uni: 0 R uni: 0	1 (1%) Bi: 0 Uni: 1 L uni: 0 R uni: 1	26 (19%) Bi: 8 Uni: 10 L uni: 3 R uni: 7	48 (19%) Bi: 11 Uni: 26 L uni: 5 R uni: 21	21 (44%) Bi: 7 Uni: 7 L uni: 3 R uni: 4	35 (80%) Bi: 15 Uni: 5 L uni: 2 R uni: 3
No. of microphthalmia@	2 (2%) Bi: 0 Uni: 2 L uni: 1 R uni: 1	1 (1%) Bi: 0 Uni: 1 L uni: 1 R uni: 0	2 (3%) Bi: 0 Uni: 2 L uni: 0 R uni: 2	7 (10%) Bi: 0 Uni: 7 L uni: 2 R uni: 5	24 (17%) Bi: 3 Uni: 18 L uni: 7 R uni: 11	95 (38%) Bi: 22 Uni: 51 L uni: 29 R uni: 22	14 (29%) Bi: 2 Uni: 10 L uni: 5 R uni: 5	8 (18%) Bi: 1 Uni: 6 L uni: 3 R uni: 3
Total no. of anophthalmia and microphthalmia @	2 (2%) Bi: 0 Uni: 2 L uni: 1 R uni: 1	1 (1%) Bi: 0 Uni: 1 L uni: 1 R uni: 0	2 (3%) Bi: 0 Uni: 2 L uni: 0 R uni: 2	8 (11%) Bi: 0 Uni: 8 L uni: 2 R uni: 6	50 (36%) Bi: 16 Uni: 18 L uni: 5 R uni: 13	143 (58%) Bi: 52 Uni: 39 L uni: 15 R uni: 24	35 (73%) Bi: 15 Uni: 5 L uni: 2 R uni: 3	43 (98%) Bi: 21 Uni: 1 L uni: 0 R uni: 1
Non-ocular defects								
No. of fetuses with exencephaly ^	0 (0%)	0 (0%)	0 (0%)	0 (0%)	23 (33%)	40 (32%)	0 (0%)	0 (0%)
No. of fetuses with cleft palate ^	0 (0%)	0 (0%)	0 (0%)	0 (0%)	6 (9%)	17 (14%)	5 (21%)	5 (23%)

^ Percentage represented captioned defect over the total number of fetuses examined.
@ Percentage represented captioned defect over the total number of fetal eyes examined.
Bi Bilateral
L uni Left, unilateral
R uni Right, unilateral
Uni Unilateral, either side

anophthalmia and microphthalmia after RA treatment was 58%, which was higher than that of ICR homozygous fetuses but lower than heterozygous fetuses with parents of reciprocal strains and C57 homozygous fetuses.

In my study, 21 out of 22 fetuses (95%) of anophthalmia and microphthalmia in RA-treated C57 homozygous fetuses were bilateral whereas in RA-treated ICR homozygous fetuses, only 16 out of 69 fetuses (23%) displayed bilateral anophthalmia and / or microphthalmia. Moreover, similar percentage of RA-treated ICR homozygous fetuses developed unilateral anophthalmia and / or microphthalmia (18 out of 69, 26%) as the bilateral cases. Since most of the eyes in RA-treated C57 homozygous fetuses were found to be bilaterally affected, therefore only 1 out 22 fetuses (4.5%) was found to be unilaterally affected. In the heterozygous fetuses obtained from matings of C57♂ x ICR♀, 52 out of 124 fetuses (42%) were classified as bilateral anophthalmia and / or microphthalmia whereas in the heterozygous fetuses obtained from matings of ICR♂ x C57♀, 15 out of 24 fetuses (62.5%) were classified as bilateral anophthalmia and / or microphthalmia. It is, therefore, after exogenous RA administration, bilateral anophthalmia and / or microphthalmia were more prominent in homozygous C57 fetuses and heterozygous fetuses obtained from matings of C57♂ x ICR♀ and ICR♂ x C57♀ than unilateral anophthalmia and / or microphthalmia. At the moment, although no defined explanation has been proposed to explain the underlying mechanism of unilaterality and bilaterality of congenital eye defects, it is commonly believed that bilaterality is more severe than unilaterality.

To determine if genotype has effect on rendering the heterozygous fetuses

more prone to RA-induced ocular defects, data were analyzed by logistic regression. In this part, there are 2 factors that can contribute to difference in the frequency of eye defects, they are the paternal and maternal genotypes. First, I have generated an equation for logistic regression by SPSS and by taking these 2 factors into account and the equation is as follow:

Logit = 0.733 (paternal genotype) + 2.158 (maternal genotype) - 0.103

The predicted probability of different genotypic combinations in developing ocular defects based on the logistic regression equation was calculated and shown in Table 3-23. Predicted probability is an estimate, based on several factors, of how likely an outcome is to occur. It is usually between the values "0" to "1". The higher the predicted probability, the more likely the expected outcome is to occur. In this case, it is very likely that fetuses obtained from mating of C57♂ x C57♀ will develop ocular defects after RA treatment as the predicted probability of such is 0.94, while for fetuses obtained from mating of ICR♂ x ICR♀, only half of them (0.49) may have chances to develop ocular defects after RA treatment.

Table 3-23 The predicted probability of different genotypic combination in developing ocular defects upon low dose of RA treatment based on the logistic regression equation.

Genotype of fetuses	Predicted probability of fetuses having anophthalmia or microphthalmia
ICR♂ x ICR♀	0.47
C57♂ x ICR♀	0.65
ICR♂ x C57♀	0.89
C57♂ x C57♀	0.94

When compared with the ICR genotypes, logistic regression showed that

the C57 genotype of both paternal or maternal origin could significantly cause the fetuses to develop ocular defects (p = 0.042 and p = 0.00011, respectively). This indicates that C57 has genotypic dominance upon RA administration in causing fetuses more prone to develop ocular defects.

In the logistic regression model, it is possible to find out the strength of a factor in causing the expected outcome, in this case, the total frequency of anophthalmia or microphthalmia.

Odd ratio of paternal genotype: $\frac{\text{C57}}{\text{ICR}}$ = 2.1 (95% CI: 1.028 to 2.547)

Odd ratio of maternal genotype: $\frac{\text{C57}}{\text{ICR}}$ = 8.7 (95% CI: 2.897 to 25.863)

The first equation is an adjusted odd ratio which has already eliminated the contribution of maternal influence and examined the paternal factor in causing ocular defects. The value of 2.1 means that the C57 paternal genotype is 2 times more likely to cause fetal ocular defects than the ICR paternal genotype. In other words, the strength of the C57 paternal genotype in causing fetal ocular defects is about 2 times higher than that of ICR. On the other hand, in the second equation, the C57 maternal genotype, i.e. the maternal factor, is nearly 9 times more likely to cause fetal ocular defects when compared with the ICR maternal genotype. In other words, the strength of the C57 maternal genotype in causing fetal ocular defects is about 9 times higher than that of ICR. This indicates that the strength of the C57 maternal genotype is more significant than that of the paternal genotype as their 95% CI values did not overlap with each other.

In summary, the C57 genotype poses influence in causing the fetus more prone to develop eye defects and the C57 maternal factor has additional influences in causing eye defects.

3.4.7.2 Frequency of exencephaly

To further investigate if C57 genotype and/or maternal factor only exert influence in causing the fetuses more prone to develop anophthalmia and microphthalmia, I have also examined whether there are genotypic dominance and maternal effects in causing exencephaly and cleft palate.

There was no spontaneously developed exencephaly in all heterozygous and homozygous fetuses. However, when low dose of RA was administered, the frequency of exencephaly in heterozygous fetuses obtained from mating of C57♂ x ICR♀ was 32%, which was similar to the ICR homozygous fetuses (33%). However, no exencephaly could be found in both C57 homozygous fetuses and heterozygous fetuses obtained from mating of ICR♂ x C57♀. Logistic regression was therefore employed to determine if genotype has effect on rendering the heterozygous fetuses more prone to RA-induced exencephaly.

An equation for logistic regression was generated by SPSS by taking the maternal and paternal genotype into account and list as follow:

Logit = 0 (paternal genotype) + 0 (maternal genotype) – 1.147

The equation showed that the contribution of paternal and maternal genotypes were eliminated after performing logistic regression as the zero-value was

generated for these factors. This indicated that paternal and maternal genotype did not pose any contributing factor in causing fetuses to develop exencephaly.

3.4.7.3 Frequency of cleft palate

There was no spontaneously developed cleft palate in all heterozygous and homozygous fetuses. However, when subjected to low dose of RA administration, the frequency of cleft palate in heterozygous fetuses obtained from mating of C57♂ x ICR♀ was 14% whereas in homozygous ICR fetuses, 9% of them had cleft palate. Similar frequency of cleft palate after RA treatment was found in heterozygous fetuses obtained from mating of ICR♂ x C57♀ (21%) and homozygous C57 fetuses (23%).

To better understand whether paternal and maternal genotype had effects in causing fetuses more prone to develop cleft palate, the data were tested by logistic regression and the equation is as follow:

$$\text{Logit} = 0\ (\text{paternal genotype}) + 0.821\ (\text{maternal genotype}) - 2.108$$

The equation showed that the contribution of paternal genotype was eliminated after performing logistic regression, suggesting that paternal genotype did not pose any contributing factor in causing fetuses to develop cleft palate. Moreover, when compared with the ICR genotype, logistic regression showed that the C57 genotype of maternal origin could not significantly cause the fetuses to develop cleft palate (p = 0.074). This indicated that C57 has no genotypic dominance upon RA administration in causing fetuses more prone to develop cleft palate.

3.5 DISCUSSION

The aim of this chapter is to determine if there is any strain differential susceptibility to RA-induced ocular defects. I have employed two mouse strains and they are C57, a strain sensitive to developing eye defects (Smith et al., 1994; Ozeki and Shirai, 1998; Ozeki et al., 1999), and ICR, a strain resistant to developing eye defects (Sulik et al., 1995). Indeed results show that there is strain specific differential susceptibility to RA-induced malformations, including ocular defects, which is time- and dose-dependent.

First, maternal administration of RA caused resorption in a dose-dependent manner. Medium and high doses of RA resulted in higher resorption rate in comparison to low dose of RA (Graphs 3-1 and 3-2). The same dose of RA administered at E7 caused higher resorption rate in C57 than in ICR fetuses. Moreover, nearly 100% of resorption was observed when RA was applied in later embryonic stages, i.e. E7.25 and E7.5, which suggested that RA application at these stages may pose irreversible changes in the embryo and thus resulting in embryolethality.

As an initial step to estimate the overall frequency of ocular defects after maternal RA administration, I have grouped all observable ocular defects into "total number of malformed eyes". Results show that 4% of ICR fetal eyes spontaneously develop eye defect while 13% of C57 fetal eyes developed eye defects without any RA treatment. C57 has long been recognized as the "standard model" for studying ocular biology and its spontaneous rate of developing ocular defects is reported as 10% (Smith et al., 1994), which is comparable with the result in this study. After low

dose of RA treatment at all 3 gestational days, C57 fetuses were significantly more prone to develop eye defects in comparison to ICR fetuses. These results are consistent with the finding in Sulik et al. (1995) that after low dose of RA treatment, C57 strain was more prone to develop ocular defects while ICR strain was prone to develop exencephaly.

RA treatment results in different severity of eye defects. Other than comparing the total number of malformed eyes, I have also compared the total frequency of fetal eyes classified as anophthalmia or microphthalmia in order to determine whether RA can cause not only an increase in the overall frequency of eye defects but also the most severe type. It was found that in C57, maternal administration of RA at all 3 gestational days significantly increased the total frequency of anophthalmia and microphthalmia, with increasing susceptibility at later gestational days. However, there was lower total frequency of anophthalmia and microphthalmia in ICR fetuses after RA treatment at all gestational days. When comparing the differences in strain susceptibility to RA, low dose of RA caused statistically significantly higher total frequency of anophthalmia and microphthalmia in C57 fetuses than in ICR fetuses. Moreover, in RA-treated C57 fetuses, the majority was anophthalmia whereas in RA-treated ICR fetuses, there was a shift towards to the less severe microphthalmia.

Other than ocular defects, several types of non-ocular malformations could be identified in this study including exencephaly and cleft palate. Regarding exencephaly, there was a strain-specific response in which ICR was more sensitive to develop exencephaly even when low dose of RA was applied (section 3.4.3.1).

However C57 was not much responsive to RA administration in this regard. This result is indeed consistent with previous findings reported in Sulik et al. (1995) indicating that low dose of RA resulted in exencephaly in ICR as a dominant phenotype but not in C57. Moreover, exencephaly is often associated with other defects such as fetal eyes without eyelids. In my study, I have also compared the frequency of fetal eyes without eyelids. As expected, ICR strain was significantly more sensitive to low dose of RA in developing no eyelids and this was consistent with the frequency of exencephaly reported in the present study.

The reason for ICR exhibiting higher frequencies of exophthalmia and eyes without eyelids after RA insult is not known. The embryonic origin of the eyelid is from the surface ectoderm. In the mouse embryo, normal eyelid closure occurs at around E16 and its malformation is shown to be associated with the alteration of proliferation and differentiation of eyelid primordial cells at this stage (Findlater et al., 1993; Zhang et al., 2005). For congenital exophthalmia, it is suggested to be associated with the formation of shallower orbit (Baujat et al., 2006). Apparently, the fact that ICR strain is more prone to RA-induced eye without eyelids and exophthalmia may be due to some unknown alteration in events in late stages of eye development.

There are several factors that could account for the difference in response exhibited by the two mouse strains to the teratogenic effect of RA. First, difference in developmental stages could be one of the factors as the teratogenic effect of RA is highly stage-dependent (Shenefelt, 1972). By counting the somite number, which is a general parameter for embryonic growth (van Maele-Fabry et al., 1992), it was

found that there is indeed differences in the developmental stage of these 2 strains at the time of RA injection and also during the early period of organogenesis, such that ICR embryos are developmentally more advance than C57 embryos by about 6 hours. This finding is not surprising as previous study by Thiel et al. (1993) already reported that there might be a delay of half a day in embryonic development between different strains of mice. Hence, in comparing strains susceptibility to a teratogen, it is essential to take into account the possibility of differences in the rate of embryonic development, so that the response should be compared between embryos of different strains at equivalent developmental stage rather than at the same gestational day.

To determine if the 6-hour difference in developmental stages between ICR and C57 embryos could result in the differential strain susceptibility to RA-induced ocular defects, I have compared the total frequency of anophthalmia and microphthalmia in ICR and C57 fetuses that had been injected with low dose of RA at equivalent developmental stage i.e. E7 for ICR and E7.25 for C57. Statistical analyses showed that significant differential strain susceptibility to RA-induced ocular defects still existed, with C57 strain demonstrating greater susceptibility. Hence, differences in the developmental stage between embryos of the two strain is not a contributory factor in causing strain difference found in this study.

Other than differences in the developmental stage of embryos when exposed to RA insult, genotype dominance and maternal effects could also account for strain differences in susceptibility to RA. I have compared the total frequency of anophthalmia or microphthalmia in fetuses obtained by reciprocal mating of the two

strains of mice. Result showed that in the CON group, the spontaneous rate of developing anophthalmia or microphthalmia in heterozygous fetuses was very low when compared with C57 homozygous fetuses. However, when subjected to maternal RA administration, both heterozygous fetuses obtained from mating of ICR♂ x C57♀ and C57♂ x ICR♀ showed higher total frequency of anophthalmia and microphthalmia. Statistical analysis by logistic regression shows that the C57 genotype from both paternal and maternal origins can cause a significant increase in the frequency of ocular defects in heterozygous fetuses. This can be concluded that C57 has genotypic dominance upon RA treatment in causing fetuses more prone to develop ocular defects. In fact, many previous studies have already reported that there are differences in strain responses to various types of teratogens. For example, in response to RA treatment, the C57 strain was more prone to the induction of embryolethality and forelimb ectrodactyly while the SWV strain was more susceptible for the induction of thymus and tail agenesis (Collins et al., 2006).

As the frequency of ocular defects developed in heterozygous fetuses obtained from mating of ICR♂ x C57♀ (73%) is higher than that in heterozygous fetuses obtained from mating of C57♂ x ICR♀ (58%), therefore it is possible that C57 mother has additional effects that may make the fetuses more prone to develop eye defects. Statistical analyses show that other than genotypic dominance, C57 has exerted maternal effects in significantly enhancing the embryo's susceptibility to develop ocular defects after RA treatment. In fact, it has been reported that C57 has maternal effects in enhancing ethanol teratogenesis (Gilliam and Irtenkauf, 1990). Furthermore, analyses on whether C57 has genotypic dominance and/or maternal effects in causing non-ocular defects, i.e. exencephaly and cleft palate, show that

C57 has neither genotypic dominance nor maternal effect in making fetuses more prone to develop non-ocular defects. This finding further indicates that C57 confers susceptibility to RA-induced ocular defects restrictedly but not non-ocular defects.

Although my findings showed that ICR embryos are developmentally 6 hours more advance than C57 embryos, when comparison was made on both ICR and C57 receiving low doses of RA treatment at the same time point (gestation day) but not at equivalent developmental stages, significant difference still existed. Hence comparison was made on the susceptibility of these 4 types of embryos to RA injection at same time point.

To conclude, in this chapter, I have successfully developed a mouse model to study the differential strain response to RA treatment in a time- and dose-specific manner. Moreover, I have attempted to elucidate the reasons for such differences in the strain response to RA treatment. First, difference in the developmental stages is not accountable for such difference. However, C57 exerts genotypic dominance and maternal effects in causing the fetus more prone to ocular defects but not non-ocular defects.

CHAPTER 4

Early Morphological and Histological Changes in RA-treated Embryos

4.1 INTRODUCTION

RA is essential for many processes of embryogenesis including ocular development. Animal studies show that both excess and deficiency of RA can inhibit ocular formation (Shenefelt, 1972; Avantaggiato et al., 1996; Hyatt et al., 1996; Dickman et al., 1997). However, the underlying mechanism is poorly understood. In ***Chapter 3***, I have reported that there is strain difference in susceptibility to RA teratogenicity; the C57 strain being more prone to develop eye defects than the ICR strain in response to a teratogenic dose of RA administered at presomitic stage. The spontaneous rate of having congenital eye defects such as microphthalmia in the C57 strain is about 10% (Smith et al., 1994). It is possible that maternal RA administration exacerbates the susceptibility of C57 embryos in developing eye defects.

In fact, several pathogenic mechanisms have been proposed to explain RA-induced malformations in various organs. As mentioned in section 1.3.2, these suggested mechanisms include alteration of cell migration (Ozeki and Shirai, 1998), inhibition of cell proliferation (Lai et al., 2003; Bohnsack et al., 2004) and excessive cell death (Kochhar et al., 1993; Shum et al., 1999; Tse et al., 2005). Moreover, high doses of RA resulted in alteration of several crucial embryonic transcription factors such as *Shh* and *Patched* (Helms et al., 1997).

In ***Chapter 3***, I have reported that maternal exposure to low doses of RA at pre-somitic stages, at which optic primordial tissues have not yet formed, resulted in a high frequency of anophthalmia and microphthalmia. Moreover, previous reports

showed that maximum concentration of RA in the embryo was attained 3 hours after administration and that RA level of tissue returned to pre-treatment level within 8 hours, indicating that the effect of RA administration could only last for a very short period of time (Satre and Kochhar, 1989). These facts raise a question on how such low doses of RA applied at a time well before any optic primordial cells have formed can result in severe eye defects.

As review in section 1.1, eye is formed from 3 different types of embryonic tissues, including neural ectoderm, surface ectoderm and mesenchyme. Normal ocular developmental processes require dynamic and complicated interactions between these embryonic tissues, as well as between individual cells within each tissue (Wright, 1997; Laemle et al., 1999; Chow and Lang, 2001). Death of cells in predictable locations and at precise developmental stages is called apoptosis (Jacobson et al., 1997; Lang, 1997; Milligan and Schwartz, 1997). Several reasons have been proposed for elimination of cells by apoptosis during embryonic development (Jacobson et al., 1997). Some of these reasons may also be applicable to ocular development, such as control of cell numbers and elimination of abnormal cells (Laemle et al., 1999). Many crucial diffusible molecules such as growth factors and morphogens like RA have been shown to be indispensable for normal eye development (Chow and Lang, 2001). Uncontrolled or improper cell death of ocular primordial cells can result from deficient or excessive production of these factors required for differentiation, or production of these factors at inappropriate embryonic stages, or receiving opposing signals. All these events can lead to developmental arrest or resulted in absence of particular ocular primordial tissues and eventually failure in eye formation.

4.2 EXPERIMENTAL DESIGN

In ***Chapter 3***, I have reported that low doses of RA injection at presomitic stages resulted in anophthalmia and/or microphthalmia in near-term fetuses, with the C57 strain showing significantly higher frequencies than the ICR strain. To understand the underlying mechanism of RA-induced ocular malformations and differences in strain susceptibility, it is important to examine whether there were any changes in the embryo shortly after RA injection. In this chapter, morphological, histological and ultra-structural studies were conducted in embryos during the 48 hours period after RA-injection. Somite number as a general growth parameter was also counted to see if RA caused developmental retardation.

As mentioned in section 4.1, cell death at early stages can be one of the possible pathways that leads to failure in embryonic eye development by arresting the development of the optic primordia such as optic pit or vesicles after RA treatment. In this chapter, first, detection of apoptosis on superficial embryonic cells was conducted on the whole embryo. To further understand the distribution of apoptotic cells, detection of apoptosis on histological sections was performed, which could provide additional information on whether maternal RA administration elicited a specific spatial and temporal pattern of cell death.

Experimental Design

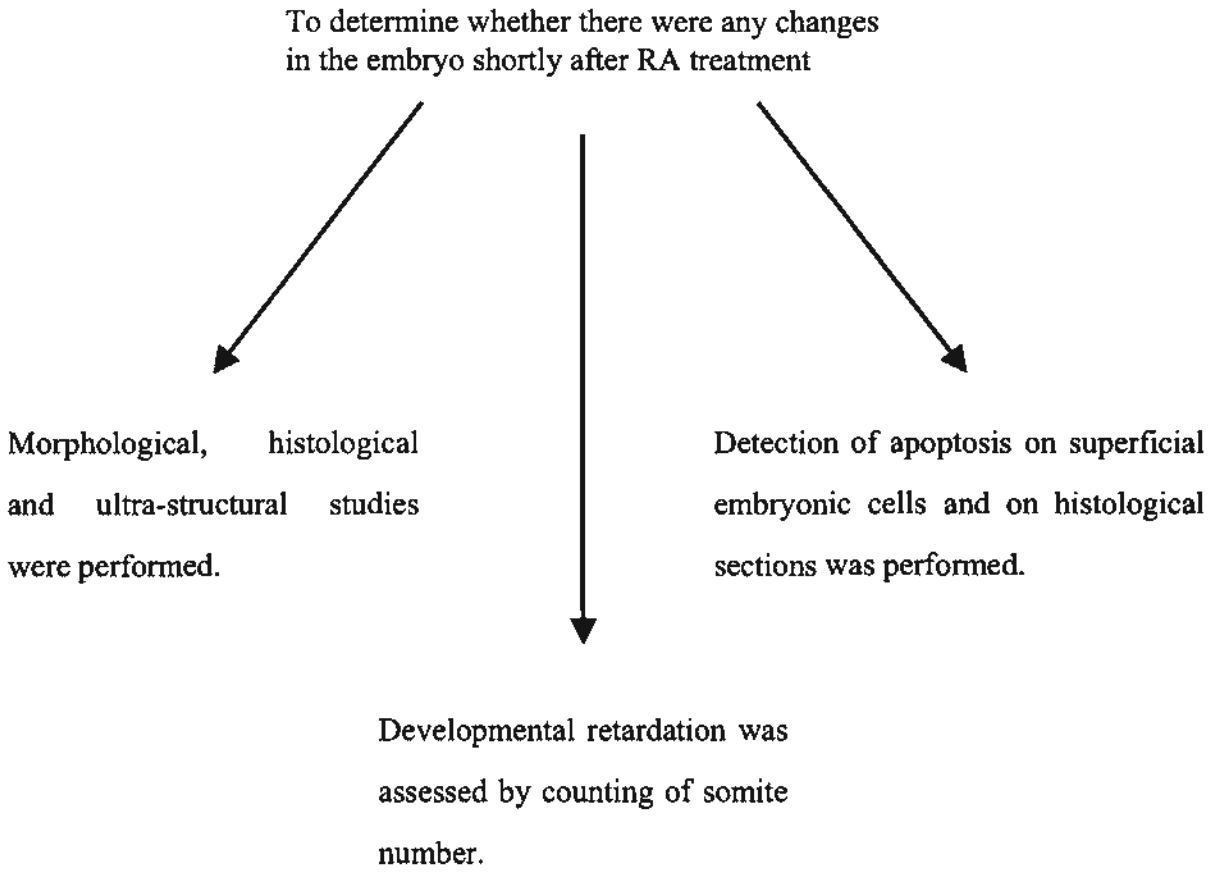

4.3 MATERIALS AND METHODS

4.3.1 RA treatment and somite counting

The preparation of RA was the same as that mentioned in section 2.1. RA at a dose of 6.25 mg/kg was administered to pregnant C57 and ICR mice on E7.25 and E7 respectively. To determine whether maternal RA treatment caused embryonic growth retardation, the somite number of embryos of both mouse strains at equivalent developmental stages, as described in Table 4-1, was determined as mentioned in section 3.3.1.

Table 4-1 Equivalent embryonic stages of ICR and C57 strains for comparison

Equivalent embryonic stages	
ICR	**C57**
E7.75	E8.0
E8.25	E8.5
E8.75	E9.0
E9.25	E9.5

4.3.2 Gross morphology

To prepare embryos for imaging of gross morphology, embryos were first dissected in ice-cold PBI medium supplemented with 1% bovine serum albumin and then washed twice with PBS before being fixed in 4% paraformaldehyde for overnight. Embryos were washed twice with PBS and then cleared in increasing concentrations of glycerol in distilled water (50%, 75%, 100%). Images were then captured with digital camera (DFC480, *Leica*), fitted onto the stereomicroscope

(MZ16, *Leica*). Between 22 to 39 bembryos were examined for each group.

4.3.3 Histology

To examine early histological changes in the embryo after maternal RA administration, control and RA-treated embryos at different stages were collected and prepared as paraffin sections as mentioned in section 2.4. Haematoxylin and eosin-stained sections were examined by light microscopy (Axioplan, *Zeiss*). Between 12 to 21 embryos were examined in each group.

4.3.4 Scanning electron microscopy (SEM)

Other than performing histological analysis on embryos, detailed morphological analysis were carried out by using SEM. In brief, embryos were dissected out in ice-cold 0.1 M phosphate buffer (PB) (pH = 7.2) and then pre-fixed in 0.25% glutaldehyde in sterile 0.1 M PB for no longer than 24 hours.

After removal of fixatives, samples were washed slightly 3 times with 0.1 M PB for 5 minutes each time. Samples were then post-fixed in 1% osmium in distilled water at room temperature for 1 hour. After post-fixation, samples were washed 5 times with distilled water for 5 minutes each time. Samples were then dehydrated once with 50%, 70%, 80% and 90% ethanol and twice with absolute ethanol for 30 minutes in each solution. After complete dehydration, samples were subjected to critical point dried by liquid CO_2. Afterwards, samples were mounted onto aluminum stub with double-sided tape, and sputter coated with gold palladium. Samples were then examined by SEM microscopy (JSM-6301F, *JOEL*). Between 15

to 21 embryos were examined in each group.

4.3.5 Terminal deoxynucleotidyl transferase dUTP nick end labeling (TUNEL) staining of whole mount embryos

To examine if there was any apoptosis on superficial embryonic epithelial cells after maternal RA treatment, embryos were dissected out in ice-cold PBS and fixed in 4% PFA overnight at 4°C. Embryos were washed twice in PBS containing 1% Tween-20 (*Sigma*) (PBT) for 20 minutes and then dehydrated by passing through once in ascending concentrations of methanol solution (25%, 50% and 75% in PBT) and then twice in absolute methanol. All dehydration procedures were carried out at 4°C. Embryos were then kept at -20°C until use. To perform the experiment, embryos were placed in 2 ml micro-centrifuge tubes and all procedures were carried out at room temperature unless specified. Samples were gradually rehydrated in 75%, 50% and 25% methanol in PBS containing 2 mM levamisole (*Sigma*) (PBSL) for at least 20 minutes in each solution. Embryos were washed 5 times in PBSL for 30 minutes each time. Embryos were then soaked in permeabilization buffer [0.1% Triton X-100 (*Sigma*), 0.01% sodium citrate in autoclaved water] for 15 minutes, followed by washing in autoclaved water for 15 minutes. Embryos were washed 3 times in PBSL containing 0.01% Triton X-100 (PBLT) for 20 minutes each time. Embryos were then incubated with 5 µl of terminal deoxynucleotidyl transferase (TdT) enzymes in 45 µl of reaction buffer (provided in *In Situ* Cell Death Detection Kit, *Roche Diagnostic Ltd*) for 3 hours at 37°C in dark. After incubation, embryos were washed 4 times in PBLT for 30 minutes each time. Embryos were then incubated with PBLT containing 20% sheep serum and 3% BSA with gentle shaking. Incubation was kept overnight at 4°C.

On the next day, after draining off the incubation buffer, embryos were immediately incubated with 60 µl of Converter-AP solution (provided in *In Situ* Cell Death Detection Kit, *Roche Diagnostic Ltd*) for 3 hours at room temperature in dark. After washing for 4 times in PBLT, embryos were soaked in Tris-buffer [0.1 mM Tris (pH 9.2)] for 5 minutes. Embryos were transferred to a glass vial and incubated with 17.5 µl of BCIP and 22.5 µl of NBT in 5 ml of Tris-buffer in dark for signal development. It normally took less than 1 hour for complete signal development. When optimal signal intensity was reached, reaction was stopped by washing 3 times in PBS for 15 minutes each time. Embryos were then post-fixed in 4% PFA overnight at 4°C. On the next day, embryos were washed briefly twice in PBT and then twice in PBS for 15 minutes each time. Embryos were cleaned by passing through ascending concentrations of glycerol in autoclaved water (50%, 75% and 100%). Images were captured by digital camera fitted onto a stereomicroscope.

4.3.6 TUNEL staining of paraffin-sectioned embryos

To further determine if apoptosis occurred in cell populations other than those on the surface, TUNEL staining of paraffin-sectioned embryo was also performed. In brief, embryos were dissected out in ice-cold PBS and fixed overnight in 4% PFA at 4°C. On the next day, embryos were first washed twice in normal saline for 20 minutes each. Embryos were dehydrated and then embedded in paraffin as described in sections 2.4.1 and 2.4.2. Serial sections at a thickness of 6 µm cut at transverse plane of the embryo were prepared. Serial sections were laid on TESPA-coated slides.

Before staining paraffin-sectioned slides were first briefly melted on slide

dryer at 60°C for 1 minute and then cooled down to room temperature for a couple of minutes. Sections were then dewaxed in three changes of xylene at 15 minutes intervals and then rehydrated through a series of ethanol with descending concentrations (100%, 95%, 80%, 70% in autoclaved water). The sections were then washed in several changes of distilled water for a few minutes before washing in PBS for 5 minutes. Endogenous peroxidase in the tissue was quenched by addition of 3% H_2O_2 in PBS for 5 minutes at room temperature followed by washing 3 times in PBS for 5 minutes each time. Sections were then subjected to TUNEL staining using the Apoptag Plus Peroxidase *In Situ* Apoptosis Detection Kit (*Chemicon*) by procedures according to the manufacturer's instruction with minor modifications. In brief, after washing with PBS, slides were incubated with "Equilibration Buffer" for 1 minute at room temperature. After removal of excess Equilibration Buffer, TdT enzyme was immediately added to the slide. Slides were then incubated in a humidified slide chamber at 37°C for 1 hour. Enzymatic reaction was stopped by addition of "Stop/Wash Buffer" for 10 minutes at room temperature. Slides were then washed with 3 changes of distilled water followed by several changes of PBS for at least 5 minutes in each charge. After washing, slides were incubated with anti-DIG-peroxidase-conjugated antibody at room temperature in a humidified chamber for 30 minutes. After incubation, slides were washed at least 4 times in TBS [50 mM Tris-base, 0.8% NaCl (pH7.5)] for 2 minutes each time.

Signal development was achieved by using *p*-dimethylaminoazobenzene (DAB, 100 μg/ml in TBS) as substrate and 0.01% H_2O_2 as catalyst. When optimal signal intensity was reached, reaction was stopped by washing under running tap water for 15 minutes. The slides were then counterstained with 0.5% methyl green

(in 0.1M sodium acetate, pH 4.0) for 60 minutes. Afterwards, slides were washed in tap water for 15 minutes and then dehydrated once in ascending concentrations of ethanol (70%, 80%, and 95%) and then twice in absolute ethanol. Slides were cleared 3 times in xylene and then mounted in Permount (*Fisher Chemicals*). Darkly-stained apoptotic body/bodies found within a single cell, which was counter-stained by methyl green, I was counted as a positive signal. For E7.75 (ICR) / E8 (C57) and E.8.25 (ICR) / E8.5 (C57) embryos, positively stained apoptotic cells in the neuroepithelium and mesenchyme under the neural fold of the future forebrain in 5 and 8 alternate sections were counted respectively. Results were expressed in apoptotic bodies over the total number of cells in the region concerned.

4.3.7 Statistical analysis

Differences in the number of somites and apoptotic bodies between control and RA-treated embryos of the same strain were tested by Independent sample *t* test. All statistical analyses were carried out using SPSS software (*SPSS*), with statistical significance level set at $p < 0.05$.

4.4 RESULTS

4.4.1 RA caused developmental retardation

There was linear increase in somite number from E7.75 (2.42 ± 0.17) to E9.25 (16.70 ± 0.21) in ICR embryos (Table 4-2 and Graph 4-1). Moreover, from E8.25 onwards, the somite number of RA-treated embryos was statistically significantly smaller than that of control embryos suggesting that RA caused developmental retardation at early stages.

In C57 embryos, there was linear increase in somite number from E8 (2.52 ± 0.19) to E9.5 (21.88 ± 0.39) (Table 4-3 and Graph 4-2). Maternal RA treatment resulted in statistically significant reduction in somite number from E8.5 onwards suggesting that RA caused developmental retardation at early stages.

4.4.2 RA caused failure in formation of optic primordial tissues and alteration in future forebrain

4.4.2.1 Gross morphological examination

In ICR embryos, at E7.75, there was no observable difference in the gross morphology of control (Figure 4-1 A) and RA-treated embryos (Figure 4-1 B). At E8.25, there was slight reduction in the size of the anterior neural plate of RA-treated embryos (Figure 4-1 D) in comparison to that of control embryos (Figure 4-1 C). At E8.75, the size of the future forebrain of control (Figure 4-2 A) and RA-treated embryos (Figure 4-2 B) was similar. Moreover, optic vesicles have

Table 4-2 Somite number of ICR embryos with or without RA treatment.

Gestational day	E7.75		E8.25		E8.75		E9.25	
Treatment groups	CON	RA	CON	RA	CON	RA	CON	RA
No. of litters	7	8	8	5	6	7	6	7
No. of implantations	97	106	109	70	76	98	77	99
No. of resorptions	2	5	4	4	0	6	1	8
% of resorption	2.0	4.7	3.5	5.4	0.0	5.7	1.5	9
No. of viable embryos	95	101	105	66	76	92	76	91
Somite no. (± SE)	2.42 ± 0.17	2.04 ± 0.12	8.94 ± 0.12	7.88 ± 0.12	16.70 ± 0.21	15.47 ± 0.12	21.91 ± 0.19	20.88 ± 0.11
p-value	0.063		< 0.001*		< 0.001*		< 0.001*	

* *Statistically significant*

Table 4-3 Somite number of C57 embryos with or without RA treatment.

Gestational day	E8		E8.5		E9		E9.5	
Treatment groups	**CON**	**RA**	**CON**	**RA**	**CON**	**RA**	**CON**	**RA**
No. of litters	4	7	10	8	9	9	9	10
No. of implantations	25	43	59	48	60	60	55	65
No. of resorptions	2	4	5	9	6	13	6	13
% of resorption	7.8	8.9	8.7	18.0	9.9	21.1	10.3	18.8
No. of viable embryos	23	39	54	39	54	47	49	52
Somite no. (± SE)	2.52 ± 0.19	2.77 ± 0.20	8.81 ± 0.36	7.38 ± 0.38	16.2 ± 0.38	14.36 ± 0.34	21.88 ± 0.39	19.38 ± 0.54
***p*-value**	0.374		0.007*		< 0.001*		< 0.001*	

** Statistically significant*

started to form in both groups of embryos (Figures 4-2 C and D). At half a day later, the optic vesicles were well-developed in control (Figures 4-3 A and C) and RA-treated embryos (Figures 4-3 B and D).

In C57 embryos, no observable changes could be found at E8 after RA treatment (Figures 4-4 A and B). However, at E8.5, the size of the anterior neural plate of RA-treated embryos (Figure 4-4 D) was noticeably smaller than that of control embryos (Figure 4-4 C). As a result, at E9, a smaller forebrain was formed (compare Figures 4-5 A and B). Moreover, as shown in higher magnification, while optic vesicles have formed in control embryos (Figure 4-5 C), no optic vesicle could be found in RA-treated embryos (Figure 4-5 D). When embryos were examined at half a day later, there was still no sign of optic vesicles formation in RA-treated embryos (Figures 4-6 B and D), but optic vesicles in control embryos were well-developed (Figures 4-6 A and C).

4.4.2.2 Histological examination

Histological examination on haematoxylin and eosin stained paraffin section showed that in ICR embryos, at E7.75, no obvious changes could be found in the neuroepithelium and the underlying mesenchyme after RA treatment (Figures 4-7 A and B). Later on, at E8.25, 2 deep depressions called optic pits were found in the neuroepithelium (Figure 4-8 A). The epithelium of the future forebrain of both control (Figure 4-8 A) and RA-treated (Figure 4-8 B) embryos was pseudostratified columnar in shape with no observable difference in their thickness. At half a day later (E8.75), a pair of deeply evaginated optic vesicles had formed in both control and RA-treated embryos (Figures 4-9 A and B).

For C57 embryos, at E8, there were plenty of mesenchymal cells underlying the neuroepithelium in control embryos (Figure 4-10 A) whereas in RA-treated embryos, there were obviously much less mesenchymal cells (Figure 4-10 B). At E8.5, two optic pits had developed in the neuroepithelium (Figure 4-11 A). However, no optic pits were found in RA-treated embryos (Figure 4-11 B). Moreover, while mesenchymal cells underlying the neuroepithelium were densely packed in control embryos (Figure 4-11 A), limited mesenchymal cells could be found in RA-treated embryos (Figure 4-11 B). At E9, in C57 CON embryo, two shapely evaginated optic vesicles could be found on both sides of the forebrain in control embryos (Figure 4-12 A). However, no optic vesicles could be found in RA-treated embryos at the corresponding level (Figure 4-12 B) and the size of the forebrain was also much smaller.

4.4.2.3 SEM examination

To further study the ultra-structural differences in the surface feature of the two mouse strains upon RA treatment, scanning electron microscopy was conducted. At E7.75, in ICR embryos, there were no observable differences in the shape and the size of the anterior neural plate between control and RA-treated groups (Figure 4-13). At E8.25, in control embryos, there were sharp borders along the forebrain, midbrain and hindbrain neural plate (Figure 4-14 A). Similar contour was also found in RA-treated embryos (Figures 4-14 B and C). Moreover, two optic pits could be found on the two sides of the future forebrain in both control and RA-treated embryos (Figures 4-14 C and D), although the optic pits were shallower in some of the RA-treated embryos (Figures 4-14 E and F, orange arrows).

In C57 embryos, similarly at E8.0, there were no observable changes between control and RA-treated groups (Figure 4-15). The epithelial surface was smooth without blebbing of cells. At E8.5, in control embryos, there were sharp borders along the forebrain, midbrain and hindbrain neural plate (Figure 4-16 A). However, maternal RA exposure resulted in abnormal shaping of the future forebrain (Figures 4-16 B and C). Moreover, a pair of optic pits, which were present in the future forebrain region in control embryos (Figure 4-16 D) were completely missing in RA-treated embryos (Figures 4-16 E and F). Apart from this, RA treatment also resulted in underdevelopment of the forebrain neural plate (Figure 4-16 F).

4.4.3 RA treatment caused cell death

As mentioned in section 4.1, one of the possible teratogenic actions of RA is induction of cell death. To determine if RA treatment resulted in increase of apoptosis, whole mount TUNEL staining was carried out to examine the distribution of apoptotic bodies on superficial cells of the embryo. At E.7.75, in ICR embryos, apoptotic cells were found on the headfold (Figures 4-17 A and B). Maternal RA administration did not result in any observable differences in embryos of the same strain (Figures 4-17 C and D). Similar pattern of distribution of apoptotic bodies were found in control C57 embryos at equivalent stage, i.e. E8 (Figures 4-17 E and F). There was no observable change in C57 embryos of C57 strain after RA treatment (Figures 4-17 G and H).

At half a day later, positively stained apoptotic bodies were found along the neural fold of the forebrain, midbrain and hindbrain in ICR control embryos at E8.25 (Figures 4-18 A and B). Maternal RA administration resulted in more

apoptotic bodies in neural fold of midbrain and hindbrain as well as anterior neural fold (Figures 4-18 C and D). Similarly, in C57 control embryos at equivalent embryonic stage, i.e. E8.5, apoptotic bodies were found along the neural fold of forebrain, midbrain and hindbrain (Figures 4-18 E and F). Maternal RA administration resulted in more apoptotic bodies in the neural fold of midbrain and hindbrain (Figures 4-18 G and H).

After having an overview of distribution of apoptotic bodies on the superficial layer of the embryo, further examination on the tissue distribution of apoptotic bodies were conducted on the paraffin-section. Scattering of apoptotic bodies could be found in both the neuroepithelium and the mesenchyme under the neural fold of the future forebrain. The number of apoptotic bodies were counted and shown in Tables 4-4 to 4-7.

First, the percentage of positively labeled apoptotic bodies in the mesenchyme under the neural fold of the future forebrain was counted and presented in Table 4-5, with representative images shown in Figures 4-19 and 4-20. In ICR embryos, there was a decrease in the percentage of apoptotic bodies in the mesenchyme of RA-treated embryos when compared with control embryos, though there was no significant differences between these 2 groups (Table 4-4 and Graph 4-3).

Table 4-4 Apoptotic bodies in the mesenchyme of ICR and C57 embryos at E7.75 and E8 respectively.

Mouse strain	ICR E7.75		C57 E8	
Treatment group	CON	RA	CON	RA
No. of embryos counted	7	6	6	6
% of dead cells in mesenchyme (± SE)	3.07 ± 0.006	1.64 ± 0.006	2.37 ± 0.003	1.82 ± 0.004
p-value	0.121		0.323	

In C57 embryos at equivalent developmental stage, i.e. E8, there was no significant difference in the percentage of apoptotic bodies after RA treatment (Graph 4-3).

At half a day later, there was no increase in the percentage of apoptotic bodies in the mesenchyme of RA-treated ICR embryos at E8.25 (Table 4-5 and Graph 4-4) and RA-treated C57 embryos at equivalent developmental stage i.e. E8.5. Representative images were shown in Figure 4-20.

Table 4-5 Apoptotic bodies in the mesenchyme of ICR and C57 embryos at E8.25 and E8.5 respectively.

Mouse strain	ICR E8.25		C57 E8.5	
Treatment group	CON	RA	CON	RA
No. of embryos counted	6	6	6	6
% of dead cells in mesenchyme (± SE)	2.05 ± 0.004	2.14 ± 0.004	2.42 ± 0.003	1.89 ± 0.008
p-value	0.873		0.467	

In comparing the percentage of apoptotic bodies in the neuroepithelium, there was no significant difference between control and RA-treated groups at E7.75

and E8 of ICR and C57 embryos respectively (Table 4-6, Graph 4-5).

Table 4-6 Apoptotic bodies in the neuroepithelium of ICR and C57 embryos at E7.75 and E8 respectively.

Mouse strain	ICR E7.75		C57 E8	
Treatment group	CON	RA	CON	RA
No. of embryos counted	7	6	6	6
% of dead cells in neuroepithelium (± SE)	1.36 ± 0.003	1.20 ± 0.004	3.12 ± 0.010	2.22 ± 0.004
p-value	0.764		0.444	

Similarly, no significant difference in the percentage of apoptotic bodies in the neuroepithelium could be observed in control and RA-treated embryos at E8.25 of ICR and E8.5 of C57 strains respectively (Table 4-7, Graph 4-6).

Table 4-7 Apoptotic bodies in the neuroepithelium of ICR and C57 embryos at E8.25 and E8.5 respectively.

Mouse strain	ICR E8.25		C57 E8.5	
Treatment group	CON	RA	CON	RA
No. of embryos counted	6	6	6	6
% of dead cells in neuroepithelium (± SE)	2.22 ± 0.005	1.34 ± 0.003	1.83 ± 0.003	3.40 ± 0.009
p-value	0.127		0.147	

4.5 DISCUSSION

The aims of this chapter were to examine the early changes in the embryo after RA treatment and to determine if there were any strain differences between ICR and C57 embryos. First, I have investigated if RA caused developmental retardation and examined early morphological changes. Results showed that low doses of RA caused statistically significant reduction in somite number from 30 hours after RA treatment in both ICR and C57 embryos. In fact, RA is well known to cause embryonic developmental retardation (Morriss-Kay and Ward, 1999; Ross et al., 2000; Mark et al., 2006). It was reported that addition of RA to mouse embryos in culture caused significant embryonic growth retardation in a dose-dependent manner (Watanabe et al., 1988). Growth retardation was accompanied by increased cell death and decreased proliferation rate of mesenchymal cells (Watanabe et al., 1988).

Apart from developmental retardation, gross, histological and scanning electron microscopic examinations showed that RA caused failure in formation of optic primordial tissues including the optic pit and optic vesicle in C57 embryos. However, these optic primordial tissues could still be found in RA-treated ICR embryos.

Other than affecting the optic primordial tissues, RA treatment also caused underdevelopment of the anterior neural plate and future forebrain. In fact, besides playing a crucial role in eye development, RA is also indispensable for proper forebrain development (Niederreither et al., 2002; Mic et al., 2004; Ribes et al.,

2006; Halilagic et al., 2007). Ribes et al. (2006) showed that *Raldh2*, the earliest expressed RA synthesizing enzymes in the embryo, was responsible for RA synthesis in the forebrain and craniofacial regions in early embryogenesis. *Raldh2*$^{-/-}$ knockout embryos exhibited defective morphogenesis of various forebrain derivatives such as optic vesicles. In my study, smaller forebrain formation was accompanied by missing of optic primordial tissues. Could these 2 events be resulted from disruption of RA synthesis? In fact, *Raldh2* is expressed from about E7.5 in the mouse embryo (Niederreither et al., 1999). In my study, RA was injected at a time well before any optic primordial tissues have formed (E7 in ICR and E7.25 in C57), yet it could lead to failure of optic pit /vesicle formation. Thus, it is tempting to suggest that RA treatment could interfere with the normal onset or proper functioning of *Raldh2* and thus resulted in defects in eye and forebrain development. This part was examined and discussed in ***Chapter 5***.

In histological examination, it was found that RA treatment resulted in reduced number of mesenchymal cells under the neural folds of the future forebrain in early stages of C57 embryos. However, this phenomenon was not obvious in RA-treated ICR embryos. These results again suggest that there are strain differences in susceptibility to RA-induced teratogenicity with the C57 strain being more vulnerable to RA insult. It has been reported that teratogenic doses of 13-*cis* RA, a retinoid with lower potency than that of all-*trans* RA, can induce cell death and reduction in cell number in the mesenchyme (Watanabe et al., 1988). Hence it is possible that in this study, RA caused a decrease in the number of mesenchymal cells via several mechanisms such as reduction in cell proliferation rate.

It is commonly believed that teratogenic insult of RA will lead to massive cell death (Sulik et al., 1988). In this study, I have reported that there were similar patterns of distribution of apoptotic bodies in the headfold regions of both control and RA-treated embryos of C57 and ICR strains (Figure 4-17). At a later stage, more apoptotic bodies were observed in the midbrain and hindbrain regions of embryos of both strains (Figure 4-18). However, by conducting cell counting on paraffin sections of embryos stained by TUNEL method, there was no statistically significant difference in the number of apoptotic bodies in the neuroepithelium and the underlying mesenchyme of the future forebrain between the control and the RA-treated embryos of both strains. Although cell death has been proposed to be one of the major pathogenic mechanisms of RA teratogenicity, there may be other possible mechanisms that can lead to changes in cell population, such as alteration in the migratory pathway of mesenchymal cells (Morriss-Kay and Ward, 1999; Ross et al., 2000).

To conclude, in this chapter, it was found that early changes in the embryos after RA treatment included developmental retardation, reduction in the size of the anterior neural plate and subsequently the forebrain and failure in optic pits / vesicles formation. Moreover, there was strain differences in terms of the severity of these changes, with C57 embryos being affected to a greater extent than ICR embryos. In the following chapters, I have investigated the mechanisms that may lead to failure in formation of the optic primordial tissues.

CHAPTER 5

Expression Analyses of RA-Regulatory and Early Eye Development Genes

5.1 INTRODUCTION

It has been well-recognized that ocular development is dependent upon homeostatic retinoic acid signaling. Litters without eyes were delivered from pigs kept on vitamin A deficient diet (Hale, 1933). Other studies also show that vitamin A deficiency result in a range of ocular defects in different severity, including anophthalmia, microphthalmia, coloboma, abnormal folding of retina, anterior chamber defects, gaps between the neural and pigmented retina, thickened retrolenticular membrane filling the vitreous cavity, delayed lens differentiation and a denser periocular mesenchyme (Hale, 1933; Dickman et al., 1997; Morriss-Kay and Ward, 1999). Interestingly, overdose of vitamin A or RA during pregnancy is also teratogenic and causes a range of ocular defects that closely resemble those caused by vitamin A deficiency (Cook and Sulik, 1988; Sulik et al., 1995; Ozeki and Shirai, 1998). Such similarities have prompted the idea that both excess and deficiency of RA induce defects via common mechanisms.

Among different developing organs, eye is very susceptible to excess and deficiency of RA. Apparently, it may be due to the fact that the eye is a site of intense RA synthesis. Different RA synthesizing and catabolizing enzymes can be located in the developing eye with distinct compartmentalization (McCaffery et al., 1992; McCaffery et al., 1999; Blentic et al., 2003; Luo et al., 2006). Moreover, RA can be detected in both dorsal and ventral regions of the eye and its relative amount changes with the developmental age (McCaffery and Dräger, 1993; Mey et al., 1997; McCaffery et al., 1999; Molotkov et al., 2006). In fact, the temporal and spatial distributions of endogenous concentrations of RA among different regions are

regulated by the balancing act of the RA synthesizing enzyme retinaldehyde dehydrogenase (RALDH) and the RA catabolizing enzyme CYP26, a member of the cytochrome P450 family (Mey et al., 1997; McCaffery et al., 1999; Dobbs-McAuliffe et al., 2004; Reijntjes et al., 2005).

Raldh has 3 subtypes: *Raldh1*, *Raldh2* and *Raldh3*. *Raldh2*, being the earliest expressed RA synthesizing enzyme in the embryo, is transiently expressed at the anterior neural ridge surrounding the optic pit at about E8.5 (Wagner et al., 2000) and in the neuroepithelium of the optic vesicle at E9 (Haselbeck et al., 1999; Mic et al., 2004). Interestingly, this key RA synthesizing enzyme does not express in the optic cup from E9.5 onwards but instead, expresses in the periocular mesenchyme (Niederreither et al., 1997; Niederreither et al., 1999; Haselbeck et al., 1999; Matt et al., 2005; Molotkov et al., 2006). By using the RARE-*lacZ* reporter transgenic mouse, it is found that the expression pattern of *Raldh2* correlates well with regions of RA production in the embryo (Niederreither et al., 1997; Niederreither et al., 2002). Another RA synthesizing enzyme *Raldh3* starts to express in the surface ectoderm overlying the ventral optic pit at E8.5 and then extends into the neural ectoderm and eventually in the ventral retina from E9 onwards (McCaffery et al., 1999; Mic et al., 2000). *Raldh1* starts to express dorsally in the optic cup from E9.5 onwards (McCaffery et al., 1991; McCaffery et al., 1992; Molotkov et al., 2006).

A series of knockout mouse models of RA synthesizing enzymes has been proven to be invaluable in unveiling the mechanisms and pathways of RA signalling in embryonic development. *Raldh2* null mutant embryos die at midgestation with various defects, suggesting that *Raldh2* is indispensible for

embryogenesis (Niederreither et al., 1997; Mic et al., 2002). *Raldh2*$^{-/-}$ embryos exhibit shortening along the antero-posterior body axis without undergoing axial rotation. They also have defects in heart tube formation and truncation in the frontonasal region (Niederreither et al., 1999). In particular, *Raldh2*$^{-/-}$ embryos lack RA synthesis in the optic vesicle, which then fail to invaginate to become the optic cup and no lens is formed. These phenotypes suggest that *Raldh2* plays a crucial role in early ocular morphogenesis (Mic et al., 2004; Ribes et al., 2006). To overcome the limitation due to early lethality of *Raldh2* mouse null mutants, researchers rescued these embryos by maternal dietary supplementation of RA in dosages within the normal physiological range at various early- to mid-gestational periods (Mic et al., 2004; Matt et al., 2005; Ribes et al., 2006; Molotkov et al., 2006; Halilagic et al., 2007).

It has been suggested that the presence of normal levels of *Raldh1* and *Raldh3* in the developing optic cup may compensate for the loss of RA synthesized by *Raldh2* (Matt et al., 2005). *Raldh3*$^{-/-}$ mice die at birth as a result of nasal defects (Dupe et al., 2003) and exhibit mild ocular defects such as mild shortening of the ventral retina, abnormal retrolenticular membrane and thickening of the ventral periocular mesenchyme (Dupe et al., 2003; Matt et al., 2005; Molotkov et al., 2006). *Raldh1* null mutant embryos exhibit no noticeable defects in eye development (Fan et al., 2003). *Raldh1/Raldh2* double null mutant embryos showed similar degrees of abnormality in optic cup formation as the single *Raldh2* null mutant with no additional regions of abnormality (Mic et al., 2004). On the other hand, *Raldh1/Raldh3* double null mutant embryos showed a greater degree of abnormality in the same structure as the single *Raldh3* mutant but with no additional regions of

abnormality (Matt et al., 2005; Molotkov et al., 2006). *Raldh2/Raldh3* double knockout mouse mutants have more severe eye abnormalities than single null mutants (Halilagic et al., 2007). Moreover, knockout studies also suggest that there is functional redundancy between *Raldh1* and *Raldh3, s*ince the absence of one enzyme is compensated by the presence of the other (Matt et al., 2005; Molotkov et al., 2006).

Three subtypes of RA catabolizing enzymes have been identified. They are *Cyp26a1, Cyp26b1* and *Cyp26c1*. *Cyp26a1* first expresses in the developing eye in an equatorial region between the two RA-rich compartments created by the dorsally expressed *Raldh1* and ventrally expressed *Raldh3* from E11 onwards (Fujii et al., 1997; McCaffery et al., 1999; Wagner et al., 2000). At E15, *Cyp26c1* forms a wispy horizontal stripe across the retina at a similar location as *Cyp26a1,* which may reinforce *Cyp26a1* in later stage of retinal development (Sakai et al., 2004). However, *Cyp26b1* is undetectable in the embryonic and postnatal mouse optic tissues (MacLean et al., 2001; Tahayato et al., 2003). The promoter regions of both *Cyp26a1* and *Cyp26c1* contain RA-responsive elements and therefore expressions of these genes are inducible by RA (Fujii et al., 1997; Ray et al., 1997; Reijntjes et al., 2003).

Although there are distinctive temporal and spatial expression domains of *Cyp26* in the developing retina, no single null mutant mouse models of *Cyp26a1, Cyp26b1* nor *Cyp26c1* showed observable ocular defects (Abu-Abed et al., 2001; Sakai et al., 2001; Yashiro et al., 2004; Ribes et al., 2007; Uehara et al., 2007). Instead, exencephaly, hindbrain mispatterning, caudal regression and spina bifida were observed in *Cyp26a1* null mutant embryos (Abu-Abed et al., 2001; Sakai et al.,

2001; Ribes et al., 2007). However, *Cyp26a1/c1* double null mutant embryos have elevated levels of endogenous RA and exhibited pronounced anterior truncation of the brain, reduced ocular region and antero-posterior patterning defects (Uehara et al., 2007). These phenotypes suggest that increased level of RA is responsible for malformation of the forebrain as well as the eye.

It has been suggested that the morphogenetic role of RA in the developing embryo is controlled by turning on and off the RA synthesizing and catabolizing enzymes in a spatially and temporally regulated manners (Niederreither et al., 1997; Reijntjes et al., 2005). Niederreither et al. (1997) demonstrated that exogenous administration of RA by oral gavage at E8.5 caused downregulation of *Raldh2* expression at 6-12 hours after injection, showing that there is a susceptible window for RA-induced *Raldh2* downregulation. Moreover, it was reported that in zebrafish embryos, upon being challenged with exogenously applied RA, there was coordinated induction of *Cyp26a1* and repression of *Raldh2* in a time, concentration and tissue-dependent manner (Dobbs-McAuliffe et al., 2004). Although *Raldh2* does not contain RARE, it has been shown that the negative feedback mechanism regulating the RA production in the presence of exogenous RA directly acts on the *Raldh2* promotor region in which its activity is repressed by exogenous RA (Dobbs-McAuliffe et al., 2004). These feedback mechanisms exist to give a precise control of endogenous RA synthesis to maintain a homeostatic retinoid level.

Other than RA synthesizing and catabolizing enzymes, several important early-expressed genes have also been identified to be important for normal ocular development. *Pax6* is a gene crucially involved in ocular development

(Chow and Lang, 2001; Hever et al., 2006). Its expression begins in the early anterior neural plate and can be detected in the optic pit of the neural ectoderm from which the optic vesicle forms (Li et al., 1994; Grindley et al., 1995). It expresses throughout in the optic vesicle (Li et al., 1994; Grindley et al., 1995; Stoykova et al., 2000) and in the prospective lens field and later in the surface ectoderm overlying the optic cup where it plays a crucial role in lens and retinal development (Marquardt et al., 2001; Lang, 2004). Downregulation of *Pax6* in the optic vesicle neuroepithelium affects the survival of optic vesicle cells and the transformation of the optic vesicle into a normal optic cup (Canto-Soler and Adler, 2006). Mutation of *Pax6* in humans and overexpression of *Pax6* in mouse resulted in many phenotypes including microphthalmia (Schedl et al., 1996; Azuma et al., 1999). It has been suggested that in P19 embryonic carcinoma (P19) cells, RA induces the expression of members of the FGF and Delta families of ligands via activation of Cdc42-mTOR pathways and subsequently leads to upregulation of the expression of *Pax6* (Endo et al., 2009).

Hes1 has also been shown to be crucial in early eye development (Tomita et al., 1996; Lee et al., 2005). *Hes1* expresses in the anterior neural plate and optic vesicles, which is shown to be necessary for proper growth, morphogenesis and differentiation of these tissues (Lee et al., 2005). These expression sites coincide with that of the eye specification genes *Pax6* (Walther and Gruss, 1991; Koroma et al., 1997). It was found that in P19 cells, the presence of RA could induce neural differentiation by means of upregulation of *Hes1* expression (Wakabayashi et al., 2000).

5.2 EXPERIMENTAL DESIGN

Many studies have been conducted to examine the temporal and spatial expression patterns and physiological roles of RA synthesizing and catabolizing enzymes in early ocular development. However, not much is known if they play any role in the pathogenesis of ocular defects such as anophthalmia and microphthalmia resulted from exposure to excess RA in presomitic stages. A discussed in section 4.5, injection of RA at presomitic stages, which was E7 in ICR mice and E7.25 in C57 mice, caused ocular defects with strain differences, in which C57 strain was more susceptible to RA teratogenic insult. Since it has shown that RA can be rapidly metabolized within 3-6 hours (Satre and Kochhar, 1989), this raises a question on how such low dose of RA applied at presomitic stages, when optic primordial tissues have not yet formed, can exert its teratogenic effect in arresting ocular development that occurs 30 hours later. Hence, it is more likely that the exogenously applied RA may act on some upstream events that will subsequently affect eye development. Since in my study, the ocular defects developed in RA-treated fetuses are phenotypically similar to those found in *Raldh2* null mutant fetuses, it leads to the speculation that the exogenously administered RA may, as a negative feedback mechanism, alter the spatial and temporal expression domains of RA synthesizing enzymes. Moreover, the expression of RA catabolizing enzymes may also change as a result of distorted RA homeostasis caused by the RA insult. If these are the cases, alterations in RA regulatory enzymes may reduce the endogenous RA content and thus affect the expression of some genes crucial for early eye development such as *Pax6* and *Hes1*. Disrupted expressions of these genes in early optic primordial tissues may eventually cause failure in optic vesicle formation.

The objectives of this chapter were first to determine whether the temporal and spatial expression patterns of *Raldh2*, *Raldh3* and *Cyp26a1* during early eye development would be altered by exogenously administered RA and secondly, to determine whether ICR and C57 mouse strains would display differences in the expression levels of these RA regulatory enzymes. Thirdly, to investigate whether RA insult would alter the expression of *Pax6* and *Hes1* and therefore led to failure in optic vesicle formation.

To achieve these objectives, the expression patterns of *Raldh2, Raldh3, Cyp26a1*, *Pax6* and *Hes1* were compared between embryos of ICR and C57 mouse strains at equivalent embryonic stages by whole mount *in situ* hybridization. In doing so, the spatial and temporal mRNA expression patterns of the aforementioned genes could be visualized and analyzed comprehensively. Real-time quantitative RT-PCR was then employed to further quantify the expression levels of these genes.

Experimental Design

To study the temporal and spatial expression patterns and to further quantify the mRNA expression levels of RA-regulating enzymes (*Raldh2*, *Raldh3* & *Cyp26a1*) and early eye development genes (*Pax6* and *Hes1*) shortly after RA treatment.

Whole mount in situ hybridization and real-time quantitative RT-PCR were performed.

5.3 MATERIALS AND METHODS

5.3.1 Sample collection

C57 and ICR pregnant mice were injected with 6.25 mg/kg RA at E7.25 and E7 respectively. At various time points after RA treatment, control and RA-treated embryos of C57 and ICR mouse strains at equivalent developmental stages were collected for whole mount *in situ* hybridization or real-time quantitative RT-PCR studies.

5.3.2 Whole mount *in situ* hybridization

Embryos were dissected in DEPC-treated ice-cold PBS and freed from all decidual tissues and extraembryonic membranes. They were fixed in 4% paraformaldehyde and then processed for whole mount *in situ* hybridization as described in section 2.7. The particulars of the cDNA plasmids employed in this study are as follow:

cDNA plasmid	Insertion size (bp)	Anti-sense restriction enzyme	Anti-sense RNA Polymerase	Sources and references
Raldh2 (Aldh1a2)	2,300	Xba I	T3	Peter McCaffery (Li et al., 2000)
Raldh3 (Aldh1a3)	800	Not I	T7	Ursula Dräger (Mic et al., 2000)
Cyp26a1	600	EcoR1	T7	Hiroshi Hamada (Sakai et al., 2001)
Pax6	640	BamH I	T3	Claudia Walther (Walther and Gruss, 1991)
Hes1	1400	Hind III	T3	Ryoichiro Kageyama (Ishibashi et al., 1994)

To make a better comparison between different groups of embryos, throughout the whole process of conducting *in situ* hybridization, the head region of control ICR embryos were used as an internal control. It was achieved by adding the internal control into tubes containing the control and RA-treated embryos of both strains at equivalent developmental stages to undergo the same treatment in all procedures. The signal was then developed in NBT/BCIP solution for the same period of time after it had been fully developed. Between 16 to 41 embryos were examined in each group.

5.3.3 Real-time Quantitative RT-PCR

C57 embryos at E8.5 and ICR embryos at E8.25 were dissected in DEPC-treated ice-cold PBS and freed from all decidual tissues and extraembryonic membranes. These specific embryonic stages were selected as an initial step for mRNA quantitation of RA-synthesizing and catabolizing enzymes as well as early eye development genes. To separately quantify the relative expression levels of the gene in the head and trunk regions, embryos were cut at a virtual line perpendicular to superior boundary of the heart tube. The head and trunk portions of the control and RA-treated ICR (E8.25) and C57 (E8.5) embryos of the same litter were separately pooled together and immediately stored in RNA*later* RNA Stabilization Reagent as described in section 2.8.1. In ***Chapter 4,*** I have reported that there was morphological changes occurred at E8.5 in C57 RA-treated embryos. I speculated that the exogenous RA administration to embryos at pre-somatic stages may lead to important changes and therefore embryos at E8.5 (C57) and E8.25 (ICR) were first selected for quantitative analysis on mRNA expression level of concerned genes.

Total RNA extraction and first-strand cDNA synthesis by RT were conducted as described in sections 2.8.2 and 2.8.3 respectively.

After RT reaction, expression levels of *Raldh2*, *Raldh3* and *Cyp26a1* were determined by real-time quantitative PCR. β-actin was used as the internal control for normalization of PCR products. The PCR conditions were as described in section 2.8.4. To quantify the amount of the aforementioned genes, a set of cDNA standards was co-amplified in each PCR. The standards were prepared as described in section 2.8.5. The cDNA plasmids of mouse *Raldh2*, *Raldh3*, *Cyp26a1* and β-actin were kindly provided by Peter McCaffery, Ursula Dräger, Hiroshi Hamada and Ronald Wang respectively. The PCR products amplified were a 201 bp sequence corresponding to nucleotide sequences 886-905 and 1067-1086 of mouse *Raldh2*, a 195 bp sequence corresponding to nucleotide sequences 2851-2871 and 3027-3046 and of mouse *Raldh3*, a 221 bp sequence corresponding to nucleotide sequences 504-523 and 706-725 of mouse *Cyp26a1*, a 247 bp sequence corresponding to nucleotide sequences 1768-1787 and 1996-2015 and of mouse *Pax6*, a 188 bp sequence corresponding to nucleotide sequences 1115-1134 and 1284-1303 and of mouse *Hes1*, and a 164 bp sequence corresponding to nucleotide sequences 304-323 and 449-468 of mouse β-actin. The sequences of primers for amplification of partial sequence of the target genes were as follow:

Primer sequences

Raldh2	forward primer:	5'-TTG CAG ATG CTG ACT TGG AC-3'
	reverse primer:	5'-TCT GAG GAC CCT GCT CAG TT-3'
Raldh3	forward primer:	5'-CCA AAA TTC AGT GTC CGA AG-3'
	reverse primer:	5'-GAT AAA GTT GGG CTG AGC AA-3'

Cyp26a1	forward primer:	5'-CAG TGC TAC CTG CTC GTG AT-3'
	reverse primer:	5'-AGA GAA GAG ATT GCG GGT CA-3'
Pax6	forward primer	5'-TAC GCA AAG GTC CTT GGT TC-3'
	reverse primer	5'-GTG TCA GTT CCC GTC CAA GT-3'
Hes1	forward primer	5'-AGG CGC AAT CCA ATA TGA AC-3'
	reverse primer	5'-CTA GCC CAC CTC TCT CTT CT-3'
β-actin	forward primer:	5'-TGT TAC CAA CTG GGA CGA CA-3'
	reverse primer:	5'-GGG GTG TTG AAG GTC TCA AA-3'

After PCR, expression levels of these target genes were analyzed by ABI Prism®7000 SDS Software (*Applied Biosystems*).

The relative mRNA expression level of the target gene was presented in terms of the ratio of target gene to *β-actin* (target gene/*β-actin*). This value was calculated by dividing of the amount of target gene (ng) by the amount of β-actin (ng) detected in the sample. The quantity of gene was measured from the cDNA standard curve, plotting the log amount of plasmid against the threshold CT value.

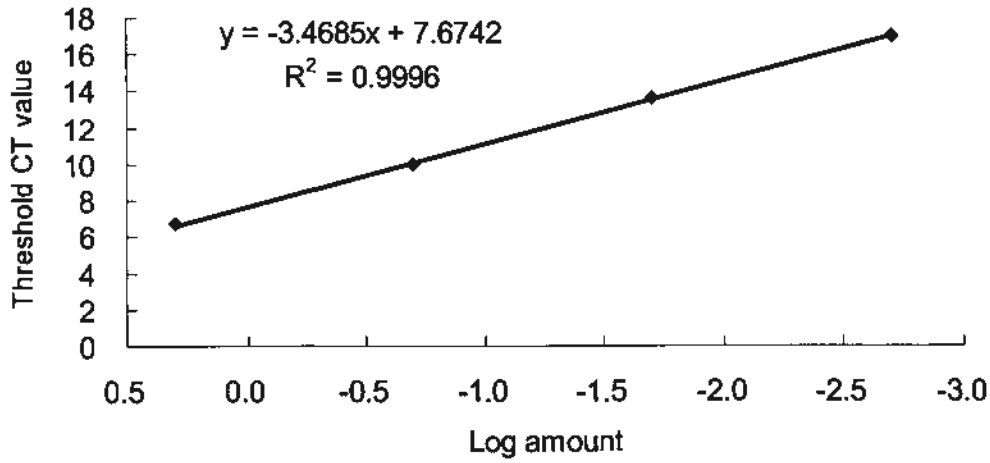

5.3.4 Statistical analysis

The relative expression levels of *Raldh2*, *Raldh3*, *Cyp26a1*, *Pax6* and *Hes1* were compared between control and RA-treated embryos of the same strain by Independent sample *t* test. Contrast test was performed to see if there was any significant difference in strain responses to the extent of RA-induced changes. All statistical analyses were carried out using SPSS (*SPSS*), with statistical significance level set at $p < 0.05$.

5.4 RESULTS

5.4.1 RA-regulatory genes

5.4.1.1 *Raldh2* expression

5.4.1.1.1 *In situ* hybridization patterns of *Raldh2*

In late headfold stage, i.e. E8, in control embryos of C57 mice, *Raldh2* was highly expressed in the whole body axis except the cephalic region (Figure 5-1 A). Similar expression domains of *Raldh2* were observed in RA-treated C57 embryos (Figure 5-1 B). Control and RA-treated embryos of ICR mice at equivalent developmental stage, i.e. E7.75, showed no difference in *Raldh2* expression domains from that of C57 embryos (Figures 5-1 C and D).

As development proceeded, in both control C57 and ICR embryos at E8.25 and E8 respectively, expression of *Raldh2* in the trunk became restricted to the somitic mesoderm, while no expression was observed in the presomitic region except at the base of the allantois (Figures 5-2 A and C).

In the cephalic region, *Raldh2* started to express in the future forebrain area where the optic primordium developed. However, RA treatment suppressed the expression of *Raldh2* in this forebrain region in C57 embryos (Figure 5-2 B), while there was no observable difference in expression levels and domains in the trunk region in comparison to the control C57 embryos (Figure 5-2 A). As for RA-treated ICR embryos, *Raldh2* did express in the forebrain region (Figure 5-2 D) but to a much reduced level when compared with control ICR embryos (Figure 5-2 B).

At E8.5, in both control and RA-treated C57 embryos, *Raldh2* continued to express at high levels in the somitic mesoderm and also at the base of the allantois (Figures 5-3 A and B). However, cranially, while *Raldh2* specifically expressed in the optic pit region there was no observable expression of *Raldh2* in the forebrain region in control C57 embryos (Figure 5-3 A) in RA-treated C57 embryos (Figure 5-3 B). As for control and RA-treated embryos of ICR embryos at equivalent developmental stage (E8.25), similar expression domains of *Raldh2* were found in the somitic mesoderm and at the base of the allantois (Figures 5-3 C and D). However, there was reduced *Raldh2* expression in the optic pit region in RA-treated ICR embryos (Figure 5-3 C) in comparison to that of control ICR embryos (Figure 5-3 D).

At E9, while expression levels of *Raldh2* in the trunk region remained high in both control and RA-treated C57 embryos (Figures 5-4 A and B), there was only low level of *Raldh2* expression at the posterior peripheral region of the optic vesicle in control C57 embryos (Figure 5-4 A). Expression of *Raldh2* in such region was barely observable in RA-treated C57 embryos (Figure 5-4 B). In ICR embryos at equivalent developmental stage (E8.75), *Raldh2* expression around the posterior optic vesicle region was also very low, although the difference between control (Figure 5-4 C) and RA-treated ICR embryos (Figure 5-4 D) was less than that between control (Figure 5-4 A) and RA-treated C57 embryos (Figure 5-4 B).

At E9.5 and E9.25 respectively for C57 and ICR embryos, the mRNA level of *Raldh2* in the trunk region remained high in both control (Figures 5-5 A and C) and RA-treated embryos (Figures 5-5 B and D). In the head region, *Raldh2*

expression was only observed in the temporal optic mesenchyme in control C57 (Figure 5-5 A) and ICR embryos (Figure 5-5 C). However, *Raldh2* expression was barely observable in this region in RA-treated C57 (Figure 5-5 B) and ICR (Figure 5-5 D) embryos.

Taken together, results of *in situ* hybridization studies showed that exogenously applied RA caused regional-specific suppression of *Raldh2* expression, particularly in tissues involved in ocular development in embryos of both strains. However, the effect of RA on the optic primordial tissues was more severe in C57 than in ICR embryos.

5.4.1.1.2 Expression levels of *Raldh2* determined by real-time quantitative RT-PCR

To further quantitatively compare the expression level of *Raldh2*, more sensitive real-time quantitative RT-PCR study was conducted to measure the expression levels of *Raldh2* in the head as well as the trunk regions of E8.5 C57 and E8.25 ICR embryos with or without RA treatment.

Head region

The relative expression levels of *Raldh2* in the head region of control and RA-treated C57 and ICR embryos are summarized in Tables 5-1 and 5-2 and presented in Graph 5-1.

Table 5-1 **Relative expression levels of *Raldh2* in the head region of ICR and C57 embryos with or without RA treatment.**

MOUSE STRAIN	ICR		C57	
Treatment group	CON	RA	CON	RA
No. of litters	5	5	5	5
No. of embryos	25	25	25	25
Relative expression levels of *Raldh2* (± SE)	0.1208 ± 0.0223	0.0838 ± 0.0128	0.0892 ± 0.0117	0.0235 ± 0.0049

Table 5-2 **Statistical analysis of relative expression levels of *Raldh2* in the head region of ICR and C57 embryos with or without RA treatment.**

Groups for comparison	*p*-value
ICR (CON) vs ICR (RA) [a]	0.015*
C57 (CON) vs C57 (RA) [a]	< 0.001*
ICR (CON) vs C57 (CON) [a]	0.028*
ICR (RA) vs C57 (RA) [a]	< 0.001*
Difference between ICR (CON) & ICR (RA) vs C57 (CON) & C57 (RA) [b]	0.049*

[a] Data were analyzed by Independent sample *t* test

[b] Data were analyzed by Contrast test

* Statistically significant

In the presence of RA, there was a 4-fold reduction in the relative expression levels of *Raldh2* in the head region of C57 embryos, which was statistically significant ($p < 0.001$) when compared with control C57 embryos. In the ICR strain, RA treatment also significantly suppressed *Raldh2* expression ($p = 0.015$). There is strain difference in the basal level of *Raldh2* in which the expression level of *Raldh2* in control ICR embryos was significantly higher than that in the control C57 embryos ($p = 0.028$). Moreover, when subject to RA treatment, the

extent of suppression of *Raldh2* expression levels in the head region of C57 embryos was statistically significantly greater than that of ICR embryos [$p = 0.049$, difference between ICR (CON) & ICR (RA) vs C57 (CON) & C57 (RA)].

Trunk region

The relative expression levels of *Raldh2* in the trunk region of control and RA-treated C57 and ICR embryos are summarized in Tables 5-3 and 5-4 and presented in Graph 5-2.

Table 5-3 Relative expression levels of *Raldh2* in the trunk region of ICR and C57 embryos with or without RA treatment.

MOUSE STRAIN	ICR		C57	
Treatment group	CON	RA	CON	RA
No. of litters	5	5	5	5
No. of embryos	25	25	25	25
Relative expression levels of *Raldh2* (± SE)	1.0429 ± 0.0733	1.0072 ± 0.0518	1.0205 ± 0.0637	0.9121 ± 0.0299

Table 5-4 Statistical analysis of relative expression levels of *Raldh2* in the trunk region of ICR and C57 embryos with or without RA treatment.

Groups for comparison	*p*-value
ICR (CON) vs ICR (RA) [a]	0.695
C57 (CON) vs C57 (RA) [a]	0.162
ICR (CON) vs C57 (CON) [a]	0.824
ICR (RA) vs C57 (RA) [a]	0.150
Difference between ICR (CON) & ICR (RA) vs C57 (CON) & C57 (RA) [b]	0.521

[a] Data were analyzed by Independent sample *t* test

[b] Data were analyzed by Contrast test

* Statistically significant

When the trunk region of the embryo was analyzed, in the absence of RA, the relative expression level of *Raldh2* was over 10 times more abundant than that in the head region of both strains. In the presence of RA, there was no statistically significant difference in *Raldh2* expression levels in the trunk regions of both strains when compared with corresponding control groups.

Hence, taken together results of whole mount *in situ* hybridization and real-time quantitative RT-PCR, it appeared that exogenously applied RA suppressed the expression of *Raldh2* in the optic primordial tissue in the head region. C57 embryos were much more susceptible to this RA induced suppression than ICR embryos.

5.4.1.2 *Raldh3* expression

5.4.1.2.1 *In situ* hybridization expression patterns of *Raldh3*

Raldh3 expression was first initiated in early organogenesis period. i.e. E8.5 of C57 and E8.25 of ICR embryos. The expression pattern of *Raldh3* was solely restricted to the future forebrain region in which a band of expression was located in the surface ectoderm overlying the posterior optic recess (Figures 5-6 A and C). However, *Raldh3* expression was greatly suppressed in RA-treated embryos. The extent of suppression was greater in C57 (Figure 5-6 B) than in ICR embryos (Figure 5-6 D).

At half a day later, *Raldh3* continued to express in the forebrain region where it expressed in the surface ectoderm overlying the optic vesicles and in the

maxillary primordium of the first brachial arch in embryos of C57 and ICR mice at E9 and E8.75 respectively (Figures 5-7 A and C). In response to exogenously administered RA, the level of *Raldh3* expression in the surface ectoderm overlying the forebrain was greatly reduced in C57 embryos, whereas in the maxillary primordium of the first brachial arch, expression could still be clearly observed (Figure 5-7 B). Similar patterns of reduction in *Raldh3* expression were also noticeable in RA-treated ICR embryos (Figure 5-7 D) but occurred to a lesser extent in comparison to RA-treated C57 embryo (Figure 5-7 B).

As development proceeded to E9.5 in C57 control embryos, more widespread domains of *Raldh3* expression were found overlying the optic vesicles (Figure 5-8 A). In control ICR embryos at equivalent developmental stage (E9.25) the expression of *Raldh3* was found to be more eccentric to the optic vesicle whereas weaker signal was detected in the central region of the optic vesicle (Figure 5-8 C). In response to RA treatment, the expression of *Raldh3* around the optic vesicle region was noticeably reduced in both C57 (Figure 5-8 B) and ICR embryos (Figure 5-8 D).

Taken together, it appeared that in response to RA, downregulation of *Raldh3* was observed in and around the optic vesicles in both C57 and ICR embryos.

5.4.1.2.2 Expression levels of *Raldh3* determined by real-time quantitative RT-PCR

To determine if there were any statistically significant differences in the expression level of *Raldh3*, control and RA-treated embryos at E8.5 of C57 and

E8.25 of ICR embryos were compared by quantitative RT-PCR. As mentioned in section 5.4.1.2.1, *Raldh3* was solely restricted to the future forebrain region, therefore the quantitation of the expression levels of *Raldh3* in the head region was conducted.

Head region

The relative expression levels of *Raldh3* in the head region of control and RA-treated C57 and ICR embryos are summarized in Tables 5-5 and 5-6 and presented in Graph 5-3.

Table 5-5 Relative expression levels of *Raldh3* in the head region of ICR and C57 embryos with or without RA treatment.

MOUSE STRAIN	ICR		C57	
Treatment group	CON	RA	CON	RA
No. of litters	5	5	5	5
No. of embryos	25	25	25	25
Relative expression levels of *Raldh3* (± SE)	0.0011 ± 0.0001	0.0008 ± 0.0001	0.0011 ± 0.0001	0.0007 ± 0.0001

Table 5-6 Statistical analysis of relative expression levels of *Raldh3* in the head region of ICR and C57 embryos with or without RA treatment.

Groups for comparison	*p*-value
ICR (CON) vs ICR (RA) [a]	0.053
C57 (CON) vs C57 (RA) [a]	0.013*
ICR (CON) vs C57 (CON) [a]	0.403
ICR (RA) vs C57 (RA) [a]	0.598
Difference between ICR (CON) & ICR (RA) vs C57 (CON) & C57 (RA) [b]	0.361

[a] Data were analyzed by Independent sample *t* test

[b] Data were analyzed by Contrast test

* Statistically significant

In C57 embryos, RA treatment resulted in statistically significant (p = 0.013) reduction of *Raldh3* expression level in the head region. Although reduced expression of *Raldh3* could also be observed in ICR embryos, the extent was not yet statistically significant (p = 0.053).

Taken together results of whole mount *in situ* hybridization and real-time quantitative RT-PCR, studies showed that C57 embryos were more susceptible to RA induced downregulation of *Raldh3* in the optic primordial tissue than that in ICR embryos.

5.4.1.3 *Cyp26a1* expression

5.4.1.3.1 *In situ* hybridization expression patterns of *Cyp26a1*

During early embryogenesis, at E8.5 in C57 embryos, *Cyp26a1* was strongly expressed in the caudal end (Figures 5-9 A and B). Cranially, low level of expression was also observed in the second rhombomere as well as in the region underlying the optic pit (Figure 5-9 A). However expressions at these cranial sites were greatly reduced in RA-treated C57 embryos (Figure 5-9 B). RA treatment also led to reduced expression in these domains in ICR embryos (Figure 5-9 D) when compared with control ICR embryos (Figure 5-9 C).

As development proceeded to E9 in control C57 embryos, other than being highly expressed in the caudal end, *Cyp26a1* expression became highly upregulated cranially in the ventral optic mesenchyme, in the first brachial arch region, in the hindbrain region and around the otic vesicles (Figure 5-10 A). Similar patterns of expression could be observed in E8.75 control ICR embryos (Figure 5-10

C). Exogenously administered RA resulted in slightly downregulated expressions of *Cyp26a1* in the ventral optic region of ICR embryo (Figure 5-10 D). However, RA administration exerted a greater reduction in *Cyp26a1* expression levels in the ventral optic region, in the first brachial arch and around the otic vesicles in RA-treated C57 embryos (Figure 5-10 B) while high level of expression was still observed in the hindbrain region.

At a half day later, *Cyp26a1* was highly expressed in both the caudal end and cranial regions of C57 and ICR embryos at E9.5 and E9.25 respectively (Figures 5-11 A and C). Moreover, RA treatment noticeably reduced the expression level of *Cyp26a1* in the cranial domains of ICR embryos (Figure 5-11 D) and to a greater extent in C57 embryos (Figure 5-11 B).

In summary, *in situ* hybridization results showed that RA treatment caused downregulation of *Cyp26a1* in the cranial region of both C57 and ICR embryos.

5.4.1.3.2 Expression levels of *Cyp26a1* determined by real-time quantitative RT-PCR

To determine if differences in expression levels of *Cyp26a1* observed by *in situ* hybridization were statistically significant, control and RA-treated embryos at E8.5 of C57 and at E8.25 of ICR embryos were compared by quantitative RT-PCR.

Head region

The relative expression levels of *Cyp26a1* in the head region of control and RA-treated C57 and ICR embryos are summarized in Tables 5-7 and 5-8 and presented in Graph 5-4.

Table 5-7 Relative expression levels of *Cyp26a1* in the head region of ICR and C57 embryos with or without RA treatment.

MOUSE STRAIN	ICR		C57	
Treatment group	CON	RA	CON	RA
No. of litters	5	5	5	5
No. of embryos	25	25	25	25
Relative expression levels of *Cyp26a1* (± SE)	0.0025 ± 0.0002	0.0022 ± 0.0001	0.0032 ± 0.0002	0.0027 ± 0.0004

Table 5-8 Statistical analysis of relative expression levels of *Cyp26a1* in the head region of ICR and C57 embryos with or without RA treatment.

Groups for comparison	*p*-value
ICR (CON) vs ICR (RA) [a]	0.630
C57 (CON) vs C57 (RA) [a]	0.021*
ICR (CON) vs C57 (CON) [a]	0.054
ICR (RA) vs C57 (RA) [a]	0.002
Difference between ICR (CON) & ICR (RA) vs C57 (CON) & C57 (RA) [b]	0.236

[a] Data were analyzed by Independent sample *t* test

[b] Data were analyzed by Contrast test

* Statistically significant

Consistent with the finding of *in situ* hybridization studies, RA treatment resulted in statistically significant downregulation of *Cyp26a1* in the head regions of C57 embryos. However, no significant difference between control and RA-treated embryos was found in the ICR strain. These results showed that C57

strain was more susceptible to RA-induced downregulation of *Cyp26a1* than ICR strain.

Trunk region

The relative expression levels of *Cyp26a1* in the trunk region of control and RA-treated C57 and ICR embryos are summarized in Table 5-9 & 10 and presented in Graph 5-5.

Table 5-9 Relative expression levels of *Cyp26a1* in the trunk region of ICR and C57 embryos with or without RA treatment.

MOUSE STRAIN	ICR		C57	
Treatment group	CON	RA	CON	RA
No. of litters	5	5	5	5
No. of embryos	25	25	25	25
Relative expression levels of *Cyp26a1* (± SE)	0.0103 ± 0.0007	0.0112 ± 0.0004	0.0112 ± 0.0003	0.0111 ± 0.0006

Table 5-10 Statistical analysis of relative expression levels of *Cyp26a1* in the trunk region of ICR and C57 embryos with or without RA treatment.

Groups for comparison	*p*-value
ICR (CON) vs ICR (RA) [a]	0.290
C57 (CON) vs C57 (RA) [a]	0.951
ICR (CON) vs C57 (CON) [a]	0.235
ICR (RA) vs C57 (RA) [a]	0.958
Difference between ICR (CON) & ICR (RA) vs C57 (CON) & C57 (RA) [b]	0.376

[a] Data were analyzed by Independent sample *t* test

[b] Data were analyzed by Contrast test

* Statistically significant

There was no significant difference in *Cyp26a1* expression levels in the

trunk region between control and RA-treated embryos of both C57 and ICR strains, suggesting that RA teratogenicity is region specific in which the cranial region shows greater susceptibility to RA than the caudal region.

5.4.2 Early eye development genes

5.4.2.1 *Pax6* expression

5.4.2.1.1 *In situ* hybridization expression patterns of *Pax6*

Being a crucial gene in eye development, *Pax6* was found to be broadly expressed cranially in the anterior neural plate of the future forebrain region as well as the optic pit in control embryos of both C57 (Figure 5-12 A) and ICR mice (Figure 5-12 C) at E8.5 and E8.25 respectively. Moreover, *Pax6* was also highly expressed in the developing somites in the trunk region. There was no obvious change in the *Pax6* expression levels and domains in the trunk region in response to RA administration in both C57 and ICR embryos (Figures 5-12 B and D). In the future forebrain region, although in a smaller domain, *Pax6* was strongly expressed in both mouse strains.

5.4.2.1.2 Expression levels of *Pax6* determined by real-time quantitative RT-PCR

Since the expression domain of *Pax6* is broad and intense in the head region of the embryos, it is difficult to quantitate the difference in expression level between the groups by the results of the whole mount *in situ* hybridization. Real-time quantitative RT-PCR study was therefore conducted to measure the expression levels of *Pax6* in the head region of E8.5 C57 and E8.25 ICR embryos with or without RA treatment. As the aim of this part was to identify whether RA treatment altered the

eye development genes, thus only the head region of the embryo was selected for quantitation.

Head region

The relative expression levels of *Pax6* in the head region of control and RA-treated C57 and ICR embryos are summarized in Tables 5-11 and 5-12 and presented in Graph 5-6.

Table 5-11 Relative expression levels of *Pax6* in the head region of ICR and C57 embryos with or without RA treatment.

MOUSE STRAIN	ICR		C57	
Treatment group	CON	RA	CON	RA
No. of litters	5	5	5	5
No. of embryos	25	25	25	25
Relative expression levels of *Pax6* (± SE)	0.234 ± 0.016	0.184 ± 0.007	0.183 ± 0.005	0.124 ± 0.004

Table 5-12 Statistical analysis of relative expression levels of *Pax6* in the head region of ICR and C57 embryos with or without RA treatment.

Groups for comparison	*p*-value
ICR (CON) vs ICR (RA) [a]	0.024*
C57 (CON) vs C57 (RA) [a]	<0.001*
ICR (CON) vs C57 (CON) [a]	0.018*
ICR (RA) vs C57 (RA) [a]	<0.001*
Difference between ICR (CON) & ICR (RA) vs C57 (CON) & C57 (RA) [b]	0.628

[a] Data were analyzed by Independent sample *t* test

[b] Data were analyzed by Contrast test

* Statistically significant

In the presence of RA, there was significant reduction in the relative

expression levels of *Pax6* in the head region of C57 embryos ($p < 0.001$). In the ICR strain, RA treatment also significantly suppressed *Pax6* expression ($p = 0.024$). There is strain difference in the basal level of *Pax6* in which the expression level of *Pax6* in the control C57 embryo was significantly lower than that in the control ICR embryo ($p = 0.018$).

5.4.2.2 *Hes1* expression

5.4.2.2.1 *In situ* hybridization expression patterns of *Hes1*

During the early stage of ocular development, i.e. E8.5 in C57 and E8.25 in ICR embryos, *Hes1* mRNA expression domain could be found in the forebrain region where high levels of expression were observed in and around the optic pit. *Hes1* was also expressed in the caudal end (Figures 5-13 C and A). However, exogenously administered RA greatly reduced the expression level of *Hes1* in the cranial sites but not the caudal domains of C57 embryos (Figure 5-13 B). Reduction of *Hes1* expression was also observed in RA-treated ICR embryos (Figure 5-13 D).

5.4.2.2.2 Expression levels of *Hes1* determined by real-time quantitative RT-PCR

It seemed that exogenous RA administration led to downregulation of expression level of *Hes1*, particularly in the head region. To determine if differences in expression levels of *Hes1* observed by in situ hybridization were statistically significant, control and RA-treated embryos at E8.5 of C57 and E8.25 of ICR embryos were compared by quantitative RT-PCR. As the aim of this part was to identify whether RA altered *Hes1* expression in the optic region, thus only the head region of the embryo was selected for quantitation.

Head region

The relative expression levels of *Hes1* in the head region of control and RA-treated C57 and ICR embryos are summarized in Tables 5-13 and 5-14 and presented in Graph 5-7.

Table 5-13 Relative expression levels of *Hes1* in the head region of ICR and C57 embryos with or without RA treatment.

MOUSE STRAIN	ICR		C57	
Treatment group	CON	RA	CON	RA
No. of litters	5	5	5	5
No. of embryos	25	25	25	25
Relative expression levels of *Hes1* (± SE)	0.379 ± 0.019	0.316 ± 0.014	0.361 ± 0.013	0.320 ± 0.007

Table 5-14 Statistical analysis of relative expression levels of *Hes1* in the head region of ICR and C57 embryos with or without RA treatment.

Groups for comparison	*p*-value
ICR (CON) vs ICR (RA) [a]	0.035*
C57 (CON) vs C57 (RA) [a]	0.027*
ICR (CON) vs C57 (CON) [a]	0.476
ICR (RA) vs C57 (RA) [a]	0.769
Difference between ICR (CON) & ICR (RA) vs C57 (CON) & C57 (RA) [b]	0.429

[a] Data were analyzed by Independent sample *t* test

[b] Data were analyzed by Contrast test

* Statistically significant

In the presence of RA, there were statistically significant reductions in *Hes1* expression levels in the head regions of both strains when compared with corresponding control groups.

5.5 DISCUSSION

The objectives of this chapter were to determine whether the mRNA expression levels of RA synthesizing and catabolizing enzymes and of early eye development gene would be changed after RA exposure in presomitic stages. Results showed that exogenously administered RA suppressed the normal expression of *Raldh2* in the head region of C57 embryos at early stages while reduced expression occurred to a lesser extent in ICR embryos. Moreover, results also showed that the expression levels of *Raldh3* and *Cyp26a1* in the head regions were all downregulated after RA-treatment, and embryos of C57 mice showed a greater sensitivity towards RA teratogenicity. As for the two early eye development genes, result showed that the expression levels of *Pax6* and *Hes1* in the cranial regions were all downregulated after exogenously administered RA.

In the embryo, the expression of *Raldh2* and *Cyp26a1* are thought to be regulated by RA and correlated with retinoid levels in the tissue (Niederreither et al., 1997; MacLean et al., 2001; Liu and Gudas, 2005; Loudig et al., 2005), therefore, I have used these genes as molecular markers to monitor the retinoid homeostasis of C57 and ICR embryos. Results showed that exogenous administration of RA to presomitic stage embryo at E7.25 first suppressed the expression of *Raldh2* in C57 embryos at E8. At E8.5, the expression of *Raldh3* and *Cyp26a1* became reduced specifically in the cephalic region. Reduced expression of *Raldh2, Raldh3* and *Cyp26a1* were also observed in the cephalic region of RA-treated ICR embryos at all stages examined, but to a lesser extent in comparison to that in C57 embryos.

These results agree with previous findings that administration of a teratogenic dose of RA to pregnant mice at E8.5 results in severe downregulation of *Raldh2* in the caudal region of the mouse embryo (Niederreither et al., 1997). Hence, it is speculated that, as a negative feedback mechanism to protect the embryo from the teratogenicity of excess RA, the exogenously applied RA may cause prolonged suppression of *Raldh2* expression to reduce endogenous RA synthesis. This may eventually lead to RA deficiency and thereby disrupt normal oculogenesis. In fact, suppression of *Raldh2* expression in the optic region at early stages is consistent with the preliminary work in our laboratory on kidney development in which we have found that a teratogenic dose of RA caused prolonged downregulation of *Raldh2* in kidney primordial tissues. Supplementation with low doses of RA after RA insult can resume kidney development (unpublished data).

RA teratogenicity is highly developmental stage-dependent. I have reported in ***Chapter 3*** that the developmental stage at which RA was injected was specifically teratogenic to the cephalic region therefore, it is not surprising that no changes in *Raldh2* expression were observed in the trunk region. Moreover, maintenance of *Raldh2* expression in the trunk region after RA treatment may also be due to higher endogenous levels of RA in this region as supported by studies on detecting RA concentrations in different regions of the embryo using the RARE-*lacZ* transgenic mice (Haselbeck et al., 1999; Mic et al., 2002; Niederreither et al., 2002).

There is functional redundancy among the different subtypes of RA synthesizing enzymes and *Raldh3* was shown to play compensatory role to

synthesize RA in *Raldh2* null mutant embryos (Mic et al., 2002; Molotkov et al., 2006). However, results in this study showed that the expression level of *Raldh3* was also down-regulated at E8.5 in the cephalic region of C57 embryos after RA treatment while such downregulation in ICR embryos occurred to a lesser extent. This finding further supports my hypothesis that exogenously administered RA can downregulate RA synthesizing enzymes and therefore may lead to RA deficiency.

Cyp26a1 expression was downregulated in the cephalic region of RA-treated C57 embryos at E8.5, but to a lesser extent in ICR embryos. This finding was consistent with previous studies in which injection of a teratogenic dose of RA to mouse embryos at early stages resulted in downregulation of *Cyp26a1* (Fujii et al., 1997). Since *Cyp26a1* contains RARE in the promoter and is a RA-responsive gene, the downregulation of *Cyp26a1* expression observed in the present study gives further support that exogenously administered RA probably leads to deficiency of endogenous RA production in the cephalic region of the embryo.

In this study it was found that there was a strain difference in susceptibility to RA teratogenicity, in which C57 mice were more sensitive to RA-induced downregulation of RA synthesizing and catabolizing enzymes. If such suppression of *Raldh2* expression and downregulation of *Raldh3* are contributory to depletion of RA synthesis, it may lead to more severe RA deficiency, as indicated by downregulation of *Cyp26a1* expression, and can therefore subsequently affect oculogenesis more extensively in C57 mice than in ICR mice. Thus it may provide a clue to explain why the C57 mouse strain shows higher susceptibility to RA-induced eye defects than the ICR mouse strain. If this is the case, it gives further insight into

understanding the mechanisms of how deficiency and excess of RA can both lead to ocular malformations. Indeed, in our laboratory, we have demonstrated that excess RA could disrupt kidney development and led to defects that were phenotypically similar to those caused by vitamin A deficiency (Tse et al., 2005).

RA itself is a key morphogen. A proper spatiotemporal gradient of RA concentrations in corresponding tissues to timely control the onset of developmental genes is required for early eye development (Morriss-Kay and Ward, 1999; Ross et al., 2000; Mark et al., 2006; Luo et al., 2006). Hence, downregulation of *Raldh2* and subsequent depletion of endogenous RA may disrupt gene actions that are essential for oculogenesis. This study revealed that downregulation of *Raldh2* and *Raldh3* was accompanied by downregulation of *Pax6* in the head region of embryos of both strains. In fact, other studies have reported that *Pax6* and other important transcription factors for eye development were still normally expressed but in a lesser extent and smaller domain in the optic vesicle in the absence of RA signalling in *Raldh2* single and *Raldh2/Raldh3* double null mutant embryos (Mic et al., 2004; Halilagic et al., 2007), which is consistent with the finding of the present study. Apart from downregulated *Pax6* expression levels, exogenous RA-induced downregulation of *Hes1*. Previous studies showed that the phenotypes of *Pax6* and *Hes1* single null mutants are microphthalmia (Schedl et al., 1996; Tomita et al., 1996) whereas *Pax6/Hes1* double null mutants are anophthalmia (Lee et al., 2005). It is therefore very possible that the underlying mechanism of RA-induced anophthalmia and microphthalmia is associated with the extent of downregulation of both *Pax6* and *Hes1*.

Taken together the results of this study, it is concluded that there is a strain difference in susceptibility to RA-induced developmental ocular defects in which RA homeostasis is being altered in a strain-specific manner. This study may also provide insight into the mechanisms of how exogenously applied RA can lead to endogenous RA deficiency and thus may explain why both excess and deficiency of RA can lead to ocular malformations with comparable phenotypes. Moreover, RA-induced developmental ocular defect is associated with downregulation of *Pax6* and *Hes1* expression levels. To further elucidate this hypothesis, in the following chapter, I have investigated whether downregulation of *Raldh2* and *Raldh3* caused by exogenously applied RA led to depletion of endogenous RA.

CHAPTER 6

Exogenously Administered RA Causes Endogenous RA Deficiency

6.1 INTRODUCTION

As mentioned in ***Chapter 1***, homeostatic distribution of endogenous RA in the embryo relies on well-coordinated interplay between RA synthesizing and catabolizing enzymes. I have shown in ***Chapter 5*** that exogenous administration of RA to embryos at the presomitic stage resulted in reduced mRNA expression of the key RA synthesizing enzymes, *Raldh2* and *Raldh3,* in the head region, with C57 embryos showing a greater teratogenic response to RA than ICR embryos. This might lead to RA deficiency, as indicated by downregulation of *Cyp26a1*, an RA-inducible enzyme. Particularly, embryos of C57 strain showed downregulation of *Cyp26a1* to a greater extent than those of ICR strain. These results provide strong support to our hypothesis that exogenously administered RA may lead to insufficient production of endogenous RA. To determine if this hypothesis is correct, it is essential to measure the concentration of endogenous RA in embryos that have or have not been treated with an exogenous dose of RA.

Rossant et al. (1991) developed a transgenic reporter mice for visualizing the distribution of endogenous RA in the embryo. These transgenic mice carry a construct composed of a RARE upstream of the reporter β-galactosidase. These mice express β-galactosidase in cells that contain activated RARs and thus the *in situ* distribution of RA in the embryo can be visualized by staining for β-galactosidase activity to change the substrate X-gal into a colored product. Hence, the higher the concentration of endogenous RA, the more intense the colored product in the corresponding regions. Many previous studies using this RARE-*lacZ* transgenic mice have reported that regions expressing *Raldh1*, *Raldh2*, or *Raldh3* are

superimposable with regions expressing β-galactosidase throughout embryonic development (Moss et al., 1998; Mic et al., 2002; Mic et al., 2004; Molotkova et al., 2007).

To determine the endogenous RA concentration in the embryo, several methods have been developed. High pressure liquid chromatography (HPLC) is the most commonly used method to detect RA concentrations in different organs of adult tissues (Hupert et al., 1991; Pappas et al., 1993; Kane et al., 2005) as well as embryonic tissues (Maden et al., 1998; Sakhi et al., 1998; Hoover et al., 2001). Using HPLC analysis, the level of endogenous all-*trans* RA and all-*trans* retinol in the mouse embryo at E9 was found to be 76 pg and 279 pg per embryo respectively (Sakhi et al., 1998). However, this level of RA is close to the detection limit. To overcome this limitation, a large amount of embryonic tissues is therefore required. This analytical method is very labor intensive and of relatively poor sensitivity, which makes the determination of endogenous RA concentrations in embryos at early stages infeasible. As shown by the RARE-*lacZ* transgenic embryos, the distribution of endogenous RA is not homogenous in the embryo. In fact, the spatial distribution of endogenous RA can be differentially localized within the same organ. For instance, the concentration of RA in the ventral embryonic retina is higher than that of the dorsal portion (McCaffery et al., 1992). Moreover, it is well-known that there is a RA concentration gradient in the embryonic central nervous system, with higher levels being found in the developing neural tube and very low levels in the forebrain (Horton and Maden, 1995). Thus, it is infeasible to measure the spatial distribution of endogenous RA in the embryo by using HPLC. This problem has been circumvented recently by the development of high pressure liquid

chromatography/mass spectrometry (HPLC/MS) which has higher sensitivity and specificity. By using HPLC/MS, McCaffery et al. (2002) reported that the concentration of endogenous RA in the retina of the mouse embryo at E15 was about 20.75 pg/μg protein. However, although sensitive, this method is very expensive.

Apart from the abovementioned analytical methods, RA-responsive cell lines have also been extensively employed for detecting RA distribution in the embryo. In a study where the ectoderm of the head region of mouse embryos at E9.5 was directly placed on top of the RA-responsive cell line, RA bioavailability was readily detectable in the surrounding edges of the co-cultured tissues (Enwright, III and Grainger, 2000). However, this qualitative method of determining endogenous RA cannot provide quantitative comparison of different tissue types. Moreover, the efficacy of this method is entirely reliant on how well the tested samples can adhere to the cell line throughout the experiment. To utilize these cell lines and to overcome the abovementioned technical problems, in this chapter, I have employed an *in vitro* bioassay method to determine the endogenous RA concentrations in the embryonic head, which contains a low level of RA (Horton and Maden, 1995).

6.2 EXPERIMENTAL DESIGN

The aim of this chapter was to determine whether reduced expressions of *Raldh2* and *Raldh3* in the head region would eventually lead to endogenous deficiency of RA in the corresponding region.

The RA responsive cell line was kindly provided by Prof. Peter McCaffery (University of Aberdeen, U.K.). Our laboratory has previously conducted a comprehensive characterization of the cell line (Lee, 2007). Based on this information and together with other established protocols (Yamamoto et al., 2000; Mey et al., 2001), I have further fine-tuned an *in vitro* bioassay method to compare the endogenous RA concentrations in the head regions of C57 and ICR embryos that had or had not been exposed to an exogenous dose of RA.

Head explants of C57 embryos at E8.5 and ICR embryos at E8.25 of both control and RA-treated groups were harvested. Since only trace amounts of endogenous RA were present in the head region, a large number of embryonic tissues were used in order to overcome the detection limit of the RA responsive cell line.

Experimental Design

To study whether endogenous RA levels showed any changes after RA treatment, head explants of C57 (E8.5) and ICR (E8.25) embryos of control and RA-treated groups were harvested

Endogenous RA level of each group was quantitated by the RA-responsive cell line.

6.3 MATERIALS AND METHODS

A RA responsive cell line, derived from the F9 teratocarcinoma cell line that has been stably transfected with the β-galactosidase gene, was used to determine the concentration of endogenous RA in the head explants. The expression of β-galactosidase in this RA responsive cell line is under the control of the RARE of RAR_β (Wagner et al., 1992) and different levels of β-galactosidase is expressed in response to different concentrations of RA.

6.3.1 Cell culture

Cells stored under liquid nitrogen was thawed in a water bath at 37°C. Once thawed, cells were pipetted out and added to 10 ml of Hanks' medium (*Gibco*) to dilute the toxic effect of dimethyl sulfoxide (DMSO) in the freezing medium. The cell suspension was centrifuged at 3,000 rpm for 3 minutes. The supernatant was discarded and the cell pellet was resuspended in 5 ml of culture medium [Dulbecco's Modified Eagle's Medium (DMEM, *Gibco*) supplemented with 10% fetal bovine serum (*Gibco*), 2 mg/ml G418 (*Sigma*), 100 units/ml penicillin G (*Sigma*) and 0.1 mg/ml streptomycin (*Sigma*)]. Prior to seeding, a 25 cm^2 culture flask (*Nunc*) was precoated with gelatin. This was achieved by covering the bottom of the culture flask with a 0.1% gelatin solution for half an hour and then washed with Hanks' medium immediately prior to use. Cells at a density of 4×10^4 cells were cultured on the gelatin-coated culture flask in a 5% CO_2 incubator at 37°C for 24 to 30 hours.

To detach cells from the surface of the culture flask, cells were incubated with 3 ml of 0.05% trypsin in Hanks' medium at 37°C for 1 minute. The reaction

was stopped by mixing the cell suspension with 10 ml of culture medium. The cell suspension was centrifuged at 3,000 rpm for 3 minutes. The supernatant was discarded and the cell pellet was resuspended in culture medium. The cell density was then determined by cell counting using a hematocytometer.

6.3.2 Seeding onto a 96-well plate

Ninety-six well plates (*Nunc*) were precoated (as described above) in gelatin prior to use. Cells were seeded at a density of 4 $x10^4$ cells in 100 µl of culture medium per well and allowed to grow until they reached 80% confluence (usually within 16 hours of incubation after seeding).

To analyze the relative amount of RA in the embryo extract, 90 µl of the RA containing sample was added to each well as described below in section 6.3.4

6.3.3 Collection and storage of samples

ICR and C57 pregnant mice were injected with 6.25 mg/kg RA on E7 and E7.25 respectively. Embryos from control and RA-treated ICR and C57 mice at E8.25 and E8.5 respectively were dissected out in ice-cold L15 medium (*Gibco*) in a dark room under dim red light. Head explants of embryos at 8-10 somite stage were harvested according to the cutting site mentioned in section 5.3.4.1 and collected into a 1.7 ml microfuge tube. The head explants were washed 2 times with L15 medium. The L15 medium was removed as much as possible. To avoid the tissues from being oxidized, the microfuge tube containing the tissue was gassed with pure nitrogen. The tube was immediately sealed with parafilm and wrapped with

aluminum foil, then snap frozen in liquid nitrogen. Samples were stored at -80°C until used.

6.3.4 Extraction of endogenous RA

Twenty head explants were pooled together into a new microfuge tube. One hundred microlitre of DMEM medium containing 10% FBS was added to each tube. To block endogenous CYP26-mediated enzymatic degradation of RA during the extraction process, 100 nM of R115866, (1 μl of 5 μM stock solution in DMEM, a gift from Johnson and Johnson) (Stoppie et al., 2000), a highly potent CYP26 inhibitor, was added to the medium. To obtain the endogenous RA, the head explants were lysed by trituration with a 20 μl pipette tip until homogenous. Tissues were then incubated in a 5% CO_2 incubator at 37°C for 6 hours in dark, with gentle shaking by hand on hourly basis, to allow adequate time for RA to be released into the medium. After incubation, the samples were centrifuged at 1,500 rpm for 5 minutes in order to remove tissue flakes. Ninety microlitre of the supernatant of each sample was added to a single well of a 96-well plate grown with RA responsive cells. Cells were incubated in a 5% CO_2 incubator at 37°C for 18 hours to allow transcriptional activation of the β-galactosidase reporter gene.

For both C57 and ICR embryos, head explants of 20 embryos were pooled together to obtain sufficient amount of endogenous RA in medium. Five trunk explants of embryos were randomly collected and used as the internal positive control. Medium without tissues served as the negative control.

6.3.5 Preparation of RA stock solution

The protocol used in this part was adopted from Lee (2007). All of the following procedures were carried out in a safety cabinet for tissue culture under dim red light which prevent *all-trans* RA from photo-degradation. To make a 100 mM *all-trans* RA stock solution, DMSO (*Sigma*) at a volume of 1.66 ml, was added to 50 mg of all-trans RA. All stock solution in 30 µl aliquots then gassed with nitrogen and then snap frozen in liquid nitrogen. The aliquots were kept in microfuge tubes sealed with parafilm and wrapped with aluminum foil. It was stored at -80°C and used within 2 months.

6.3.6 Preparation of RA standard solutions

Serial dilution was by diluting the 100 mM RA stock solution to 10^{-5} M following the procedures as shown in Table 6-1. After that, RA standard solutions from 10^{-6} M to 10^{-15} M were obtained by 10-fold serial dilution with culture medium in a stepwise manner to prevent precipitation.

Table 6-1 Procedures for preparation of RA standard solutions in DMSO.

Final concentration of RA	Volume of RA solution	Volume of DMSO	Volume of culture medium
10 mM	10 µl of 100 mM RA	90 µl	-----
1 mM	10 µl of 10 mM RA	90 µl	-----
500 µM	50 µl of 1 mM RA	-----	50 µl
10 µM (10^{-5} M) *	20 µl of 500 µM RA	-----	980 µl
10^{-6} - 10^{-15} M	10-fold serial dilution with culture medium		

* RA solution in 1% DMSO

6.3.7 Staining of cells

The activity of β-galactosidase to convert the substrate 5-bromo-4-chloro-3-idolyl-β-galactopyranoside (X-gal, *Gibco*) into a coloured product allowed quantification of the induction level of β-galactosidase. Cells were fixed with 1% glutaraldehyde in PBS for 10 minutes at room temperature and then washed 3 times with 200 µl of 0.1 M PBS. They were then incubated with 70 µl (per well) of staining solution [0.1 M PBS containing 3.3 mM $K_4Fe(CN)_6 \cdot 3H_2O$, 3.3 mM $K_3Fe(CN)_6 \cdot 3H_2O$, 6 mM $MgCl_2$ and 2 mg/ml X-gal (*Gibco*, dissolved in dimethyl formamide as 40 mg/ml aliquots)] for 16 hours at 37°C. The staining solution was removed. Cells were washed 3 times with 200 µl of 0.1 M PBS. One hundred microlitre of 75% glycerol was added to each well. The level of transcriptional activation of the β-galactosidase reporter gene was quantified by measuring the OD at 650 nm using an ELISA plate reader (SpectraMax25, *Biomolecular Device*).

6.3.8 Statistical analysis

Endogenous RA concentrations in head explants of embryos of same strains with or without maternal RA treatment as well as control groups of both strains were tested by Independent sample *t* test. Contrast test was performed to see if there was any significant difference in strain responses to the extent of RA-induced RA deficiency. All statistical analyses were carried out using SPSS (*SPSS*), with statistical significant level sought at $p < 0.05$.

6.4 RESULTS

To determine whether exogenously administered RA could eventually lead to deficiency of endogenous RA in the head region of embryos, endogenous RA concentrations in head explants of control and RA-treated embryos of C57 and ICR mice at E8.5 and E8.25 respectively were compared. Results were shown in Tables 6-2 and 6-3 and presented in Graph 6-1.

Table 6-2 Endogenous RA concentrations in head explants of ICR and C57 embryos with or without exogenous RA treatment.

MOUSE STRAIN	ICR		C57	
Treatment group	CON	RA	CON	RA
No. of litters	11	13	15	17
No. of embryos	100	100	60	60
No. of samples †	5	5	3	3
RA concentrations per sample (nM ± SE)	0.0269 ± 0.00115	0.0174 ± 0.00118	0.0208 ± 0.00098	0.0101 ± 0.00187

† 20 head explants per sample

Table 6-3 Statistical analysis of endogenous RA concentrations in head explants of ICR and C57 embryos with or without exogenous RA treatment.

Groups for comparison	*p*-value
ICR (CON) vs ICR (RA) [a]	< 0.001*
C57 (CON) vs C57 (RA) [a]	0.007*
ICR (CON) vs C57 (CON) [a]	0.012*
ICR (RA) vs C57 (RA) [a]	0.011*
Difference between ICR (CON) & ICR (RA) vs C57 (CON) & C57 (RA) [b]	0.655

[a] Data were analyzed by Independent sample *t*-test

[b] Data were analyzed by Contrast test

* Statistically significant

Results showed that after exogenous administration of RA, the endogenous RA concentration in the head region of C57 embryos were significantly reduced when compared with that of control embryos [p = 0.007, C57 (CON) vs C57 (RA)].

Exogenously administered RA also resulted in statistically significant reduction in the endogenous RA concentration in the head region of ICR embryos when compared with that of control embryos [$p < 0.001$, ICR (CON) vs ICR (RA)].

Moreover, the endogenous RA concentration in the head region of control C57 embryos was statistically significantly lower than that of control ICR embryos [p = 0.012, ICR (CON) vs C57 (CON)] suggesting that there is strain difference in basal level of endogenous RA concentrations.

There was no significant difference between the extent of reduction in endogenous RA concentrations in the head region of C57 embryos than that in ICR embryos when subjected to an exogenous teratogenic dose of RA [p = 0.655, ICR (CON) & ICR (RA) vs C57 (CON) & C57 (RA)]. Despite this, there was about 35% reduction of endogenous RA concentrations in the head region of ICR embryos after RA treatment. However, RA insult resulted in about 51% reduction in endogenous RA concentrations in the head region of C57 embryos, suggesting that exogenous RA administration causes greater impact on C57 strain.

6.5 DISCUSSION

The aim of this chapter was to examine whether exogenous administration of a teratogenic dose of RA would subsequently lead to a deficiency in endogenous RA and whether there was any strain difference. Indeed, I have found that the basal level of endogenous RA concentrations in the head region of control C57 embryos is significantly lower than that of control ICR embryos. Moreover, I have found that exogenous administration of RA could cause a significant reduction in endogenous RA concentrations in the head region of both C57 and ICR embryos. However, there is no strain difference in the extent of reduction.

To my knowledge, this is the first report to show that exogenous administration of RA to pregnant mice can subsequently lead to embryonic RA deficiency. These results are consistent with findings in ***Chapter 5*** that there were reduced expressions of *Raldh2* and *Raldh3* in the head region of RA-treated embryos. Moreover, the extent of reduction of *Raldh2* in C57 embryos was more severe than that in ICR embryos. Furthermore, results of this chapter show that the endogenous RA level in the head region of control C57 embryos is significantly lower than that of control ICR embryos, which corresponds very well with the finding in ***Chapter 5*** that the expression level of *Raldh2* in the head region of C57 embryos is significantly lower than that of ICR embryos (Tables 5-1 and 5-2). These strain differences in *Raldh2* expression level and endogenous RA concentrations may shed light on understanding the pathogenic mechanisms of why C57 embryos are more susceptible to RA-induced ocular defects. RA itself is crucial for ocular development (Chow and Lang, 2001). The lower the basal expression level of

Raldh2 and endogenous RA concentrations in the head region of C57 embryos, the higher the chance to develop spontaneous ocular defects.

The RARE-*lacZ* transgenic mouse has been widely employed for visualizing the spatial distribution of endogenous RA under normal and abnormal circumstances (Niederreither et al., 2002; Matt et al., 2005; Molotkov et al., 2006; Halilagic et al., 2007). For instance, there was a study that employed the RARE-*lacZ* mouse to examine the individual and combinational biological functions and functional redundancy of *Raldh1, Raldh2* and *Raldh3* in the formation of the retina. It was found that *Raldh1*, *Raldh2* and *Raldh3* single, double and triple null mice exhibited progressively less or no RA synthesis in the eye (Molotkov et al., 2006). It seems that this transgenic mouse may be suitable for examining detailed spatial and temporal patterns of distribution of endogenous RA in the embryo in response to exogenous RA administration. However, once RA molecules bind to RAR, the complex will bind to the RARE and lead to transcription of the downstream gene *β-galactosidase*. It will then be translated into β-galactosidase protein and present in the cytoplasm. As it would take some time for β-galactosidase protein to return to base level, therefore, whether this transgenic mouse strain is suitable for registering endogenous RA level after the teratogenic insult remains questionable.

It is well-documented that in humans, both excess intake and deficiency of RA are associated with ocular malformations such as microphthalmia (Mic et al., 2004; Ribes et al., 2006). However, the underlying pathogenic mechanism remains unclear. I have reported in ***Chapter 5*** that exogenously administered RA suppressed the expression of *Raldh2* and *Raldh3* in the head region of embryos and in this

chapter, I have shown that such suppression of RA-synthesizing enzymes was accompanied by a reduction in RA concentrations. These results support my hypothesis that a teratogenic dose of RA may subsequently lead to endogenous RA deficiency, and shed light on why excess intake and deficiency of RA can both result in the same type of ocular defect. It is speculated that exogenous RA administration would not lead to a reduction in endogenous RA concentrations in the trunk region of the embryos as no suppression of *Raldh2*, being the sole RA-synthesizing enzymes in the trunk region, can be found in there.

Apart from ocular defects, our laboratory also demonstrated that maternal administration of a teratogenic dose of RA could cause kidney malformations that closely resemble those found in cases of vitamin A deficiency (Tse et al., 2005). Moreover, it was found that after RA treatment, there was prolonged downregulation of *Raldh2* in the kidney primordial tissues, but supplementation with low doses of RA could restore normal kidney development (unpublished data). Hence, it is very possible that deficiency of endogenous RA also occurs in the kidney primordial tissues after the RA insult.

Some groups have suggested that different mechanisms underlie the generation of similar malformations by RA excess and deficiency. For instance, with respect to the early development of the brachial arches, Mark et al. (2006) suggested that RA in excess and RA deficiency did not disrupt or share identical cellular and molecular mechanisms in causing defects in the formation of brachial arches. Exposure to excess RA at E8 resulted in hypoplasia of the first two brachial arches (Matt et al., 2003) whereas antagonizing the RA signal induced hypoplasia of the

third to the sixth brachial arches without altering the development of the first two brachial arches (Wendling et al., 2000). Since RA teratogenicity is highly developmental stage- and tissue-dependent, the underlying mechanisms of how RA excess and deficiency cause similar malformations maybe entirely different, depending on the tissue and the developmental stage when RA insult occurs. However, no matter whether or not RA excess and deficiency caused ocular defects by the same mechanism, results of the present study support that RA teratogenicity can be mediated by exogenous RA-induced endogenous RA deficiency.

CHAPTER 7

Conclusion and Future Perspectives

It is well-known that in humans, both excess intake and deficiency of vitamin A or RA during pregnancy are associated with ocular malformations such as microphthalmia (Yasuda et al., 1986; Rothman et al., 1995; Niederreither et al., 1999; Dupe et al., 2003; Mic et al., 2004; Ribes et al., 2006; Niederreither and Dolle, 2008). However, the underlying pathogenic mechanisms of how these two contrasting conditions of vitamin A or RA can cause the same type of ocular defects are far from clear. The aim of this thesis is to study the pathogenesis of RA-induced developmental ocular defects using mouse models.

To achieve this, in ***Chapter 3***, I have employed two mouse strains as the animal models, they are C57 mice that spontaneously develop ocular defects (Smith et al., 1994) and ICR mice, which are not prone to developing ocular defects (Sulik et al., 1995). By conducting detailed time and dose response studies on pregnant mice and examining the eye defects in near-term fetuses, I have found that in response to RA treatment, the frequency of the most severe ocular defects, i.e. anophthalmia and microphthalmia, was significantly higher for C57 fetuses, indicating that the C57 strain was more susceptible to RA-induced ocular defects than the ICR strain. Next, I have examined different factors that could be responsible for this strain difference. Since RA teratogenicity is highly developmental stage-dependent (Shenefelt, 1972; Simeone et al., 1995), therefore I have first investigated if any difference in developmental stages exist between these two mouse strains. Indeed, I have found that ICR embryos developed approximately 6 hours ahead of C57 embryos at the time of RA treatment as well as all embryonic stages examined in this study. Hence, C57 embryos receiving RA injection at E7.25 should be compared with ICR embryos at the corresponding stage, i.e. at E7.0.

However, even when fetuses of the two mouse strains were compared at equivalent developmental stages, C57 fetuses were still 3 times more prone to developing ano/microphthalmia than ICR fetuses. Hence, the factor of differences in the developmental stage in causing differential strain susceptibility to RA-induced ocular defects can be excluded. Next, I have investigated whether genetic predisposition and maternal factors are involved in causing differential strain susceptibility. This was achieved by comparing the frequency of RA-induced anophthalmia and microphthalmia in heterozygous fetuses obtained from reciprocal matings between C57 and ICR mice with that in homozygous ICR and C57 fetuses. It was found that the C57 genotype, from paternal or maternal origin, can significantly increase the frequency of ocular defects in heterozygous fetuses in comparison to that of ICR homozygous fetuses, suggesting that C57 has genotypic dominance in causing fetuses more susceptible to ocular defects upon RA treatment. Apart from exerting genotypic dominance, I have also demonstrated that C57 has exhibited maternal effects in significantly enhancing the susceptibility of embryos to RA-induced ocular defects. Taken together, the result of ***Chapter 3*** demonstrated that C57 mice have genotypic dominance and maternal effects in causing fetuses more susceptible to RA-induced ocular defects than ICR mice. On the other hand, difference in developmental stages of embryos does not contribute to strain difference in susceptibility to RA teratogenicity.

To follow on, in ***Chapter 4***, I have evaluated whether RA treatment caused early changes with strain differences in C57 and ICR embryos. First I have demonstrated that RA caused developmental retardation in both mouse strains. Moreover, by gross morphological, histological and SEM examinations, it was

found that RA treatment reduced the size of the anterior neural plate and altered the formation of optic primordial tissues, including the optic pit and optic vesicle. There were much less mesenchymal cells under the neural fold of the future forebrain that became underdeveloped. All these features were observed in embryos of both strains, but C57 embryos were more severely affected. However, no abnormal pattern of apoptosis was observed in RA-treated embryos of both ICR and C57 strains.

Since the types of spontaneous eye defects developed in C57 mice mimic those caused by excess or deficiency of RA, this leads to the speculation that differences in RA-associated mechanisms may be involved in causing differential strain response to RA-induced ocular defects. To prove this hypothesis, in ***Chapter 5***, I have demonstrated that exogenously administered RA suppressed the normal expression of *Raldh2* and *Raldh3* in the head region, but not in the trunk, of C57 embryos at early stages (E8.5), while reduced expression also occurred in ICR embryos (E8.25) but to a lesser extent. This finding supports my hypothesis that exogenously administered RA can downregulate RA synthesizing enzymes and therefore may lead to RA deficiency. Being an RA-inducible gene, *Cyp26a1* downregulated to a greater extent in the head region of RA-treated C57 embryos than that of ICR embryos, further supporting that deficiency of endogenous RA production may exist after exogenous administration of RA.

Though RA treatment resulted in downregulation of *Pax6* and *Hes1* in the head region of embryos of both strains, it is still unclear how alteration in RA regulatory mechanisms may eventually lead to failure of optic primordial tissues formation. In fact, many of the early eye development genes are expressed in both

optic primordial tissues as well as the forebrain, which makes the analysis of gene expression profile more difficult because of their co-expression in broad domains. In fact, other early eye development genes such as *Otx2* (Ragge et al., 2005; Hever et al., 2006) and *Rx* (Mathers et al., 1997) have been demonstrated to play important roles in normal ocular development and their expressions are localized in the optic regions only. Mutation of these genes in humans resulted in congenital eye defects (Hever et al., 2006). Hence, further investigation on how RA treatment leads to ocular defects by studying the expression profile of these genes is needed.

To further elucidate the abovementioned hypothesis on endogenous RA deficiency, in ***Chapter 6***, I have found that exogenous administration of RA indeed could subsequently lead to RA deficiency in the head regions of the embryos with C57 embryos showing a greater extent of reduction in RA concentrations. These results provide strong support in favor of the hypothesis that exogenously administered RA, possibly as a feedback mechanism via suppressing the expression of RA synthesizing enzymes, leads to insufficient production of endogenous RA, which as a result, leads to failure in oculogenesis. In ***Chapter 4***, no abnormal pattern of apoptosis was found in the future forebrain region of embryos of early stages (E8/8.5 of C57 and E7.75/E8.25 of ICR). Interestingly, there is no observable abnormal cell death in the future forebrain region in *Raldh2* null mutant embryos in early stages (Niederreither et al., 2000; Niederreither et al., 2002; Ribes et al., 2006). Although RA supplementation to *Raldh2* null mutant embryos is needed to prevent embryolethality in mid-gestation, Molotkova et al. (2007) found that such supplementation of RA did not stimulate RA activity in the forebrain region. Hence, the finding of no abnormal cell death observed in the forebrain region of embryos in

my study is very comparable to what has been identified in *Raldh2* null mutant embryos, suggesting that apoptosis apparently is not directly involved in the pathogenic pathway of RA-induced ocular defects in my mouse models.

The finding that exogenous administration of RA caused endogenous RA deficiency in the head region of embryos of C57 and ICR strains is consistent with the suppression of *Raldh2* and *Raldh3* expressions caused by RA treatment. As discussed earlier, previous reports showed that maximum RA concentration in the embryo was attained 3 hours after administration and that RA levels returned to pre-treatment level by 8 hours, indicating that the effect of RA administration can only last for a very short period of time (Satre and Kochhar, 1989). RA itself is a highly diffusible molecule and its morphogenic action can be mediated via nearby tissues in paracrine manner (McCaffery and Drager, 2000; Matt et al., 2005). The earliest time of expression of *Raldh2* in the head region of C57 and ICR embryos is at E8.25 and E8 respectively. It is not known whether exogenous RA-induced endogenous RA deficiency is already in place well before the onset of *Raldh2* expression in the head region, i.e. on or before E8 and E7.75 of C57 and ICR embryos respectively. If this is the case, it can reduce the endogenous RA level in the posterior part of the embryo at very early stage and subsequently interfere with the RA level in the anterior part of the embryo which should be synthesized on time and in place to initiate normal eye development. Hence, future work should be carried out to investigate a detailed time profile of exogenous RA-induced endogenous RA deficiency in embryos of early stages. It would be a great asset to understand this unknown mysterious window.

Although this information is not available at present, it will be expected that it is related to the altered repression of RAR in early gastrula stage at which RA treatment is received. Niederreither and Dolle (2008) reviewed that in early gastrula stage, the presence of *Cyp26a1* and *Cyp26c1* in the anterior tissues is required to prevent premature activation of RARs which are in repressed state. To provide a harmonic environment for proper head structure formation, RARs in the anterior region must stay in repressed status. In my hypothesis, transient upsurge of endogenous RA due to exogenous RA administration at this stage can inappropriately activate the RARs that normally function as transcriptional repressors in the anterior region of the embryo. This premature activation of RARs in the anterior region of the embryo may thus alters the FGF and WNT signalling (Beddington and Robertson, 1998;Weinstein and Hemmati-Brivanlou, 1999). In fact, these pathways have been suggested to be regulator for *Raldh2* onset (Olivera-Martinez and Storey, 2007) and therefore, it could suppress the normal onset of *Raldh2* in the head region of C57 and ICR embryos at E8.25 and E8 respectively and *Raldh3* afterwards. Future work in an attempt to examine whether exogenous RA treatment can lead to alteration in FGF and WNT signalling will be of interest to understand the underlying mechanisms.

To this end, the severity of ocular defects caused by RA treatment can be accounted by the duration of RA deficiency, in which exposure to RA at earlier gestational day resulted in the less severe microphthalmia rather than the most severe anophthalmia (***Chapter 3***). It is speculated that premature activation of repressed RAR in the anterior region of the embryo by exposure to RA at earlier gestational day may not be that critical as those exposed to RA at later gestational

day. This is probably because there may be adequate time for RA degradation by *Cyp26a1* and *Cyp26c1* in the anterior region of the embryo and thus may not affect the onset of *Raldh2* and thus the subsequent RA deficiency.

However, other than anophthalmia / microphthalmia, RA treatment also resulted in a wide spectrum of congenital ocular defects in embryos including defects in the anterior eye chamber. The lens, cornea and eyelids start to develop after the successful formation of the optic cup, i.e. from E10 onwards. It would be expected that any malformations of these ocular structures may take place only after formation of the optic cup and therefore exogenous RA-induced endogenous RA deficiency may not be applicable in this regard. In fact, several mechanisms have been proposed for RA teratogenicity, such as excessive cell death, distorted cell proliferation and migration as well as disorganized induction and they can contribute to the induction of ocular defects in the anterior eye chamber after RA treatment.

Other than ocular defects, C57 is shown to be prone to have forelimb ectrodactyly. Shimizu et al. (2007) found that following maternal RA administration, gene-specific perturbations were observed in the C57 limb bud (such as *Fgf8, Bmp4*) whereas these genes were normally expressed in the SWV limb bud, indicating that C57 does exert genetic factors in this regard. However, endogenous RA homeostasis in response to exogenous RA was not different between the two strains as no strain-specific changes in the RA-synthesizing and degrading enzymes at the transcriptional level was found, suggesting that exogenous RA-induced endogenous RA deficiency may not be applicable to it.

Indeed, in our laboratory, it was found that there was prolonged downregulation of *Raldh2* in kidney primordial tissues after RA insult. With supplementation of low doses of RA, it could restore normal kidney development (unpublished data). It will be worthwhile to investigate whether supplementation with low doses of RA within the physiological range at an early stage, e.g. at about E7.5 and E7.25 of C57 and ICR embryos respectively, can also alleviate the occurrence of ocular defects to provide further evidence for the hypothesis of exogenous RA-induced endogenous RA deficiency in embryos after RA treatment.

Over the past few decades, the importance of eating a balanced diet of vitamin A and the therapeutic usage of RA in anti-cancer drugs and skin problems has been highly addressed. However, the underlying mechanisms of how both excess and deficiency of them can cause the same type of ocular defects are not clear. To my knowledge, this is the first report to show that exogenously administered RA can subsequently lead to endogenous RA deficiency. This result may shed light on understanding how opposite conditions of embryonic RA levels can cause similar defects in the embryo. Moreover, my findings that the C57 strain, which is more prone to spontaneous eye defects, has lower basal expression levels of the RA synthesizing enzyme and endogenous RA concentrations may provide new insight in the mechanism of differential susceptibility to eye defects in humans.

Final Conclusion

- The C57 strain is more susceptible to RA-induced most severe type of ocular defects, i.e. anophthalmia and microphthalmia, than the ICR strain.

- Difference in developmental stages between these 2 strains does not contribute to the differential strain susceptibility to RA-induced ocular defects.

- The C57 strain exerts genotypic dominance and maternal effects in causing fetuses more prone to RA-induced ocular defects than the ICR strain.

- RA-induced failure in optic primordial tissue formation is more prominent in embryos of the C57 strain than that of the ICR strain.

- Exogenously administered RA can downregulate the expressions of *Raldh2* and *Raldh3* in the head region of the embryo.

- Exogenous administration of RA can subsequently lead to RA deficiency in the head region of the embryo. This possibly acts as a negative feedback mechanism via suppressing the expression of RA synthesizing enzymes.

- The above findings support the hypothesis that exogenously administered RA leads to insufficient production of endogenous RA, which as a result, leads to failure in oculogenesis.

REFERENCES

Abbott BD, Harris MW, and Birnbaum LS (1989) Etiology of retinoic acid-induced cleft palate varies with the embryonic stage. *Teratology,* **40,** 533-553.

Abu-Abed S, Dolle P, Metzger D, Beckett B, Chambon P, and Petkovich M (2001) The retinoic acid-metabolizing enzyme, CYP26A1, is essential for normal hindbrain patterning, vertebral identity, and development of posterior structures. *Genes Dev,* **15,** 226-240.

Adams J (1993) Structure-activity and dose-response relationships in the neural and behavioral teratogenesis of retinoids. *Neurotoxicol Teratol,* **15,** 193-202.

Alles AJ and Sulik KK (1989) Retinoic-acid-induced limb-reduction defects: perturbation of zones of programmed cell death as a pathogenetic mechanism. *Teratology,* **40,** 163-171.

Alles AJ and Sulik KK (1992) Pathogenesis of retinoid-induced hindbrain malformations in an experimental model. *Clin Dysmorphol,* **1,** 187-200.

Ang HL and Duester G (1997) Initiation of retinoid signaling in primitive streak mouse embryos: spatiotemporal expression patterns of receptors and metabolic enzymes for ligand synthesis. *Dev Dyn* **208**:536-543

Arnold GL, Kirby RS, Stern TP, and Sawyer JR (1995) Trisomy 9: review and report of two new cases. *Am J Med Genet,* **56,** 252-257.

Avantaggiato V, Acampora D, Tuorto F, and Simeone A (1996) Retinoic acid induces stage-specific repatterning of the rostral central nervous system. *Dev Biol,* **175,** 347-357.

Azuma N, Yamaguchi Y, Handa H, Hayakawa M, Kanai A, and Yamada M (1999) Missense mutation in the alternative splice region of the PAX6 gene in eye anomalies. *Am J Hum Genet,* **65,** 656-663.

Balmer JE and Blomhoff R (2002) Gene expression regulation by retinoic acid. *J Lipid Res,* **43,** 1773-1808.

Bardakjian T, Weiss A, and Schneider AS (2007) Anophthalmia / Microphthalmia Overview.

Bar-Yosef U, Abuelaish I, Harel T, Hendler N, Ofir R, and Birk OS (2004) CHX10 mutations cause non-syndromic microphthalmia/ anophthalmia in Arab and Jewish kindreds. *Hum Genet,* **115,** 302-309.

Baujat B, Krastinova D, Bach CA, Coquille F and Chabolle F (2006) Orbital morphology in exophthalmos and exorbitism. *Plast Reconstr Surg* **117**:542-550

Beddington RS and Robertson EJ (1998) Anterior patterning in mouse. *Trends Genet* **14**:277-284

Beebe DC (1986) Development of the ciliary body: a brief review. *Trans Ophthalmol Soc U K,* **105 (Pt 2),** 123-130.

Benke PJ (1984) The isotretinoin teratogen syndrome. *JAMA,* **251,** 3267-3269.

Binkley N and Krueger D (2000) Hypervitaminosis A and bone. *Nutr Rev,* **58,** 138-144.

Blentic A, Gale E, and Maden M (2003) Retinoic acid signalling centres in the avian embryo identified by sites of expression of synthesising and catabolising enzymes. *Dev Dyn,* **227,** 114-127.

Blomhoff R (1994) Transport and metabolism of vitamin A. *Nutr Rev,* **52,** S13-S23.

Bohnsack BL, Lai L, Dolle P, and Hirschi KK (2004) Signaling hierarchy downstream of retinoic acid that independently regulates vascular remodeling and endothelial cell proliferation. *Genes Dev,* **18,** 1345-1358.

Bowman TA, Goonewardene IM, Pasatiempo AM, Ross AC, and Taylor CE (1990) Vitamin A deficiency decreases natural killer cell activity and interferon production in rats. *J Nutr,* **120,** 1264-1273.

Bron AJ, Tripathi RC, and Tripathi BJ (1997) *Wolff's Anatomy of the Eye and Orbit.* Chapman & Hall, London.

Bruno NP, Beacham BE, and Burnett JW (1984) Adverse effects of isotretinoin therapy. *Cutis,* **33,** 484-6, 489.

Busby A, Dolk H, and Armstrong B (2005) Eye anomalies: seasonal variation and maternal viral infections. *Epidemiology,* **16,** 317-322.

Calderone JP, Chess J, Borodic G, and Albert DM (1983) Intraocular pathology of trisomy 18 (Edwards's syndrome): report of a case and review of the literature. *Br J Ophthalmol,* **67,** 162-169.

Canto-Soler MV and Adler R (2006) Optic cup and lens development requires Pax6 expression in the early optic vesicle during a narrow time window. *Dev Biol,* **294,** 119-132.

Carlier M, Nosten-Bertrand M, and Michard-Vanhee C (1992) Separating genetic effects from maternal environmental effects. In Goldowitz,D., Wahlsten,D., and Wimer,R.E. (Eds.), *Techniques for the genetic analysis of brain and behavior: Focus on the mouse*, . Elsevier, Amsterdam, pp. 111-126.

Chalhub EG, Baenziger J, Feigen RD, Middlekamp JN, and Shackelford GD (1977) Congenital herpes simplex type II infection with extensive hepatic calcification, bone lesions and cataracts: complete postmortem examination. *Dev Med Child Neurol,* **19,** 527-534.

Chambon P (1996) A decade of molecular biology of retinoic acid receptors. *FASEB J,* **10,** 940-954.

Chang L, Blain D, Bertuzzi S, and Brooks BP (2006) Uveal coloboma: clinical and basic science update. *Curr Opin Ophthalmol,* **17,** 447-470.

Chow RL and Lang RA (2001) Early eye development in vertebrates. *Annu Rev Cell Dev Biol,* **17,** 255-296.

Clarren SK and Smith DW (1978) The fetal alcohol syndrome. *N Engl J Med,* **298,** 1063-1067.

Coberly S, Lammer E, and Alashari M (1996) Retinoic acid embryopathy: case report and review of literature. *Pediatr Pathol Lab Med,* **16,** 823-836.

Cogan DG and Kuwabara T (1964) Ocular Pathologi of the 13-15 trisomy syndrome. *Arch Ophthalmol,* **72,** 246-253.

Collins MD, Eckhoff C, Weiss R, Resnick E, Nau H, and Scott WJ, Jr. (2006) Differential teratogenesis of all-trans-retinoic acid administered on gestational day 9.5 to SWV and C57BL/6N mice: emphasis on limb dysmorphology. *Birth Defects Res A Clin Mol Teratol,* **76,** 96-106.

Collins MD and Mao GE (1999) Teratology of retinoids. *Annu Rev Pharmacol Toxicol,* **39,** 399-430.

Colon-Teicher LS, Dugyala RR, and Sharma RP (1996) Temporal expression of retinoic acid receptors in hamster fetus during organogenesis and alteration by retinoic acid treatment. *Comp Biochem Physiol C Pharmacol Toxicol Endocrinol,* **114,** 71-78.

Cook CS and Sulik KK (1988) Keratolenticular dysgenesis (Peters' anomaly) as a result of acute embryonic insult during gastrulation. *J Pediatr Ophthalmol Strabismus,* **25,** 60-66.

Cook CS and Sulik KK (1986) Sequential scanning electron microscopic analyses of normal and spontaneously occurring abnormal ocular development in C57B1/6J mice. *Scan Electron Microsc,* 1215-1227.

Darby WJ, McGanity WJ, McLaren DS, Paton D, Alemu Z, and Gebre-Medhen M (1960) Bitot's spots and vitamin A deficiency. *Public Health Rep,* **75,** 738-743.

De La Cruz M, Sun S, Vangvanichyakorn K, and Desposito F (1984) Multiple congenital malformations associated with maternal isotretinoin therapy. *Pediatrics,* **74,** 428-430.

De Luca LM (1991) Retinoids and their receptors in differentiation, embryogenesis, and neoplasia. *FASEB J,* **5,** 2924-2933.

De Luca LM, Darwiche N, Jones CS, and Scita G (1995) Retinoids in differentiation and neoplasia. *Sci Amer Sci Med,* 28-37.

Dekaban AS (1968) Abnormalities in children exposed to x-radiation during various stages of gestation: tentative timetable of radiation injury to the human fetus. *I. J Nucl Med,* **9,** 471-477.

Dickman ED, Thaller C, and Smith SM (1997) Temporally-regulated retinoic acid depletion produces specific neural crest, ocular and nervous system defects. *Development,* **124,** 3111-3121.

Dobbs-McAuliffe B, Zhao Q, and Linney E (2004) Feedback mechanisms regulate retinoic acid production and degradation in the zebrafish embryo. *Mech Dev,* **121,** 339-350.

Downs KM and Davies T (1993) Staging of gastrulating mouse embryos by morphological landmarks in the dissecting microscope. *Development,* **118,** 1255-1266.

Duester G (1996) Involvement of alcohol dehydrogenase, short-chain dehydrogenase/reductase, aldehyde dehydrogenase, and cytochrome P450 in the control of retinoid signaling by activation of retinoic acid synthesis. *Biochemistry,* **35,** 12221-12227.

Dupe V, Matt N, Garnier JM, Chambon P, Mark M, and Ghyselinck NB (2003) A newborn lethal defect due to inactivation of retinaldehyde dehydrogenase type 3 is prevented by maternal retinoic acid treatment. *Proc Natl Acad Sci U S A,* **100,** 14036-14041.

Emmanouil-Nikoloussi EN, Goret-Nicaise M, Foroglou CH, Katsarma E, Dhem A, Dourov N, Persaud TV, and Thliveris JA (2000) Craniofacial abnormalities induced by retinoic acid: a preliminary histological and scanning electron microscopic (SEM) study. *Exp Toxicol Pathol,* **52,** 445-453.

Endo M, Antonyak MA and Cerione RA (2009) Cdc42-mTOR signaling pathway controls Hes5 and Pax6 expression in retinoic acid-dependent neural differentiation. *J Biol Chem* **284**:5107-5118

Enwright JF, III and Grainger RM (2000) Altered retinoid signaling in the heads of small eye mouse embryos. *Dev Biol,* **221,** 10-22.

Fan X, Molotkov A, Manabe S, Donmoyer CM, Deltour L, Foglio MH, Cuenca AE, Blaner WS, Lipton SA, and Duester G (2003) Targeted disruption of Aldh1a1 (Raldh1) provides evidence for a complex mechanism of retinoic acid synthesis in the developing retina. *Mol Cell Biol,* **23,** 4637-4648.

Fantes J, Ragge NK, Lynch SA, McGill NI, Collin JR, Howard-Peebles PN, Hayward C, Vivian AJ, Williamson K, van H, V, and Fitzpatrick DR (2003) Mutations in SOX2 cause anophthalmia. *Nat Genet,* **33,** 461-463.

Ferda PE, Ploder LA, Yu JJ, Arici K, Horsford DJ, Rutherford A, Bapat B, Cox DW, Duncan AM, Kalnins VI, Kocak-Altintas A, Sowden JC, Traboulsi E, Sarfarazi M, and McInnes RR (2000) Human microphthalmia associated with mutations in the retinal homeobox gene CHX10. *Nat Genet,* **25,** 397-401.

Fields AL, Soprano DR, and Soprano KJ (2007) Retinoids in biological control and cancer. *J Cell Biochem,* **102,** 886-898.

Findlater GS, McDougall RD and Kaufman MH (1993) Eyelid development, fusion and subsequent reopening in the mouse. *J Anat* **183** (Pt 1):121-129

Francis PJ, Berry V, Moore AT, and Bhattacharya S (1999) Lens biology: development and human cataractogenesis. *Trends Genet,* **15,** 191-196.

Francis PJ and Moore AT (2004) Genetics of childhood cataract. *Curr Opin Ophthalmol,* **15,** 10-15.

Fraunfelder FT, LaBraico JM, and Meyer SM (1985) Adverse ocular reactions possibly associated with isotretinoin. *Am J Ophthalmol,* **100,** 534-537.

Fujii H, Sato T, Kaneko S, Gotoh O, Fujii-Kuriyama Y, Osawa K, Kato S, and Hamada H (1997) Metabolic inactivation of retinoic acid by a novel P450 differentially expressed in developing mouse embryos. *EMBO J,* **16,** 4163-4173.

Fujita H, Yoshii A, Maeda J, Kosaki K, Shishido S, Nakai H, and Awazu M (2004) Genitourinary anomaly in congenital varicella syndrome: case report and review. *Pediatr Nephrol,* **19,** 554-557.

Fulton AB, Howard RO, Albert DM, Hsia YE, and Packman S (1977) Ocular findings in triploidy. *Am J Ophthalmol,* **84,** 859-867.

Gale TF (1991) Effects of in vivo exposure of pregnant hamsters to glucose. 1. Abnormalities in LVG strain fetuses following intermittent multiple treatments with two isomers. *Teratology,* **44,** 193-202.

Geelen JA (1979) Hypervitaminosis A induced teratogenesis. *CRC Crit Rev Toxicol,* **6,** 351-375.

Geelen JA, Langman J, and Lowdon JD (1980) The influence of excess vitamin A on neural tube closure in the mouse embryo. *Anat Embryol (Berl),* **159,** 223-234.

Germain P, Chambon P, Eichele G, Evans RM, Lazar MA, Leid M, de Lera AR, Lotan R, Mangelsdorf DJ, and Gronemeyer H (2006) International Union of Pharmacology. LX. Retinoic acid receptors. *Pharmacol Rev,* **58,** 712-725.

Gilkes MJ and Strode M (1963) Ocular anomalies in association with developmental limb abnormalities of drug origin. *Lancet,* **1,** 1026-1027.

Gilliam DM and Irtenkauf KT (1990) Maternal genetic effects on ethanol teratogenesis and dominance of relative embryonic resistance to malformations. *Alcohol Clin Exp Res,* **14,** 539-545.

Gilliam DM, Mantle MA, Barkhausen DA, and Tweden DR (1997) Effects of acute prenatal ethanol administration in a reciprocal cross of C57BL/6J and short-sleep mice: maternal effects and nonmaternal factors. *Alcohol Clin Exp Res,* **21,** 28-34.

Ginsberg J, Ballard ET, and Soukup S (1981) Pathologic features of the eye in triploidy. *J Pediatr Ophthalmol Strabismus,* **18,** 48-55.

Glaser T, Jepeal L, Edwards JG, Young SR, Favor J, and Maas RL (1994) PAX6 gene dosage effect in a family with congenital cataracts, aniridia, anophthalmia and central nervous system defects. *Nat Genet,* **7,** 463-471.

Golz S, Lantin C, and Mey J (2004) Retinoic acid-dependent regulation of BMP4 and Tbx5 in the embryonic chick retina. *Neuroreport,* **15,** 2751-2755.

Gregory-Evans CY, Williams MJ, Halford S, and Gregory-Evans K (2004) Ocular coloboma: a reassessment in the age of molecular neuroscience. *J Med Genet,* **41,** 881-891.

Gregory-Evans K (2000) Developmental disorders of the globe. In Moore,A. and Lightman,S. (Eds.), *Fundamentals of clinical ophthalmology: paediatric ophthalmology*, . London, pp. 53-61.

Grindley JC, Davidson DR, and Hill RE (1995) The role of Pax-6 in eye and nasal development. *Development,* **121,** 1433-1442.

Grondona JM, Kastner P, Gansmuller A, Decimo D, Chambon P, and Mark M (1996) Retinal dysplasia and degeneration in RARbeta2/RARgamma2 compound mutant mice. *Development,* **122,** 2173-2188.

Gudas LJ (1994) Retinoids and vertebrate development. *J Biol Chem,* **269,** 15399-15402.

Hagstrom SA, Pauer GJ, Reid J, Simpson E, Crowe S, Maumenee IH, and Traboulsi EI (2005) SOX2 mutation causes anophthalmia, hearing loss, and brain anomalies. *Am J Med Genet A,* **138,** 95-98.

Hale F (1933) Pigs born without eyeballs. *Journal of Heredity,* **24,** 105-106.

Hale F (1935) The relation of vitamin A to anophthalmos in pigs. *Am J Ophthalmol,* **18,** 1087-1093.

Halilagic A, Ribes V, Ghyselinck NB, Zile MH, Dolle P, and Studer M (2007) Retinoids control anterior and dorsal properties in the developing forebrain. *Dev Biol,* **303,** 362-375.

Hansen LA and Pearl GS (1985) Isotretinoin teratogenicity. Case report with neuropathologic findings. *Acta Neuropathol,* **65,** 335-337.

Hanson N and Leachman S (2001) Safety issues in isotretinoin therapy. *Semin Cutan Med Surg,* **20,** 166-183.

Harris SS, Hunt CE, Alvarez CJ, and Navia JM (1978) Vitamin A deficiency and new bone growth: histologic changes. *J Oral Pathol,* **7,** 85-90.

Haselbeck RJ, Hoffmann I, and Duester G (1999) Distinct functions for Aldh1 and Raldh2 in the control of ligand production for embryonic retinoid signaling pathways. *Dev Genet,* **25,** 353-364.

Hay ED (1979) Development of the vertebrate cornea. *Int Rev Cytol,* **63,** 263-322.

Heilig CW, Saunders T, Brosius FCI, Moley K, Heilig K, Baggs R, Guo L, and Conner D (2003) Glucose transporter-1-deficient mice exhibit impaired development and deformities that are similar to diabetic embryopathy. *Proc Natl Acad Sci U S A,* **100,** 15613-15618.

Helms JA, Kim CH, Hu D, Minkoff R, Thaller C, and Eichele G (1997) Sonic hedgehog participates in craniofacial morphogenesis and is down-regulated by teratogenic doses of retinoic acid. *Dev Biol,* **187,** 25-35.

Henderson RA, Williamson K, Cumming S, Clarke MP, Lynch SA, Hanson IM, Fitzpatrick DR, Sisodiya S, and van H, V (2007) Inherited PAX6, NF1 and OTX2 mutations in a child with microphthalmia and aniridia. *Eur J Hum Genet,* **15,** 898-901.

Hever AM, Williamson KA, and van H, V (2006) Developmental malformations of the eye: the role of PAX6, SOX2 and OTX2. *Clin Genet,* **69,** 459-470.

Holson RR, Adams J, and Ferguson SA (1999) Gestational stage-specific effects of retinoic acid exposure in the rat. *Neurotoxicol Teratol,* **21,** 393-402.

Holson RR, Gazzara RA, Ferguson SA, and Adams J (1997a) Behavioral effects of low-dose gestational day 11-13 retinoic acid exposure. *Neurotoxicol Teratol,* **19,** 355-362.

Holson RR, Gazzara RA, Ferguson SA, Ali SF, Laborde JB, and Adams J (1997b) Gestational retinoic acid exposure: a sensitive period for effects on neonatal mortality and cerebellar development. *Neurotoxicol Teratol,* **19,** 335-346.

Hoover F, Gundersen TE, Ulven SM, Michaille JJ, Blanchet S, Blomhoff R, and Glover JC (2001) Quantitative assessment of retinoid signaling pathways in the developing eye and retina of the chicken embryo. *J Comp Neurol,* **436,** 324-335.

Hornby SJ, Adolph S, Gilbert CE, Dandona L, and Foster A (2000a) Visual acuity in children with coloboma: clinical features and a new phenotypic classification system. *Ophthalmology,* **107,** 511-520.

Hornby SJ, Gilbert CE, Rahi JK, Sil AK, Xiao Y, Dandona L, and Foster A (2000b) Regional variation in blindness in children due to microphthalmos, anophthalmos and coloboma. *Ophthalmic Epidemiol,* **7,** 127-138.

Horton C and Maden M (1995) Endogenous distribution of retinoids during normal development and teratogenesis in the mouse embryo. *Dev Dyn,* **202,** 312-323.

Hupert J, Mobarhan S, Layden TJ, Papa VM, and Lucchesi DJ (1991) In vitro formation of retinoic acid from retinal in rat liver. *Biochem Cell Biol,* **69,** 509-514.

Hutchings DE, Gibbon J, and Kaufman MA (1973) Maternal vitamin A excess during the early fetal period: effects on learning and development in the offspring. *Dev Psychobiol,* **6,** 445-457.

Hutto C, Arvin A, Jacobs R, Steele R, Stagno S, Lyrene R, Willett L, Powell D, Andersen R, Werthammer J, Ratcliff G, Christy C, and Whitley R (1987) Intrauterine herpes simplex virus infections. *J Pediatr,* **110,** 97-101.

Hyatt GA, Schmitt EA, Marsh-Armstrong N, McCaffery P, Dräger UC, and Dowling JE (1996) Retinoic acid establishes ventral retinal characteristics. *Development,* **122,** 195-204.

Hyer J, Kuhlman J, Afif E, and Mikawa T (2003) Optic cup morphogenesis requires pre-lens ectoderm but not lens differentiation. *Dev Biol,* **259,** 351-363.

Hyer J, Mima T, and Mikawa T (1998) FGF1 patterns the optic vesicle by directing the placement of the neural retina domain. *Development,* **125,** 869-877.

Ishibashi M, Moriyoshi K, Sasai Y, Shiota K, Nakanishi S, and Kageyama R (1994) Persistent expression of helix-loop-helix factor HES-1 prevents mammalian neural differentiation in the central nervous system. *EMBO J,* **13,** 1799-1805.

Jacobson MD, Weil M, and Raff MC (1997) Programmed cell death in animal development. *Cell,* **88,** 347-354.

James AW, Culver K, Hall B, and Golabi M (2007) Bifid tongue: a rare feature associated with infants of diabetic mother syndrome. *Am J Med Genet A,* **143,** 2035-2039.

Johnson GJ, Minassian DC, Weale RA, and West SK (2003) *The Epidemiology of Eye Disease.* Oxford Univ Press, New York.

Kane MA, Chen N, Sparks S, and Napoli JL (2005) Quantification of endogenous retinoic acid in limited biological samples by LC/MS/MS. *Biochem J,* **388,** 363-369.

Kaufman MH (1992) *The atlas of mouse development.* Academic Press, London.

Kaufman MH (1999) The eye and the ear. *The anatomical basis of mouse development,* . Academic, San Diego, pp. 194-208.

Klein-Szanto AJ, Martin DH, and Pine AH (1980) Cutaneous manifestations in rats with advanced vitamin A deficiency. *J Cutan Pathol,* **7,** 260-270.

Kochhar DM, Jiang H, Harnish DC, and Soprano DR (1993) Evidence that retinoic acid-induced apoptosis in the mouse limb bud core mesenchymal cells is gene-mediated. *Prog Clin Biol Res,* **383B,** 815-825.

Koroma BM, Yang JM, and Sundin OH (1997) The Pax-6 homeobox gene is expressed throughout the corneal and conjunctival epithelia. *Invest Ophthalmol Vis Sci,* **38,** 108-120.

Kuriyama M, Shigematsu Y, Konishi K, Konishi Y, Sudo M, Haruki S, and Ito H (1988) Septo-optic dysplasia with infantile spasms. *Pediatr Neurol,* **4,** 62-65.

Laemle LK, Puszkarczuk M, and Feinberg RN (1999) Apoptosis in early ocular morphogenesis in the mouse. *Brain Res Dev Brain Res,* **112,** 129-133.

Lai L, Bohnsack BL, Niederreither K, and Hirschi KK (2003) Retinoic acid regulates endothelial cell proliferation during vasculogenesis. *Development,* **130,** 6465-6474.

Lamb TD and Pugh EN, Jr. (2004) Dark adaptation and the retinoid cycle of vision. *Prog Retin Eye Res,* **23,** 307-380.

Lammer EJ, Chen DT, Hoar RM, Agnish ND, Benke PJ, Braun JT, Curry CJ, Fernhoff PM, Grix AW, Jr., Lott IT, and . (1985) Retinoic acid embryopathy. *N Engl J Med,* **313,** 837-841.

Lang RA (2004) Pathways regulating lens induction in the mouse. *Int J Dev Biol,* **48,** 783-791.

Lang RA (1997) Apoptosis in mammalian eye development: lens morphogenesis, vascular regression and immune privilege. *Cell Death Differ,* **4,** 12-20.

Lee GS, Kochhar DM, and Collins MD (2004) Retinoid-induced limb malformations. *Curr Pharm Des,* **10,** 2657-2699.

Lee HY, Wroblewski E, Philips GT, Stair CN, Conley K, Reedy M, Mastick GS, and Brown NL (2005) Multiple requirements for Hes 1 during early eye formation. *Dev Biol,* **284,** 464-478.

Lee MY (2007) A study on dysregulation of retinoic acid catabolism by *Cyp26a1* in increasing the risk of caudal regression in diabetic pregnancy. M.Phil. thesis submitted to The Chinese University of Hong Kong.

Li H, Tierney C, Wen L, Wu JY, and Rao Y (1997) A single morphogenetic field gives rise to two retina primordia under the influence of the prechordal plate. *Development,* **124,** 603-615.

Li H, Wagner E, McCaffery P, Smith D, Andreadis A, and Dräger UC (2000) A retinoic acid synthesizing enzyme in ventral retina and telencephalon of the embryonic mouse. *Mech Dev,* **95,** 283-289.

Li HS, Yang JM, Jacobson RD, Pasko D, and Sundin O (1994) Pax-6 is first expressed in a region of ectoderm anterior to the early neural plate: implications for stepwise determination of the lens. *Dev Biol,* **162,** 181-194.

Li J, Molkentin JD, and Colbert MC (2001) Retinoic acid inhibits cardiac neural crest migration by blocking c-Jun N-terminal kinase activation. *Dev Biol,* **232,** 351-361.

Lips P (2003) Hypervitaminosis A and fractures. *N Engl J Med,* **348,** 347-349.

Liu L and Gudas LJ (2005) Disruption of the lecithin:retinol acyltransferase gene makes mice more susceptible to vitamin A deficiency. *J Biol Chem,* **280,** 40226-40234.

Loudig O, Maclean GA, Dore NL, Luu L, and Petkovich M (2005) Transcriptional co-operativity between distant retinoic acid response elements in regulation of Cyp26A1 inducibility. *Biochem J,* **392,** 241-248.

Luo T, Sakai Y, Wagner E, and Dräger UC (2006) Retinoids, eye development, and maturation of visual function. *J Neurobiol,* **66,** 677-686.

MacLean G, bu-Abed S, Dolle P, Tahayato A, Chambon P, and Petkovich M (2001) Cloning of a novel retinoic-acid metabolizing cytochrome P450, Cyp26B1, and comparative expression analysis with Cyp26A1 during early murine development. *Mech Dev,* **107,** 195-201.

Maden M, Blentic A, Reijntjes S, Seguin S, Gale E, and Graham A (2007) Retinoic acid is required for specification of the ventral eye field and for Rathke's pouch in the avian embryo. *Int J Dev Biol,* **51,** 191-200.

Maden M, Gale E, Kostetskii I, and Zile M (1996) Vitamin A-deficient quail embryos have half a hindbrain and other neural defects. *Curr Biol,* **6,** 417-426.

Maden M, Sonneveld E, van der Saag PT, and Gale E (1998) The distribution of endogenous retinoic acid in the chick embryo: implications for developmental mechanisms. *Development,* **125,** 4133-4144.

Magni R, Pierro L, and Brancato R (1991) Microphthalmos with colobomatous orbital cyst in trisomy 13. *Ophthalmic Paediatr Genet,* **12,** 39-42.

Mangelsdorf DJ and Evans RM (1995) The RXR heterodimers and orphan receptors. *Cell,* **83,** 841-850.

Mangelsdorf DJ, Thummel C, Beato M, Herrlich P, Schutz G, Umesono K, Blumberg B, Kastner P, Mark M, Chambon P, and Evans RM (1995) The nuclear receptor superfamily: the second decade. *Cell,* **83,** 835-839.

Mann I (1953) *The Developmental Basis of Eye Malformations.* JB Lippincott, Philadelphia.

Marcus DF, Turgeon P, Aaberg TM, Wiznia RA, Wetzig PC, and Bovino JA (1985) Optic disk findings in hypervitaminosis A. *Ann Ophthalmol,* **17,** 397-402.

Mark M, Ghyselinck NB, and Chambon P (2006) Function of retinoid nuclear receptors: lessons from genetic and pharmacological dissections of the retinoic acid signaling pathway during mouse embryogenesis. *Annu Rev Pharmacol Toxicol,* **46,** 451-480.

Marquardt T, shery-Padan R, Andrejewski N, Scardigli R, Guillemot F, and Gruss P (2001) Pax6 is required for the multipotent state of retinal progenitor cells. *Cell,* **105,** 43-55.

Marshall H, Nonchev S, Sham MH, Muchamore I, Lumsden A, and Krumlauf R (1992) Retinoic acid alters hindbrain Hox code and induces transformation of rhombomeres 2/3 into a 4/5 identity. *Nature,* **360,** 737-741.

Mathers PH, Grinberg A, Mahon KA, and Jamrich M (1997) The Rx homeobox gene is essential for vertebrate eye development. *Nature,* **387,** 603-607.

Matt N, Dupe V, Garnier JM, Dennefeld C, Chambon P, Mark M, and Ghyselinck NB (2005) Retinoic acid-dependent eye morphogenesis is orchestrated by neural crest cells. *Development,* **132,** 4789-4800.

Matt N, Ghyselinck NB, Wendling O, Chambon P, and Mark M (2003) Retinoic acid-induced developmental defects are mediated by RARbeta/RXR heterodimers in the pharyngeal endoderm. *Development,* **130,** 2083-2093.

McAvoy JW, Chamberlain CG, de Iongh RU, Hales AM, and Lovicu FJ (1999) Lens development. *Eye,* **13 (Pt 3b),** 425-437.

McCaffery P and Dräger UC (1993) Retinoic acid synthesis in the developing retina. *Adv Exp Med Biol,* **328,** 181-190.

McCaffery P and Dräger UC (1994) Hot spots of retinoic acid synthesis in the developing spinal cord. *Proc Natl Acad Sci U S A,* **91,** 7194-7197.

McCaffery P and Dräger UC (2000) Regulation of retinoic acid signaling in the embryonic nervous system: a master differentiation factor. *Cytokine Growth Factor Rev,* **11,** 233-249.

McCaffery P, Evans J, Koul O, Volpert A, Reid K, and Ullman MD (2002) Retinoid quantification by HPLC/MS(n). *J Lipid Res,* **43,** 1143-1149.

McCaffery P, Lee MO, Wagner MA, Sladek NE, and Dräger UC (1992) Asymmetrical retinoic acid synthesis in the dorsoventral axis of the retina. *Development,* **115,** 371-382.

McCaffery P, Tempst P, Lara G, and Dräger UC (1991) Aldehyde dehydrogenase is a positional marker in the retina. *Development,* **112,** 693-702.

McCaffery P, Wagner E, O'Neil J, Petkovich M, and Dräger UC (1999) Dorsal and ventral retinal territories defined by retinoic acid synthesis, break-down and nuclear receptor expression. *Mech Dev,* **82,** 119-130.

McCarthy RW, Frenkel LD, Kollarits CR, and Keys MP (1980) Clinical anophthalmia associated with congenital cytomegalovirus infection. *Am J Ophthalmol,* **90,** 558-561.

McLaren DS (1966) Skin changes in human vitamin A deficiency. *Dermatol Int,* **5,** 43-44.

McMahon CL and Braddock SR (2001) Septo-optic dysplasia as a manifestation of valproic acid embryopathy. *Teratology,* **64,** 83-86.

Mey J, McCaffery P, and Dräger UC (1997) Retinoic acid synthesis in the developing chick retina. *J Neurosci,* **17,** 7441-7449.

Mey J, McCaffery P, and Klemeit M (2001) Sources and sink of retinoic acid in the embryonic chick retina: distribution of aldehyde dehydrogenase activities, CRABP-I, and sites of retinoic acid inactivation. *Brain Res Dev Brain Res,* **127,** 135-148.

Mic FA, Haselbeck RJ, Cuenca AE, and Duester G (2002) Novel retinoic acid generating activities in the neural tube and heart identified by conditional rescue of Raldh2 null mutant mice. *Development,* **129,** 2271-2282.

Mic FA, Molotkov A, Fan X, Cuenca AE, and Duester G (2000) RALDH3, a retinaldehyde dehydrogenase that generates retinoic acid, is expressed in the ventral retina, otic vesicle and olfactory pit during mouse development. *Mech Dev,* **97,** 227-230.

Mic FA, Molotkov A, Molotkova N, and Duester G (2004a) Raldh2 expression in optic vesicle generates a retinoic acid signal needed for invagination of retina during optic cup formation. *Dev Dyn,* **231,** 270-277.

Mic FA, Sirbu IO, and Duester G (2004b) Retinoic acid synthesis controlled by Raldh2 is required early for limb bud initiation and then later as a proximodistal signal during apical ectodermal ridge formation. *J Biol Chem,* **279,** 26698-26706.

Milligan CE and Schwartz LM (1997) Programmed cell death during animal development. *Br Med Bull,* **53,** 570-590.

Molotkov A, Molotkova N, and Duester G (2006) Retinoic acid guides eye morphogenetic movements via paracrine signaling but is unnecessary for retinal dorsoventral patterning. *Development,* **133,** 1901-1910.

Molotkova N, Molotkov A, and Duester G (2007) Role of retinoic acid during forebrain development begins late when Raldh3 generates retinoic acid in the ventral subventricular zone. *Dev Biol,* **303,** 601-610.

Moro Balbas JA, Gato A, Alonso Revuelta MI, Pastor JF, Represa JJ, and Barbosa E (1993) Retinoic acid induces changes in the rhombencephalic neural crest cells migration and extracellular matrix composition in chick embryos. *Teratology,* **48,** 197-206.

Morriss-Kay GM, Murphy P, Hill RE, and Davidson DR (1991) Effects of retinoic acid excess on expression of Hox-2.9 and Krox-20 and on morphological segmentation in the hindbrain of mouse embryos. *EMBO J,* **10,** 2985-2995.

Morriss-Kay GM and Ward SJ (1999) Retinoids and mammalian development. *Int Rev Cytol,* **188,** 73-131.

Moss JB, Xavier-Neto J, Shapiro MD, Nayeem SM, McCaffery P, Dräger UC, and Rosenthal N (1998) Dynamic patterns of retinoic acid synthesis and response in the developing mammalian heart. *Dev Biol,* **199,** 55-71.

Murphy P and Hill RE (1991) Expression of the mouse labial-like homeobox-containing genes, Hox 2.9 and Hox 1.6, during segmentation of the hindbrain. *Development,* **111,** 61-74.

Napoli JL (1999) Interactions of retinoid binding proteins and enzymes in retinoid metabolism. *Biochim Biophys Acta,* **1440,** 139-162.

Napoli JL, Posch KP, Fiorella PD, and Boerman MH (1991) Physiological occurrence, biosynthesis and metabolism of retinoic acid: evidence for roles of cellular retinol-binding protein (CRBP) and cellular retinoic acid-binding protein (CRABP) in the pathway of retinoic acid homeostasis. *Biomed Pharmacother,* **45,** 131-143.

Nau H (1986) Species differences in pharmacokinetics and drug teratogenesis. *Environ Health Perspect,* **70,** 113-129.

Nau H (1993) Embryotoxicity and teratogenicity of topical retinoic acid. *Skin Pharmacol,* **6 Suppl 1,** 35-44.

Niederreither K and Dolle P (2008) Retinoic acid in development: towards an integrated view. *Nat Rev Genet,* **9,** 541-553.

Niederreither K, McCaffery P, Dräger UC, Chambon P, and Dolle P (1997) Restricted expression and retinoic acid-induced downregulation of the retinaldehyde dehydrogenase type 2 (RALDH-2) gene during mouse development. *Mech Dev,* **62,** 67-78.

Niederreither K, Subbarayan V, Dolle P, and Chambon P (1999) Embryonic retinoic acid synthesis is essential for early mouse post-implantation development. *Nat Genet,* **21,** 444-448.

Niederreither K, Vermot J, Fraulob V, Chambon P, and Dolle P (2002) Retinaldehyde dehydrogenase 2 (RALDH2)- independent patterns of retinoic acid synthesis in the mouse embryo. *Proc Natl Acad Sci U S A,* **99,** 16111-16116.

Niederreither K, Vermot J, Schuhbaur B, Chambon P, and Dolle P (2000) Retinoic acid synthesis and hindbrain patterning in the mouse embryo. *Development,* **127,** 75-85.

Nollevaux MC, Guiot Y, Horsmans Y, Leclercq I, Rahier J, Geubel AP, and Sempoux C (2006) Hypervitaminosis A-induced liver fibrosis: stellate cell activation and daily dose consumption. *Liver Int,* **26,** 182-186.

O'Donnell J (2004) Polar hysteria: an expression of hypervitaminosis A. *Am J Ther,* **11,** 507-516.

Olivera-Martinez I and Storey KG (2007) Wnt signals provide a timing mechanism for the FGF-retinoid differentiation switch during vertebrate body axis extension. *Development* **134**:2125-2135

O'Neill JF (1998) The ocular manifestations of congenital infection: a study of the early effect and long-term outcome of maternally transmitted rubella and toxoplasmosis. *Trans Am Ophthalmol Soc,* **96,** 813-879.

O'Rahilly R (1975) The prenatal development of the human eye. *Exp Eye Res,* **21,** 93-112.

Onwochei BC, Simon JW, Bateman JB, Couture KC, and Mir E (2000) Ocular colobomata. *Surv Ophthalmol,* **45,** 175-194.

Oomen HA (1974) Vitamin A deficiency, xerophthalmia and blindness. *Nutr Rev,* **32,** 161-166.

Ozeki H and Shirai S (1998) Developmental eye abnormalities in mouse fetuses induced by retinoic acid. *Jpn J Ophthalmol,* **42,** 162-167.

Ozeki H, Shirai S, Ikeda K, and Ogura Y (1999) Critical period for retinoic acid-induced developmental abnormalities of the vitreous in mouse fetuses. *Exp Eye Res,* **68,** 223-228.

Padmanabhan R, Singh G, and Singh S (1981) Malformations of the eye resulting from maternal hypervitaminosis A during gestation in the rat. *Acta Anat (Basel),* **110,** 291-298.

Palano GM, Di Pietro M, Scuderi A, and Pratico G (2005) Microphthalmia due to congenital varicella infection: a case report. *Minerva Pediatr,* **57,** 433-439.

Pappas RS, Newcomer ME, and Ong DE (1993) Endogenous retinoids in rat epididymal tissue and rat and human spermatozoa. *Biol Reprod,* **48,** 235-247.

Pei YF and Rhodin JA (1970) The prenatal development of the mouse eye. *Anat Rec,* **168,** 105-125.

Perisse J and Polacchi W (1980) Geographical distribution and recent changes in world supply of vitamin A. *Food Nutr (Roma),* **6,** 21-27.

Ragge NK, Brown AG, Poloschek CM, Lorenz B, Henderson RA, Clarke MP, Russell-Eggitt I, Fielder A, Gerrelli D, Martinez-Barbera JP, Ruddle P, Hurst J,

Collin JR, Salt A, Cooper ST, Thompson PJ, Sisodiya SM, Williamson KA, Fitzpatrick DR, van Heyningen V, and Hanson IM (2005a) Heterozygous mutations of OTX2 cause severe ocular malformations. *Am J Hum Genet,* **76,** 1008-1022.

Ragge NK, Lorenz B, Schneider A, Bushby K, de SL, de SU, Salt A, Collin JR, Vivian AJ, Free SL, Thompson P, Williamson KA, Sisodiya SM, van H, V, and Fitzpatrick DR (2005b) SOX2 anophthalmia syndrome. *Am J Med Genet A,* **135,** 1-7.

Rahi JS and Dezateux C (2001) Measuring and interpreting the incidence of congenital ocular anomalies: lessons from a national study of congenital cataract in the UK. *Invest Ophthalmol Vis Sci,* **42,** 1444-1448.

Rahman AS, Kimura M, Yokoi K, Naher TE, and Itokawa Y (1996) Neurological disorder and excessive accumulation of calcium in brain of clinically vitamin A-deficient rats. *Biol Trace Elem Res,* **53,** 57-64.

Ray WJ, Bain G, Yao M, and Gottlieb DI (1997) CYP26, a novel mammalian cytochrome P450, is induced by retinoic acid and defines a new family. *J Biol Chem,* **272,** 18702-18708.

Reijntjes S, Blentic A, Gale E, and Maden M (2005) The control of morphogen signalling: regulation of the synthesis and catabolism of retinoic acid in the developing embryo. *Dev Biol,* **285,** 224-237.

Reijntjes S, Gale E, and Maden M (2003) Expression of the retinoic acid catabolising enzyme CYP26B1 in the chick embryo and its regulation by retinoic acid. *Gene Expr Patterns,* **3,** 621-627.

Ribes V, Fraulob V, Petkovich M, and Dolle P (2007) The oxidizing enzyme CYP26a1 tightly regulates the availability of retinoic acid in the gastrulating mouse embryo to ensure proper head development and vasculogenesis. *Dev Dyn,* **236,** 644-653.

Ribes V, Wang Z, Dolle P, and Niederreither K (2006) Retinaldehyde dehydrogenase 2 (RALDH2)-mediated retinoic acid synthesis regulates early mouse embryonic forebrain development by controlling FGF and sonic hedgehog signaling. *Development,* **133,** 351-361.

Rosa FW, Wilk AL, and Kelsey FO (1986) Teratogen update: vitamin A congeners. *Teratology,* **33,** 355-364.

Ross AJ, May-Simera H, Eichers ER, Kai M, Hill J, Jagger DJ, Leitch CC, Chapple JP, Munro PM, Fisher S, Tan PL, Phillips HM, Leroux MR, Henderson DJ, Murdoch JN, Copp AJ, Eliot MM, Lupski JR, Kemp DT, Dollfus H, Tada M, Katsanis N, Forge A, and Beales PL (2005) Disruption of Bardet-Biedl syndrome ciliary proteins perturbs planar cell polarity in vertebrates. *Nat Genet,* **37,** 1135-1140.

Ross SA, McCaffery PJ, Dräger UC, and De Luca LM (2000) Retinoids in embryonal development. *Physiol Rev,* **80,** 1021-1054.

Rossant J, Zirngibl R, Cado D, Shago M, and Giguere V (1991) Expression of a retinoic acid response element-hsplacZ transgene defines specific domains of transcriptional activity during mouse embryogenesis. *Genes Dev,* **5,** 1333-1344.

Rothman KJ, Moore LL, Singer MR, Nguyen US, Mannino S, and Milunsky A (1995) Teratogenicity of high vitamin A intake. *N Engl J Med,* **333,** 1369-1373.

Ruberte E, Dolle P, Chambon P and Morriss-Kay G (1991) Retinoic acid receptors and cellular retinoid binding proteins. II. Their differential pattern of transcription during early morphogenesis in mouse embryos. *Development* **111**:45-60

Rutledge JC, Shourbaji AG, Hughes LA, Polifka JE, Cruz YP, Bishop JB, and Generoso WM (1994) Limb and lower-body duplications induced by retinoic acid in mice. *Proc Natl Acad Sci U S A,* **91,** 5436-5440.

Sakai Y, Luo T, McCaffery P, Hamada H, and Dräger UC (2004) CYP26A1 and CYP26C1 cooperate in degrading retinoic acid within the equatorial retina during later eye development. *Dev Biol,* **276,** 143-157.

Sakai Y, Meno C, Fujii H, Nishino J, Shiratori H, Saijoh Y, Rossant J, and Hamada H (2001) The retinoic acid-inactivating enzyme CYP26 is essential for establishing an uneven distribution of retinoic acid along the anterio-posterior axis within the mouse embryo. *Genes Dev,* **15,** 213-225.

Sakhi AK, Gundersen TE, Ulven SM, Blomhoff R, and Lundanes E (1998) Quantitative determination of endogenous retinoids in mouse embryos by high-performance liquid chromatography with on-line solid-phase extraction, column switching and electrochemical detection. *J Chromatogr A,* **828,** 451-460.

Sarma V (1959) Maternal vitamin A deficiency and fetal microcephaly and anophthalmia: report of a case. *Obstet Gynecol,* **13,** 299-301.

Satre MA and Kochhar DM (1989) Elevations in the endogenous levels of the putative morphogen retinoic acid in embryonic mouse limb-buds associated with limb dysmorphogenesis. *Dev Biol,* **133,** 529-536.

Schedl A, Ross A, Lee M, Engelkamp D, Rashbass P, van H, V, and Hastie ND (1996) Influence of PAX6 gene dosage on development: overexpression causes severe eye abnormalities. *Cell,* **86,** 71-82.

Schweigert FJ, Siegling C, Tzimas G, Seeger J, and Nau H (2002) Distribution of endogenous retinoids, retinoid binding proteins (RBP, CRABPI) and nuclear retinoid X receptor beta (RXRbeta) in the porcine embryo. *Reprod Nutr Dev,* **42,** 285-294.

Scott WJ, Duggan CA, Schreiner CM, and Collins MD (1990) Reduction of embryonic intracellular pH: a potential mechanism of acetazolamide-induced limb malformations. *Toxicol Appl Pharmacol,* **103,** 238-254.

Semba RD, Muhilal, Ward BJ, Griffin DE, Scott AL, Natadisastra G, West KP, Jr., and Sommer A (1993) Abnormal T-cell subset proportions in vitamin-A-deficient children. *Lancet,* **341,** 5-8.

Shenefelt RE (1972) Morphogenesis of malformations in hamsters caused by retinoic acid: relation to dose and stage at treatment. *Teratology,* **5,** 103-118.

Shimizu H, Lee GS, Beedanagari SR and Collins MD (2007) Altered localization of gene expression in both ectoderm and mesoderm is associated with a murine strain difference in retinoic acid-induced forelimb ectrodactyly. *Birth Defects Res A Clin Mol Teratol* **79**:465-482

Shiota K (1982) Neural tube defects and maternal hyperthermia in early pregnancy: epidemiology in a human embryo population. *Am J Med Genet,* **12,** 281-288.

Shum AS, Poon LL, Tang WW, Koide T, Chan BW, Leung YC, Shiroishi T, and Copp AJ (1999) Retinoic acid induces down-regulation of Wnt-3a, apoptosis and diversion of tail bud cells to a neural fate in the mouse embryo. *Mech Dev,* **84,** 17-30.

Silverman AK, Ellis CN, and Voorhees JJ (1987) Hypervitaminosis A syndrome: a paradigm of retinoid side effects. *J Am Acad Dermatol,* **16,** 1027-1039.

Simeone A, Avantaggiato V, Moroni MC, Mavilio F, Arra C, Cotelli F, Nigro V, and Acampora D (1995) Retinoic acid induces stage-specific antero-posterior transformation of rostral central nervous system. *Mech Dev,* **51,** 83-98.

Sirbu IO and Duester G (2006) Retinoic-acid signalling in node ectoderm and posterior neural plate directs left-right patterning of somitic mesoderm. *Nat Cell Biol* **8**:271-277

Smets KJ, Barlow T, and Vanhaesebrouck P (2006) Maternal vitamin A deficiency and neonatal microphthalmia: complications of biliopancreatic diversion? *Eur J Pediatr,* **165,** 502-504.

Smith DW, Clarren SK, and Harvey MA (1978) Hyperthermia as a possible teratogenic agent. *J Pediatr,* **92,** 878-883.

Smith RS, Roderick TH, and Sundberg JP (1994) Microphthalmia and associated abnormalities in inbred black mice. *Lab Anim Sci,* **44,** 551-560.

Smith SM, Levy NS, and Hayes CE (1987) Impaired immunity in vitamin A-deficient mice. *J Nutr,* **117,** 857-865.

Smith-Thomas L, Lott I, and Bronner-Fraser M (1987) Effects of isotretinoin on the behavior of neural crest cells in vitro. *Dev Biol,* **123,** 276-281.

Sommer A (1990) Vitamin A deficiency and xerophthalmia. *Arch Ophthalmol,* **108,** 343-344.

Sommer A (1998) Xerophthalmia and vitamin A status. *Prog Retin Eye Res,* **17,** 9-31.

Sommer A, Green WR, and Kenyon KR (1981) Bitot's spots responsive and nonresponsive to vitamin A. Clinicopathologic correlations. *Arch Ophthalmol,* **99,** 2014-2027.

Soprano DR and Soprano KJ (1995) Retinoids as teratogens. *Annu Rev Nutr,* **15,** 111-132.

Stoll C, Alembik Y, Dott B, and Roth MP (1992) Epidemiology of congenital eye malformations in 131,760 consecutive births. *Ophthalmic Paediatr Genet,* **13,** 179-186.

Stoll C, Alembik Y, Dott B, and Roth MP (1997) Congenital eye malformations in 212,479 consecutive births. *Ann Genet,* **40,** 122-128.

Stoppie P, Borgers M, Borghgraef P, Dillen L, Goossens J, Sanz G, Szel H, Van HC, Van NG, Nobels G, Vanden BH, Venet M, Willemsens G, and Van WJ (2000) R115866 inhibits all-trans-retinoic acid metabolism and exerts retinoidal effects in rodents. *J Pharmacol Exp Ther,* **293,** 304-312.

Stoykova A, Treichel D, Hallonet M, and Gruss P (2000) Pax6 modulates the dorsoventral patterning of the mammalian telencephalon. *J Neurosci,* **20,** 8042-8050.

Stromland K (1985) Ocular abnormalities in the fetal alcohol syndrome. *Acta Ophthalmol Suppl,* **171,** 1-50.

Stromland K, Miller M, and Cook C (1991) Ocular teratology. *Surv Ophthalmol,* **35,** 429-446.

Sulik KK, Cook CS, and Webster WS (1988) Teratogens and craniofacial malformations: relationships to cell death. *Development,* **103 Suppl,** 213-231.

Sulik KK, Dehart DB, Rogers JM, and Chernoff N (1995) Teratogenicity of low doses of all-trans retinoic acid in presomite mouse embryos. *Teratology,* **51,** 398-403.

Sun SY and Lotan R (2002) Retinoids and their receptors in cancer development and chemoprevention. *Crit Rev Oncol Hematol,* **41,** 41-55.

Suzuki R, Shintani T, Sakuta H, Kato A, Ohkawara T, Osumi N, and Noda M (2000) Identification of RALDH-3, a novel retinaldehyde dehydrogenase, expressed in the ventral region of the retina. *Mech Dev,* **98,** 37-50.

Tahayato A, Dolle P, and Petkovich M (2003) Cyp26C1 encodes a novel retinoic acid-metabolizing enzyme expressed in the hindbrain, inner ear, first branchial arch and tooth buds during murine development. *Gene Expr Patterns,* **3,** 449-454.

Tarani L, Colloridi F, Raguso G, Rizzuti A, Bruni L, Tozzi MC, Palermo D, Panero A, and Vignetti P (1994) Trisomy 9 mosaicism syndrome. A case report and review of the literature. *Ann Genet,* **37,** 14-20.

Thiel R, Chahoud I, Jurgens M, and Neubert D (1993) Time-dependent differences in the development of somites of four different mouse strains. *Teratog Carcinog Mutagen,* **13,** 247-257.

Tomita K, Ishibashi M, Nakahara K, Ang SL, Nakanishi S, Guillemot F, and Kageyama R (1996) Mammalian hairy and Enhancer of split homolog 1 regulates differentiation of retinal neurons and is essential for eye morphogenesis. *Neuron,* **16,** 723-734.

Traboulsi EI (1999) *Genetic Diseases of the Eye.* Oxford University Press, New York.

Tse HK, Leung MB, Woolf AS, Menke AL, Hastie ND, Gosling JA, Pang CP, and Shum AS (2005) Implication of Wt1 in the pathogenesis of nephrogenic failure in a mouse model of retinoic acid-induced caudal regression syndrome. *Am J Pathol,* **166,** 1295-1307.

Tsutsui Y, Kashiwai A, Kawamura N, and Kadota C (1993) Microphthalmia and cerebral atrophy induced in mouse embryos by infection with murine cytomegalovirus in midgestation. *Am J Pathol,* **143,** 804-813.

Uehara M, Yashiro K, Mamiya S, Nishino J, Chambon P, Dolle P, and Sakai Y (2007) CYP26A1 and CYP26C1 cooperatively regulate anterior-posterior patterning of the developing brain and the production of migratory cranial neural crest cells in the mouse. *Dev Biol,* **302,** 399-411.

Valleix S, Niel F, Nedelec B, Algros MP, Schwartz C, Delbosc B, Delpech M, and Kantelip B (2006) Homozygous nonsense mutation in the FOXE3 gene as a cause of congenital primary aphakia in humans. *Am J Hum Genet,* **79,** 358-364.

van Maele-Fabry G, Delhaise F, and Picard JJ (1992) Evolution of the developmental scores of sixteen morphological features in mouse embryos displaying 0 to 30 somites. *Int J Dev Biol,* **36,** 161-167.

Voronina VA, Kozhemyakina EA, O'Kernick CM, Kahn ND, Wenger SL, Linberg JV, Schneider AS, and Mathers PH (2004) Mutations in the human RAX homeobox gene in a patient with anophthalmia and sclerocornea. *Hum Mol Genet,* **13,** 315-322.

Wagner E, McCaffery P, and Dräger UC (2000) Retinoic acid in the formation of the dorsoventral retina and its central projections. *Dev Biol,* **222,** 460-470.

Wagner M, Han B, and Jessell TM (1992) Regional differences in retinoid release from embryonic neural tissue detected by an in vitro reporter assay. *Development,* **116,** 55-66.

Wakabayashi N, Kageyama R, Habu T, Doi T, Morita T, Nozaki M, Yamamoto M and Nishimune Y (2000) A novel cis-acting element regulates HES-1 gene expression in P19 embryonal carcinoma cells treated with retinoic acid. *J Biochem* **128**:1087-1095

Walther C and Gruss P (1991) Pax-6, a murine paired box gene, is expressed in the developing CNS. *Development,* **113,** 1435-1449.

Warburg M (1993) Classification of microphthalmos and coloboma. *J Med Genet,* **30,** 664-669.

Watanabe T, Goulding EH, and Pratt RM (1988) Alterations in craniofacial growth induced by isotretinoin (13-cis-retinoic acid) in mouse whole embryo and primary mesenchymal cell culture. *J Craniofac Genet Dev Biol,* **8,** 21-33.

Weinstein DC, and Hemmati-Brivanlou A (1999) Neural induction. *Annu Rev Cell Dev Biol* **15**:411-433

Wendling O, Dennefeld C, Chambon P, and Mark M (2000) Retinoid signaling is essential for patterning the endoderm of the third and fourth pharyngeal arches. *Development,* **127,** 1553-1562.

Williams KJ, Fern VH, and Willhite CC (1984) Teratogenic dose-response relationships of etretinate in the golden hamster. *Fundam Appl Toxicol,* **4,** 977-982.

Williams SS, Mear JP, Liang HC, Potter SS, Aronow BJ, and Colbert MC (2004) Large-scale reprogramming of cranial neural crest gene expression by retinoic acid exposure. *Physiol Genomics,* **19,** 184-197.

Wilson JG (1973) *Environment and Birth Defects.* Academic Press, New York.

Wilson JG, Roth CB, and Warkany J (1953) An analysis of the syndrome of malformations induced by maternal vitamin A deficiency. Effects of restoration of vitamin A at various times during gestation. *Am J Anat,* **92,** 189-217.

World Health Organization (1998a) Safe vitamin A dosage during pregnancy and lactation. Geneva.

World Health Organization (1998b) Vitamin and mineral requirements in human nutrition: report of a joint FAO/WHO expert consultation in Bangkok, Thailand. Geneva.

World Health Organization (2000) Preventing blindness in children: report of WHO/IAPB scientific meeting. Geneva.

Wright KW (1997) Embryology and eye development. In Wright,K.W. (Ed.), *Textbook of Ophthalmology,* . Williams & Wilkins, Baltimore.

Yamamoto Y, Zolfaghari R, and Ross AC (2000) Regulation of CYP26 (cytochrome P450RAI) mRNA expression and retinoic acid metabolism by retinoids and dietary vitamin A in liver of mice and rats. *FASEB J,* **14,** 2119-2127.

Yashiro K, Zhao X, Uehara M, Yamashita K, Nishijima M, Nishino J, Saijoh Y, Sakai Y, and Hamada H (2004) Regulation of retinoic acid distribution is required for proximodistal patterning and outgrowth of the developing mouse limb. *Dev Cell,* **6,** 411-422.

Yasuda Y, Okamoto M, Konishi H, Matsuo T, Kihara T, and Tanimura T (1986) Developmental anomalies induced by all-trans retinoic acid in fetal mice: I. Macroscopic findings. *Teratology,* **34,** 37-49.

Zhang H, Hara M, Seki K, Fukuda K and Nishida T (2005) Eyelid fusion and epithelial differentiation at the ocular surface during mouse embryonic development. *Jpn J Ophthalmol* **49**:195-204

GRAPHS

Graph 3-1 Time and dose responses to RA-induced resorption in E18 ICR fetuses.

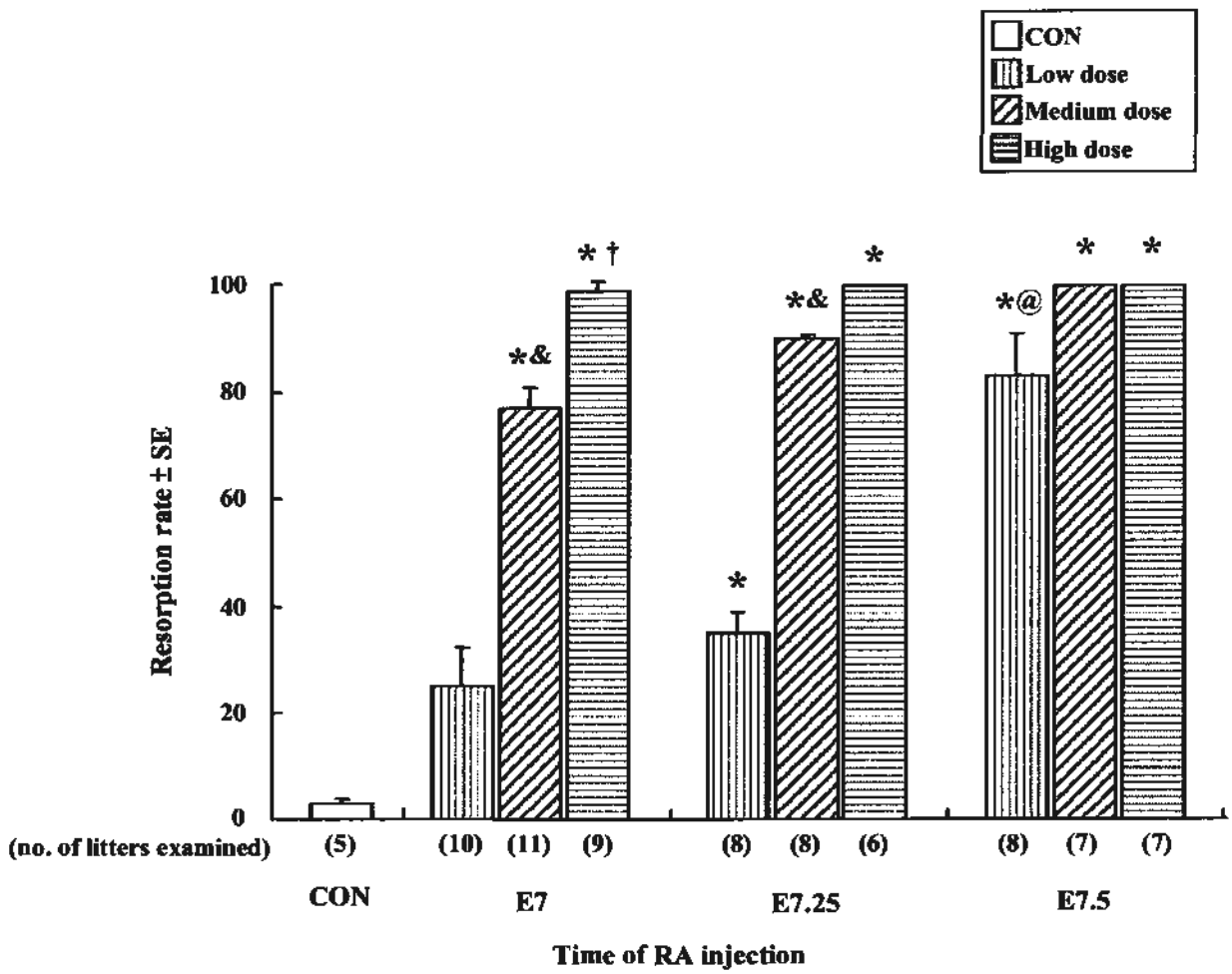

Data were analyzed by one-way ANOVA followed by Bonferroni test.

* $p < 0.05$ vs CON

& $p < 0.05$ vs low dose of RA treatment at the same gestational day

† $p < 0.05$ vs medium dose of RA treatment at the same gestational day

@ $p > 0.05$ vs E7.25 treated with the same dose of RA

There were time and dose responses in ICR fetuses after maternal RA administration.

Graph 3-2 Time and dose responses to RA-induced resorption in E18 C57 fetuses.

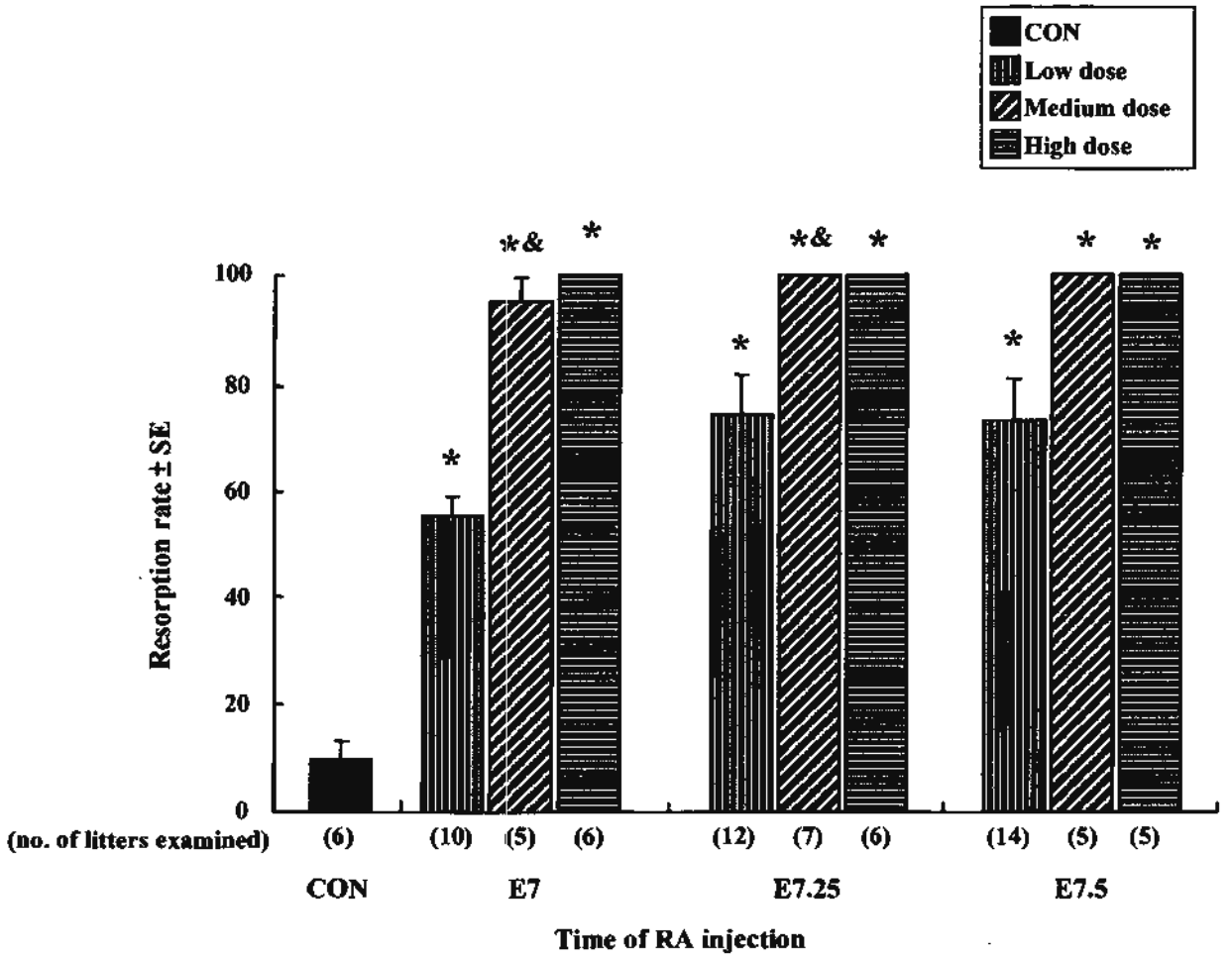

Data were analyzed by one-way ANOVA followed by Bonferroni test.

* $p < 0.05$ vs CON

& $p < 0.05$ vs low dose of RA treatment at the same gestational day

There were time and dose responses in C57 fetuses after maternal RA administration.

Graph 3-3 Strain difference in time response to RA-induced resorption in E18 fetuses.

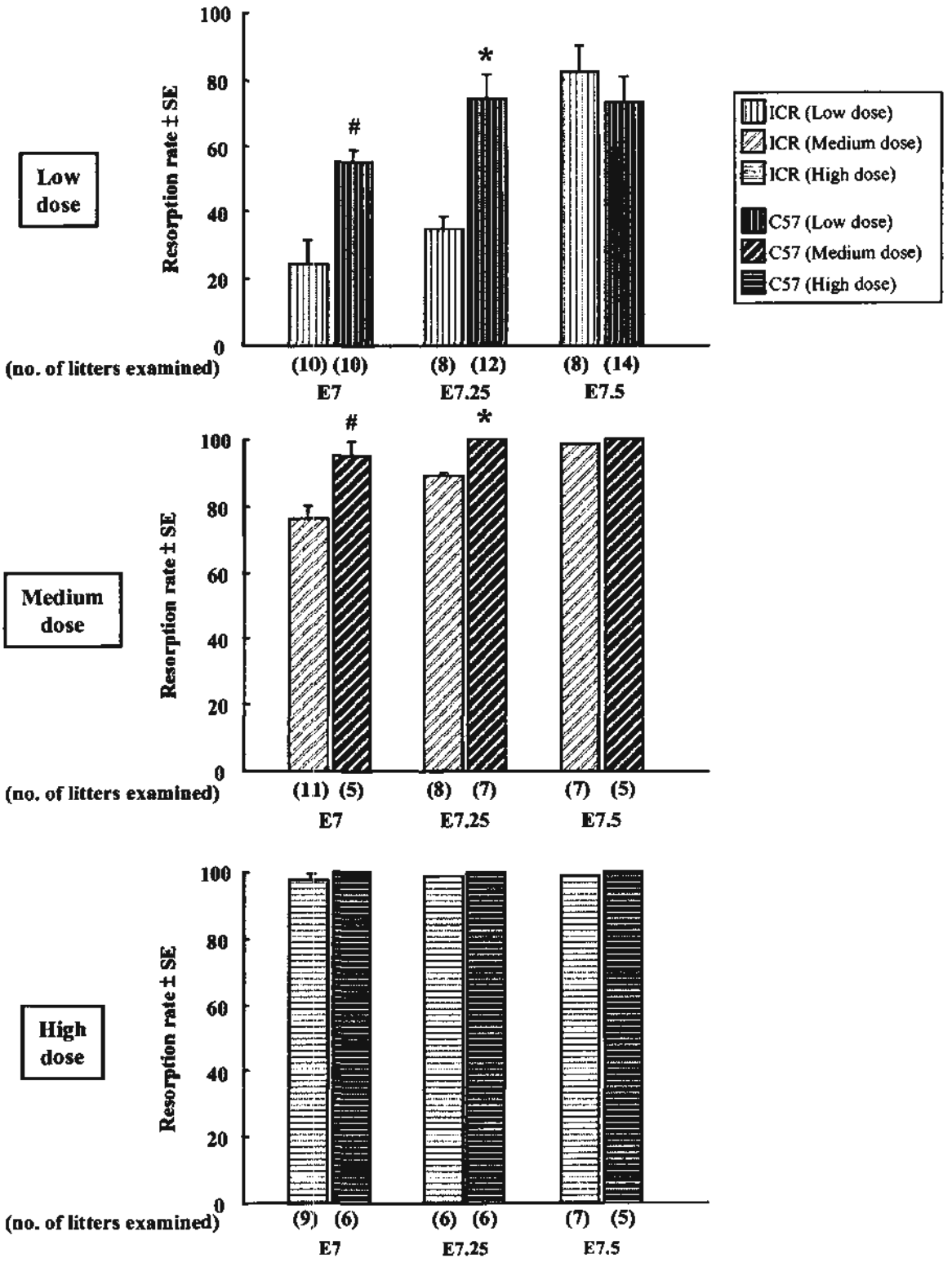

Data were analyzed by Independent sample *t* test.

# $p < 0.001$; * $p < 0.05$ vs ICR treated with RA at the same gestational day

There was significantly higher resorption rate in C57 fetuses than in ICR fetuses after low and medium doses of RA treatment at the same gestational day.

Graph 3-4 Strain difference in dose response to RA-induced resorption in E18 fetuses.

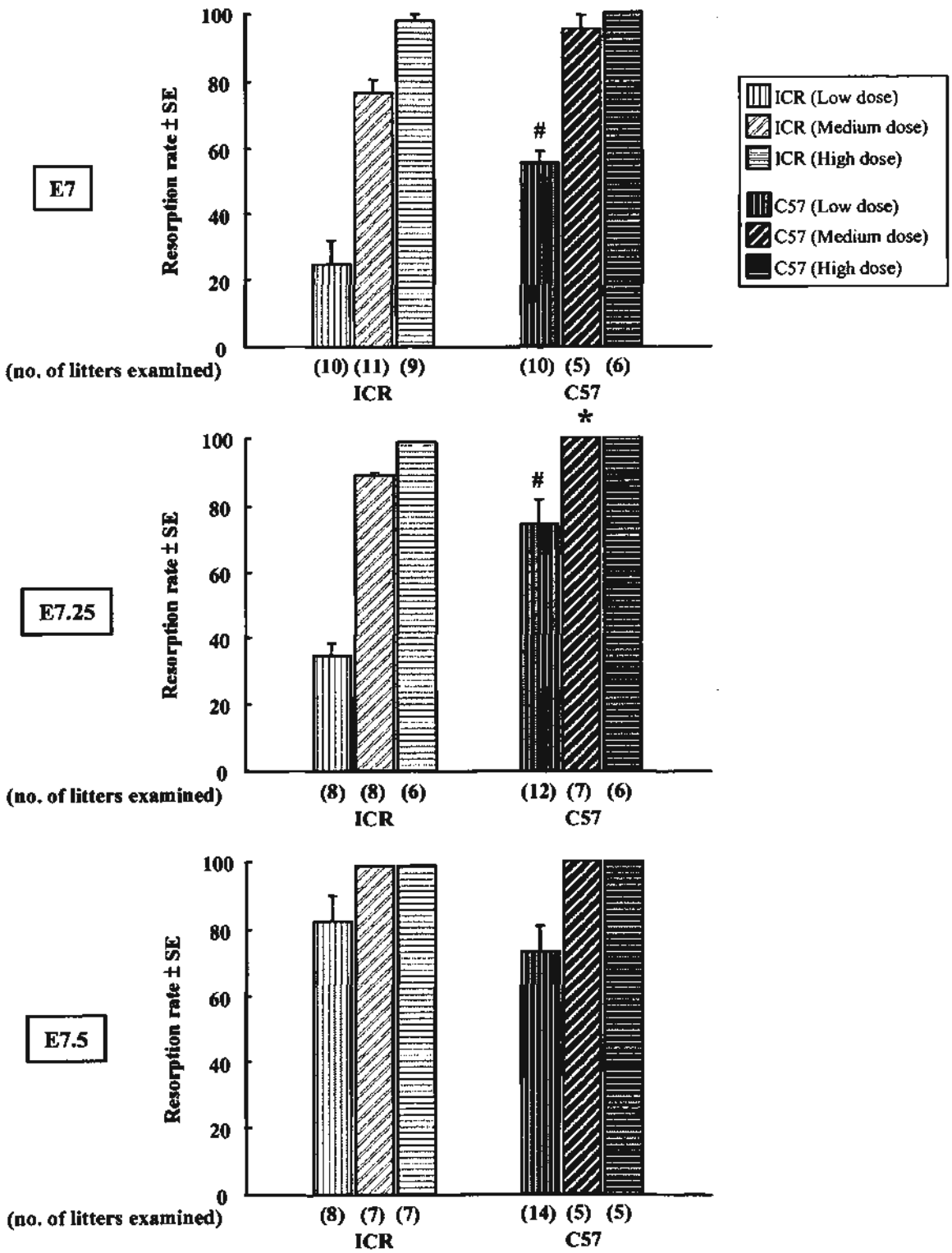

Data were analyzed by Independent sample *t* test.

$^{\#}p < 0.001$; $^{*}p < 0.05$ vs ICR treated with the same dose of RA

There was significantly higher resorption rate in C57 fetuses than in ICR fetuses after receiving the same dose of RA at different gestational days.

Graph 3-5 **Frequency of malformed eyes in E18 ICR and C57 fetuses treated with low dose of RA at different gestational days.**

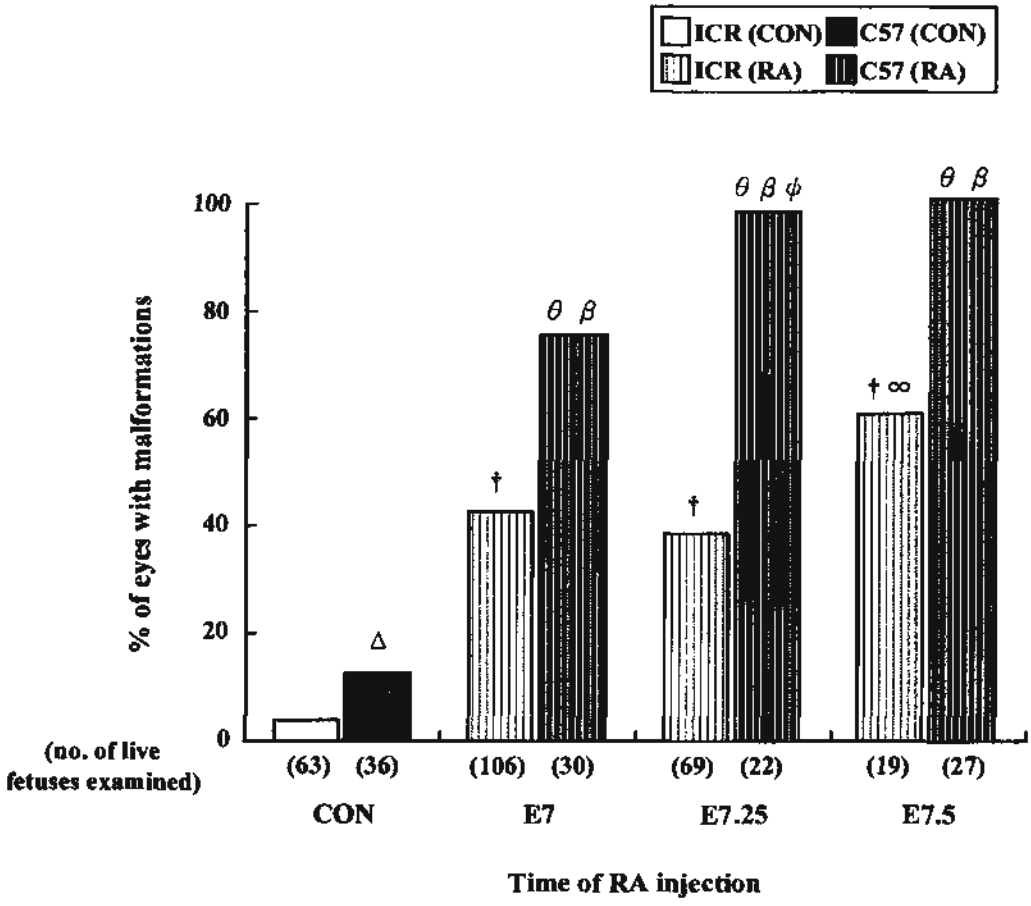

Data were analyzed by *chi*-square test.

$^{\Delta}p < 0.05$; $^{\theta}p < 0.001$ vs ICR at the same gestational day

$^{\dagger}p < 0.001$ vs ICR CON

$^{\infty}p < 0.05$ vs ICR E7.25

$^{\beta}p < 0.001$ vs C57 CON

$^{\phi}p < 0.05$ vs C57 E7

Low dose of RA treatment resulted in significantly higher frequency of malformed eyes in E18 ICR and C57 fetuses when compared with the corresponding control. C57 fetuses exhibited significantly higher frequency of malformed eyes than ICR fetuses after exposure to low dose of RA at all gestational days examined.

Graph 3-6 Frequency of anophthalmia in E18 ICR and C57 fetuses treated with low dose of RA at different gestational days.

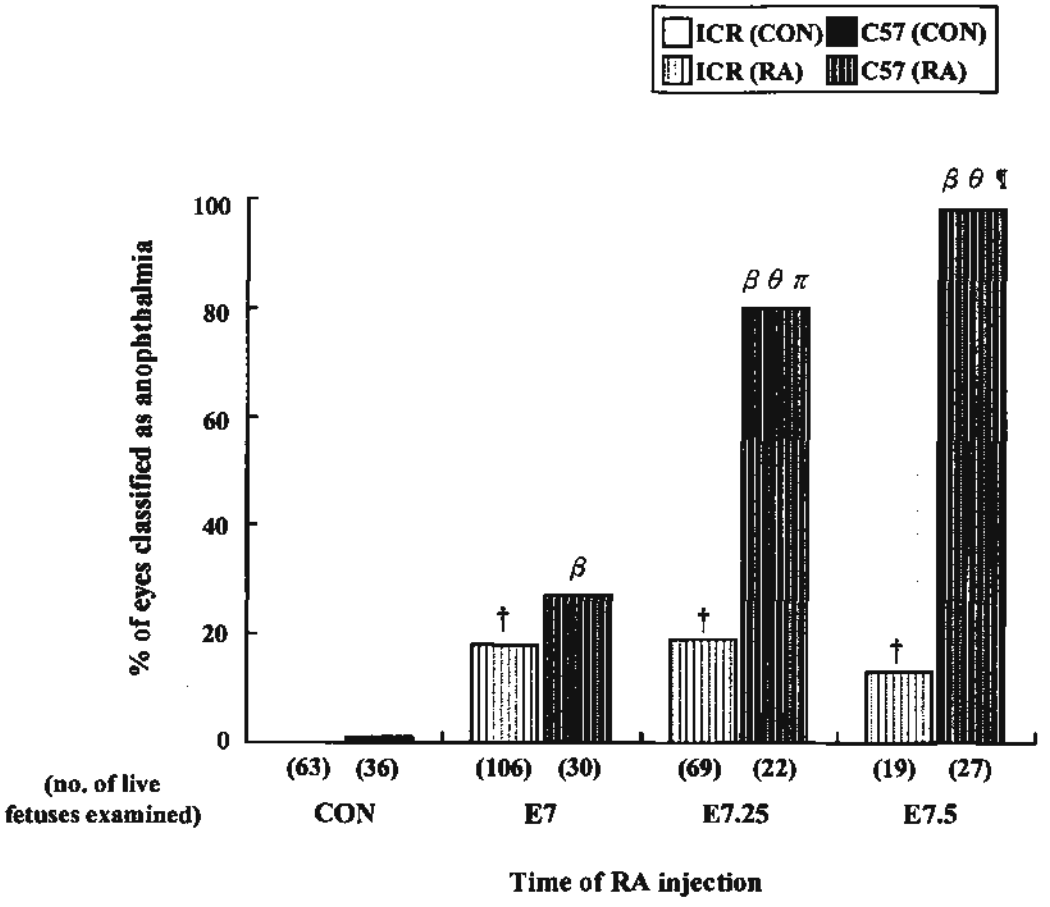

Data were analyzed by *chi*-square test.

$^{\theta}p < 0.001$ vs ICR at the same gestational day

$^{\dagger}p < 0.001$ vs ICR CON

$^{\beta}p < 0.001$ vs C57 CON

$^{\pi}p < 0.001$ vs C57 E7

$^{\P}p < 0.05$ vs C57 E7.25

Administration of low dose of RA at all gestational days examined resulted in similar frequencies of anophthalmia whereas further significant increase was resulted when RA was administered to C57 mice at later stages, i.e. at E7.25 and E7.5. There was about 4- and 7- fold increase in the frequency of anophthalmia in C57 fetuses when compared with ICR fetuses that had received RA treatment at E7.25 and E7.5 respectively.

Graph 3-7 Frequency of microphthalmia in E18 ICR and C57 fetuses treated with low dose of RA at different gestational days.

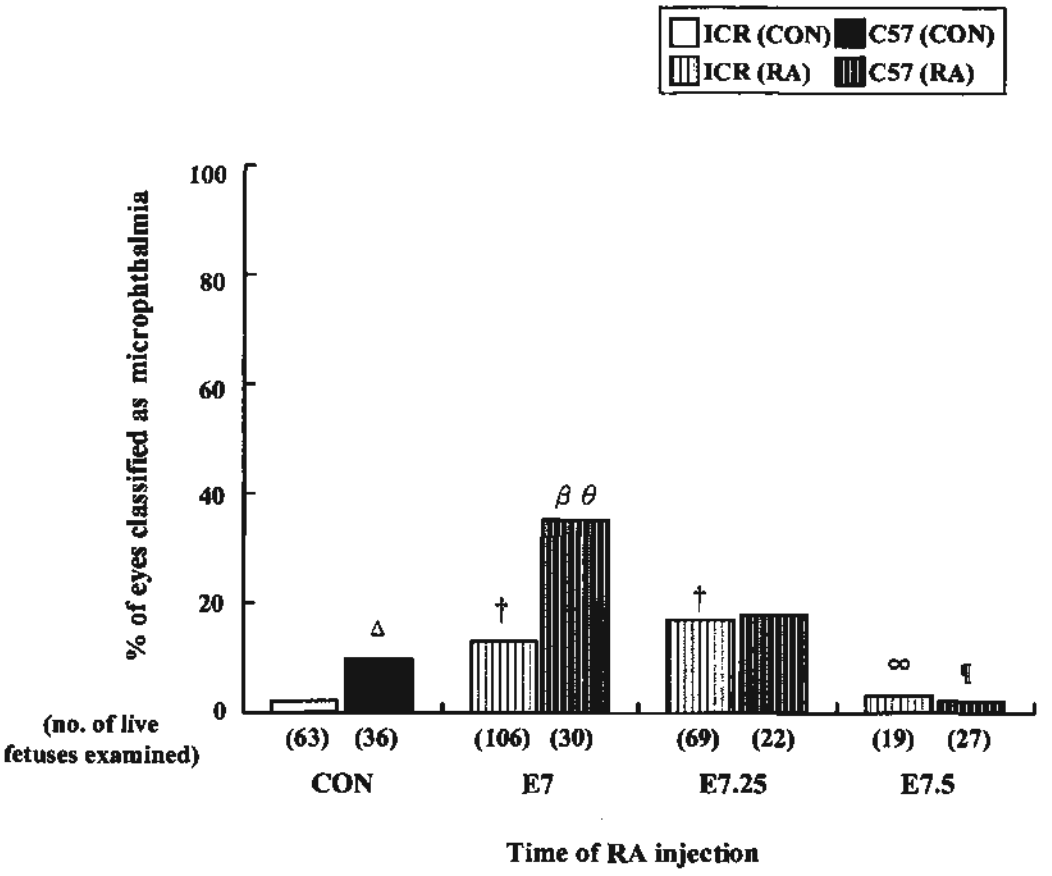

Data were analyzed by *chi*-square test.

$^{\Delta}p < 0.05$; $^{\theta}p < 0.001$ vs ICR at the same gestational day

$^{\dagger}p < 0.001$ vs ICR CON

$^{\infty}p < 0.05$ vs ICR E7.25

$^{\beta}p < 0.001$ vs C57 CON

$^{\P}p < 0.05$ vs C57 E7.25

RA treatment at E7 resulted in significant increase in the frequency of microphthalmia in ICR and C57 fetuses when compared with the corresponding CON groups. However, administration of RA at later gestational days resulted in decrease in such frequencies in C57 fetuses.

Graph 3-8 Total frequency of anophthalmia and microphthalmia in E18 ICR and C57 fetuses treated with low dose of RA at different gestational days.

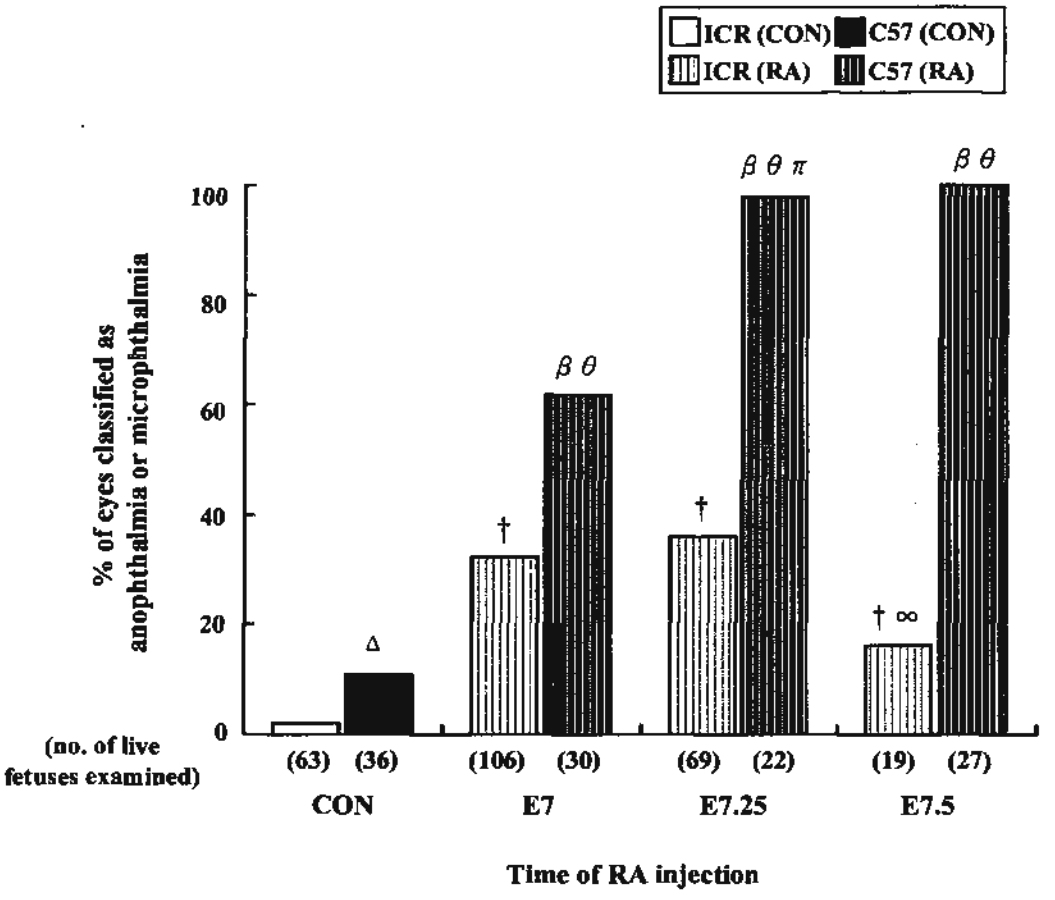

Data were analyzed by *chi*-square test.

$^{\Delta}p < 0.05$, $^{\theta}p < 0.001$ vs ICR at the same gestational day

$^{\dagger}p < 0.001$ vs ICR CON

$^{\infty}p < 0.05$ vs ICR E7.25

$^{\beta}p < 0.001$ vs C57 CON

$^{\pi}p < 0.001$ vs C57 E7

RA treatment at E7 resulted in significant increase in the captioned frequency in ICR fetuses whereas no further increase in such frequency could be found when RA was applied at later gestational stages. RA treatment at E7.5 further significantly increased the captioned frequency in C57 fetuses such that 100% of fetal eyes were classified as anophthalmia or microphthalmia. Moreover, the captioned frequencies were 2-fold, 3-fold and 6-fold higher in C57 fetuses than in ICR fetuses when RA was applied at E7, E7.25, and E7.5 respectively.

Graph 3-9 Frequency of exophthalmia in E18 ICR and C57 fetuses treated with low dose of RA at different gestational days.

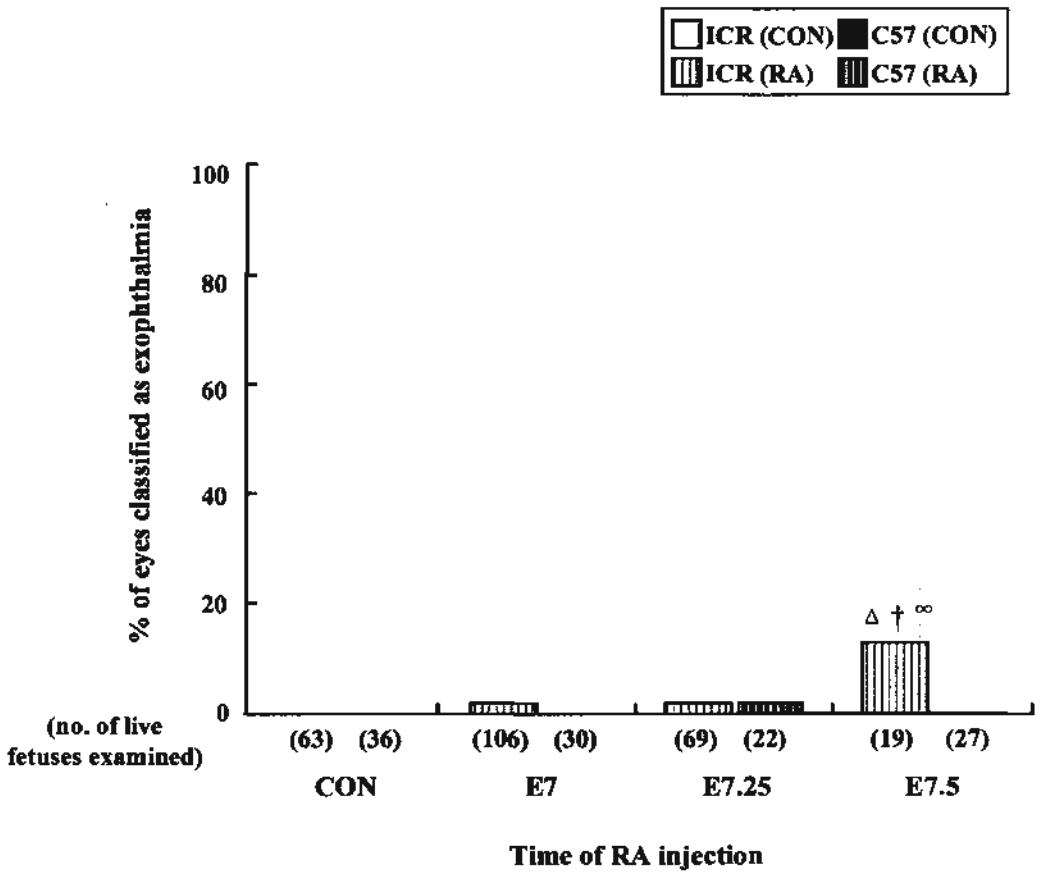

Data were analyzed by *chi*-square test.

$^{\Delta}p < 0.05$ vs ICR at the same gestational day

$^{\dagger}p < 0.001$ vs ICR CON

$^{\infty}p < 0.05$ vs ICR E7.25

RA treatment at E7.5 only resulted in low frequency of exophthalmia in ICR fetuses whereas in C57 fetuses, exophthalmia seemed to be a rare phenotype caused by RA treatment at all gestational days examined.

Graph 3-10 Frequency of eyes without eyelid in E18 ICR and C57 fetuses treated with low dose of RA at different gestational days.

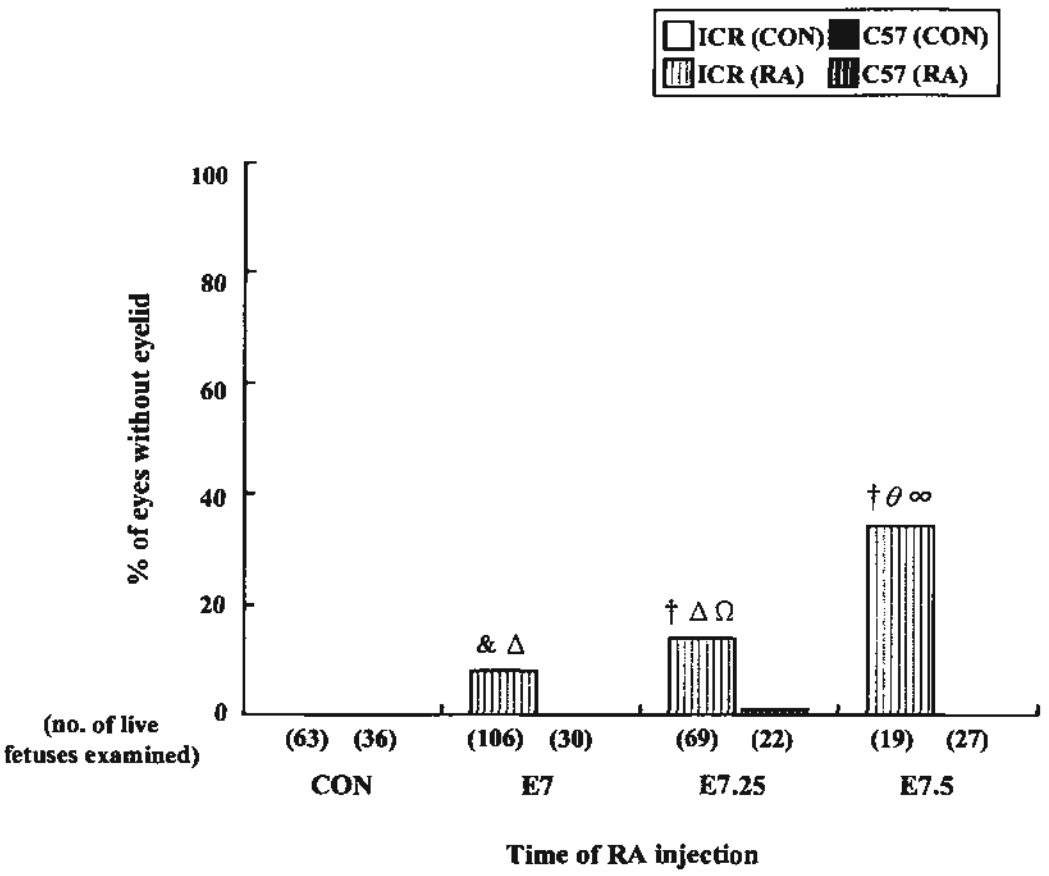

Data were analyzed by *chi*-square test.

$^{\Delta}p < 0.05$; $^{\theta}p < 0.001$ vs C57 at the same gestational day

$^{\&}p < 0.05$; $^{\dagger}p < 0.001$ vs ICR CON

$^{\Omega}p < 0.05$ vs ICR E7

$^{\infty}p < 0.05$ vs ICR E7.25

RA administration in C57 fetuses did not affect eyelid development. ICR fetuses exhibited greater sensitivity to RA-induced eyes without eyelids than C57 fetuses at all 3 gestational days of RA treatment.

Graph 3-11 Frequency of eyes with no or small lens in E18 ICR and C57 fetuses treated with low dose of RA at different gestational days.

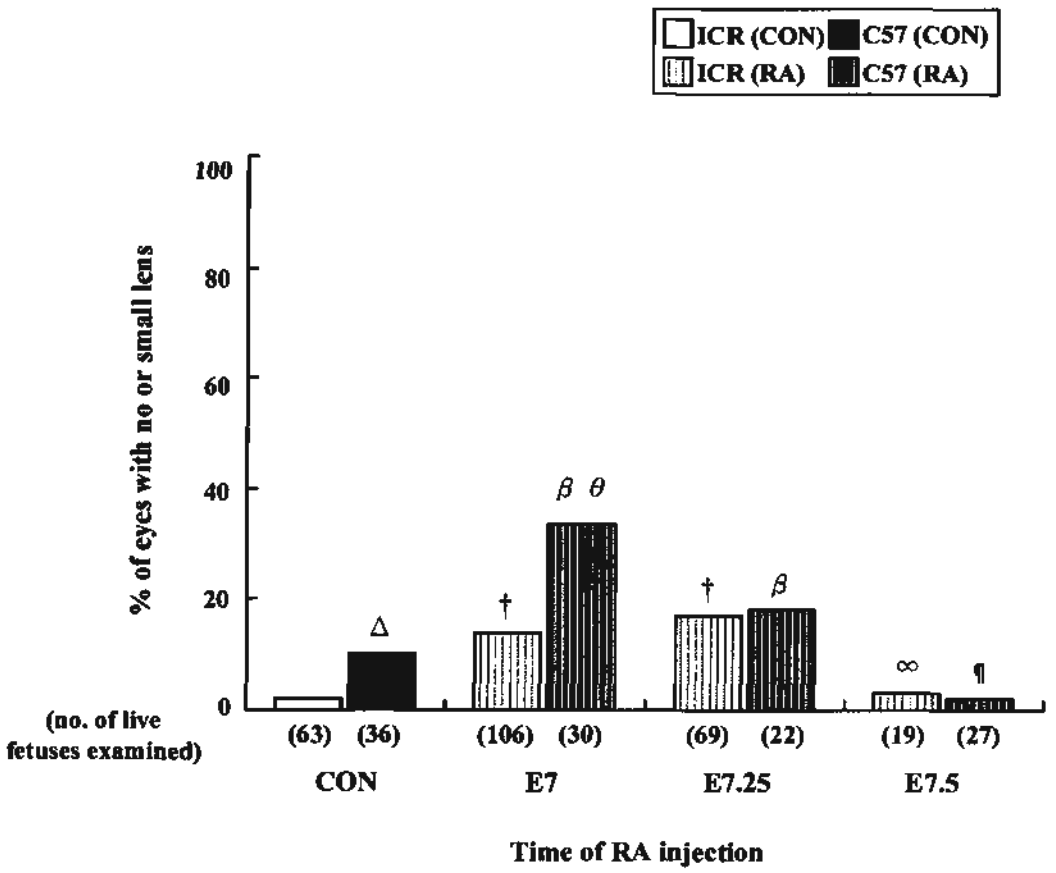

Data were analyzed by *chi*-square test.

$^{\Delta}p < 0.05$; $^{\theta}p < 0.001$ vs ICR at the same gestational day

$^{\dagger}p < 0.001$ vs ICR CON

$^{\infty}p < 0.05$ vs ICR E7.25

$^{\beta}p < 0.001$ vs C57 CON

$^{\P}p < 0.05$ vs C57 E7.25

RA treatment at E7 and E7.25 in ICR fetuses resulted in similar frequencies of eyes with lens defect whereas RA applied at E7.25 in C57 fetuses could not further enhance the captioned frequency when compared with that treated at E7.

Graph 3-12 Frequency of eyes with other minor ocular defects in E18 ICR and C57 fetuses treated with low dose of RA at different gestational days.

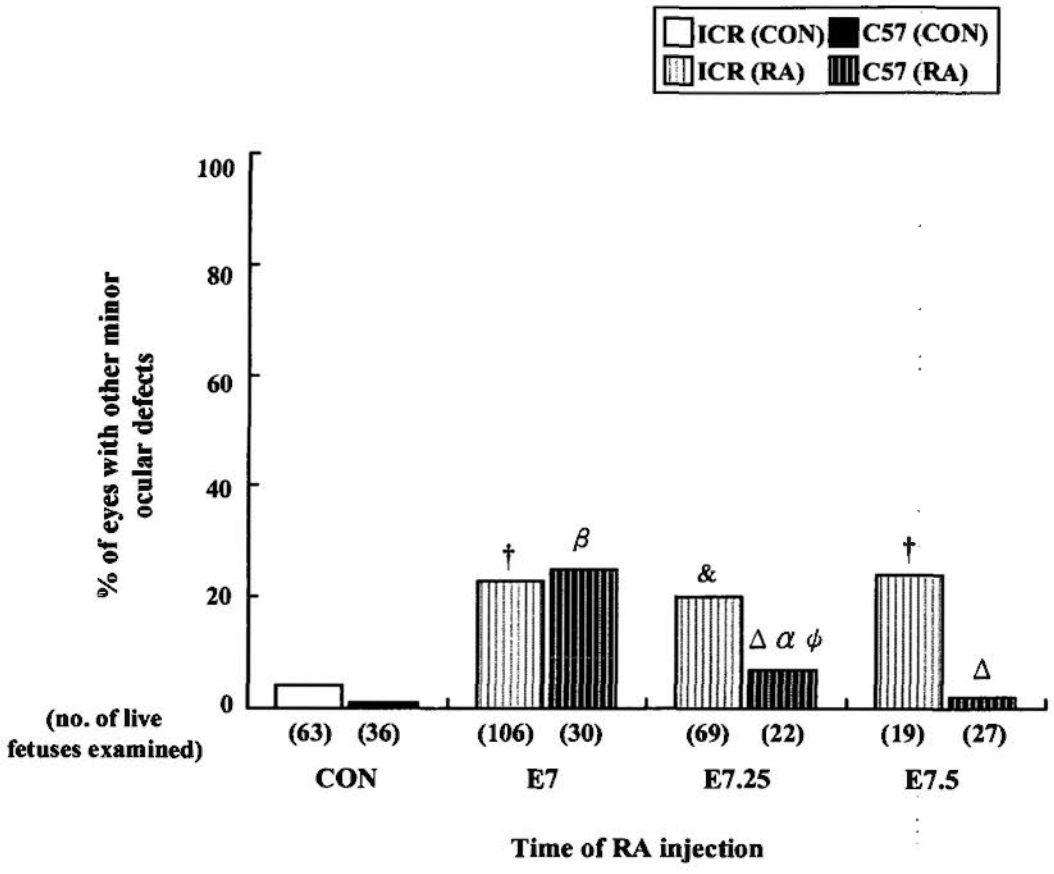

Data were analyzed by *chi*-square test.

$^{\Delta}p < 0.05$ vs ICR at the same gestational day

$^{\dagger}p < 0.001$ vs ICR CON

$^{\alpha}p < 0.05$; $^{\beta}p < 0.001$ vs C57 CON

$^{\psi}p < 0.05$ vs C57 E7

In ICR fetuses, RA treatment resulted in similar frequency of eyes with other minor ocular defects. The captioned frequency in C57 fetuses after having RA treatment at later gestational days was significantly lower than that in ICR fetuses because over 80% and 98% of C57 fetal eyes were in fact anophthalmia.

Graph 3-13 Frequency of exencephaly in E18 ICR and C57 fetuses treated with low dose of RA at different gestational days.

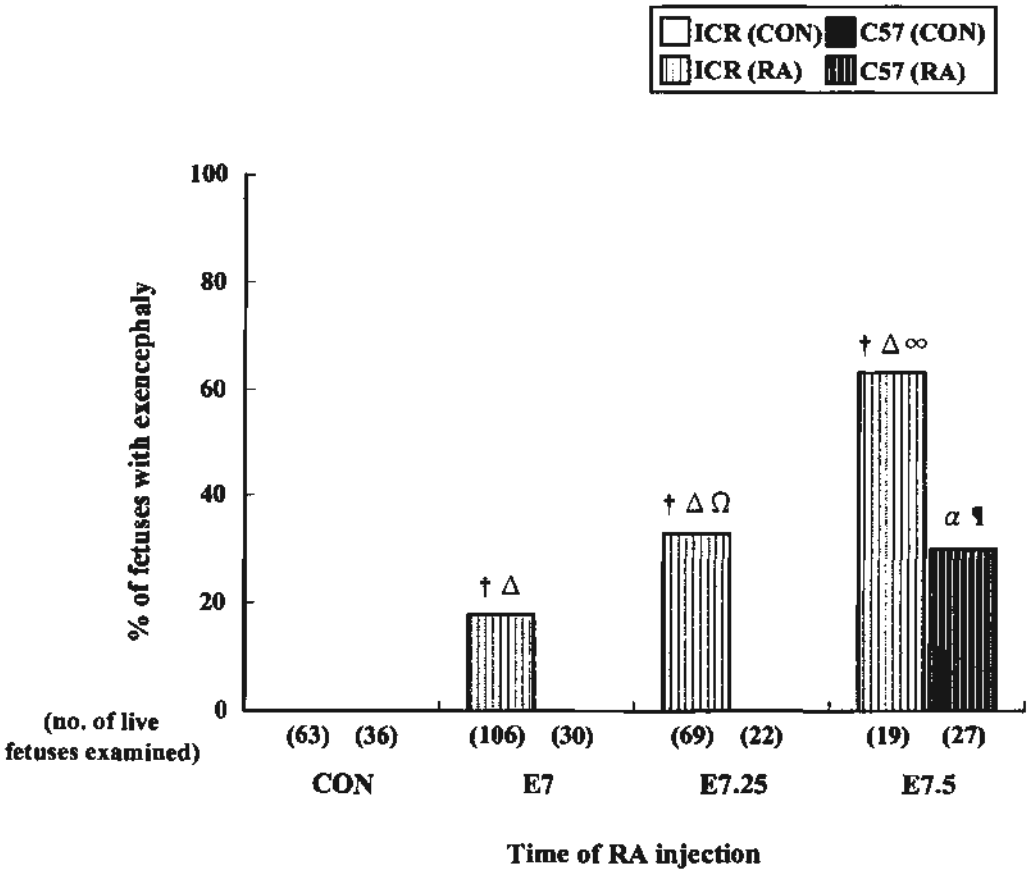

Data were analyzed by *chi*-square test.

$^{\Delta}$ $p < 0.05$ vs C57 at the same gestational day

† $p < 0.001$ vs ICR CON

$^{\Omega}$ $p < 0.05$ vs ICR E7

$^{\infty}$ $p < 0.05$ vs ICR E7.25

$^{\alpha}$ $p < 0.05$ vs C57 CON

¶ $p < 0.05$ vs C57 E7.25

RA application at later gestational days resulted in further significant increase in the captioned frequency in ICR fetuses. RA applied at E7.5 resulted in significant higher frequency in C57 fetuses than that at E7.25. Moreover, ICR fetuses was significantly more prone to develop this defect than C57 fetuses after RA treatment at all gestational days examined.

Graph 3-14 Frequency of cleft palate in E18 ICR and C57 fetuses treated with low dose of RA at different gestational days.

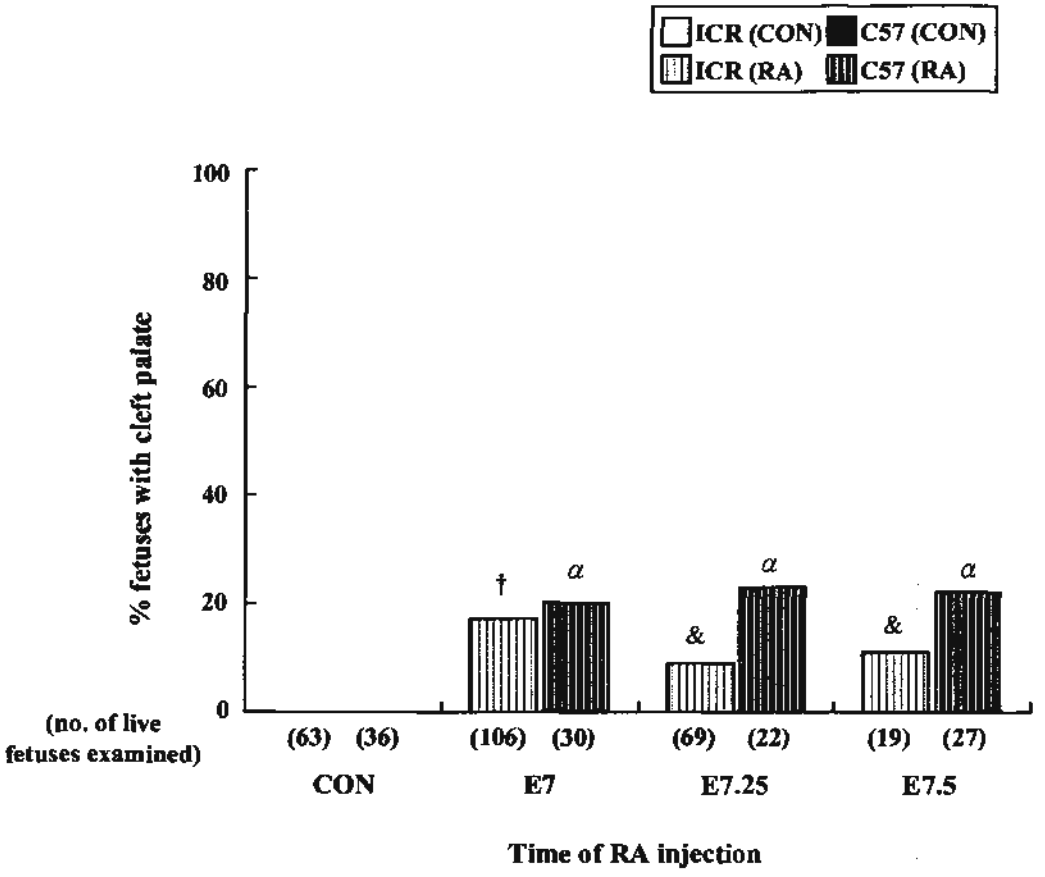

Data were analyzed by *chi*-square test.

$^{\&}p < 0.05$; $^{\dagger}p < 0.001$ vs ICR CON

$^{\alpha}p < 0.05$ vs C57 CON

Similar frequency of cleft palate was resulted in ICR and C57 fetuses when RA administered at all gestational days examined.

Graph 3-15 Comparison of somite number of ICR and C57 embryos at the same gestational day.

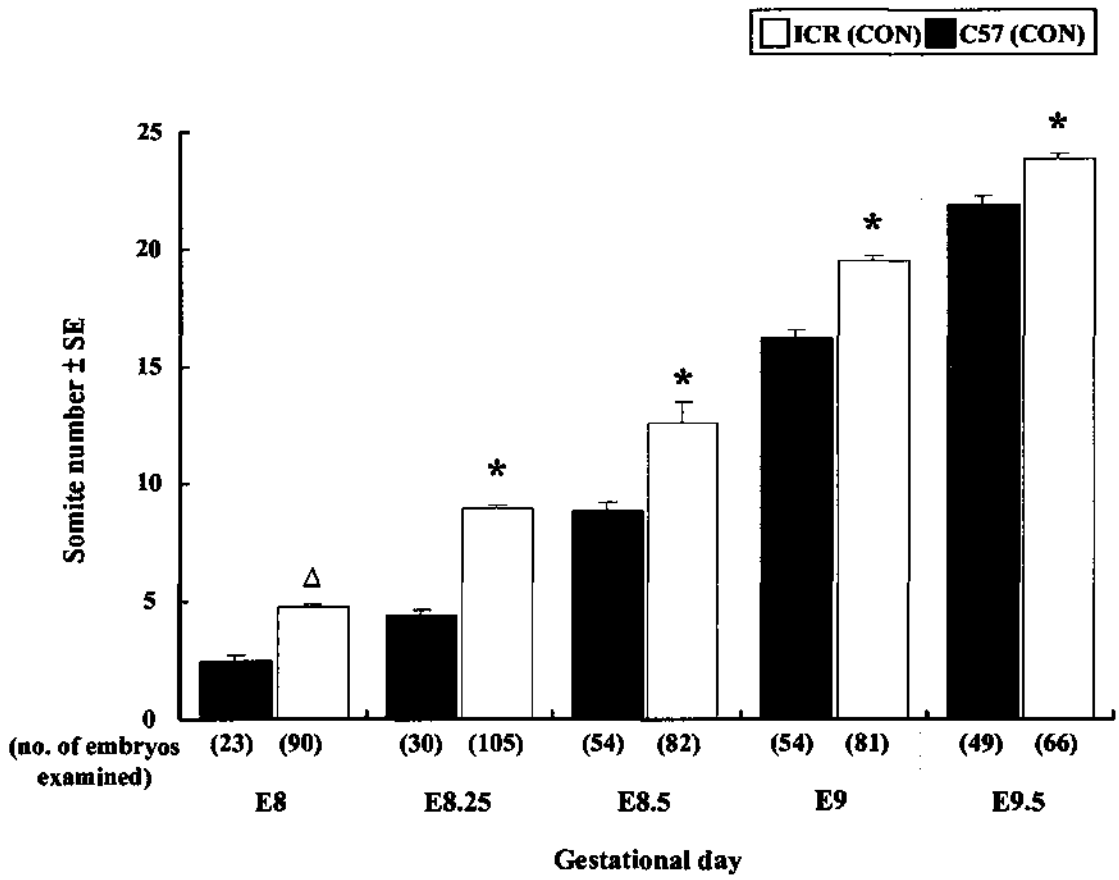

Data were analyzed by Independent sample *t* test.

$^{\Delta}p < 0.05$; $p < 0.001$ vs ICR (CON) at the same gestational day

Significant differences in somite number were found between ICR and C57 embryos were found at all gestational days examined.

Graph 3-16 Comparison of somite number of ICR and C57 embryos with 6 hour difference in gestational age.

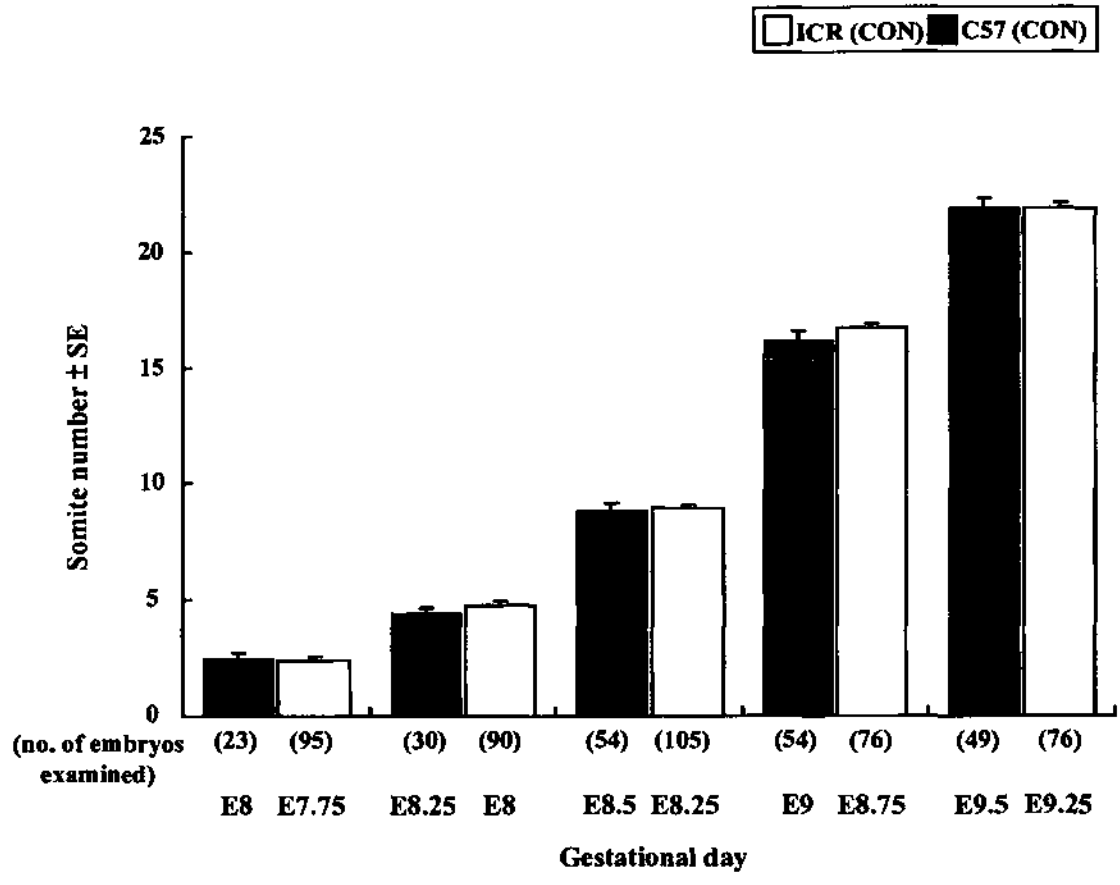

Data were analyzed by Independent sample *t* test.

There was no significant difference in somite number between C57 and ICR (6 hour behind) embryos.

Graph 3-17 Distribution patterns of ICR (E7) and C57 (E7.25) embryos at different pre-somitic stages.

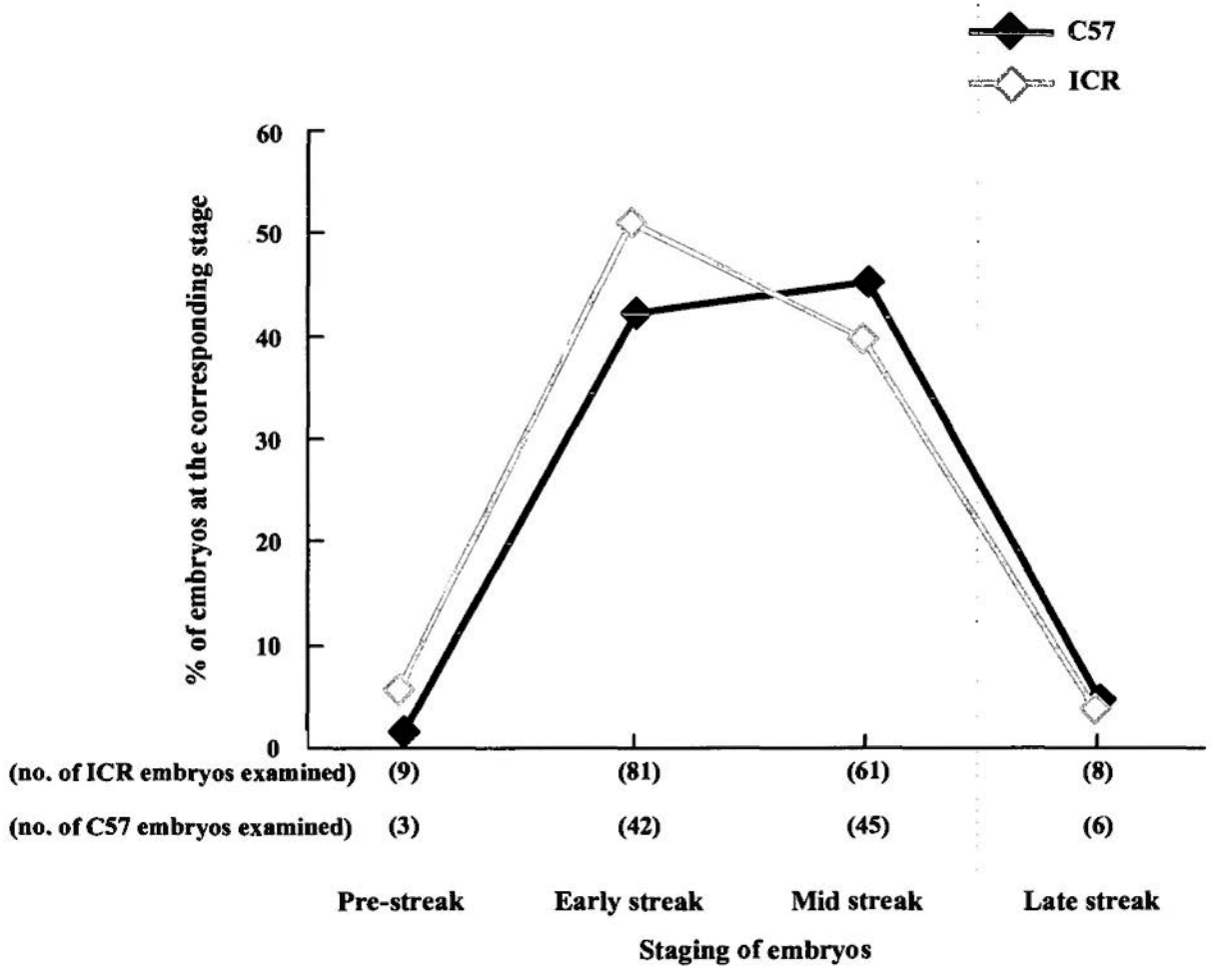

Data were analyzed by *chi*-square test.

There was no significant difference between the distribution patterns of ICR (E7) and C57 (E7.25) embryos at different pre-somitic stages.

Graph 3-18 Total frequency of anophthalmia and microphthalmia in E18 fetuses of different genotypes treated with low dose of RA at E7.25.

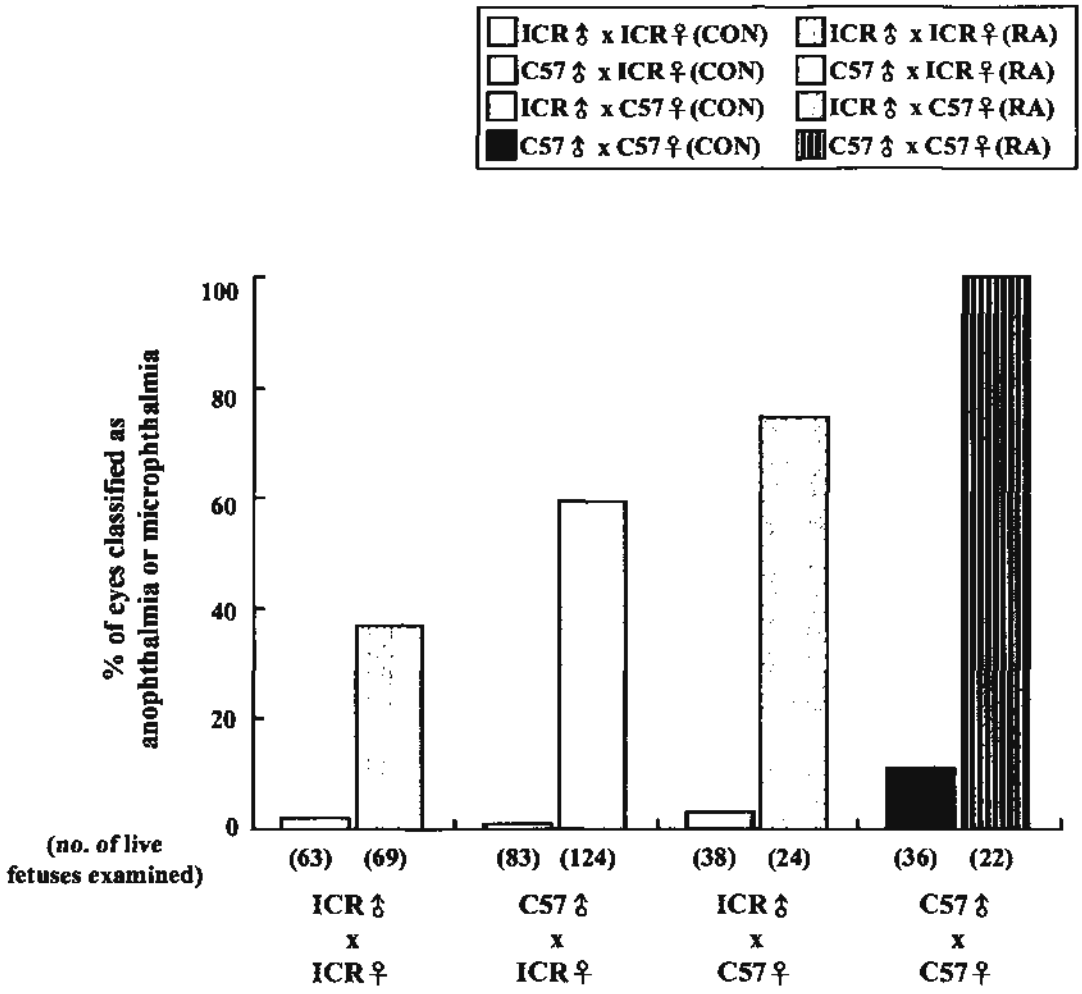

Data were analyzed by logistic regression.

The C57 strain has significant contribution of genetic dominance as well as maternal effects in causing fetuses more prone to develop ocular defects under RA influence.

For detailed information on statistical analysis, please refer to section 3.4.7.1

Graph 3-19 Frequency of exencephaly in E18 fetuses of different genotypes treated with low dose of RA at E7.25.

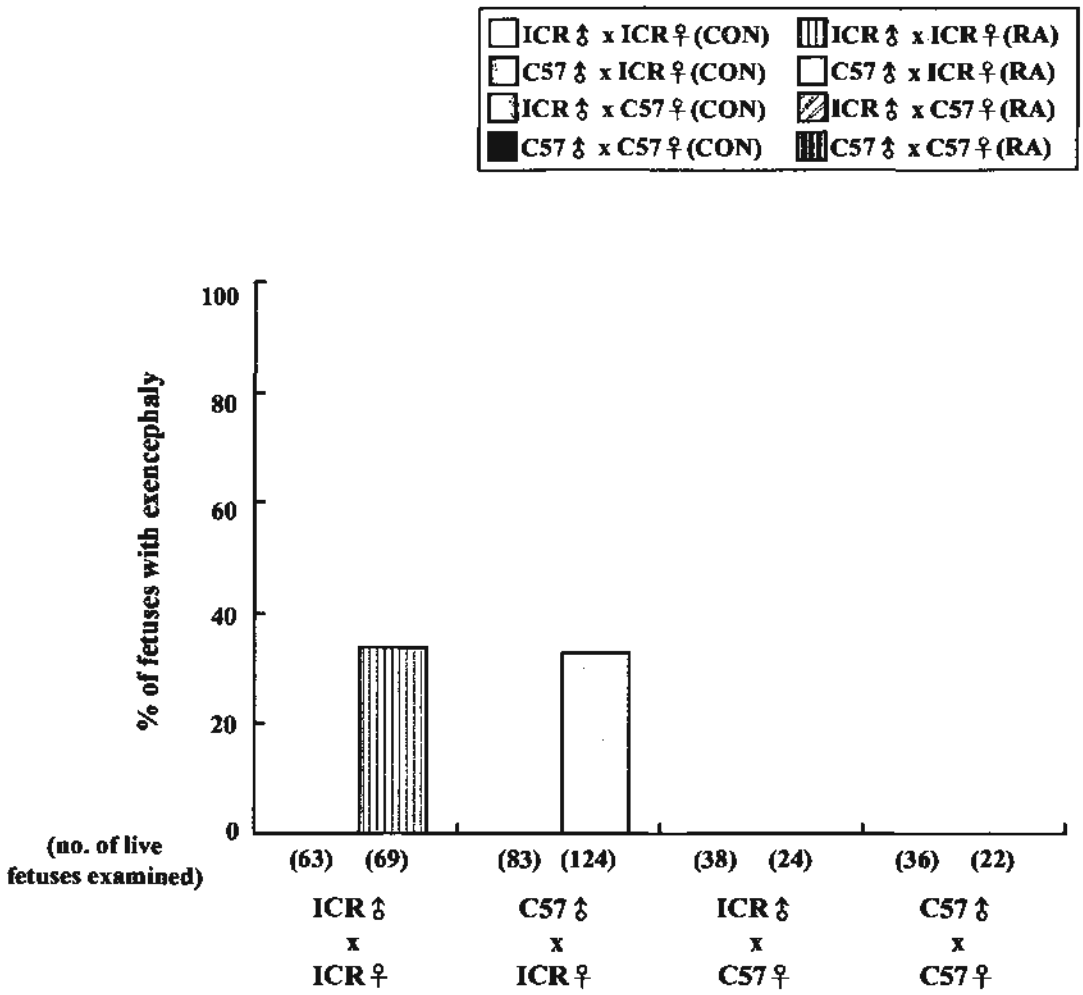

Data were analyzed by logistic regression.

The C57 strain does not have genetic dominance nor maternal effects in causing fetuses more prone to develop exencephaly under RA influence.

For detailed information on statistical analysis, please refer to section 3.4.7.2

Graph 3-20 Frequency of cleft palate in E18 fetuses of different genotypes treated with low dose of RA at E7.25.

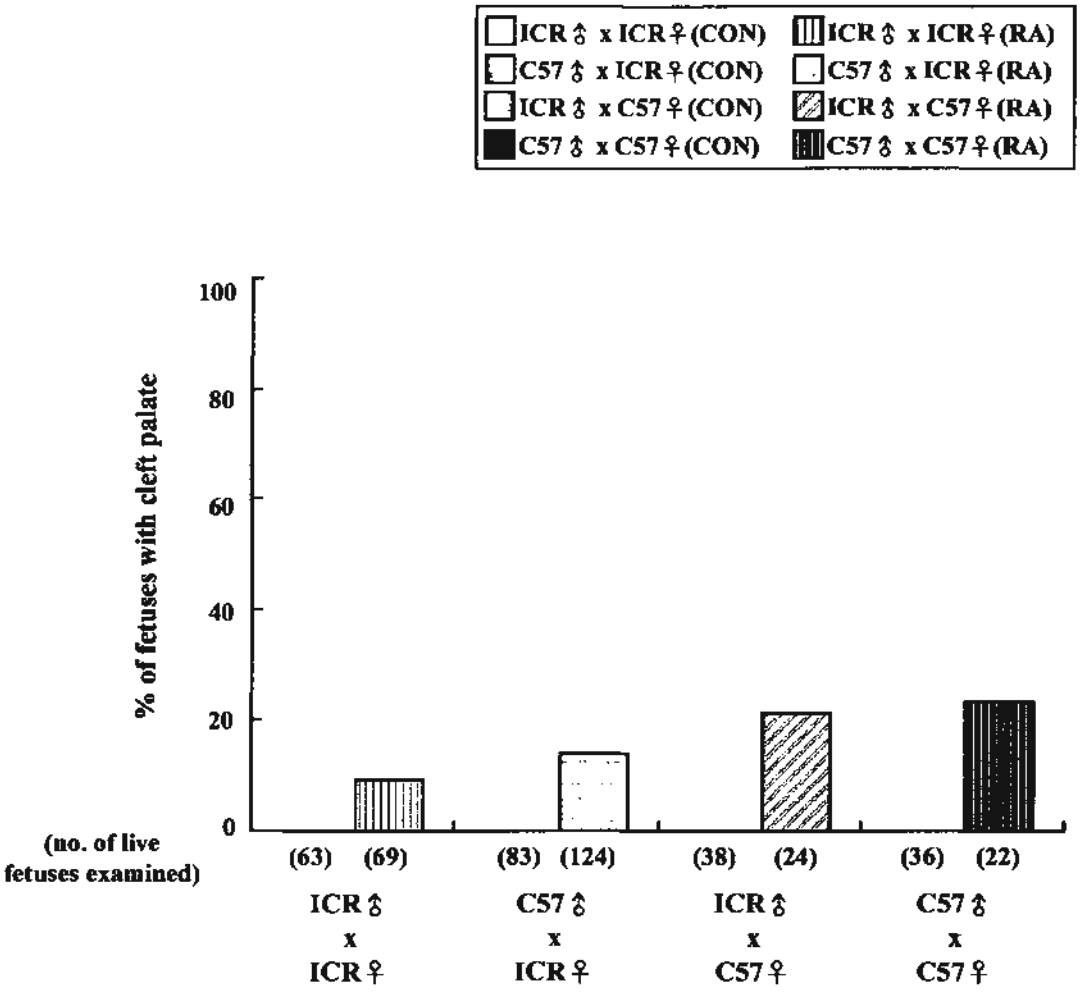

Data were analyzed by logistic regression.

The C57 strain does not have genetic dominance nor maternal effects in causing fetuses more prone to develop cleft palate under RA influence. .

For detailed information on statistical analysis, please refer to section 3.4.7.3

Graph 4-1 Comparison of somite number of ICR embryos with or without RA treatment at E7.

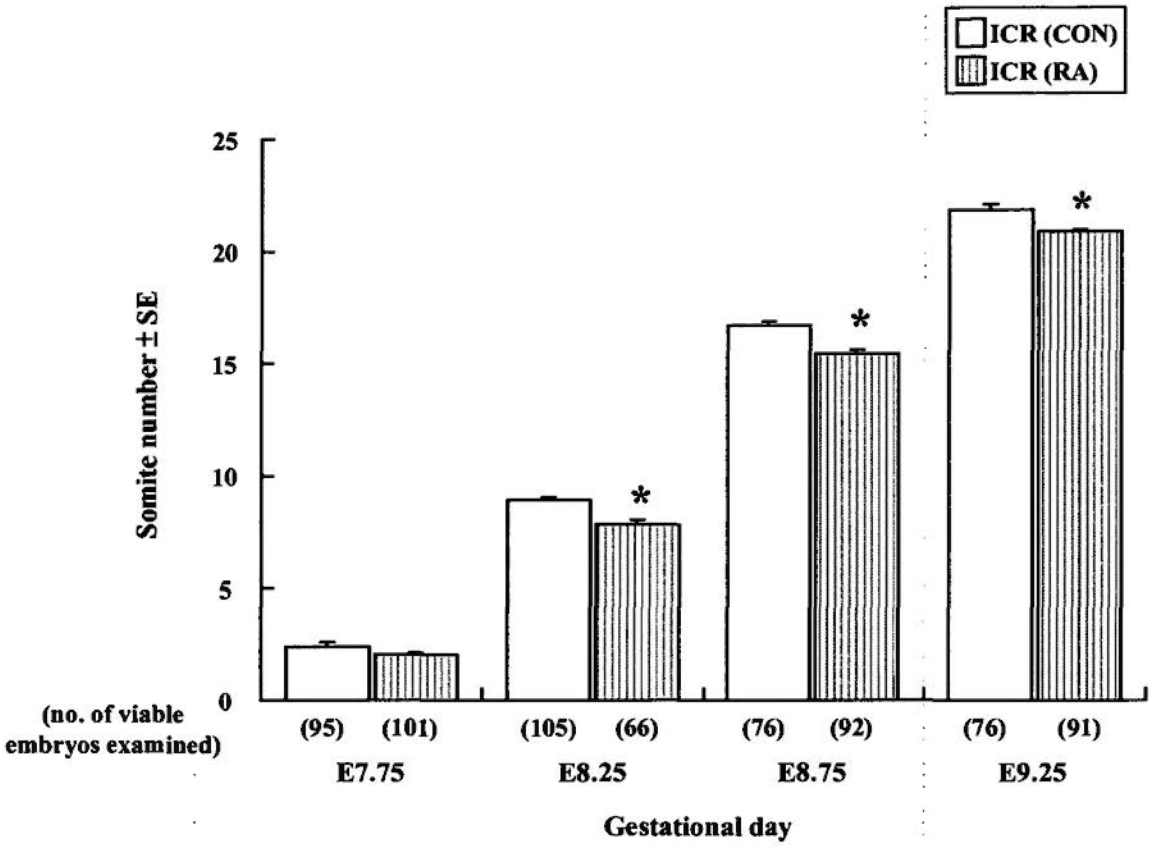

Data were analyzed by Independent sample *t* test.

* $p < 0.001$ vs CON at the same gestational day.

There was significant difference in the somite number between ICR embryos with and without RA treatment from E8.25 onwards.

Graph 4-2 Comparison of somite number of C57 embryos with or without RA treatment at E7.25.

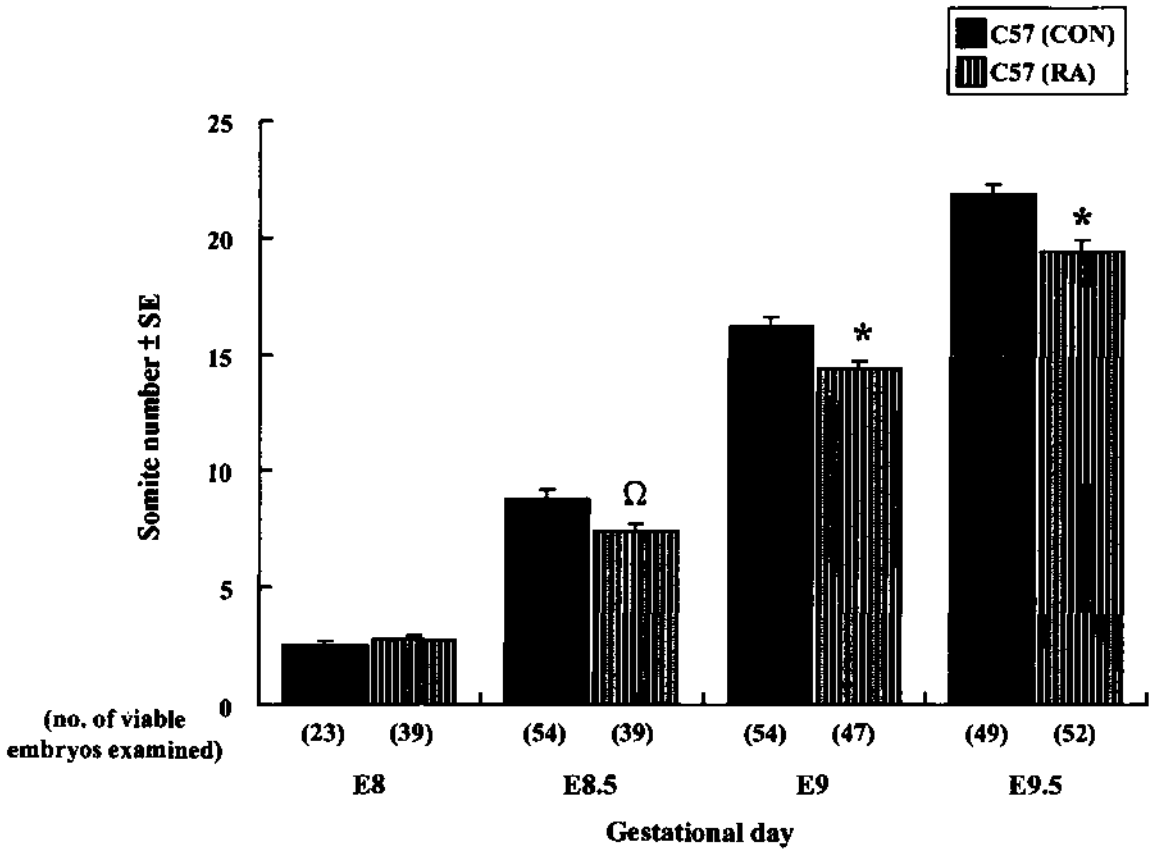

Data were analyzed by Independent sample *t* test.

* $p < 0.001$; $^{\Omega}p < 0.01$ vs CON at the same gestational day.

There was significant difference in somite number between C57 embryos with and without RA treatment was found from E8.5 onwards.

Graph 4-3 **Percentage of apoptotic bodies in the mesenchyme underlying the neuroepithelium of the future forebrain of ICR (E7.75) and C57 (E8) embryos with or without RA treatment at E7 and E7.25 respectively.**

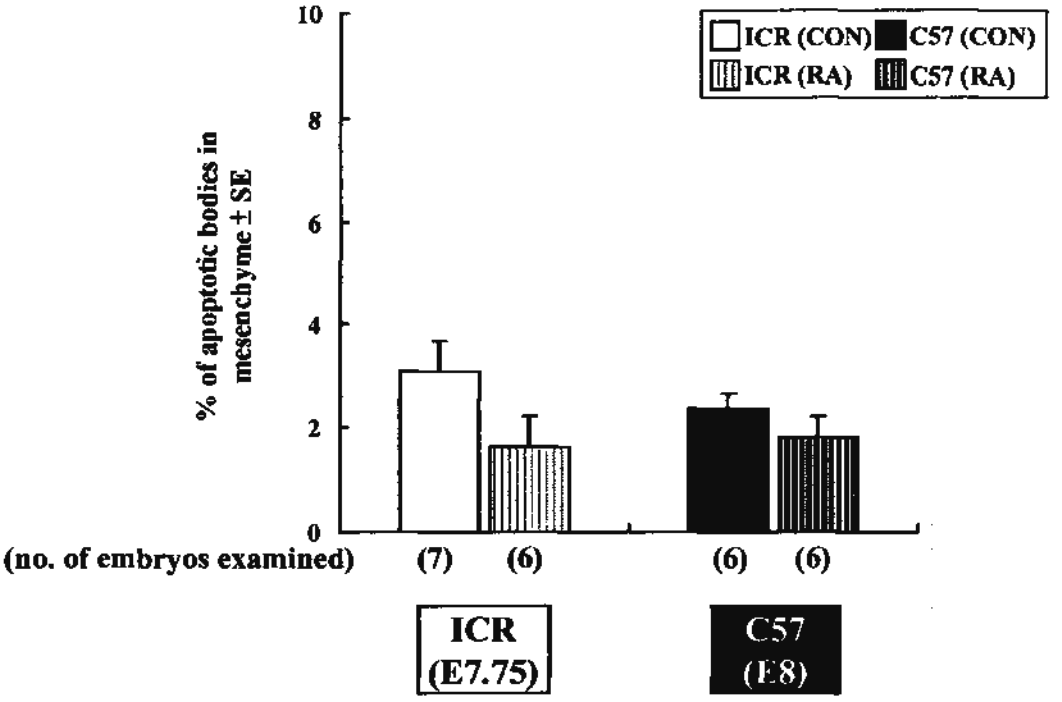

Data were analyzed by Independent sample *t* test.

There was no significant difference between the control and RA-treated embryos of the ICR strain (E7.75) as well as the C57 strain (E8).

Graph 4-4 **Percentage of apoptotic bodies in the mesenchyme underlying the neuroepithelium of the future forebrain of ICR (E8.25) and C57 (E8.5) embryos with or without RA treatment at E7 and E7.25 respectively.**

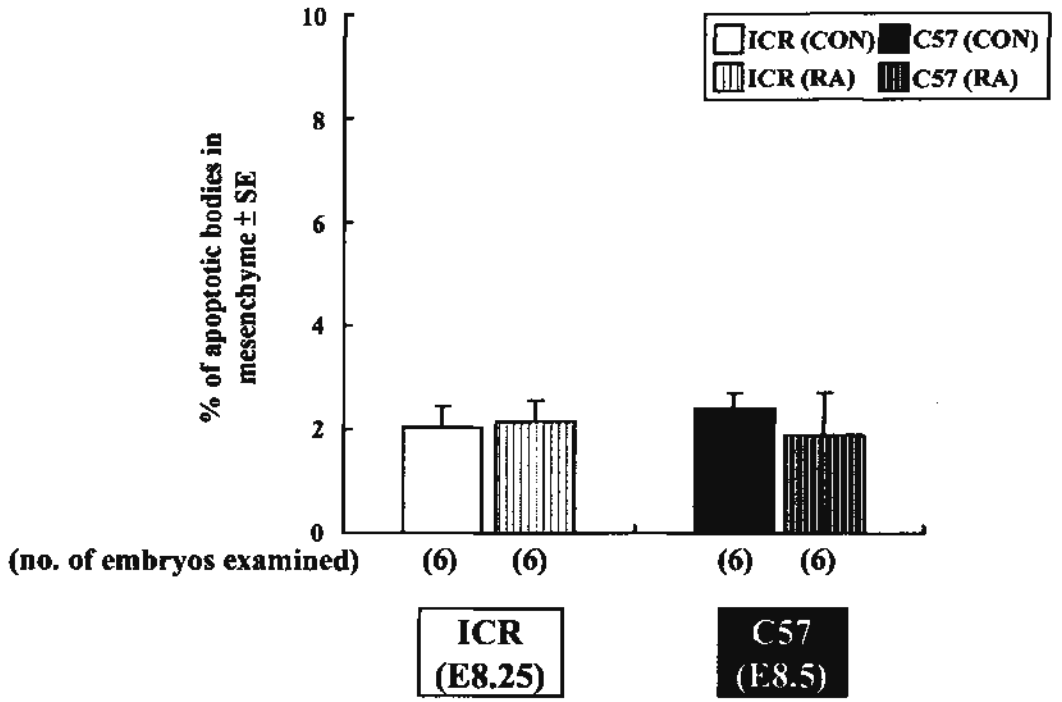

Data were analyzed by Independent sample *t* test.

There was no significant difference between the control and RA-treated embryos of the ICR strain (E8.25) as well as the C57 strain (E8.5).

Graph 4-5 **Percentage of apoptotic bodies in the neuroepithelium of the future forebrain of ICR (E7.75) and C57 (E8) embryos with or without RA treatment at E7 and E7.25 respectively.**

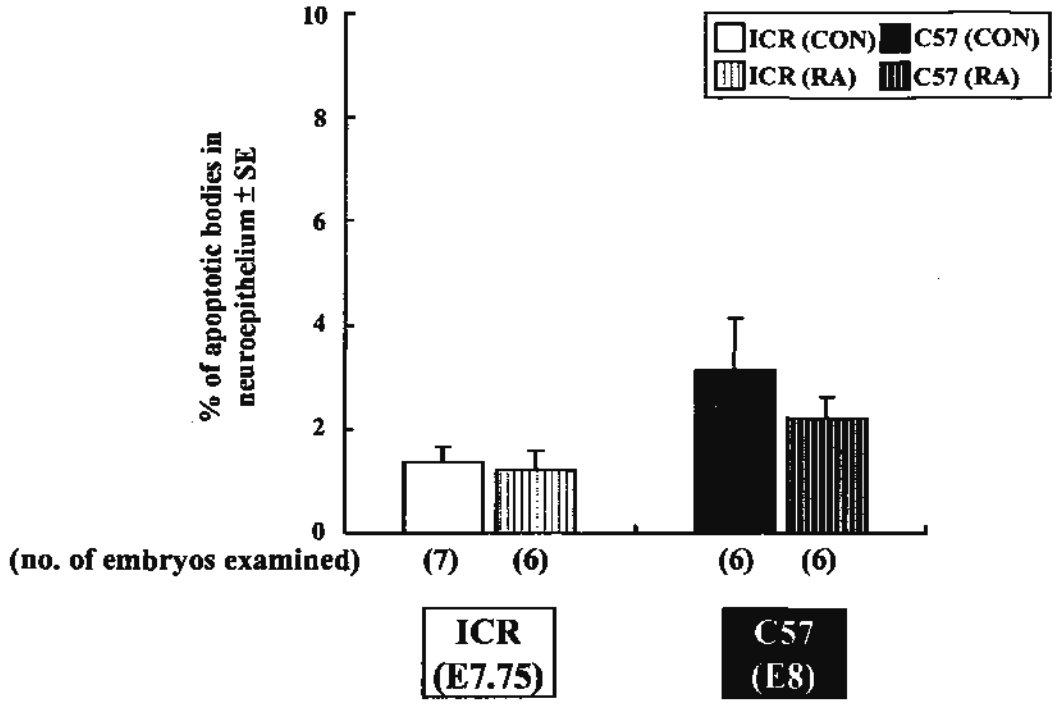

Data were analyzed by Independent sample *t* test.

There was no significant difference between the control and RA-treated embryos of the ICR strain (E7.75) as well as the C57 strain (E8).

Graph 4-6 **Percentage of apoptotic bodies in the neuroepithelium of the future forebrain of ICR (E8.25) and C57 (E8.5) embryos with or without RA treatment at E7 and E7.25 respectively.**

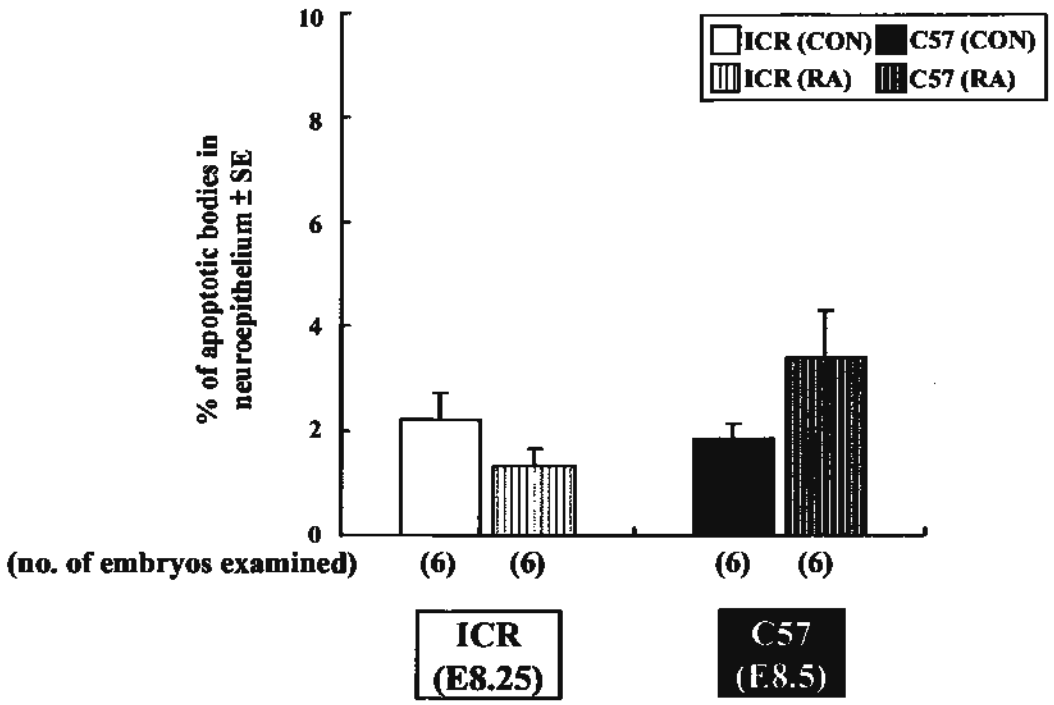

Data were analyzed by Independent sample *t* test.

There is no significant difference between the control and RA-treated embryos of the ICR strain (E8.25) as well as the C57 strain (E8.5).

Graph 5-1 **Relative expression levels of *Raldh2* in the head region of ICR (E8.25) and C57 (E8.5) embryos with or without RA treatment at E7 and E7.25 respectively.**

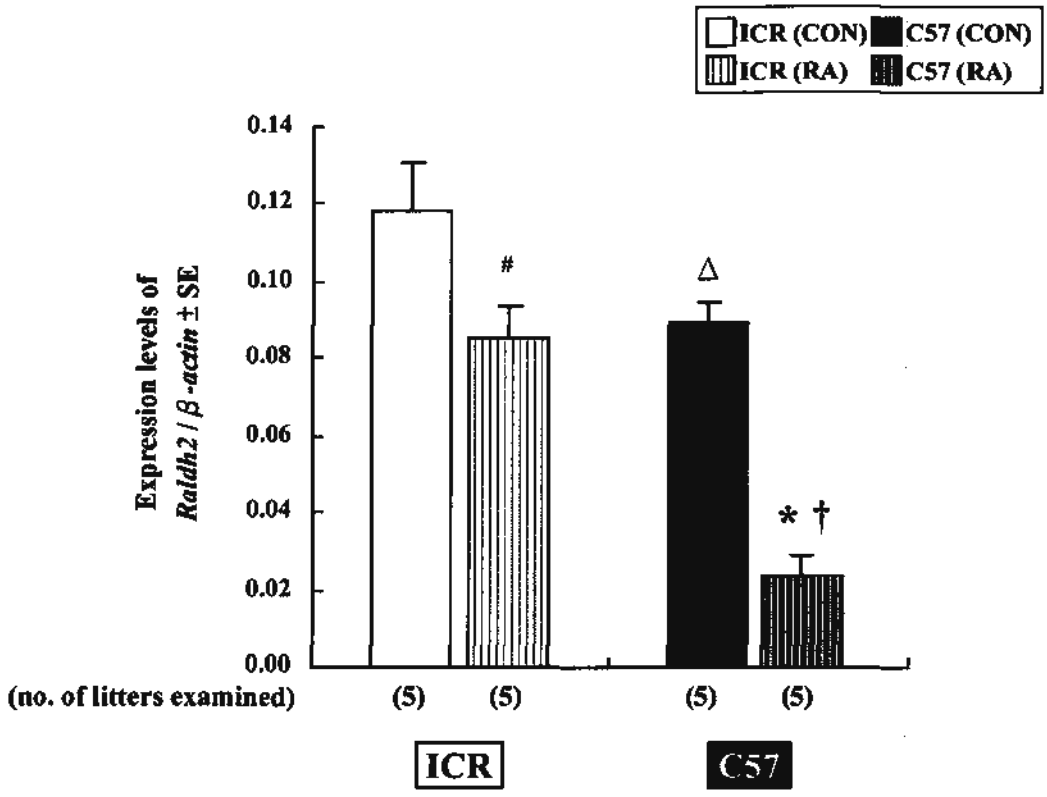

Data of control (CON) and RA-treated (RA) embryos of the same and different mouse strains were compared by Independent sample *t* test.

$^{\#}$ $p < 0.05$ vs ICR (CON)

* $p < 0.001$ vs C57 (CON)

$^{\Delta}$ $p < 0.05$ vs ICR (CON)

† $p < 0.001$ vs ICR (RA)

RA treatment resulted in significant reduction in the relative expression level of *Raldh2* in the head region of ICR and C57 embryos. Moreover, the extent of suppression of *Raldh2* expression levels in the head region of C57 embryos was significantly greater than that of ICR embryos.

Graph 5-2 **Relative expression levels of *Raldh2* in the trunk region of ICR (E8.25) and C57 (E8.5) embryos with or without RA treatment at E7 and E7.25 respectively.**

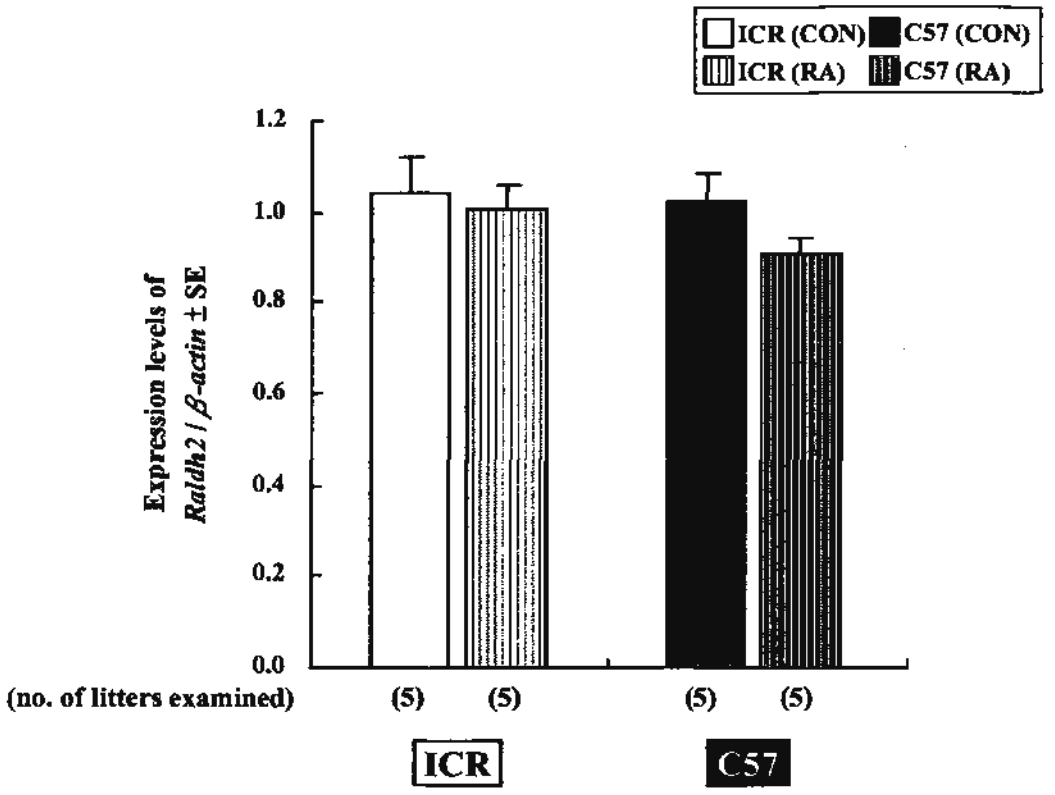

Data of control (CON) and RA-treated (RA) embryos of the same and different mouse strains were compared by Independent sample *t* test.

There was no significant difference in the relative expression level of *Raldh2* in the trunk region between the same and different mouse strains.

Graph 5-3 **Relative expression levels of *Raldh3* in the head region of ICR (E8.25) and C57 (E8.5) embryos with or without RA treatment at E7 and E7.25 respectively.**

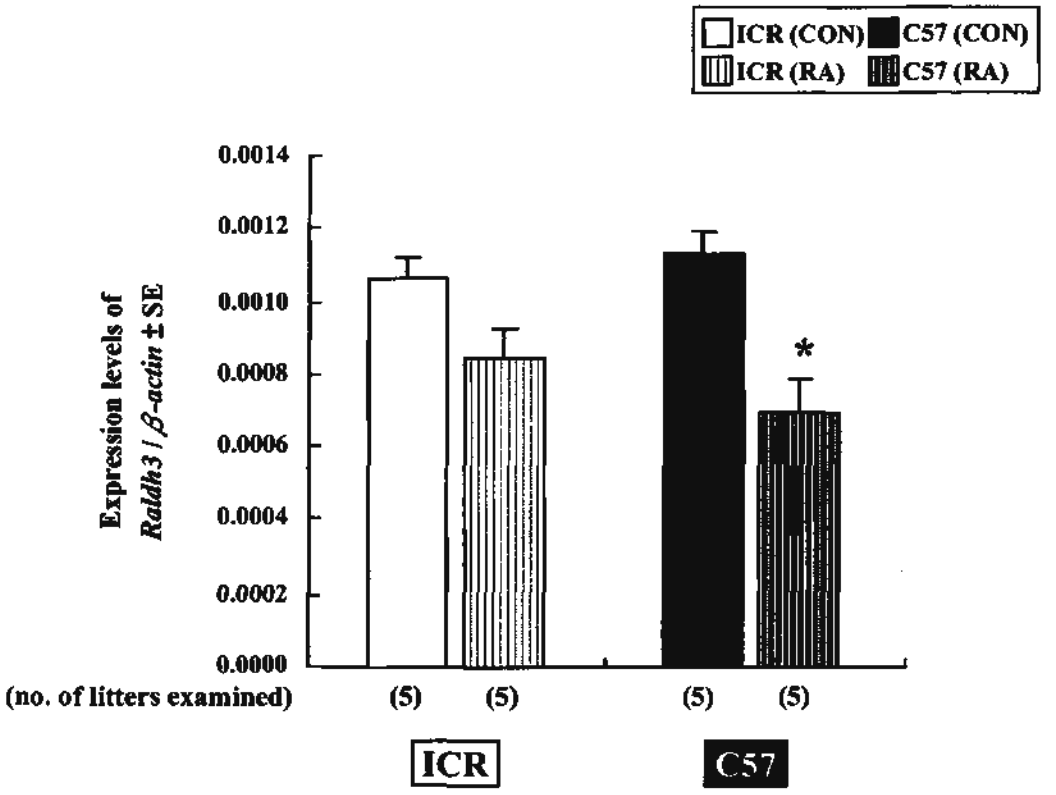

Data of control (CON) and RA-treated (RA) embryos of the same and different mouse strains were compared by Independent sample *t* test.

* $p < 0.05$ vs C57 (CON)

RA treatment resulted in significant reduction of *Raldh3* expression levels in the head region of C57 embryos.

Graph 5-4 **Relative expression levels of Cyp26a1 in the head region of ICR (E8.25) and C57 (E8.5) embryos with or without RA treatment at E7 and E7.25 respectively.**

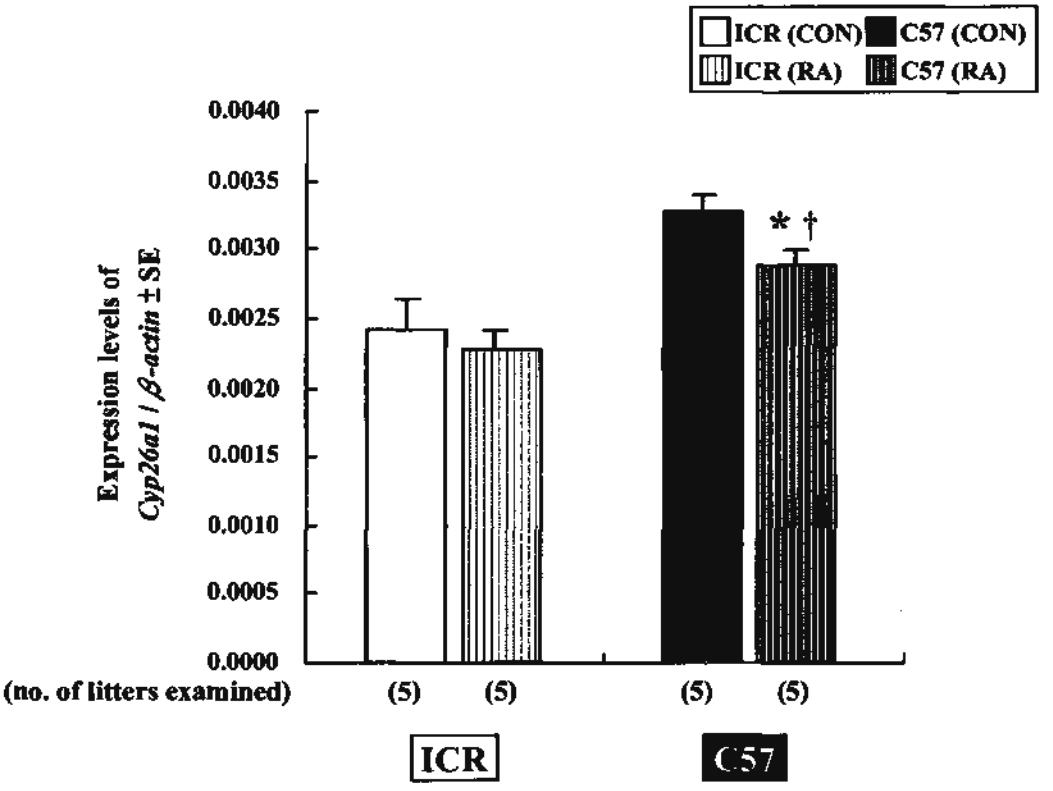

Data of control (CON) and RA-treated (RA) embryos of the same and different mouse strains were compared by Independent sample *t* test.

* $p < 0.05$ vs C57 (CON)

† $p < 0.005$ vs ICR (RA)

RA treatment resulted in significant downregulation of *Cyp26a1* in the head region of C57 embryos. However, no significant difference between control and RA-treated embryos was found in the ICR strain.

Graph 5-5 **Relative expression levels of *Cyp26a1* in the trunk region of ICR (E8.25) and C57 (E8.5) embryos with or without RA treatment at E7 and E7.25 respectively.**

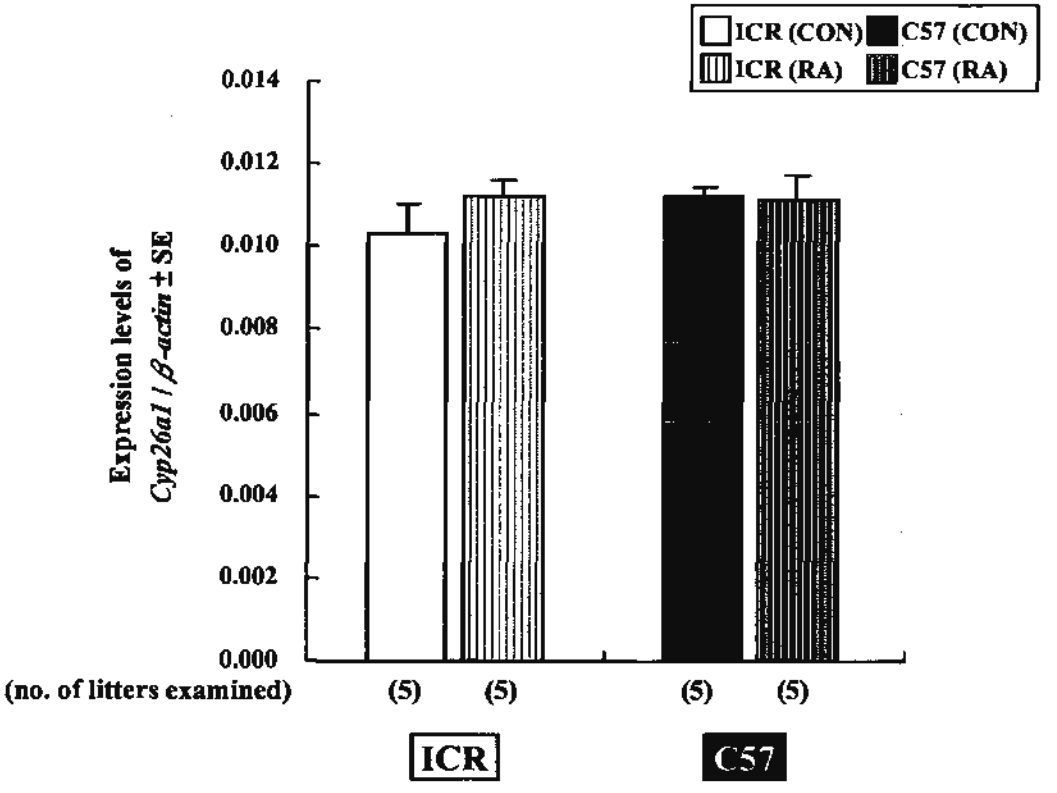

Data of control (CON) and RA-treated (RA) embryos of the same and different mouse strains were compared by Independent sample *t* test.

There was no significant difference in the expression level of *Cyp26a1* in the trunk region between the same and different mouse strains.

Graph 5-6 **Relative expression levels of *Pax6* in the head region of ICR (E8.25) and C57 (E8.5) embryos with or without RA treatment at E7 and E7.25 respectively.**

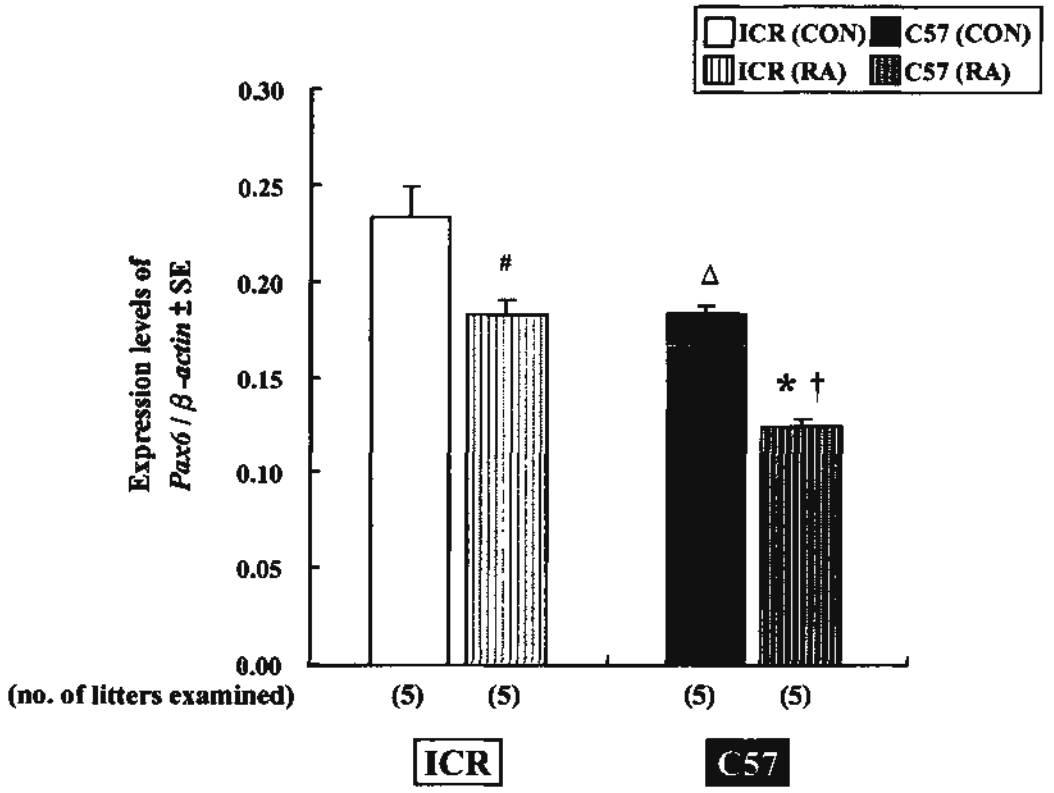

Data of control (CON) and RA-treated (RA) embryos of the same and different mouse strains were compared by Independent sample *t* test.

$^{\#}$ $p < 0.05$ vs ICR (CON)

* $p < 0.001$ vs C57 (CON)

$^{\Delta}$ $p < 0.05$ vs ICR (CON)

† $p < 0.001$ vs ICR (RA)

RA treatment resulted in significant reduction in the relative expression level of *Pax6* in the head region of C57 and ICR embryos when compared with that in the corresponding control group.

Graph 5-7 **Relative expression levels of *Hes1* in the head region of ICR (E8.25) and C57 (E8.5) embryos with or without RA treatment at E7 and E7.25 respectively.**

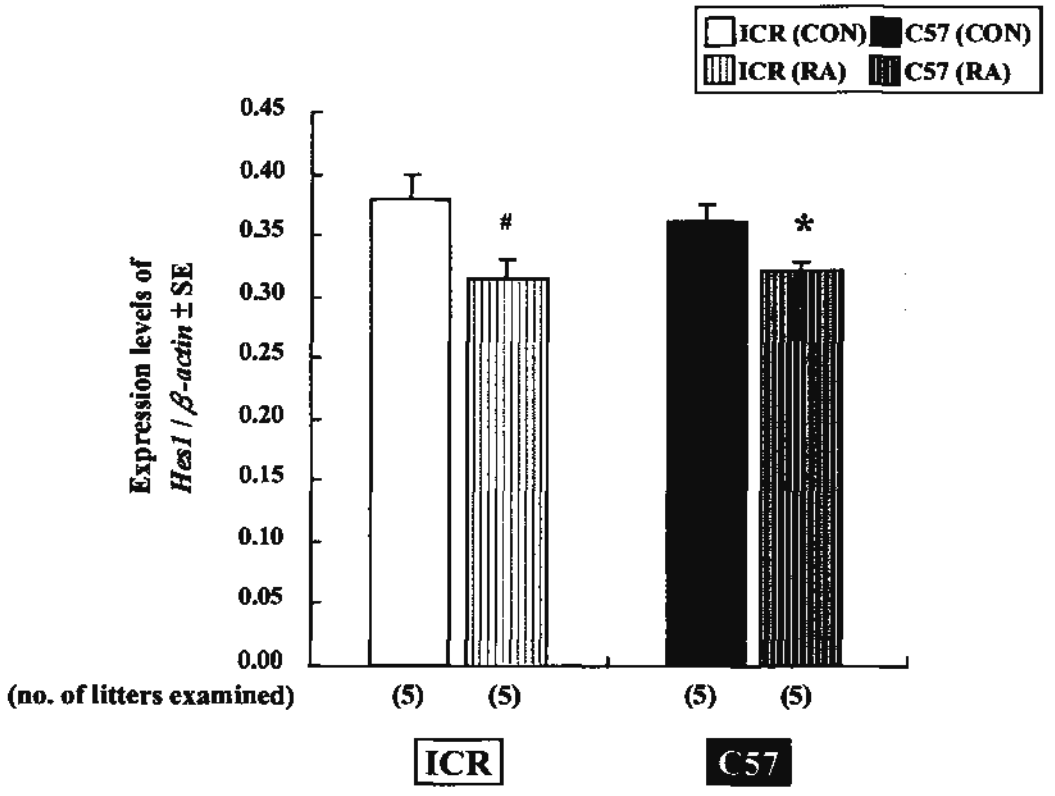

Data of control (CON) and RA-treated (RA) embryos of the same and different mouse strains were compared by Independent sample *t* test.

$^{\#}p < 0.05$ vs ICR (CON)

$^{*}p < 0.05$ vs C57 (CON)

RA treatment resulted in significant reduction in *Hes1* expression levels in the head region of ICR and C57 embryos when compared with that in the corresponding control group.

Graph 6-1 Measurement of endogenous RA concentrations in head explants of ICR (E8.25) and C57 (E8.5) embryos with or without exogenous RA treatment at E7 and E7.25 respectively.

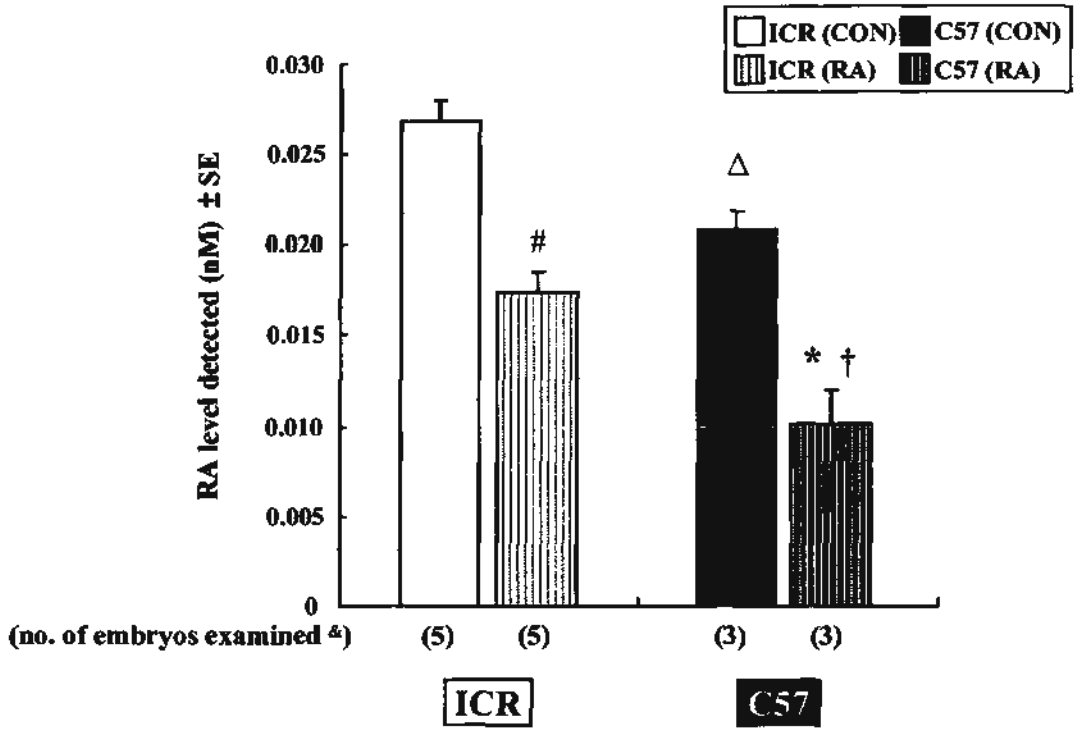

Data of control (CON) and RA-treated (RA) embryos of the same and different mouse strains were compared by Independent sample *t* test.

# $p < 0.001$ vs ICR (CON)

* $p < 0.005$ vs C57 (CON)

Δ $p < 0.05$ vs ICR (CON)

† $p < 0.05$ vs ICR (RA)

& 20 heads explants per sample

Exogenously administered RA resulted in significant reduction in endogenous RA concentrations in the head region of both ICR and C57 embryos when compared with that in the corresponding control group. Moreover, the endogenous RA concentration in the head region of C57 control embryos was significantly lower than that of ICR control embryos.

FIGURES

Figure 1-1 Schematic overview of human eye development.

A. The single central eye field splits into two lateral parts which will form optic pits.

B. Optic pit formation is initiated by an evagination of the neuroepithelium (future forebrain) as indicated by the arrow.

C. Further evagination of the optic pit will form the optic vesicle by the time of neural tube closure. Induction by close contact between the neuroepithelium and the overlying ectoderm will initiate growth and become the neural retina and lens placode respectively.

D. Further induction leads to invagination of the lens placode and neural retina. It will then gradually form the lens vesicle and cup-shaped like neural retina and collectively called bi-layered optic cup.

E. The lens fibres elongate from the posterior epithelium of the lens vesicle and fill its entire central cavity whereas the anterior epithelium forms the anterior lens epithelium.

F. Mature eye after birth.

Color codes:	blue	presumptive or differentiated lens / cornea
	green	presumptive or differentiated neural retina
	purple	presumptive or differentiated optic stalk
	red	presumptive or differentiated future forebrain
	yellow	presumptive or differentiated retinal pigmented epithelium
	others	undifferentiated tissues

Figures are modified from Chow and Lang (2001) and Graw (2003).

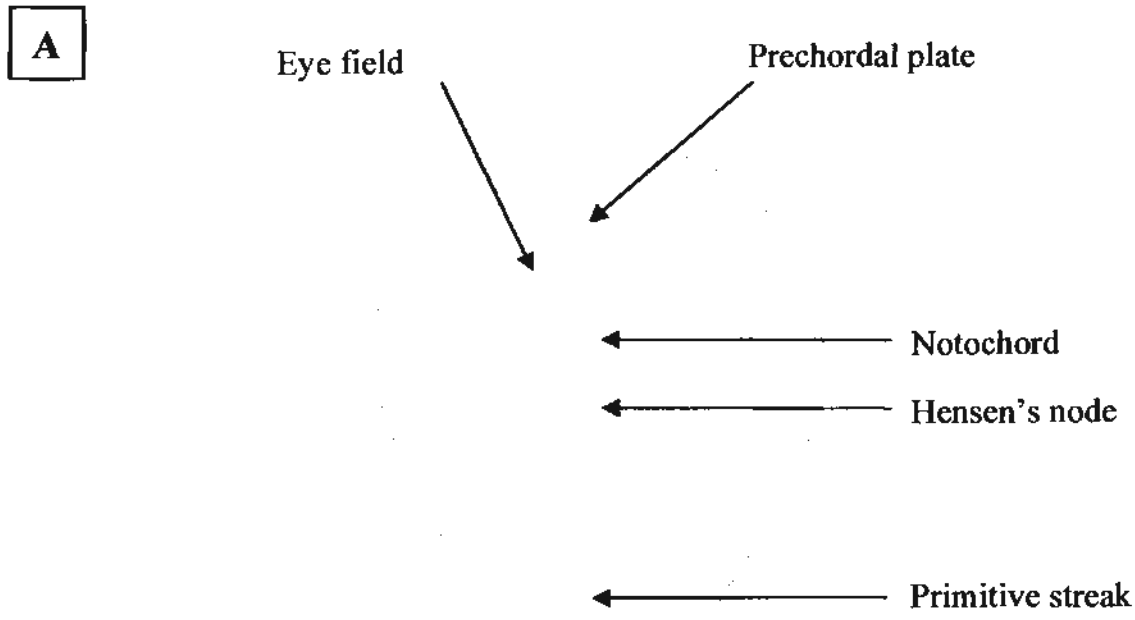
A
Eye field
Prechordal plate
Notochord
Hensen's node
Primitive streak

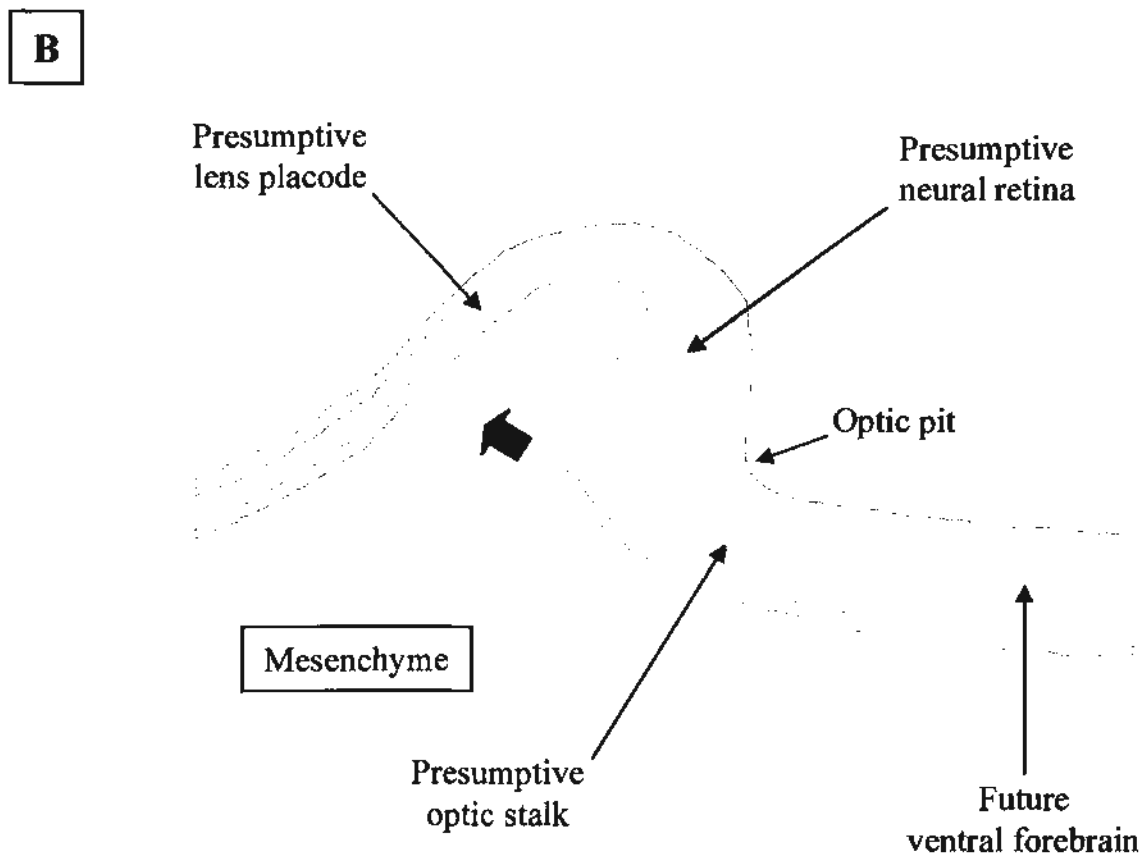
B
Presumptive lens placode
Presumptive neural retina
Optic pit
Mesenchyme
Presumptive optic stalk
Future ventral forebrain

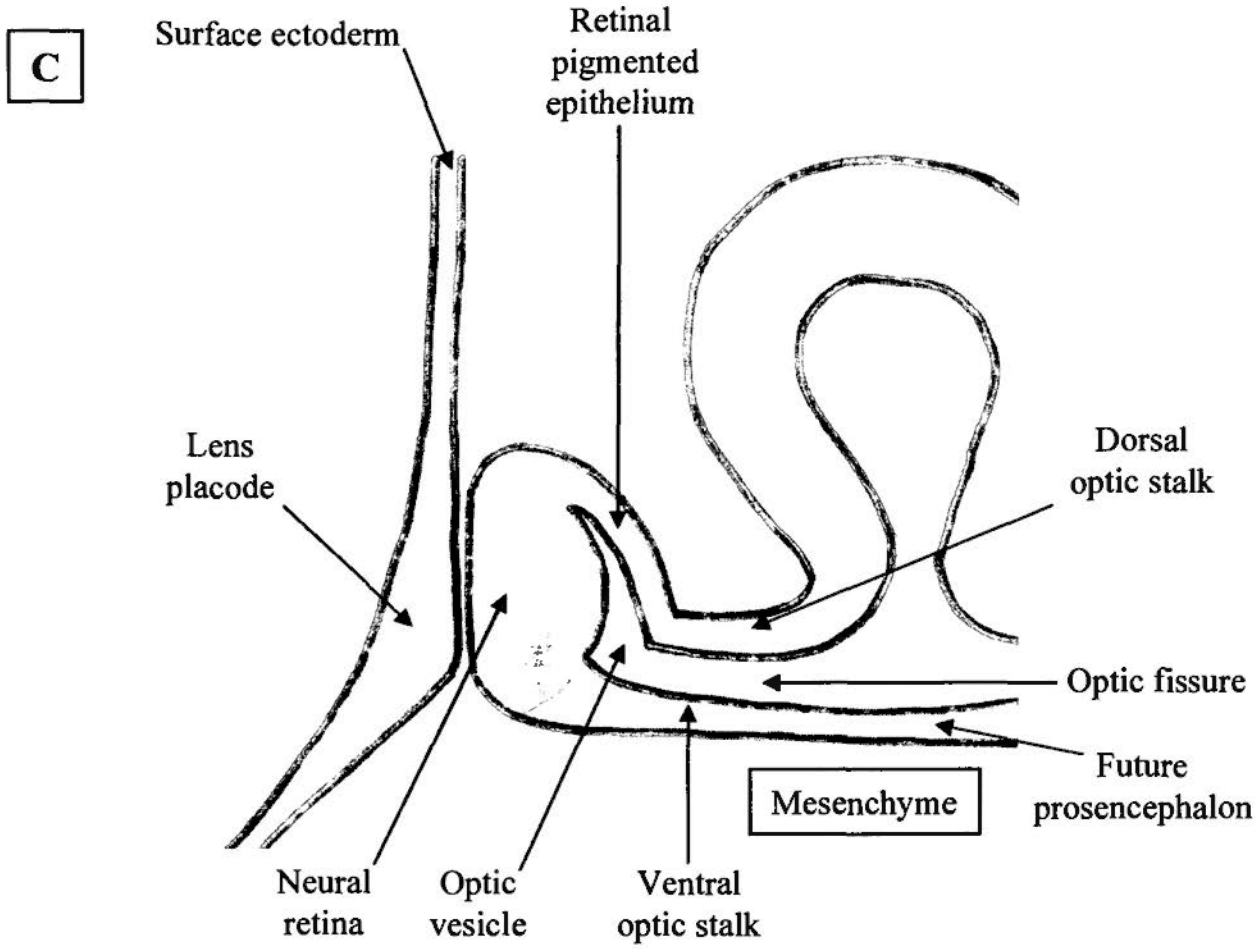
C
Surface ectoderm
Retinal pigmented epithelium
Lens placode
Dorsal optic stalk
Optic fissure
Future prosencephalon
Mesenchyme
Neural retina
Optic vesicle
Ventral optic stalk

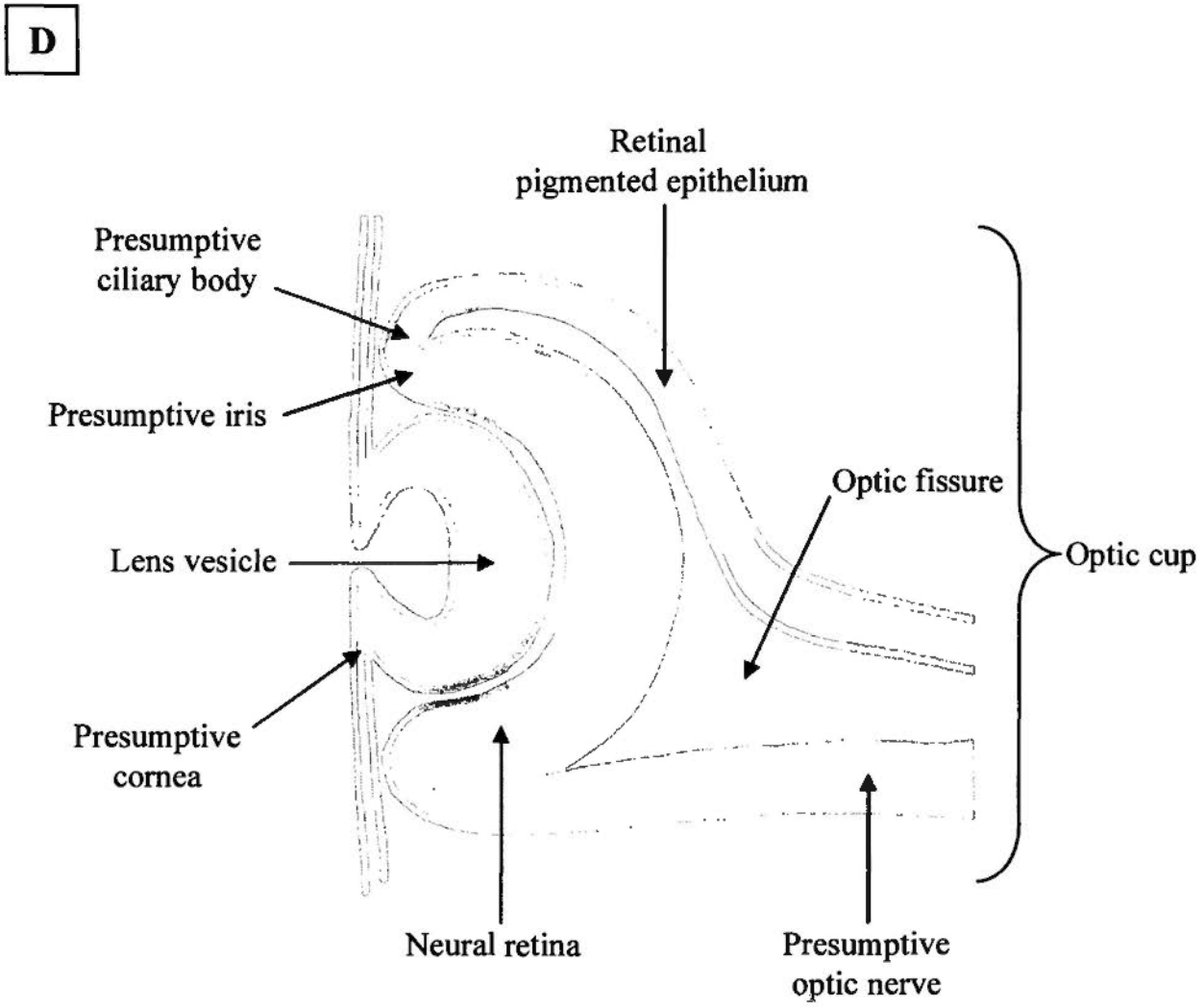
D
Retinal pigmented epithelium
Presumptive ciliary body
Presumptive iris
Optic fissure
Optic cup
Lens vesicle
Presumptive cornea
Neural retina
Presumptive optic nerve

E

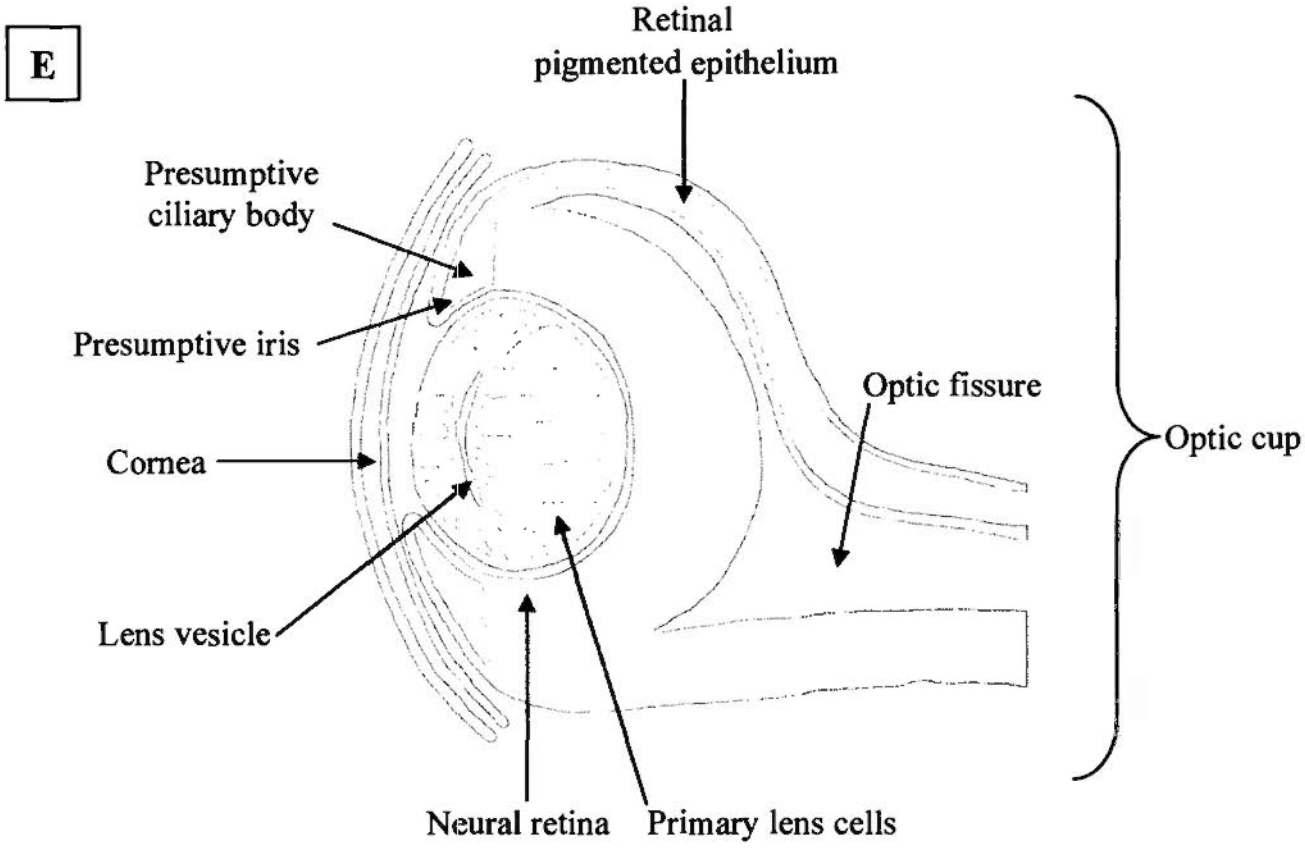
Retinal
pigmented epithelium
Presumptive
ciliary body
Presumptive iris
Optic fissure
Optic cup
Cornea
Lens vesicle
Neural retina
Primary lens cells

F

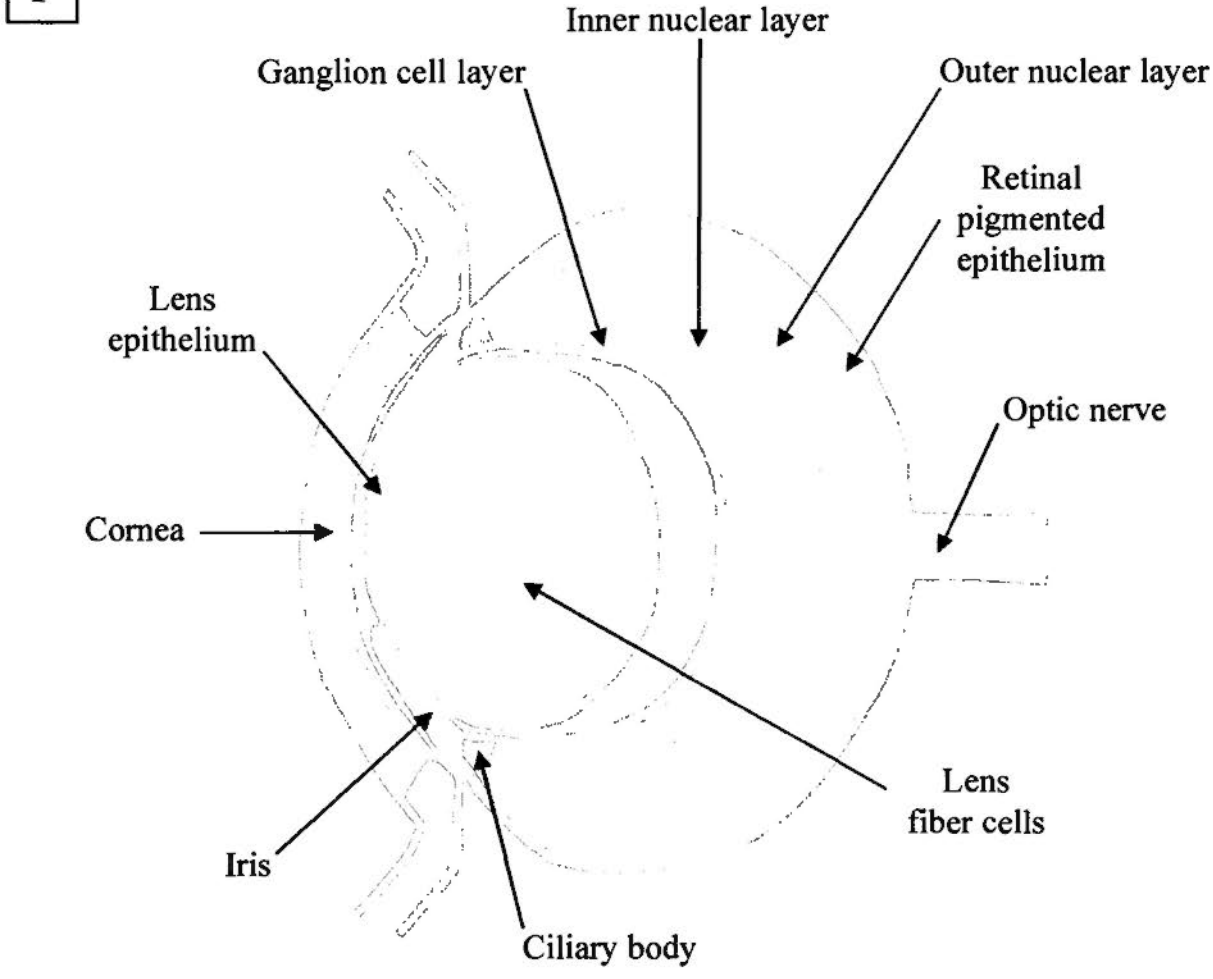
Inner nuclear layer
Ganglion cell layer
Outer nuclear layer
Retinal
pigmented
epithelium
Lens
epithelium
Optic nerve
Cornea
Lens
fiber cells
Iris
Ciliary body

Figure 3-1 Gross examination of ocular defects in near-term C57 fetuses at E18.

A. Normal eye. The black line drawn under the eye illustrates the size of a normal eye. At this stage, the fetal eye is not yet opened.

B. Eye with no eyelid. The eyeball is exposed to outside without being covered by an eyelid. This embryo also exhibited exencephaly (blue arrow).

C. Fetus with small eye (green arrow).

D. Fetus with no eye (yellow arrow).

E. Fetus with exophthalmia (orange arrow).

Labels:	Black line,	size of a normal eye
	Blue arrow,	exencephaly
	Green arrow,	small eye
	Yellow arrow,	no eye
	Orange arrow	exophthalmia

Scale bar: A to D 1 mm

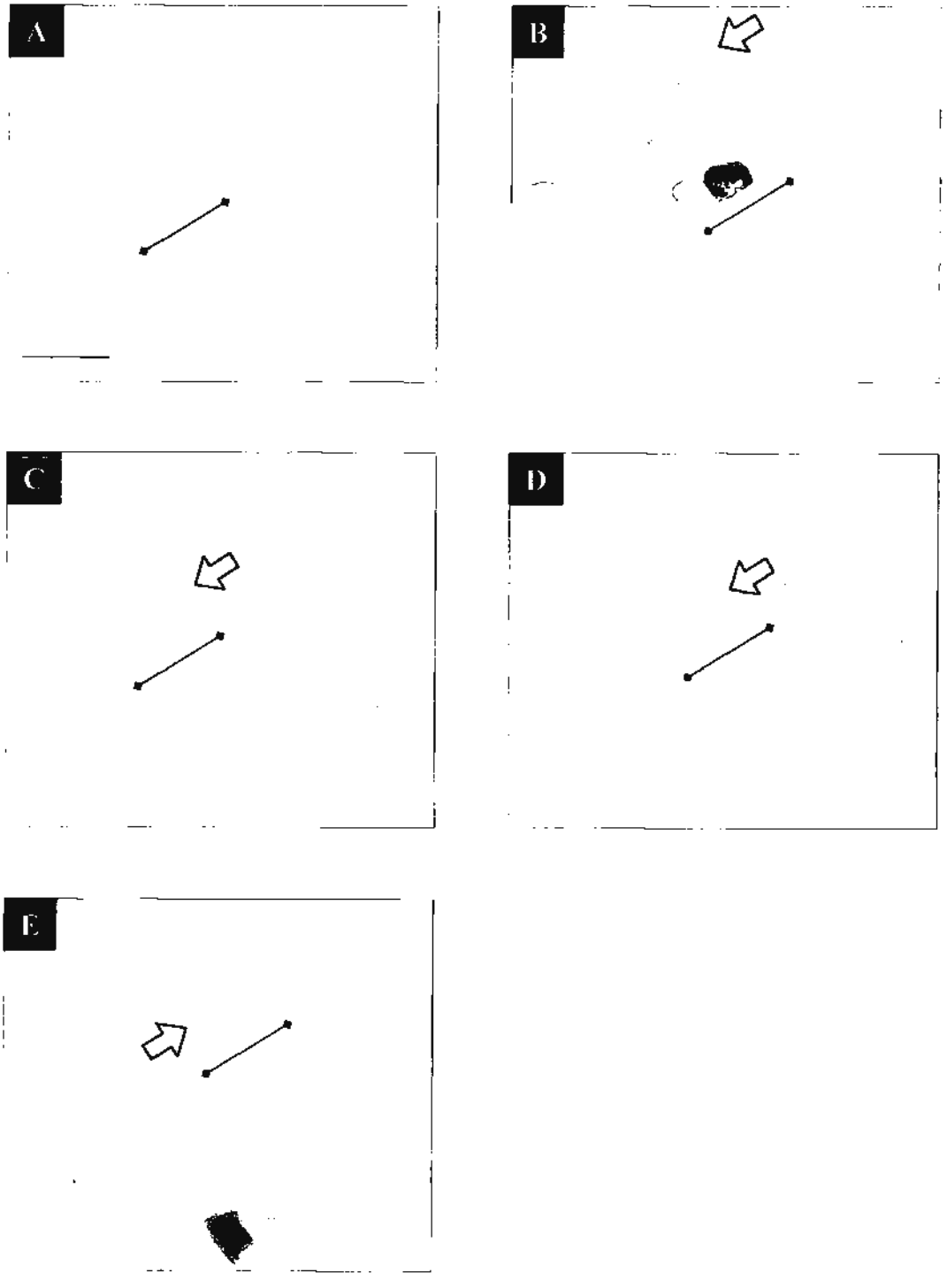
A
B
C
D
E

Figure 3-2 Different types of ocular defects identified by histological examination.

A. Normal eye covered by an eyelid. The lens, vitreous cavity (VC) and retina (R) are in place.

B. Microphthalmia with small lens (microphakia). Retina was folded and inverted into the vitreous cavity.

C. Microphthalmia without lens (aphakia). Vitreous cavity was filled with undifferentiated mesenchyme (M) and no lens rudiments could be found.

D. Anophthalmia. No eye rudiments could be found in the eye socket (yellow arrow).

E. Eye without an eyelid, resulting in the cornea (CO) being exposed to outside without coverage.

F. Eye with corneal stalk (orange arrow), a faulty separation between cornea and lens.

G. Eye with rupture in posterior lens capsule and the leaked lens cells (green arrows) were found in the vitreous cavity.

H. Eye with undifferentiated mesenchymal cells in vitreous cavity.

Labels:	Green arrow,	leaked lends cells
	Orange arrow,	corneal stalk
	Yellow arrow,	eye socket
	CO,	Cornea
	L,	Eyelid
	M,	Mesenchyme
	R,	Retina
	VC,	Vitreous cavity
Scale bar:	A to H	125 μm

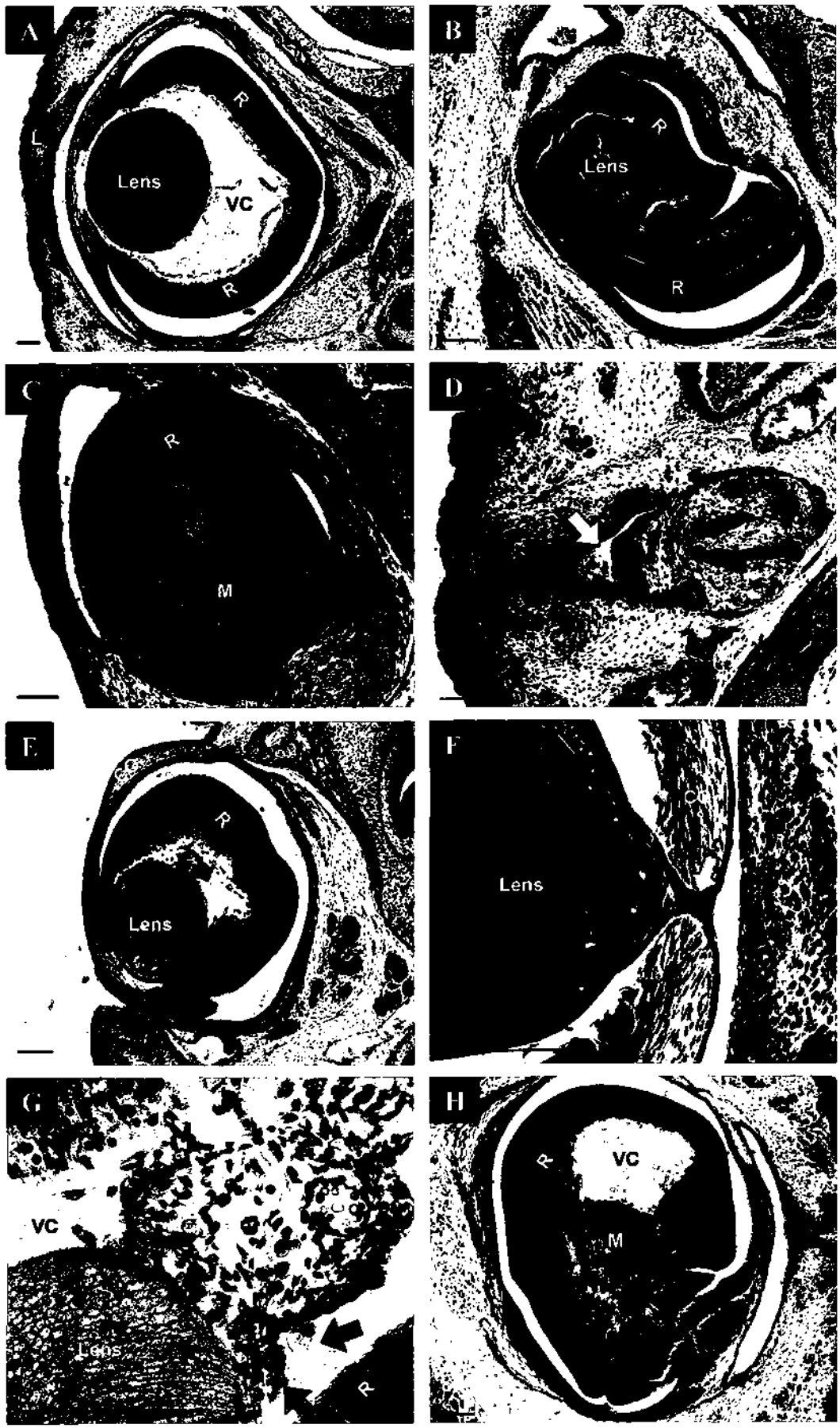
A
R
L
Lens
VC
R
B
R
Lens
R
C
R
M
D
E
P
Lens
F
Lens
G
VC
Lens
R
H
R
VC
M

Figure 3-3 Illustration on the method of counting the number of somites in a mouse embryo at the 25 somite stage.

Label: Red bracket, a single somite

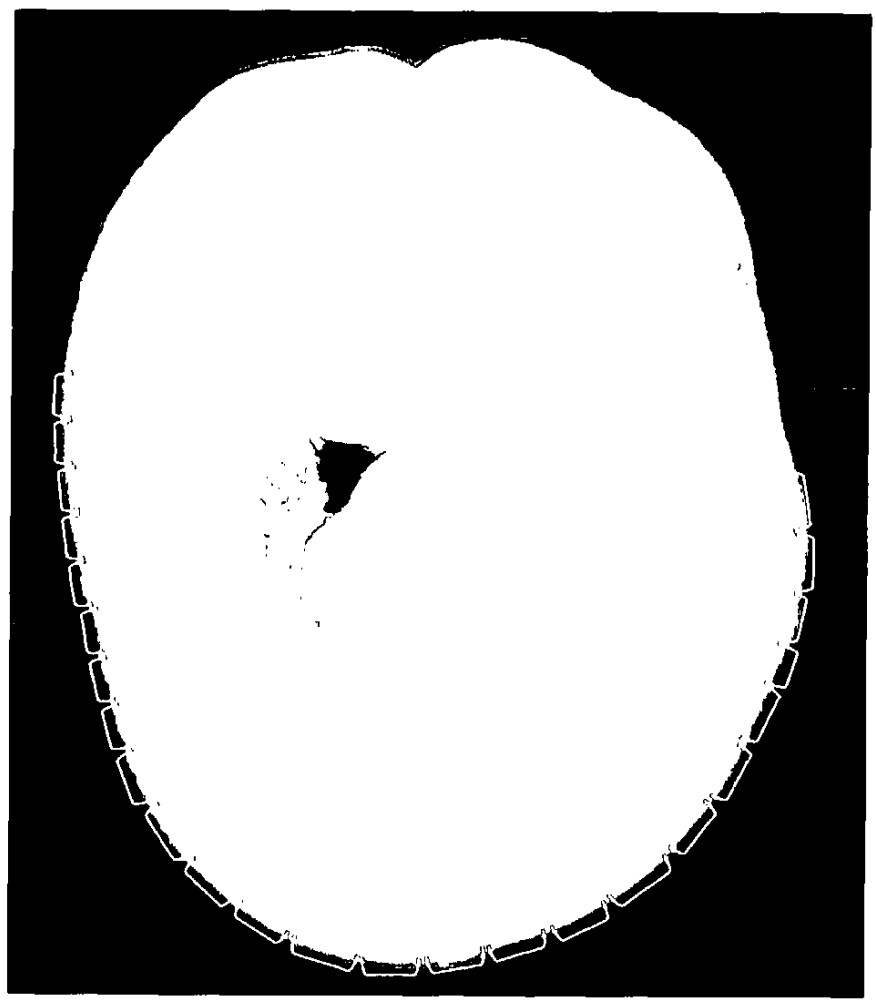

Figure 3-4 Illustration on the method of grading the developmental stage of pre-somitic embryos.

A. Embryo in pre-streak stage. Circumferential groove (arrowhead) outlines embryonic (E) and extraembryonic portions (X) of the egg cylinder. No evidence of mesoderm.

B. Embryo in early streak stage. There is small wedge of mesoderm (M) which is just visible and extended to less than 50% of the length of the posterior side.

C. Embryo in mid streak stage. The length of mesoderm exceeds 50% of the length of the posterior side of the egg cylinder.

D. Embryo in late streak stage. The posterior amniotic fold (paf) is found in between the posterior boundary of the extraembryonic and embryonic portions of the egg cylinder.

Labels:	arrowhead,	circumferential groove
	E,	embryonic portion of the egg cylinder
	M,	embryonic mesoderm
	paf,	posterior amniotic fold
	X	extraembryonic portion of the egg cylinder

Scale bar: A to D 200 μm

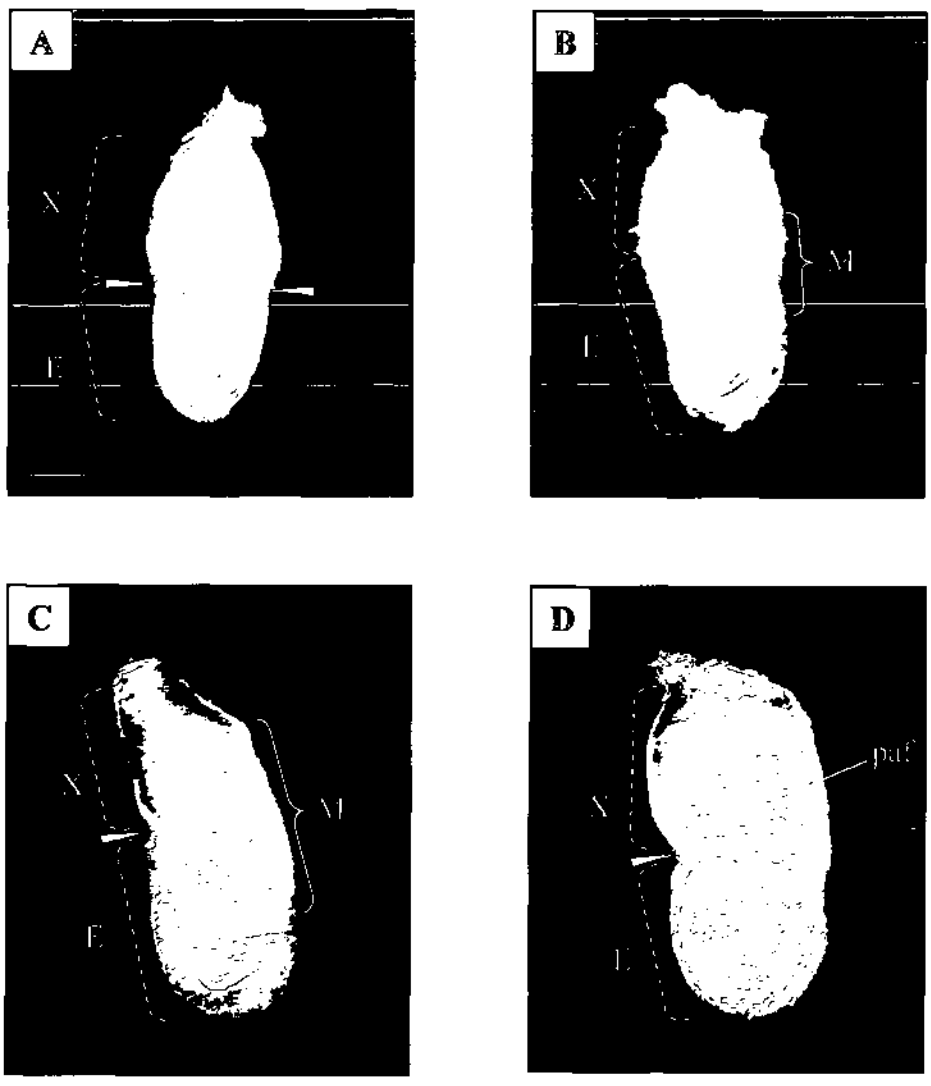
A
B
C
D
M
M
M
pat

Figure 4-1 Morphological appearances of ICR embryos at E7.75 and E8.25 with or without RA treatment.

A. At E7.75, control (CON) ICR embryos were at late head-fold stage.

B. At E7.75, RA-treated (RA) ICR embryos appeared morphologically normal.

C. At E8.25, control ICR embryos have well-developed anterior neural plate (red curved line) that would develop into the future forebrain.

D. At E8.25, RA-treated ICR embryos have slightly smaller anterior neural plate of the future forebrain.

Label: Red curved line, outline of anterior neural plate of the future forebrain

Scale bar: A and B, 0.09 mm

C and D, 0.05 mm

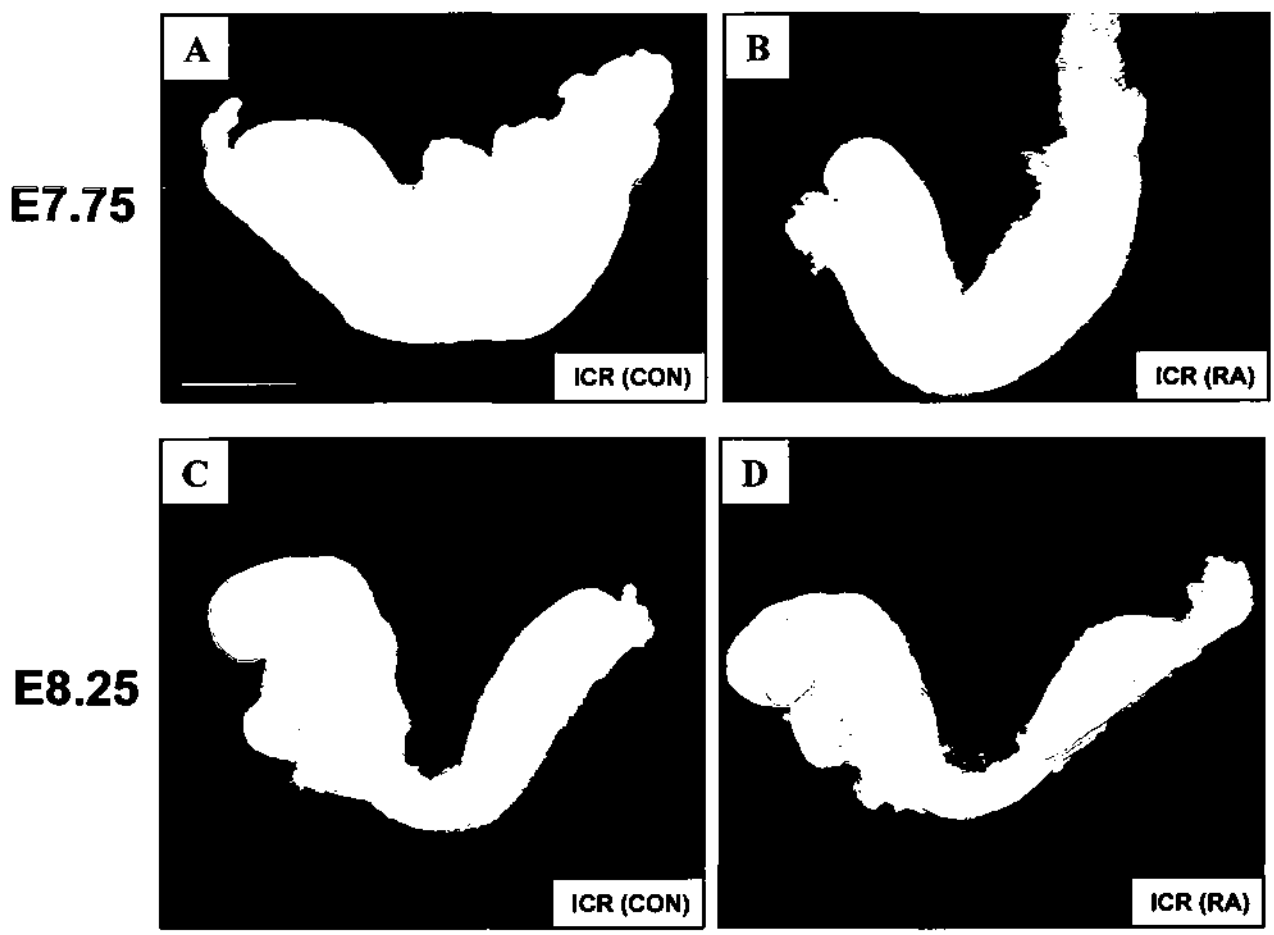
E7.75
A
ICR (CON)
B
ICR (RA)
E8.25
C
ICR (CON)
D
ICR (RA)

Figure 4-2 Morphological appearances of ICR embryos at E8.75 with or without RA treatment.

A. At E8.75, in control (CON) ICR embryos, the anterior neural plate has closed to become the forebrain (red curved line).

B. At E8.75, in RA-treated (RA) ICR embryos, the forebrain was similar in size as the control.

C. Higher magnification of the cephalic region of the control ICR embryo shown in A. The optic vesicle (green arrow) has started to develop.

D. Higher magnification of the cephalic region of the RA-treated ICR embryo shown in B. The optic vesicle (orange arrow) has started to develop as in the control.

Labels:	Arrow,	optic vesicle
	Red curved line,	outline of forebrain
Scale bar:	A and B,	1.4 mm
	C and D,	0.5 mm

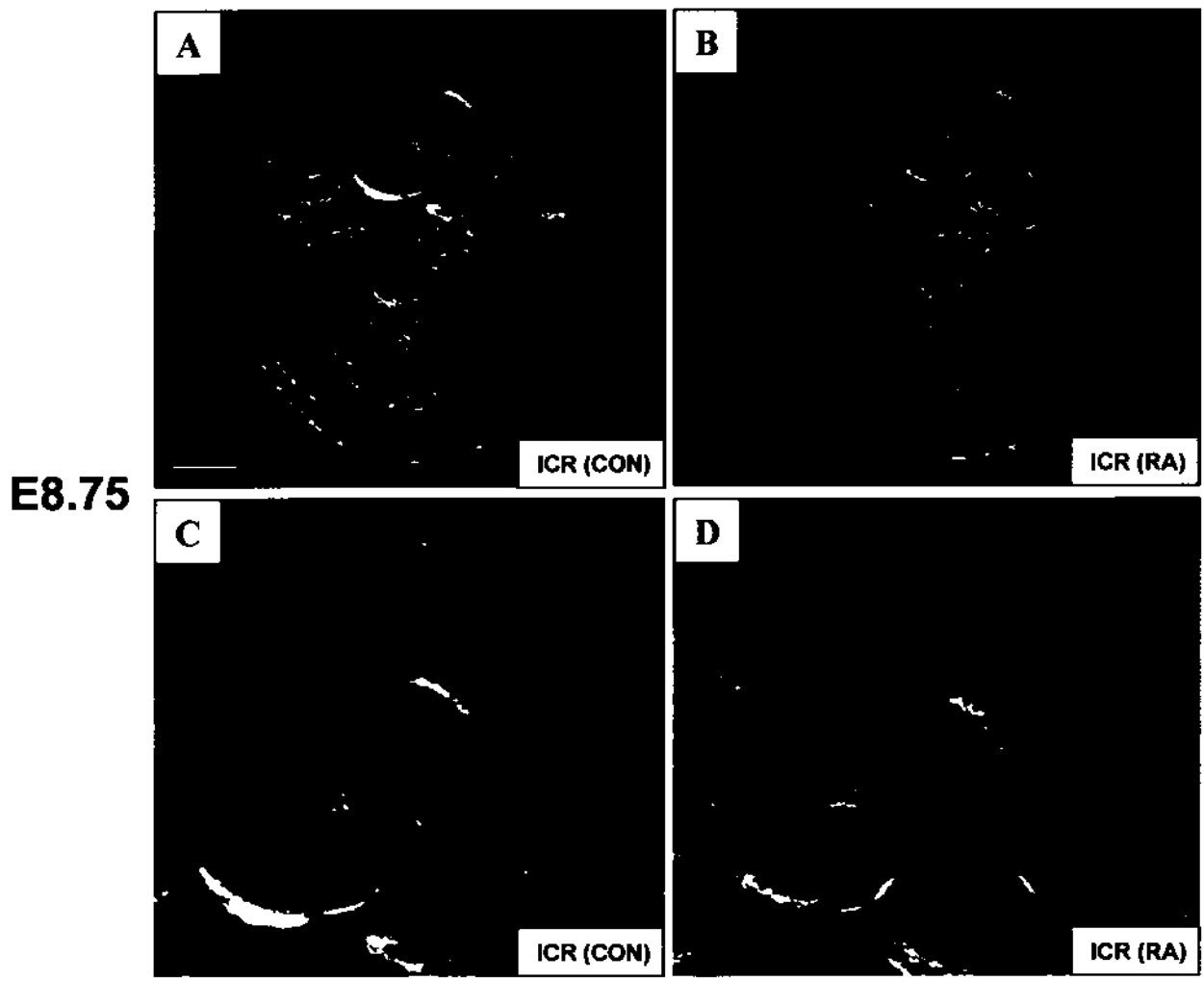
E8.75
A
ICR (CON)
B
ICR (RA)
C
ICR (CON)
D
ICR (RA)

Figure 4-3 Morphological appearances of ICR embryos at E9.25 with or without RA treatment.

A. E9.25 control (CON) embryos with forebrain outlined by red curved line.

B. At E9.25, in RA-treated (RA) ICR embryos, the forebrain appeared morphologically normal.

C. Higher magnification of the cephalic region of the control ICR embryo shown in A. The optic vesicle (green arrow) was well-developed.

D. Higher magnification of the cephalic region of the RA-treated ICR embryo shown in B. The optic vesicle (orange arrow) was well-developed as in the control.

Labels: Arrow, optic vesicle
Red curved line, outline of forebrain

Scale bar: A and B, 1.7 mm
C and D, 0.2 mm

E9.25

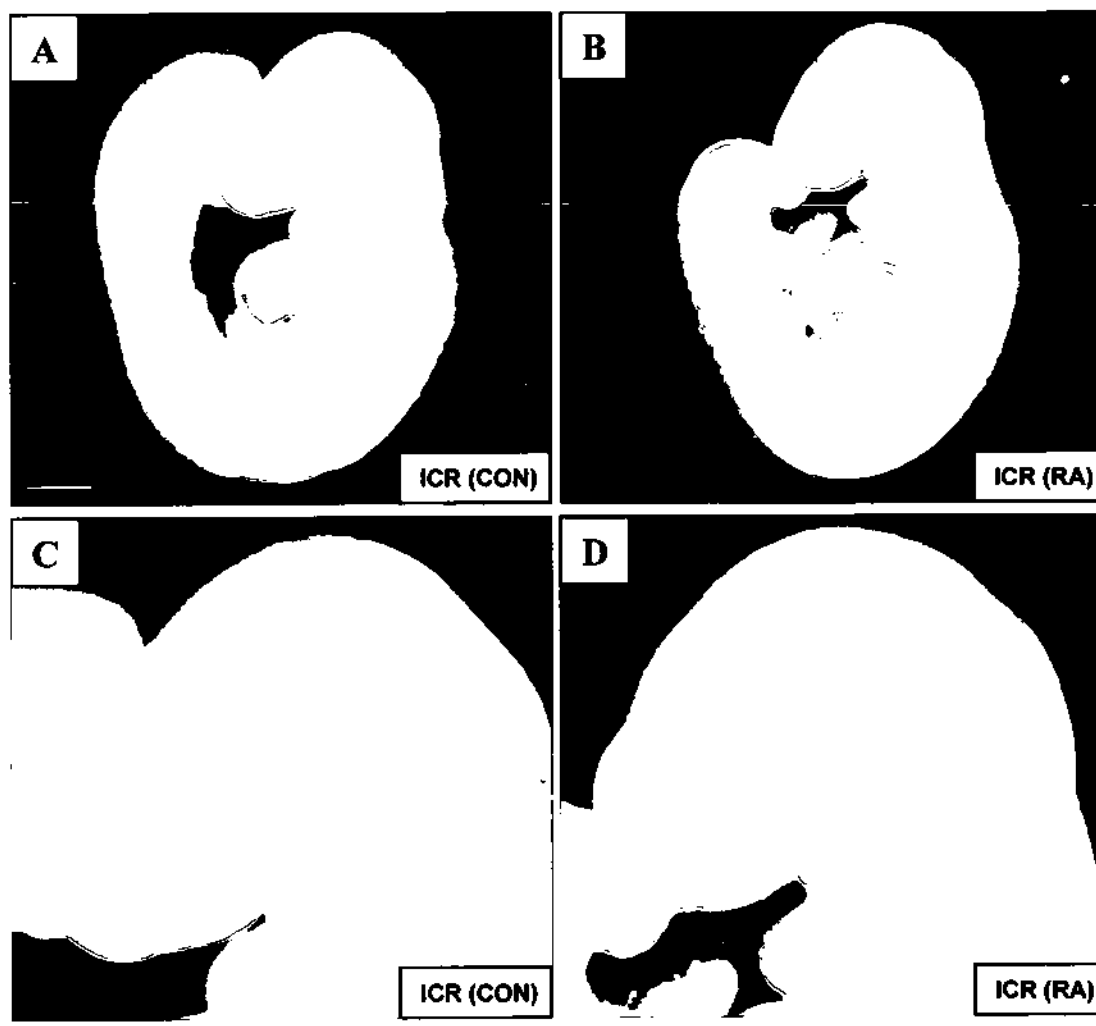

Figure 4-4 Morphological appearances of C57 embryos at E8 and E8.5 with or without RA treatment.

A. At E8, control (CON) C57 embryos were at late head-fold stage.

B. At E8, RA-treated (RA) C57 embryos appeared morphologically normal.

C. At E8.5, control C57 embryos have well-developed anterior neural plate (red curved line) that would develop into the future forebrain.

D. At E8.5, RA-treated C57 embryos have marked reduction in the size of the anterior neural plate of the future forebrain.

Label: Red curved line, outline of anterior neural plate of the future forebrain

Scale bar: A and B, 0.08 mm

C and D, 0.05 mm

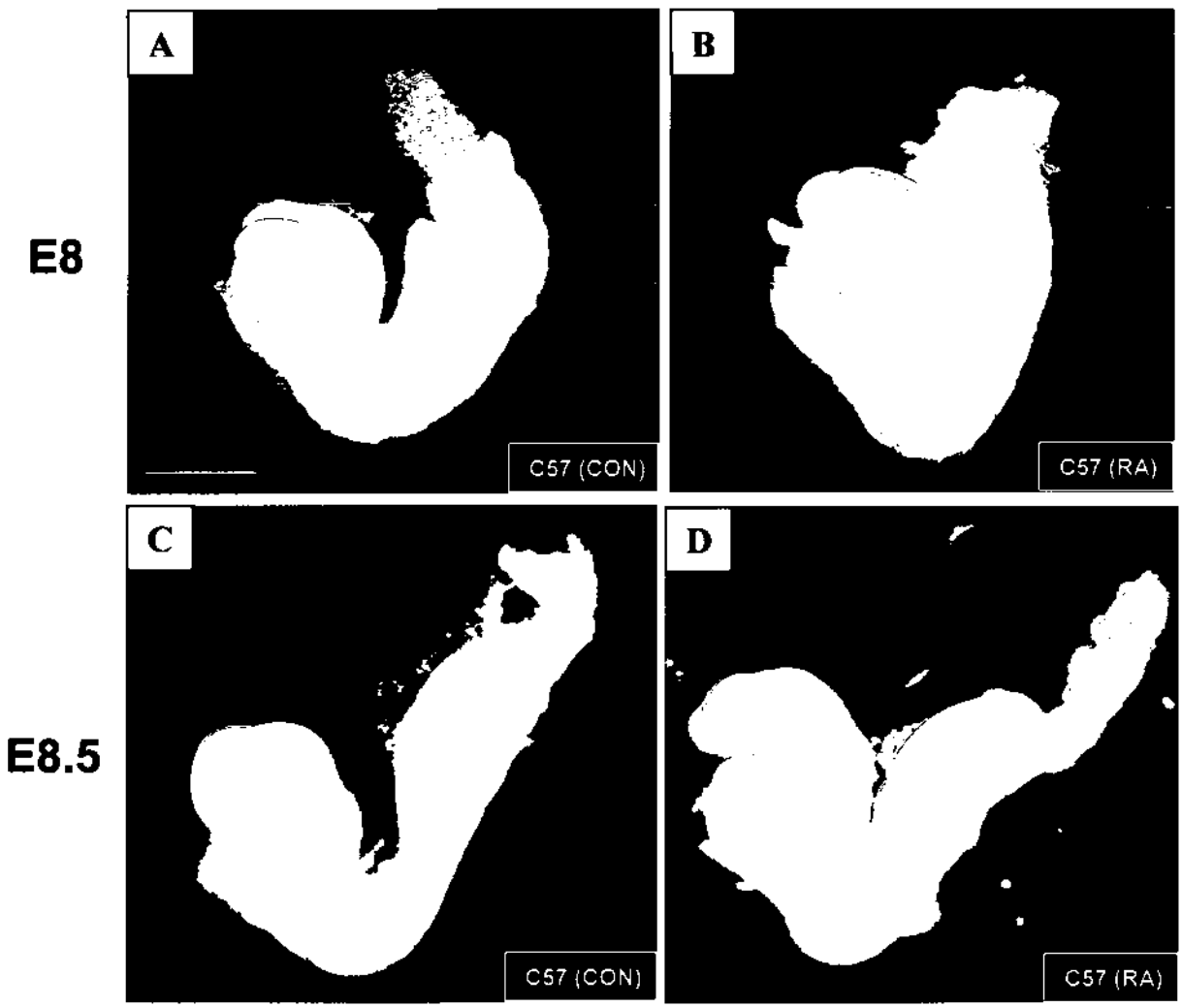
E8
E8.5
A
B
C
D
C57 (CON)
C57 (RA)
C57 (CON)
C57 (RA)

Figure 4-5 Morphological appearances of C57 embryos at E9 with or without RA treatment.

A. At E9, in control (CON) C57 embryos, the anterior neural plate has closed to become the forebrain (red curved line).

B. At E9, in RA-treated (RA) C57 embryos, the forebrain was markedly reduced in size.

C. Higher magnification of the cephalic region of the control C57 embryo shown in A. The optic vesicle (green arrow) has started to develop.

D. Higher magnification of the cephalic region of the RA-treated C57 embryo shown in B. No optic vesicle could be found. The orange arrow marked the equivalent position in the forebrain where the optic vesicle would have developed in control embryos.

Labels: Arrow, optic vesicle or equivalent position
Red curved line, outline of forebrain

Scale bar: A and B, 1.4 mm
C and D, 0.2 mm

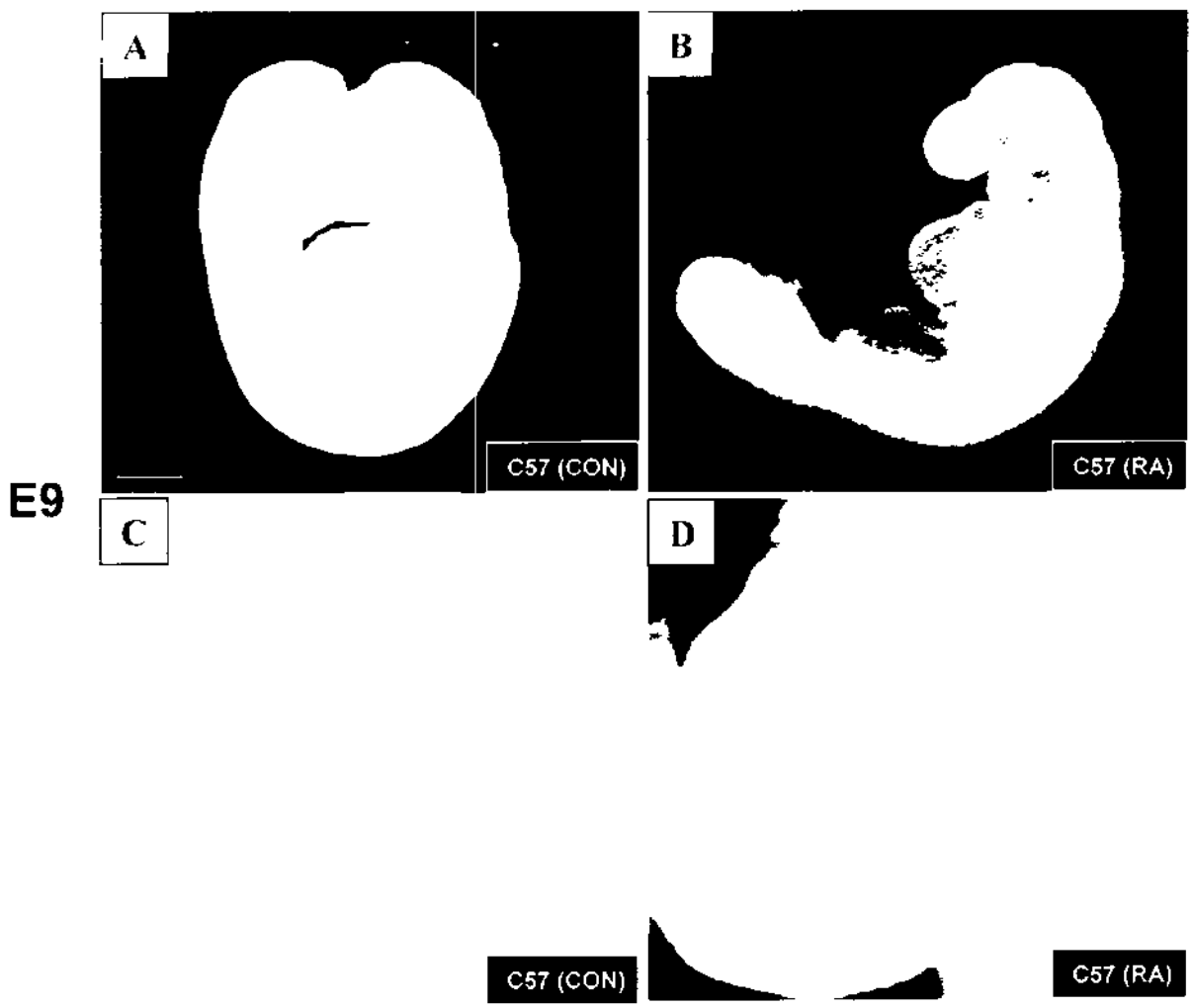
E9
A
C57 (CON)
B
C57 (RA)
C
D
C57 (CON)
C57 (RA)

Figure 4-6 Morphological appearances of C57 embryos at E9.5 with or without RA treatment.

A. E9.5, control (CON) C57 embryos with forebrain outlined by red curved line.

B. At E9.5, in RA-treated (RA) C57 embryos, the forebrain was noticeably reduced in size.

C. Higher magnification of the cephalic region of the control C57 embryo shown in A. The optic vesicle (green arrow) was well-developed.

D. Higher magnification of the cephalic region of the RA-treated C57 embryo shown in B. No optic vesicle could be found. The orange arrow marked the equivalent position in the forebrain where the optic vesicle would have developed in control embryos.

Labels: Arrow, optic vesicle or equivalent position
Red curved line, outline of forebrain

Scale bar: A and B, 1.4 mm
C and D, 0.5 mm

E9.5

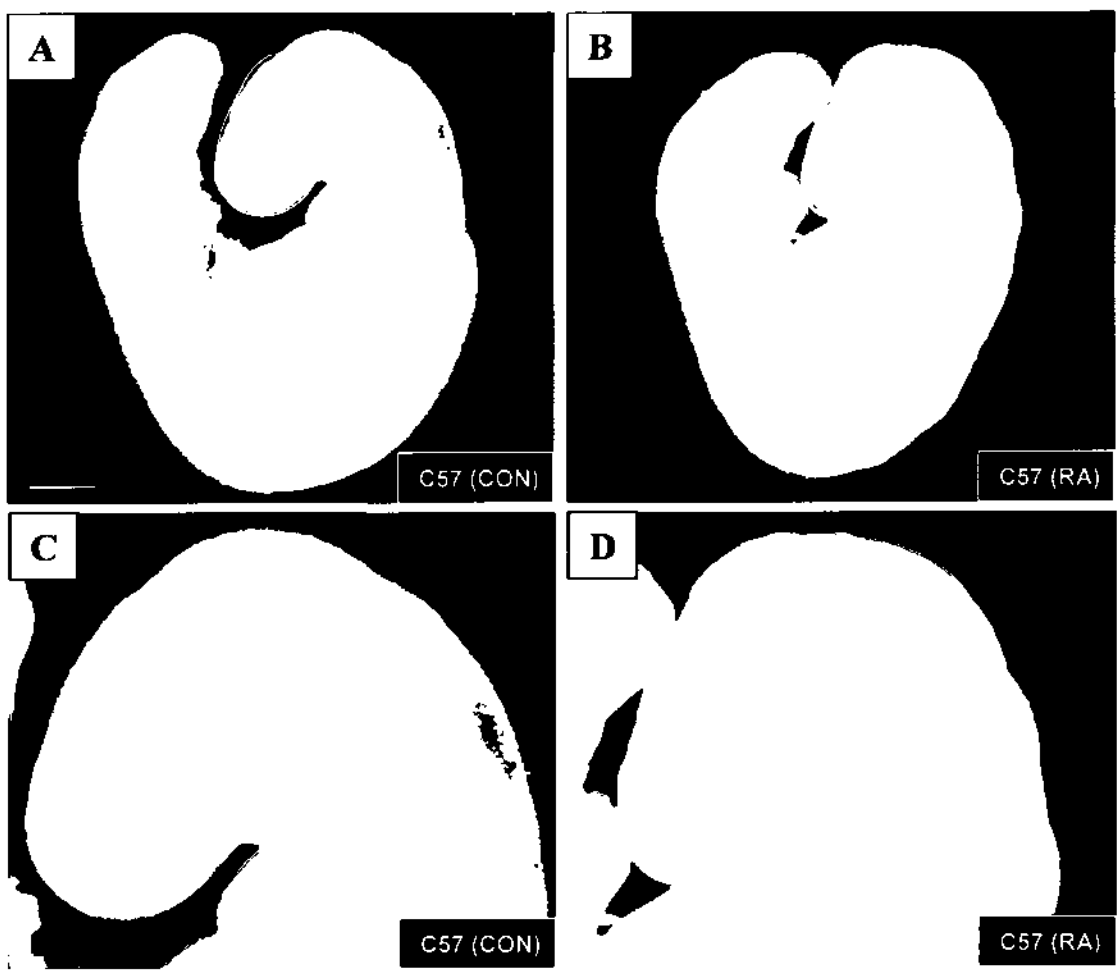

Figure 4-7 Histological analysis of ICR embryos at E7.75 with or without RA treatment.

A. Transverse section of a control (CON) ICR embryo at E7.75 at the plane indicated by the broken line. The neuroepithelium was indicated by green arrow and the underlying mesenchyme was circled in green colour.

B. Transverse section of a RA-treated (RA) ICR embryo at E7.75 at the plane indicated by the broken line. The neuroepithelium was indicated by orange arrow and the underlying mesenchyme was circled in orange colour.

Labels: Arrow, neuroepithelium
Circle, mesenchyme

Scale bar: A and B, 0.05 mm

A

E7.75

ICR (CON)

B

E7.75

ICR (RA)

Figure 4-8 Histological analysis of ICR embryos at E8.25 with or without RA treatment.

A. Transverse section of a control (CON) ICR embryo at E8.25 at the plane indicated by the broken line. The optic pits on the neuroepithelium were indicated by green arrows.

B. Transverse section of a RA-treated (RA) ICR embryo at E8.25 at the plane indicated by the broken line. A pair of optic pits (orange arrow) was clearly visible.

Labels: Arrow, optic pit
Broken line, plane of section

Scale bar: A and B, 0.1 mm

A

E8.25

ICR (CON)

B

E8.25

ICR (RA)

Figure 4-9 Histological analysis of ICR embryos at E8.75 with or without RA treatment.

A. Transverse section of a control (CON) ICR embryo at E8.75 at the plane indicated by the broken line. A pair of deeply evaginated optic vesicles (green arrows) had formed.

B. Transverse section of a RA-treated (RA) ICR embryo at E8.75 at the plane indicated by the broken line. A pair of optic vesicles (orange arrows) was clearly visible.

Labels: Arrow, optic vesicle
Broken line, plane of section

Scale bar: A and B, 0.1 mm

E8.75

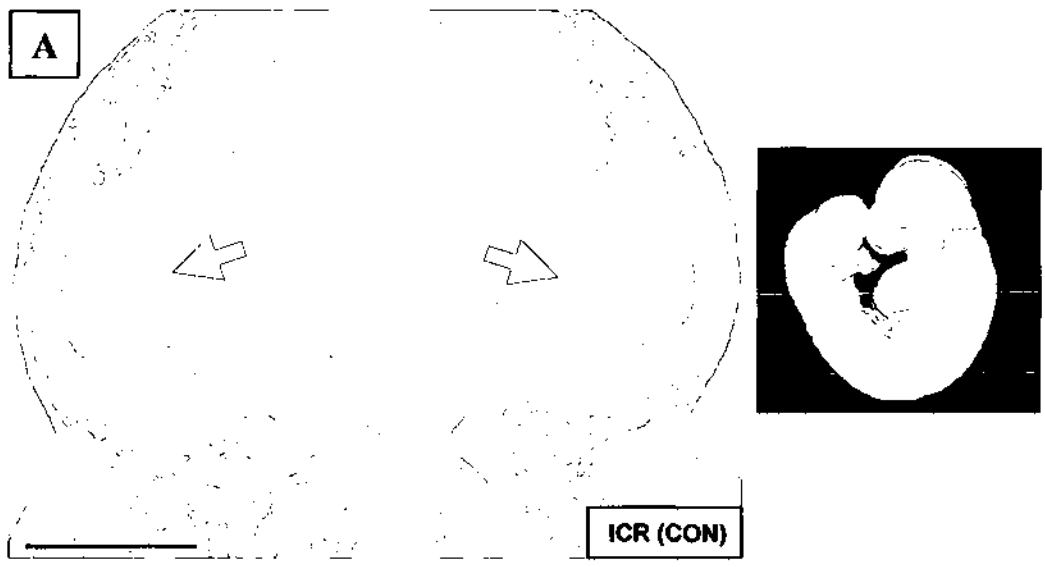

E8.75

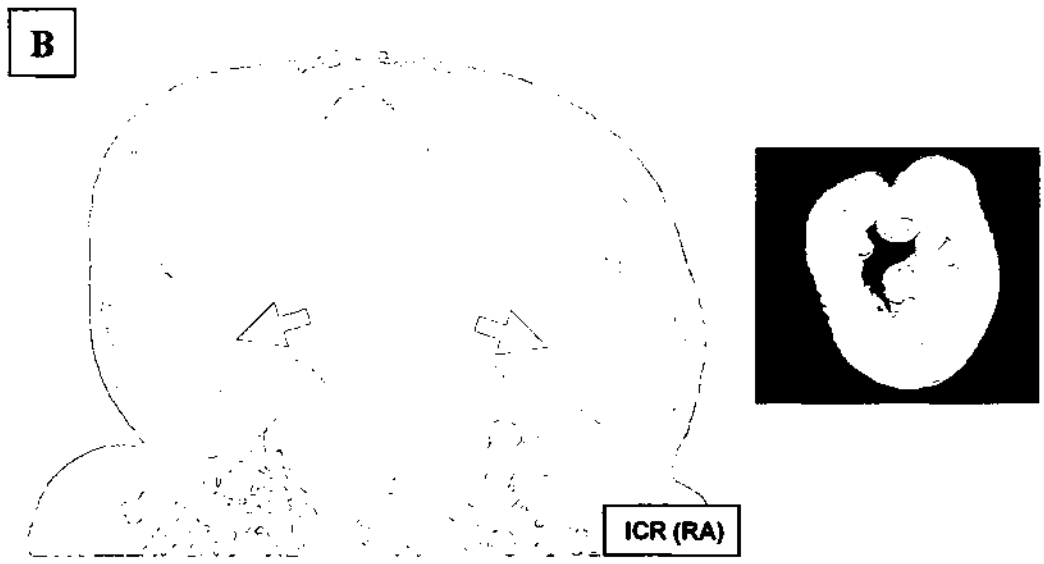

Figure 4-10 Histological analysis of C57 embryos at E8 with or without RA treatment.

A. Transverse section of a control (CON) embryo at E8 at the plane indicated by the broken line. The neuroepithelium was marked by green arrow and the underlying mesenchyme was circled in green colour.

B. Transverse section of a RA-treated (RA) C57 embryo at E8 at the plane indicated by the broken line. The neuroepithelium (orange arrow) appeared morphologically normal whereas the underlying mesenchyme (circled in orange) had less cells in comparison to the control.

Labels: Arrow, neuroepithelium
Circle, mesenchyme

Scale bar: A and B, 0.05 mm

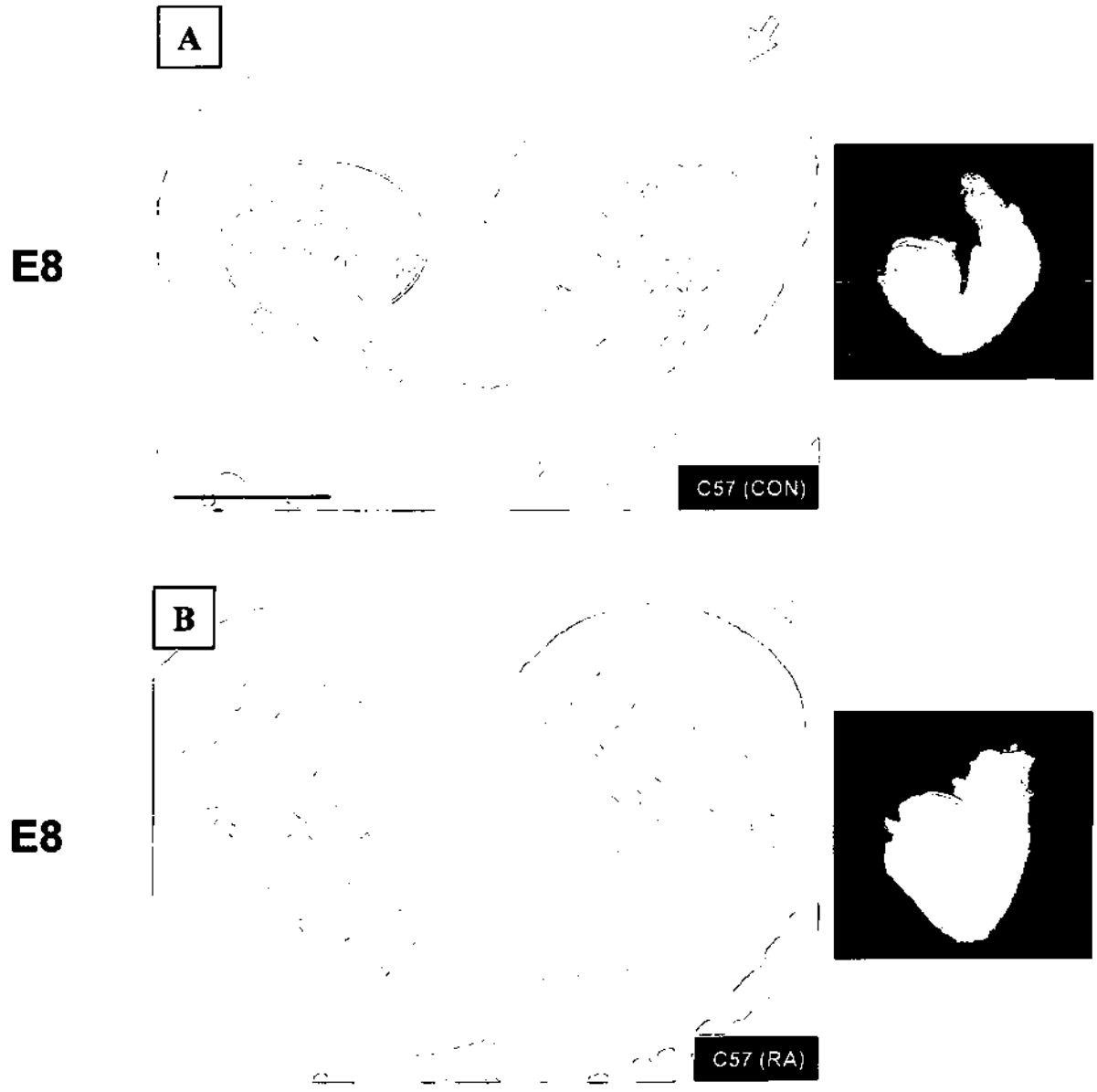
A
E8
C57 (CON)
B
E8
C57 (RA)

Figure 4-11 Histological analysis of C57 embryos at E8.5 with or without RA treatment.

A. Transverse section of a control (CON) C57 embryo at E8.5 at the plane inicated by the broken line. A pair of optic pits (green arrow) had developed in the neuroepithelium. The mesenchyme underlying the neuroepithelium was circled in green colour.

B. Transverse section of a RA-treated (RA) C57 embryo at E8.5 at the plane indicated by the broken line. No optic pits had formed in the neuroepithelium and the underlying mesenchyme (circled in orange colour) was sparsely populated at the corresponding level of the control embryo.

Labels:	Arrow,	optic pit
	Broken line,	plane of section
	Circle,	mesenchyme

Scale bar: A and B, 0.1 mm

A

E8.5

C57 (CON)

B

E8.5

C57 (RA)

Figure 4-12 Histological analysis of C57 embryos at E9 with or without RA treatment.

A. Transverse section of a control (CON) C57 embryo at E9 at the plane indicated by the broken line. A pair of deeply evaginated optic vesicles (green arrows) had formed.

B. Transverse section of a RA-treated (RA) C57 embryo at E9 at the plane indicated by the broken line. No optic vesicles had formed in the forebrain region at the corresponding level of the control embryo.

Labels: Arrow, optic vesicle
Broken line, plane of section

Scale bar: A and B, 0.1 mm

A

E9

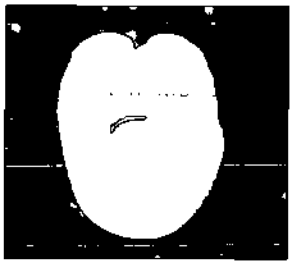

B

E9

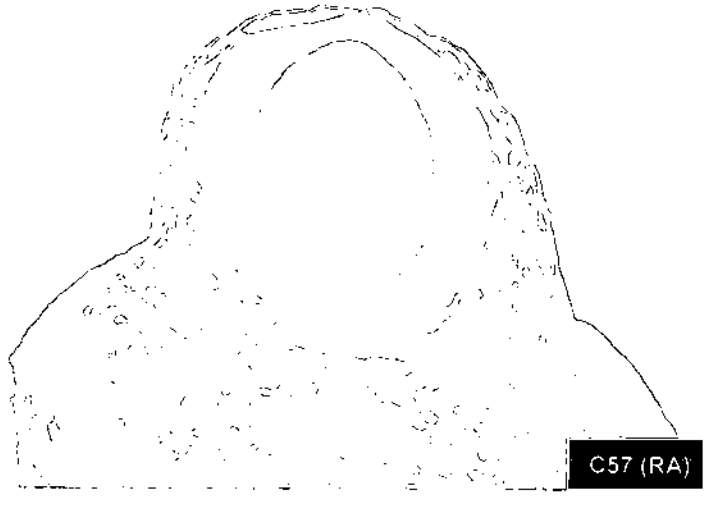

Figure 4-13 SEM images of ICR embryos at E7.75 with or without RA treatment.

A. Lateral view of a control (CON) ICR embryo at E7.75. The anterior neural plate (*) had a sharp contour.

B. Lateral view a RA-treated (RA) ICR embryo at E7.75. The anterior neural plate appeared morphologically normal in shape and size.

C. Frontal view of the control ICR embryo shown in A to show the anterior neural plate.

D. Frontal view of the RA-treated ICR embryo shown in B. The anterior neural plate appeared morphologically normal in shape and size.

Label: *, anterior neural plate

Scale bar: A and B, 0.1 mm

C and D, 0.25 mm

E7.75

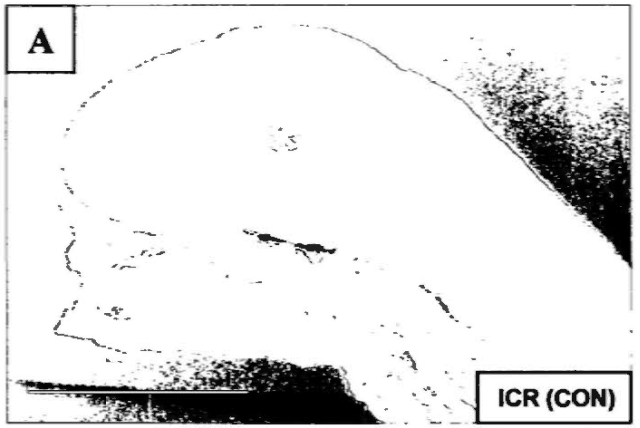

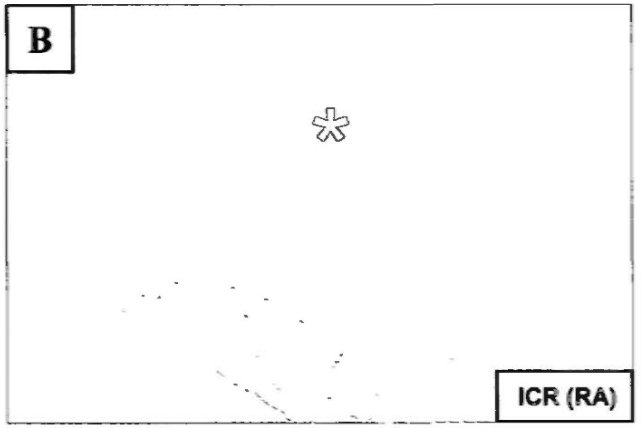

E7.75

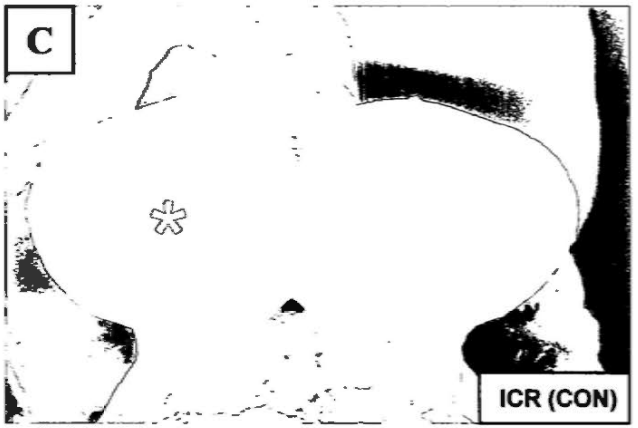

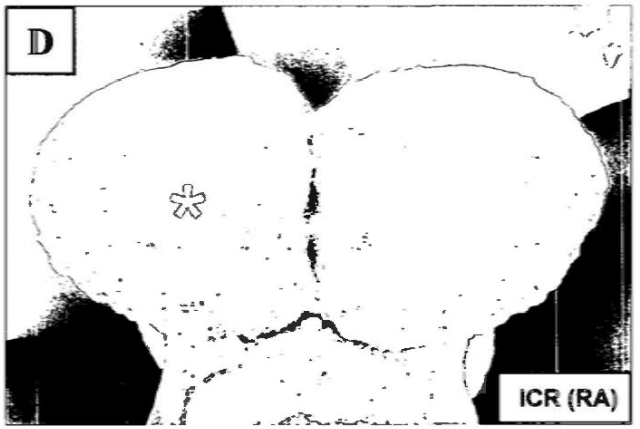

Figure 4-14 SEM images of ICR embryos at E8.25 with or without RA treatment.

A. Lateral view of a control (CON) ICR embryo at E8.25. The anterior neural plate of the future forebrain (FB), midbrain (MB) and hindbrain (HB) had sharp contours. The junction of the future FB and MB was indicated by an arrowhead.

B. Lateral view of a RA-treated (RA) ICR embryo at E8.25. The FB, MB and HB neural plate had normal appearance.

C. Lateral view of another RA-treated ICR embryo at E8.25. The FB, MB and HB neural plate had normal appearance.

D. Frontal view of the control ICR embryo shown in A. Optic pits (arrows) appeared as a pair of sharp depressions in the FB neural plate.

E. Frontal view of the RA-treated ICR embryo shown in B. A pair of optic pits (arrows) was clearly visible.

F. Frontal view of the RA-treated ICR embryo at shown in C. A pair of optic pits (arrows) was clearly visible although less deep than that of the control.

Labels:	Arrow,	optic pit
	Arrowhead,	junction of the future forebrain and midbrain
	FB,	forebrain
	MB,	midbrain
	HB,	hindbrain
Scale bar:	A to C,	0.1 mm
	D to F,	0.14 mm

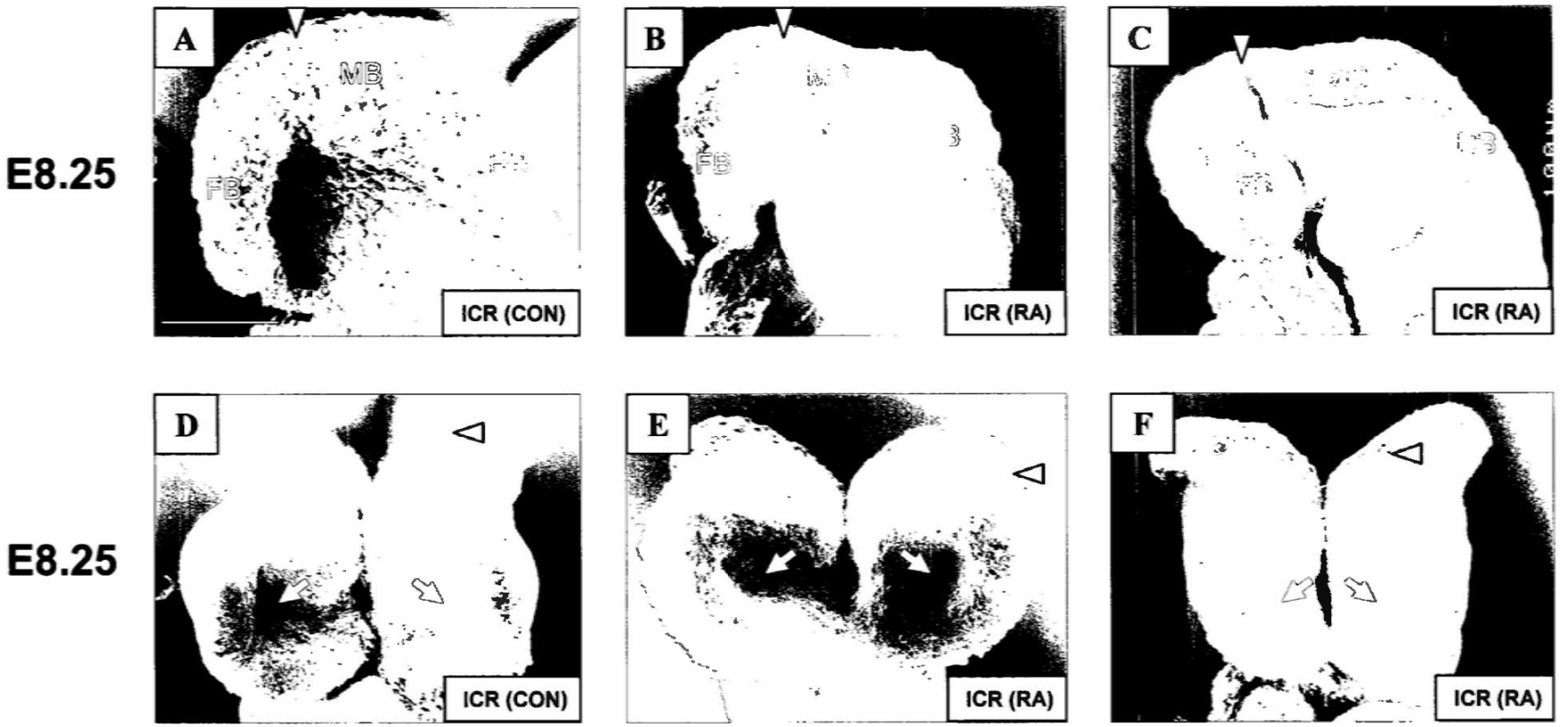
E8.25
A
MB
FB
ICR (CON)
B
FB
ICR (RA)
C
ICR (RA)
E8.25
D
ICR (CON)
E
ICR (RA)
F
ICR (RA)

Figure 4-15 SEM images of C57 embryos at E8 with or without RA treatment.

A. Lateral view of a control (CON) C57 embryo at E8. The anterior neural plate (*) had a sharp contour.

B. Lateral view of a RA-treated (RA) C57 embryo at E8. The anterior neural plate appeared morphologically normal in shape and size.

C. Frontal view of the control C57 embryo shown in A to show the anterior neural plate.

D. Frontal view of the RA-treated C57 embryo shown in B. The anterior neural plate appeared morphologically normal in shape and size.

Label: *, anterior neural plate

Scale bar: A and B, 0.1 mm

C and D, 0.25 mm

E8

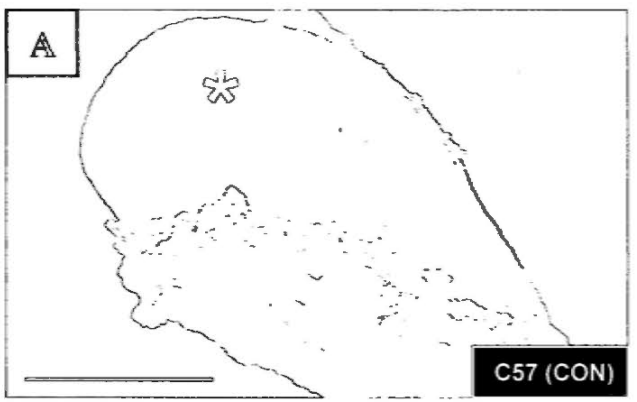

E8

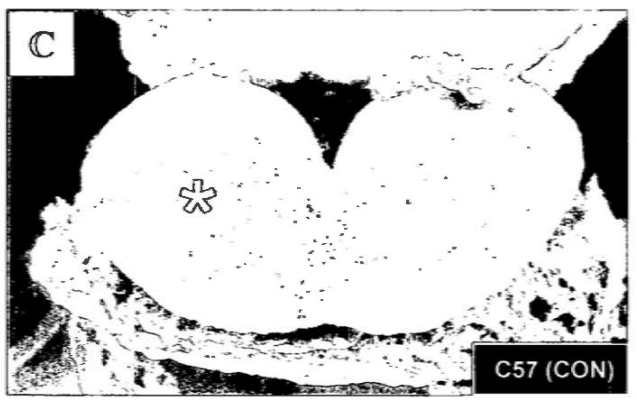

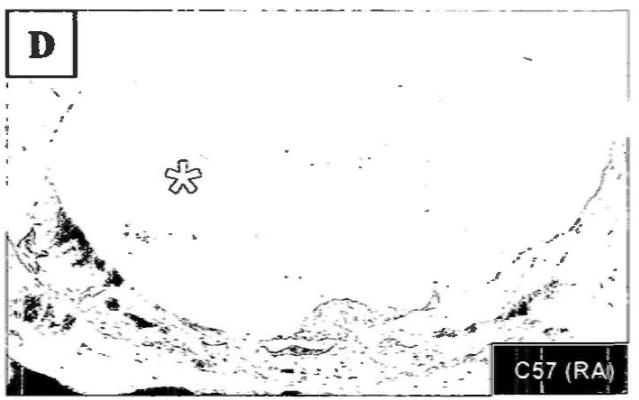

Figure 4-16 SEM images of C57 embryos at E8.5 with or without RA treatment.

A. Lateral view of a control (CON) C57 embryo at E8.5. The anterior neural plate of the future forebrain (FB), midbrain (MB) and hindbrain (HB) had sharp contours. The junction of the future FB neural and MB was indicated by an arrowhead.

B. Lateral view of RA-treated (RA) C57 embryo. The MB and HB neural plate had normal appearance whereas the FB plate appeared abnormal in shape.

C. Lateral view of another RA-treated C57 embryo. The MB and HB neural plate had normal appearance whereas the FB neural plate was much reduced in size in comparison the control.

D. Frontal view of the control C57 embryo shown in A. Optic pits (arrows) appeared as a pair of sharp depressions in the FB neural plate.

E. Frontal view of the RA-treated C57 embryo at E8.5 shown in B. No optic pits could be found. The FB neural plate had abnormally fused together in the most anterior part.

F. Frontal view of the RA-treated C57 embryo shown in C. Optic pits were missing. The FB neural plate was greatly reduced in size.

Labels:	Arrowhead,	forebrain-midbrain junction
	FB,	forebrain
	MB,	midbrain
	HB,	hindbrain
Scale bar:	A to C,	0.1 mm
	D to F,	0.14 mm

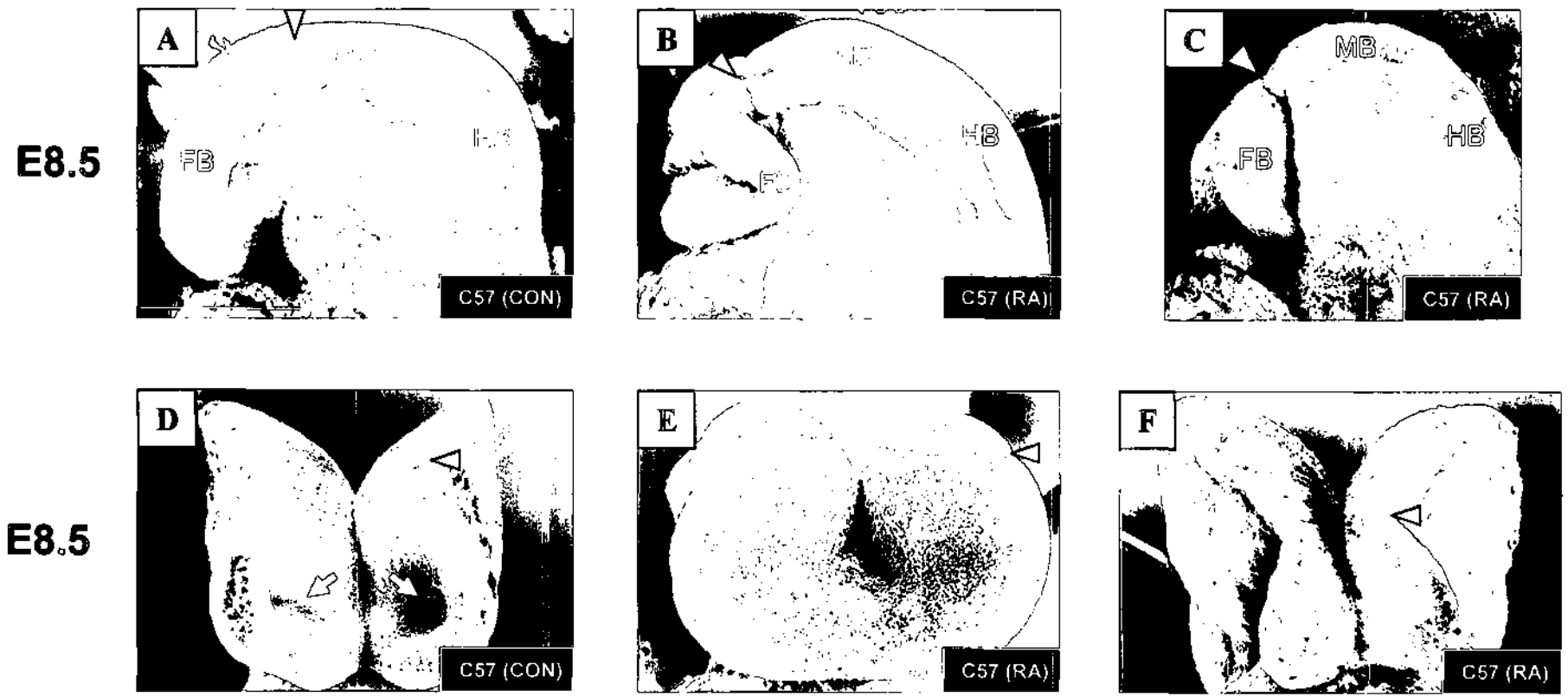
E8.5
A
FB
C57 (CON)
B
HB
C57 (RA)
C
MB
FB
HB
C57 (RA)
E8.5
D
C57 (CON)
E
C57 (RA)
F
C57 (RA)

Figure 4-17 Whole mount TUNEL staining of E7.75 ICR and E8 C57 embryos with or without RA treatment.

A. The lateral view of a control (CON) ICR embryo at E7.75. Apoptotic bodies (arrow) were found on the anterior neural plate.

B. The frontal view of the embryo shown in A. A few of apoptotic bodies were found on the anterior neural plate.

C. The lateral view of a RA-treated (RA) ICR embryo at E7.75. A scatter of apoptotic bodies were found on the anterior neural plate.

D. The frontal view of the embryo shown in B. A few of apoptotic bodies were found on the lateral ridges of the anterior neural plate which is comparable to that observed in control ICR embryo as shown in B.

E. The lateral view of a control C57 embryo at E8. Apoptotic bodies were found on the anterior neural plate which resemble to that observed in control ICR embryos as shown in A.

F. The frontal view of the embryo shown in E. RA treatment apparently did not result in prominent cell death in the headfold region

G. The lateral view of a RA-treated C57 embryo at E8. Similar pattern of distribution of apoptotic bodies was found on the anterior neural plate when compared with that of control C57 embryos.

H. The frontal view of the embryo shown in G which was similar to that in control C57 embryo (F).

Label: Arrow, apoptotic bodies

Scale bar: A, C, E, G 0.12 mm

B, D, F, H 0.2 mm

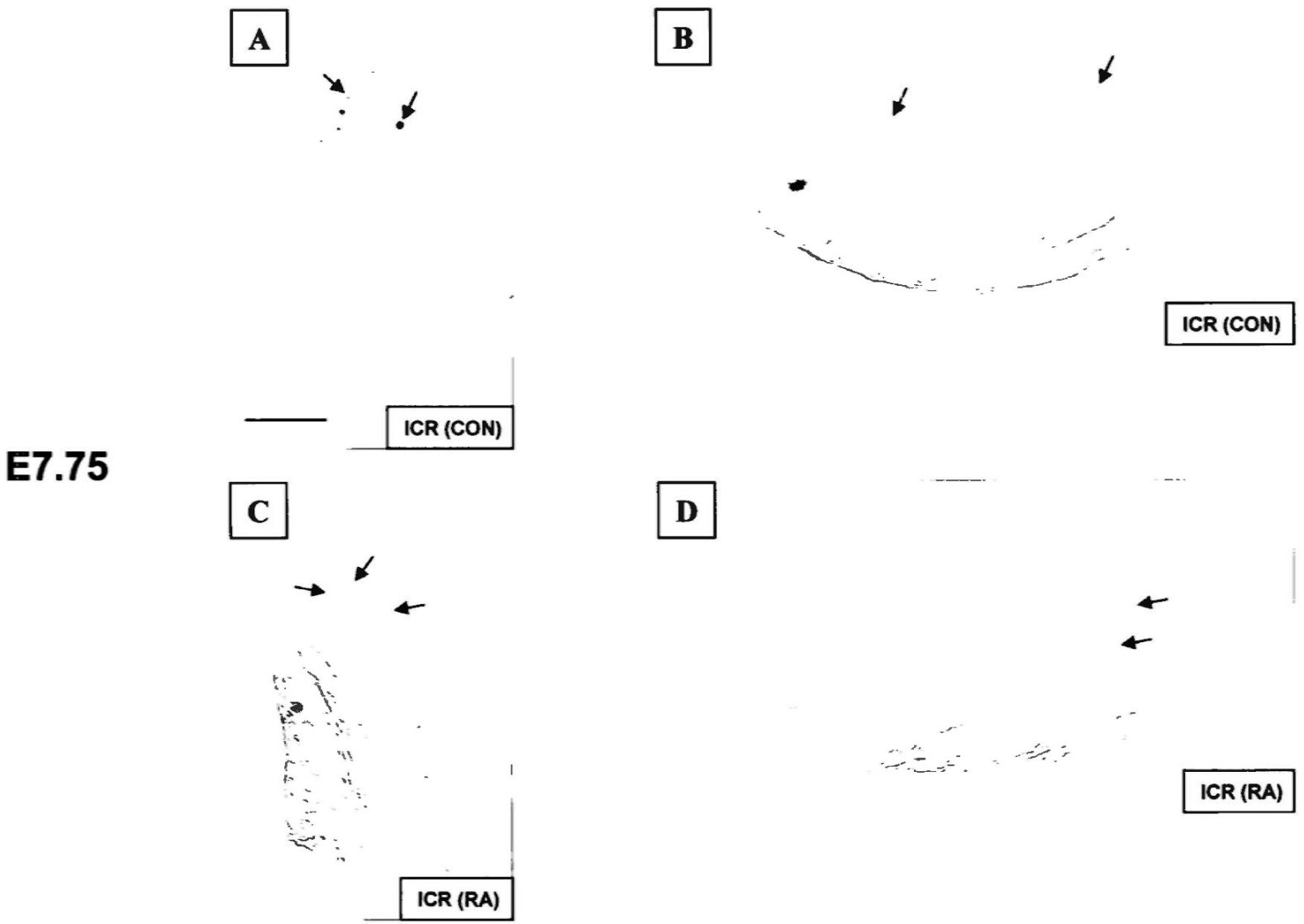
A
B
ICR (CON)
E7.75
C
D
ICR (RA)
ICR (CON)
ICR (RA)

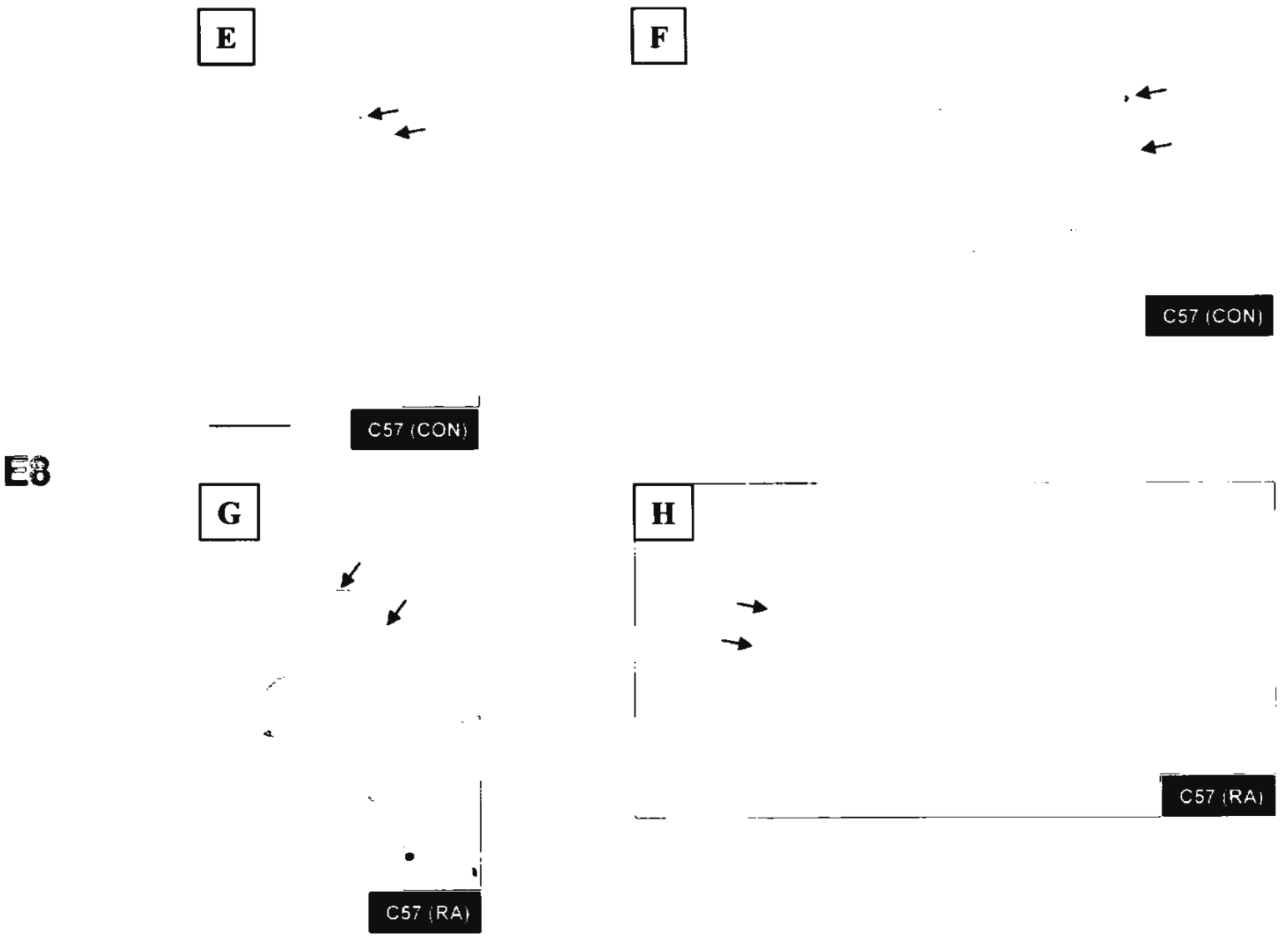
E
F
C57 (CON)
C57 (CON)
G
H
C57 (RA)
C57 (RA)

Figure 4-18 Whole mount TUNEL staining of E8.25 ICR and E8.5 C57 embryos with or without RA treatment.

A. The lateral view of a control (CON) ICR embryo at E8.25. Some of the positively stained apoptotic bodies were marked by arrows and were found scattered on the forebrain, midbrain and hindbrain neural plate.

B. The frontal view of the embryo shown in A. Positively stained apoptotic bodies were found on the forebrain neural plate.

C. The lateral view of a RA-treated (RA) ICR embryo at E8.25. Apoptotic bodies were found along the forebrain, midbrain and hindbrain neural plate. Increase in number of apoptotic bodies were observed in midbrain and hindbrain neural plates when compared with the control embryos shown in A.

D. The frontal view of the embryo shown in C. Similar pattern of distribution apoptotic bodies was found on the forebrain neural plate of the RA-treated ICR embryo when compared with the control shown in B.

E. The lateral view of a control C57 embryo at E8.5. Apoptotic bodies were found on the forebrain, midbrain and hindbrain neural plate.

F. The frontal view of the embryo shown in E. Apoptotic bodies were found on the forebrain neural plate.

G. The lateral view of a RA-treated C57 embryo at E8.5. Apoptotic bodies were found on the forebrain, midbrain and hindbrain. In comparison to the control, increase in number of apoptotic bodies was found in midbrain and hindbrain neural plate.

H. The frontal view of the embryo shown in G. Similar pattern of distribution of apoptotic bodies was found on the forebrain neural plate which was similar to the control embryo.

Label: Arrow, apoptotic bodies

Scale bar: A, C, E, G 0.08 mm

B, D, F, H 0.125 mm

E8.25

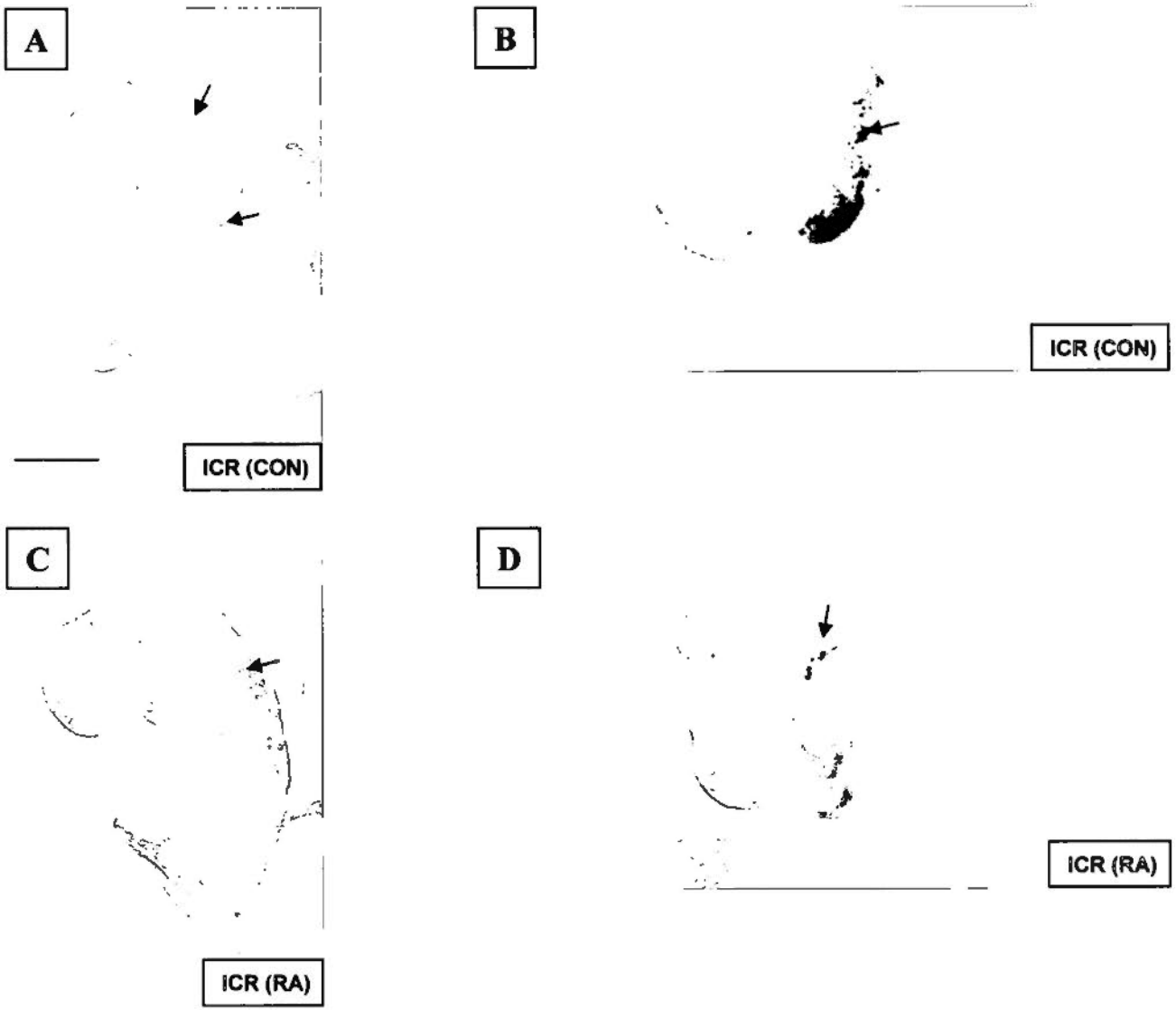

E8.5

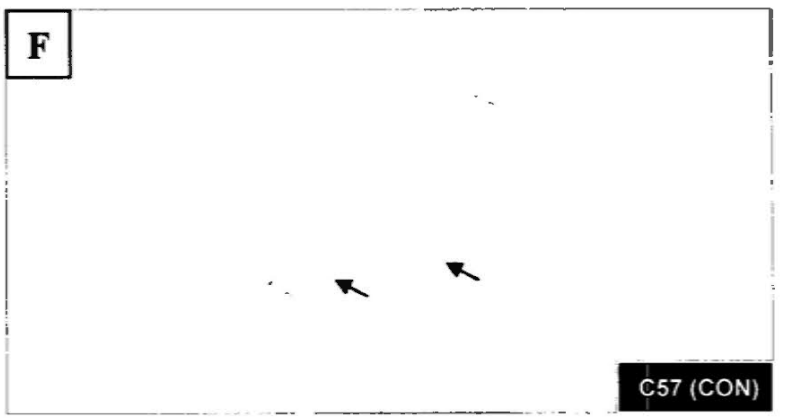

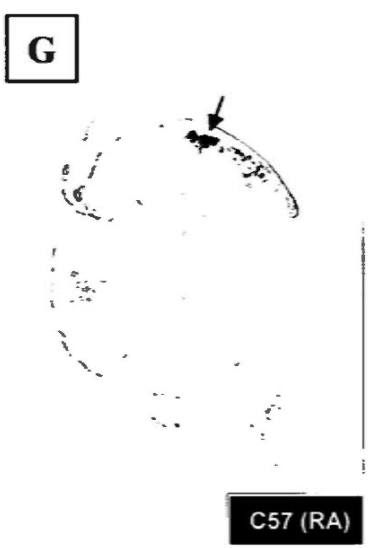

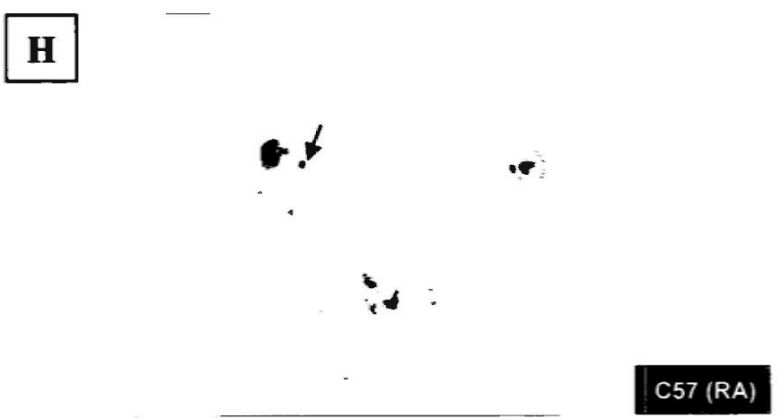

Figure 4-19 TUNEL staining on sections of E7.75 ICR and E8 C57 embryos with or without RA treatment.

A. Transverse section of the anterior neural plate of control (CON) ICR embryo at E7.75. Some positively stained apoptotic bodies were marked by arrows and were found scattered in both the neuroepithelium and the underlying mesenchyme.

B. Transverse section of the anterior neural plate of RA-treated (RA) ICR embryo at E7.75. There was no obvious difference in the distribution of apoptotic bodies in both the neuroepithelium and the underlying mesenchyme.

C. Transverse section of the anterior neural plate of control C57 embryo at E8. Positively stained apoptotic bodies were found scattered in both the neuroepithelium and the underlying mesenchyme.

D. Transverse section of the anterior neural plate of RA-treated C57 embryo at E8. There was no obvious difference in the distribution of apoptotic bodies in both the neuroepithelium and the underlying mesenchyme.

Label: Arrow, apoptotic bodies

Scale bar: A to D 0.05 mm

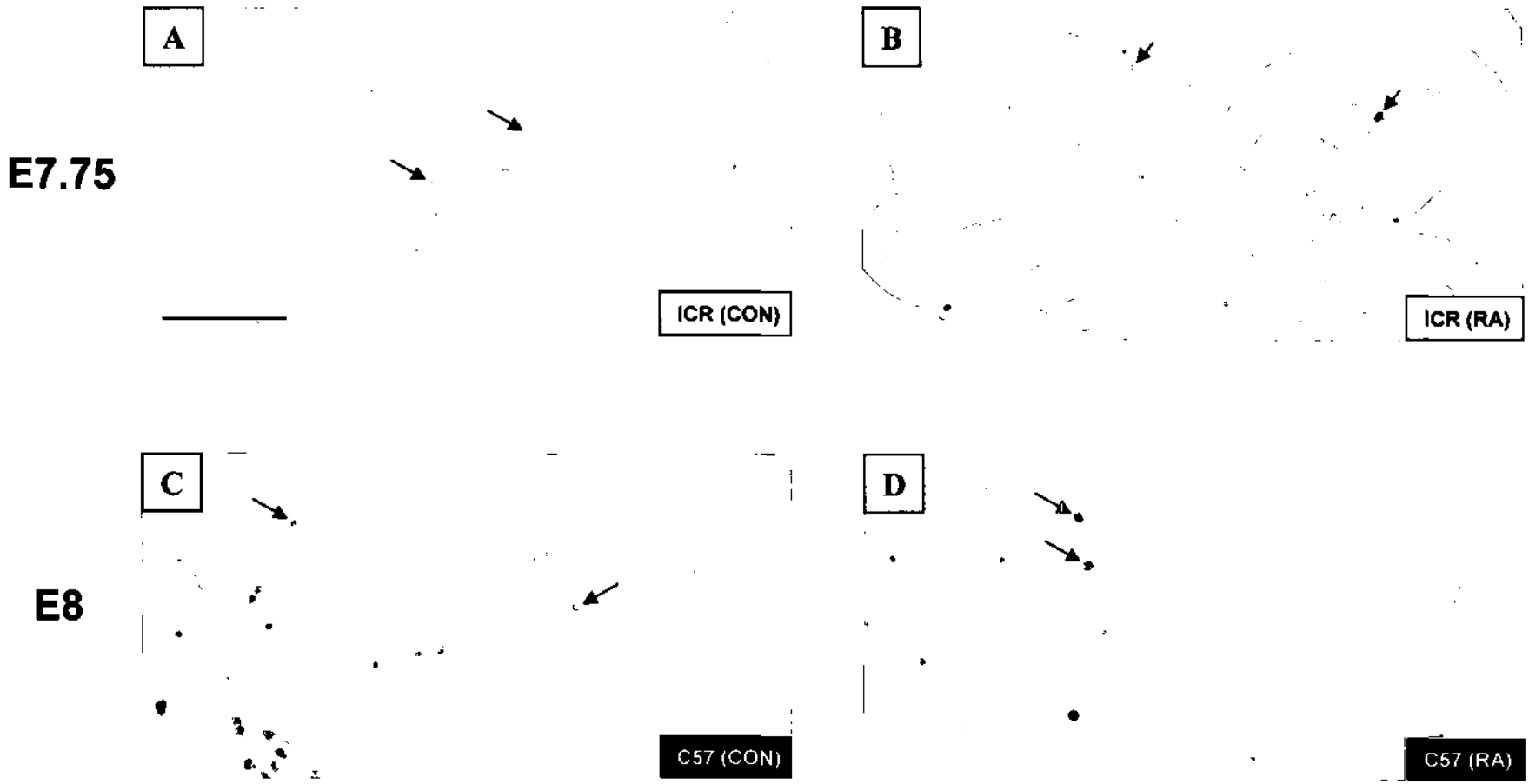
A
B
E7.75
ICR (CON)
ICR (RA)
C
D
E8
C57 (CON)
C57 (RA)

Figure 4-20 TUNEL staining on sections of E8.25 ICR and E8.5 C57 embryos with or without RA treatment.

A. Transverse section of the forebrain neural plate of control (CON) ICR embryo at E8.25. Some of the positively stained apoptotic bodies were marked by black arrows and were scattered in both the neuroepithelium and the underlying mesenchyme. A pair of optic pits was marked by green arrows.

B. Transverse section of the forebrain neural plate of RA-treated (RA) ICR embryo at E8.25. There were no increase in apoptotic bodies.

C. Transverse section of the forebrain neural plate of control C57 embryo at E8.5. Apoptotic bodies were found in both the neuroepithelium and the underlying mesenchyme. A pair of optic pits were found.

D. Transverse section of the forebrain neural plate of RA-treated C57 embryo at E8.5. There were no increase in apoptotic bodies. No optic pits could be found.

Labels:	Black arrow,	apoptotic bodies
	Green arrow,	optic pit
Scale bar:	A to D	0.01 mm

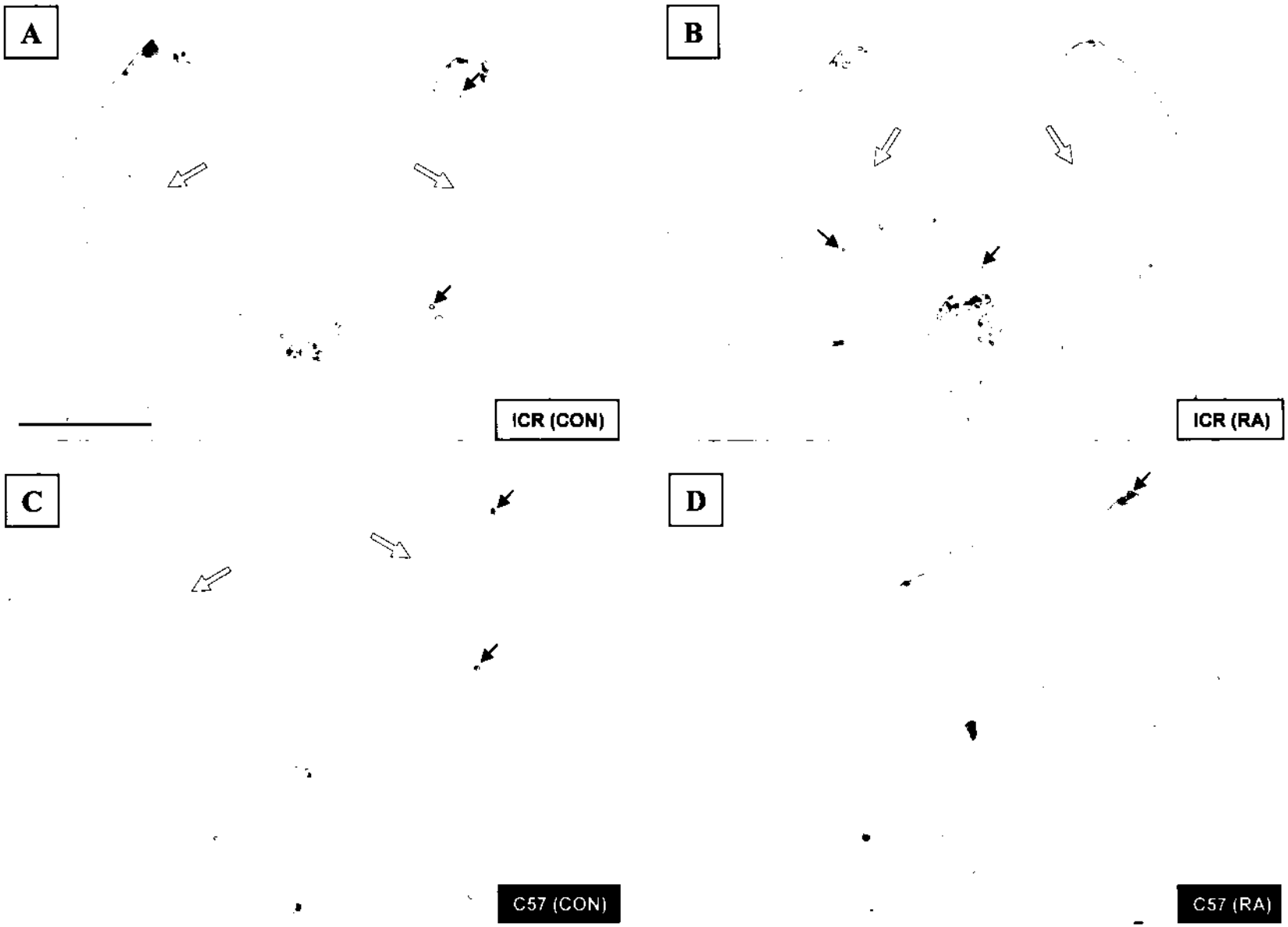
A
B
E8.25
ICR (CON)
ICR (RA)
C
D
E8.5
C57 (CON)
C57 (RA)

Figure 5-1 **Whole mount *in situ* hybridization patterns of *Raldh2* in C57 and ICR embryos at E8 and E7.75 respectively with or without RA treatment.**

A. At E8, in control (CON) C57 embryos, *Raldh2* expressed strongly in the whole body axis except the cephalic region.

B. At E8, in RA-treated (RA) C57 embryos, expression of *Raldh2* showed no observable difference from that of C57 (CON) embryos.

C. At E7.75, in control ICR embryos, expression of *Raldh2* was similar to that in C57 (CON) embryos at equivalent development stage (E8).

D. At E7.75, in RA-treated ICR embryos, expression of *Raldh2* showed no observable difference from that of ICR (CON) embryos.

Scale bar: A to D, 0.1 mm

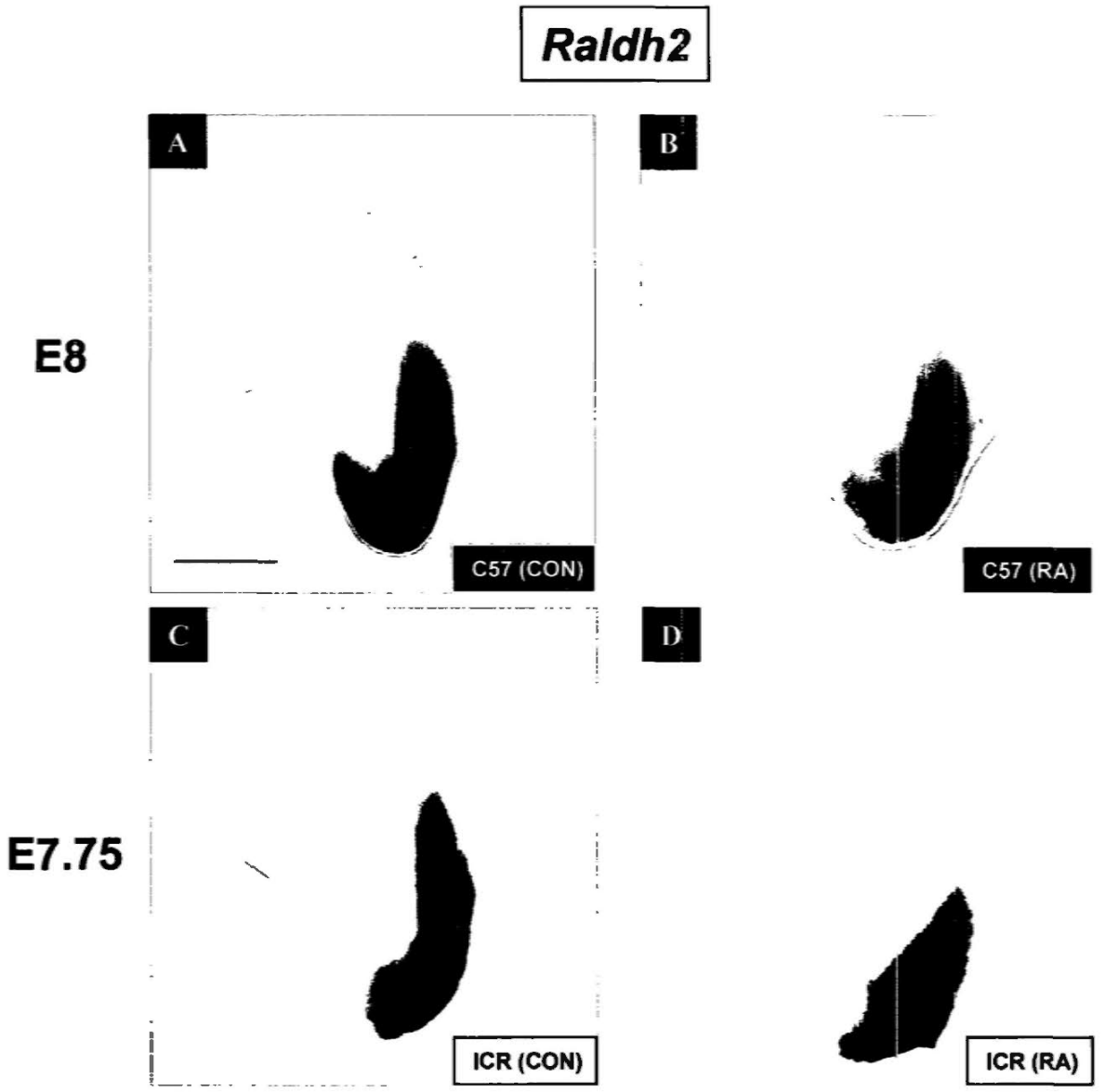
Raldh2
A
B
E8
C57 (CON)
C57 (RA)
C
D
E7.75
ICR (CON)
ICR (RA)

Figure 5-2 **Whole mount *in situ* hybridization patterns of *Raldh2* in C57 and ICR embryos at E8.25 and E8 respectively with or without RA treatment.**

A. At E8.25, in control (CON) C57 embryos, while expression levels of *Raldh2* in the trunk region remained high, it started to express cranially in an anterior rim of the future forebrain from where the optic primordium developed (arrowhead) and also caudally at the base of the allantois (arrow).

B. At E8.25, in RA-treated (RA) C57 embryos, while expression levels of *Raldh2* remained high in the trunk, there was hardly any expression detectable in the future forebrain region, although expression was observed at the base of the allantois similar to that in C57 (CON) embryos.

C. At E8, in control ICR embryos, *Raldh2* expression was similar to that in C57 (CON) embryos at equivalent developmental stage (E8.25).

D. At E8, in RA-treated ICR embryos, while expression of *Raldh2* remained high in the trunk and at the base of the allantois, there was reduced expression in the optic primordium in comparison to that in ICR (CON) embryos.

Labels: Arrow, base of allantois
Arrowhead, optic primordium

Scale bar: A to D, 0.07 mm

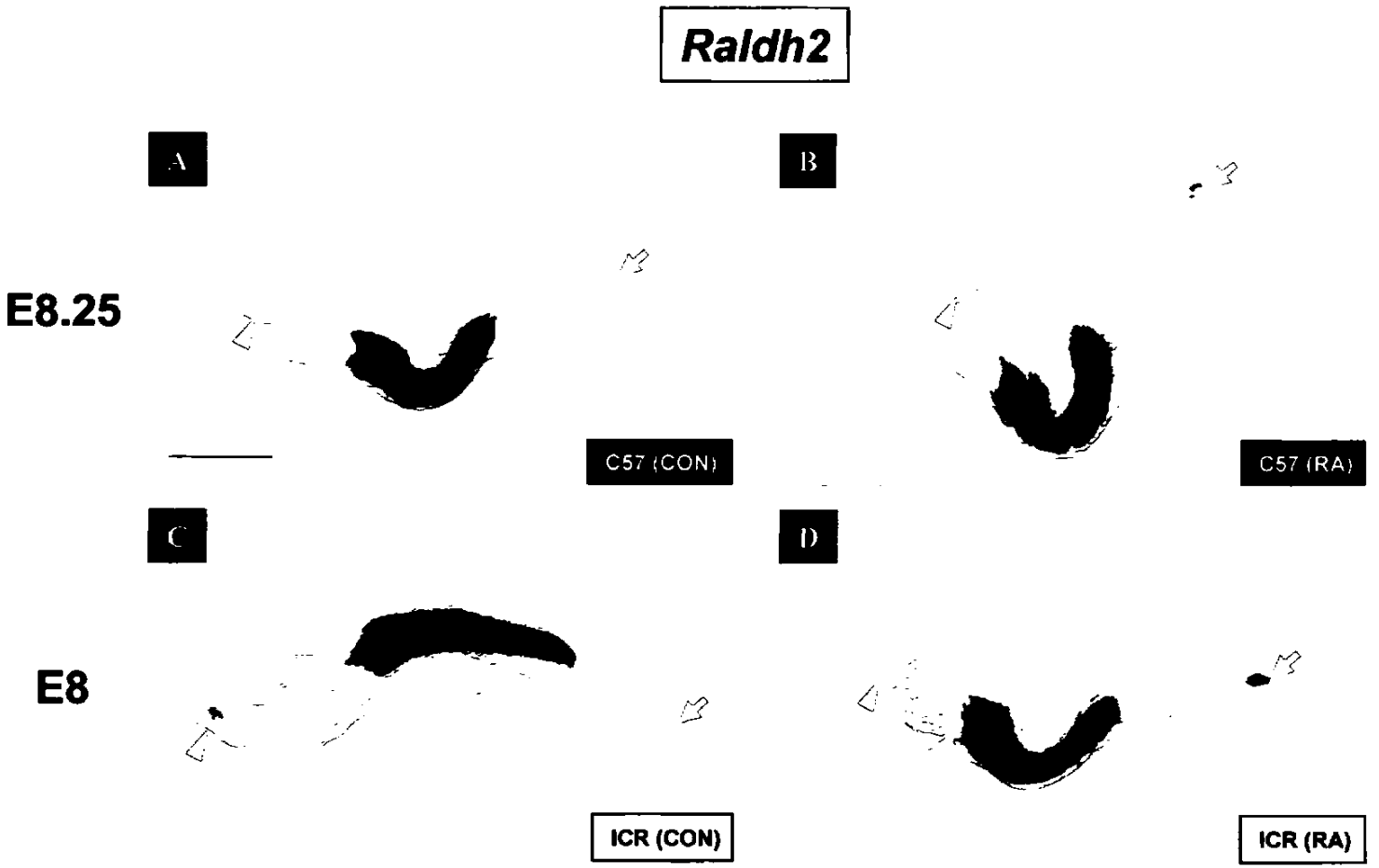
Raldh2
A
B
E8.25
C57 (CON)
C57 (RA)
C
D
E8
ICR (CON)
ICR (RA)

Figure 5-3 Whole mount *in situ* hybridization patterns of *Raldh2* in C57 and ICR embryos at E8.5 and E8.25 respectively with or without RA treatment.

A. At E8.5, in control (CON) C57 embryos, *Raldh2* expressed strongly in the trunk. Expressions were also clearly observed cranially in the optic pit (arrowhead) and caudally at the base of the allantois (arrow).

B. At E8.5, in RA-treated (RA) C57 embryos, while expressions of *Raldh2* in the trunk and at the base of the allantois were similar to that in C57 (CON) embryos, there was hardly any expression in the future forebrain region.

C. At E8.25, in control ICR embryos, expression of *Raldh2* was similar to that in C57 (CON) embryos at equivalent developmental stage (E8.5).

D. At E8.25, in RA-treated ICR embryos, while expression of *Raldh2* remained high in the trunk and at the base of the allantois, reduced expression level was found in the optic pit in comparison to that in ICR (CON) embryos.

Labels: Arrow, base of allantois
Arrowhead, optic pit

Scale bar: A to D, 0.05 mm

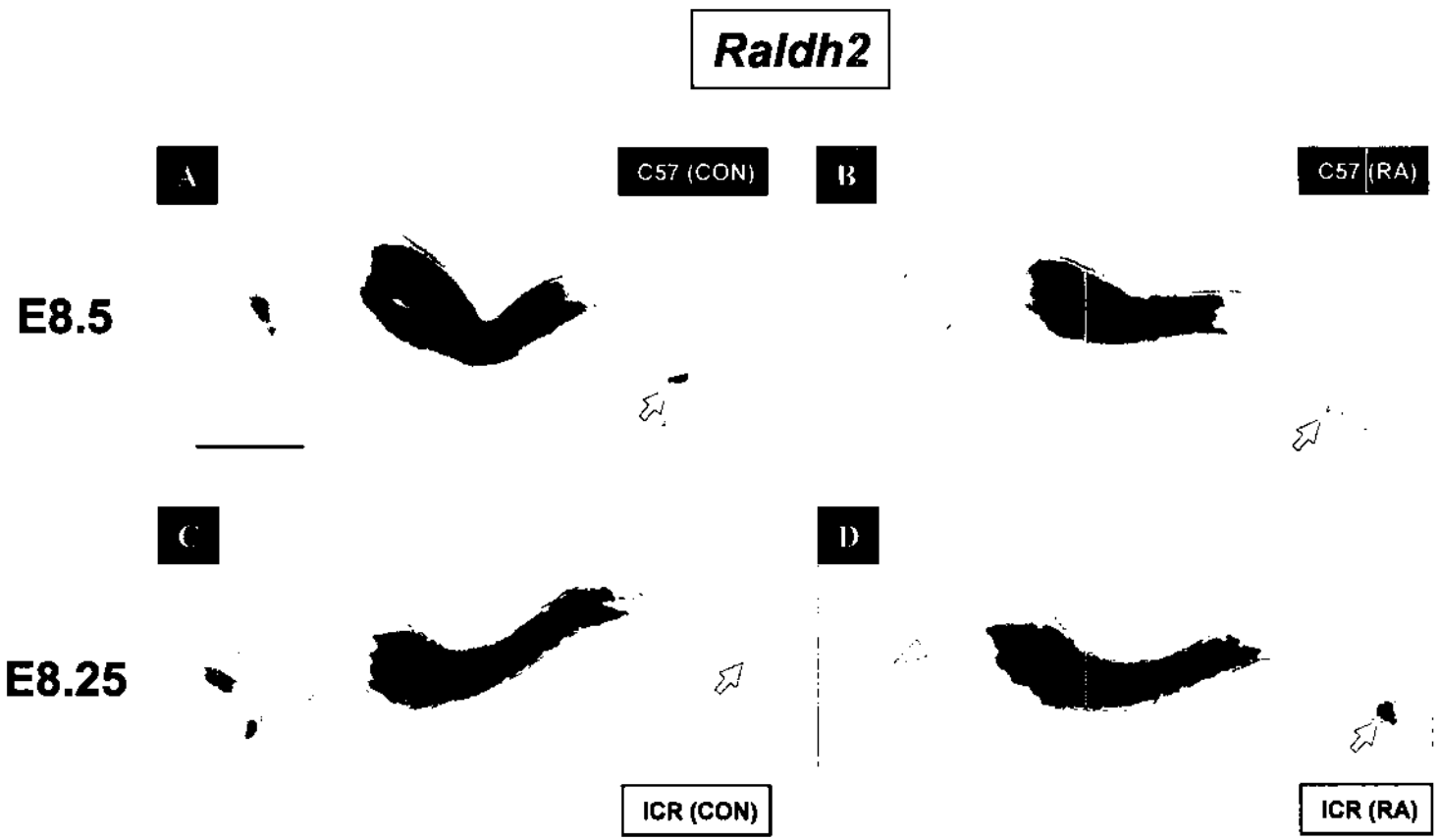
Raldh2
A
C57 (CON)
B
C57 (RA)
E8.5
C
D
E8.25
ICR (CON)
ICR (RA)

Figure 5-4 Whole mount *in situ* hybridization patterns of *Raldh2* in C57 and ICR embryos at E9 and E8.75 respectively with or without RA treatment.

A. At E9, in control (CON) C57 embryos, strong expression of *Raldh2* persisted in the trunk and in the cloacal region (arrow). Low level of expression was observed at the posterior peripheral region of the optic vesicle (arrowhead).

B. At E9, in RA-treated (RA) C57 embryos, while expression level of *Raldh2* in the trunk and cloacal regions remained high, *Raldh2* was barely detectable around the optic vesicle.

C. At E8.75, in control ICR embryos, *Raldh2* expression was similar to that in C57 (CON) embryos at equivalent developmental stage (E9).

D. At E8.75, in RA-treated ICR embryos, very low level of *Raldh2* was observed around the optic vesicle.

Labels: Arrow, cloacal region
Arrowhead, optic vesicle

Scale bar: A to D, 1.4 mm

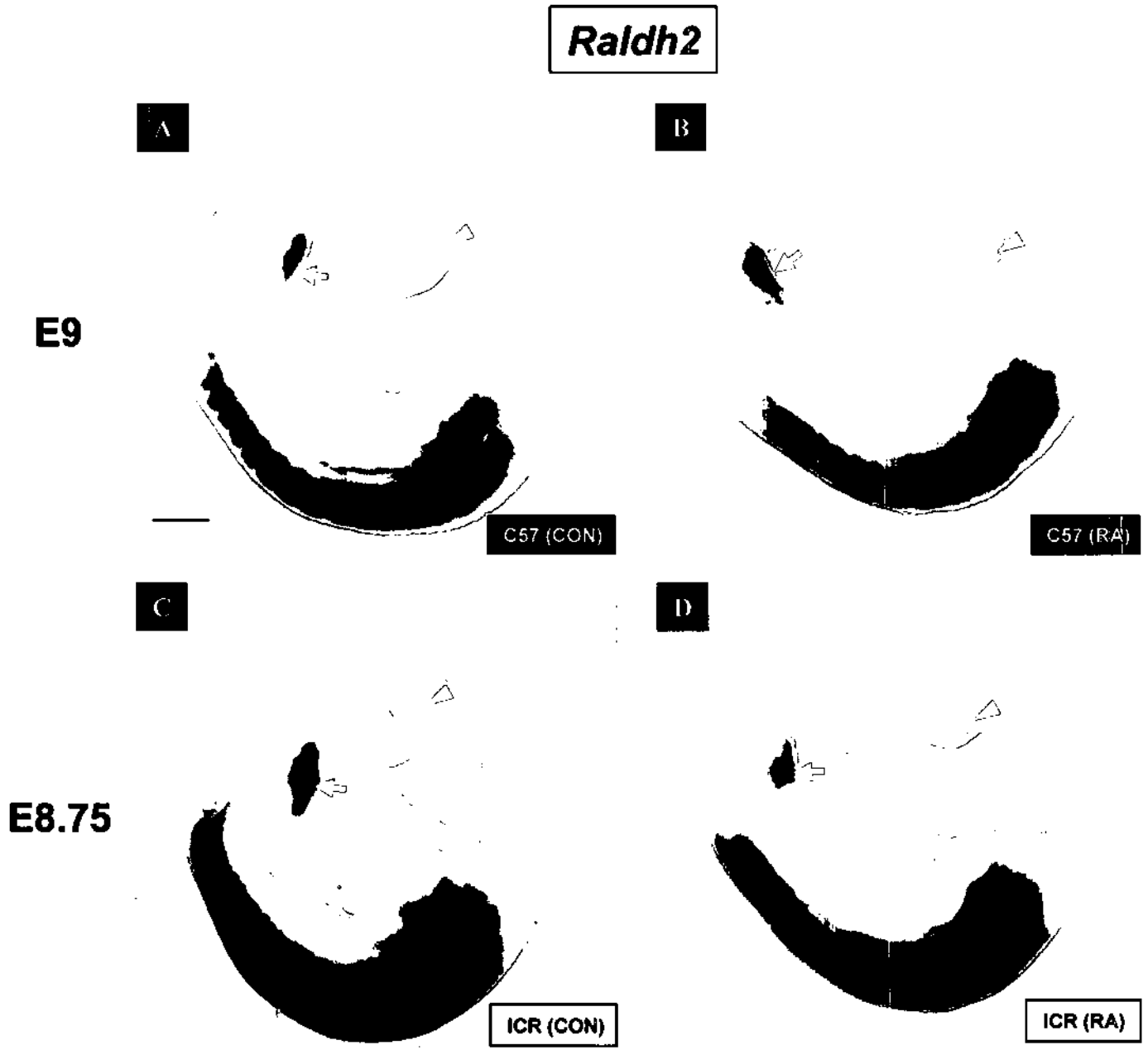
Raldh2
A
B
E9
C57 (CON)
C57 (RA)
C
D
E8.75
ICR (CON)
ICR (RA)

Figure 5-5 Whole mount *in situ* hybridization patterns of *Raldh2* in C57 and ICR embryos at E9.5 and E9.25 respectively with or without RA treatment.

A. At E9.5, in control (CON) C57 embryos, the expression level of *Raldh2* in the trunk region remained high. *Raldh2* expression could be detected in the temporal optic mesenchyme (arrowhead).

B. At E9.5, in RA-treated (RA) C57 embryos, there was hardly any *Raldh2* expression in the head region, although *Raldh2* remained highly expressed in the trunk region.

C. At E9.25, in control ICR embryos, *Raldh2* expression was similar to that in C57 (CON) embryos at equivalent developmental stage (E9.5).

D. At E9.25, in RA-treated ICR embryos, *Raldh2* expression was barely detectable in the temporal optic mesenchyme.

Label: Arrowhead, temporal optic mesenchyme

Scale bar: A to D, 1.2 mm

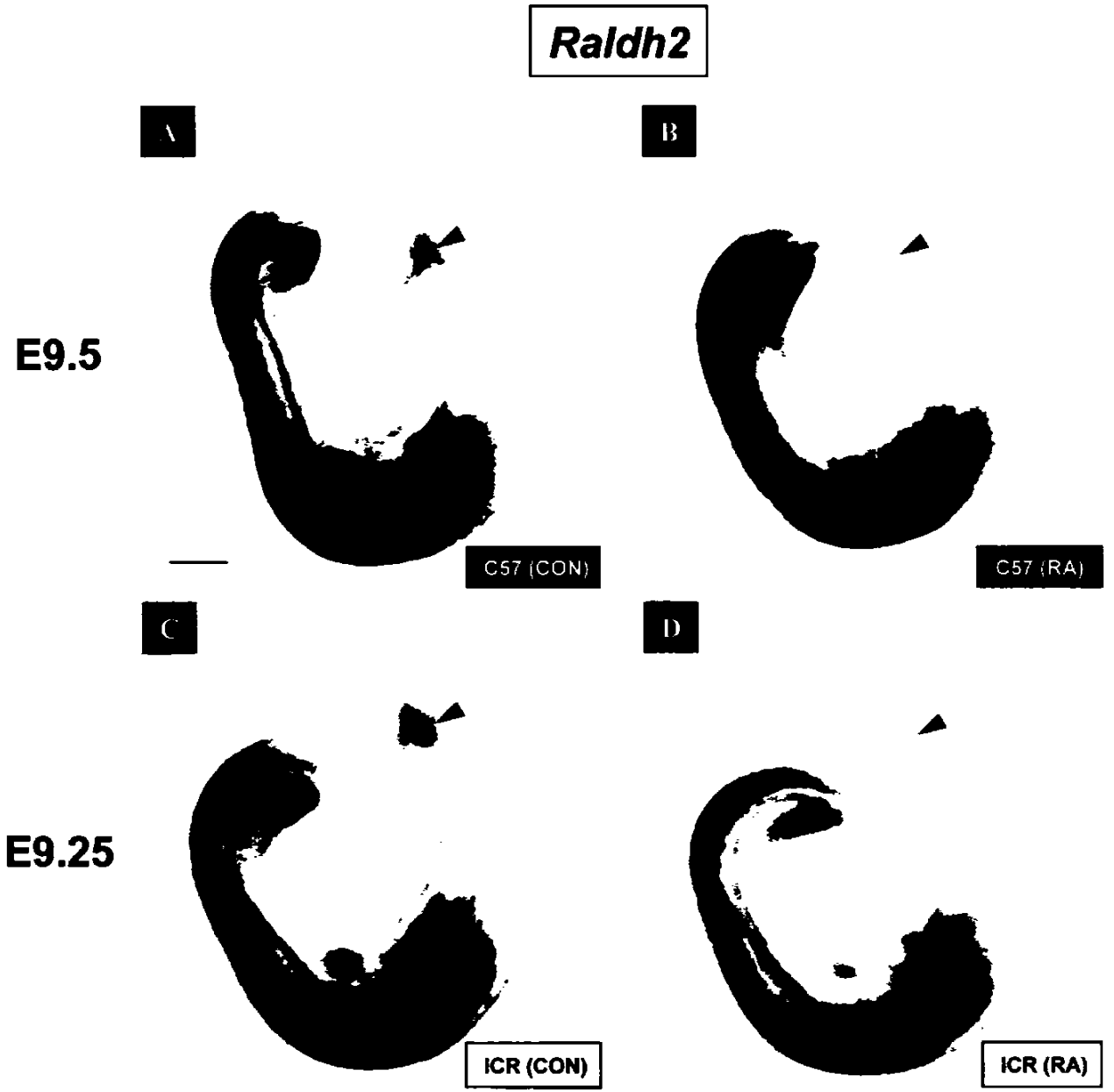
Raldh2
A
B
E9.5
C57 (CON)
C57 (RA)
C
D
E9.25
ICR (CON)
ICR (RA)

Figure 5-6 Whole mount *in situ* hybridization patterns of *Raldh3* in C57 and ICR embryos at E8.5 and E8.25 respectively with or without RA treatment.

A. At E8.5, in control (CON) C57 embryos, *Raldh3* expression was restricted to the surface ectoderm overlying the posterior optic recess (arrowhead).

B. At E8.5, in RA-treated (RA) C57 embryos, there was hardly any *Raldh3* expression in the head region.

C. At E8.25, in control ICR embryos, *Raldh3* was expressed in the same domains as C57 (CON) embryos at equivalent developmental stage (E8.5).

D. At E8.25, in RA-treated ICR embryos, there was reduced level of *Raldh3* expression in the surface ectoderm overlying the posterior optic recess in comparison to ICR (CON) embryos.

Labels: Arrowhead, posterior optic recess

Scale bar: A to D, 0.05mm

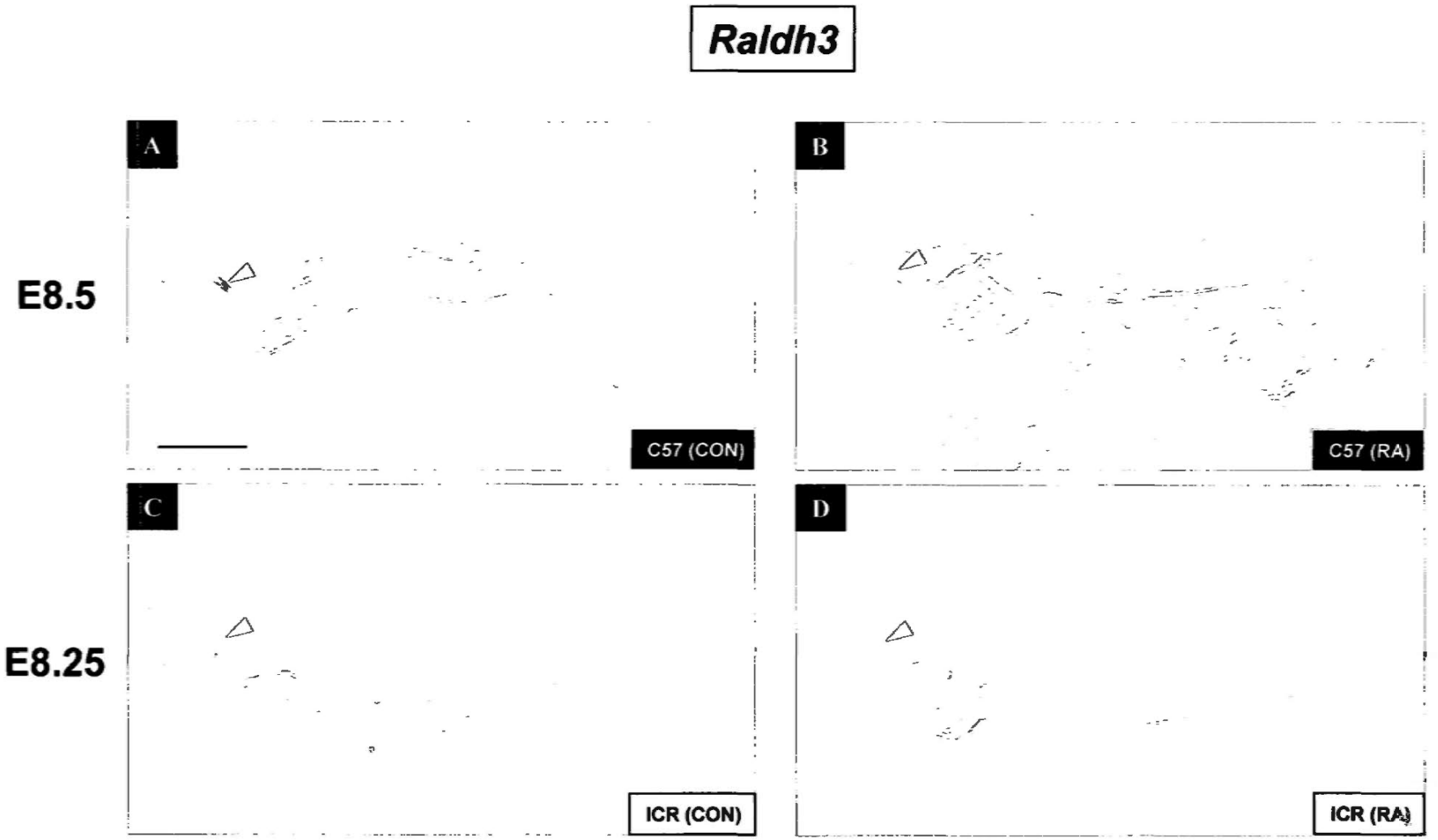
Raldh3
E8.5
E8.25
A
B
C
D
C57 (CON)
C57 (RA)
ICR (CON)
ICR (RA)

Figure 5-7 Whole mount *in situ* hybridization patterns of *Raldh3* in C57 and ICR embryos at E9 and E8.75 respectively with or without RA treatment.

A. At E9, in control (CON) C57 embryos, expression of *Raldh3* was detected in the surface ectoderm overlying the optic vesicle (arrowhead) and in the maxillary primordium of the first brachial arch (arrow).

B. At E9, in RA-treated (RA) C57 embryos, while expression of *Raldh3* was detected in the maxillary primordium of the first brachial arch, only very weak level of expression was observed in the surface ectoderm overlying the forebrain region.

C. At E8.75, in control ICR embryos, *Raldh3* was expressed in the same domains as C57 (CON) embryos at equivalent developmental stage (E9).

D. At E8.75, in RA-treated ICR embryos, *Raldh3* expression was barely detectable in the surface ectoderm overlying the optic vesicle, although its expression in the maxillary primordium of the first brachial arch remained strong.

Labels: Arrow, maxillary primordium of the first brachial arch
Arrowhead, optic vesicle

Scale bar: A to D, 1.2 mm

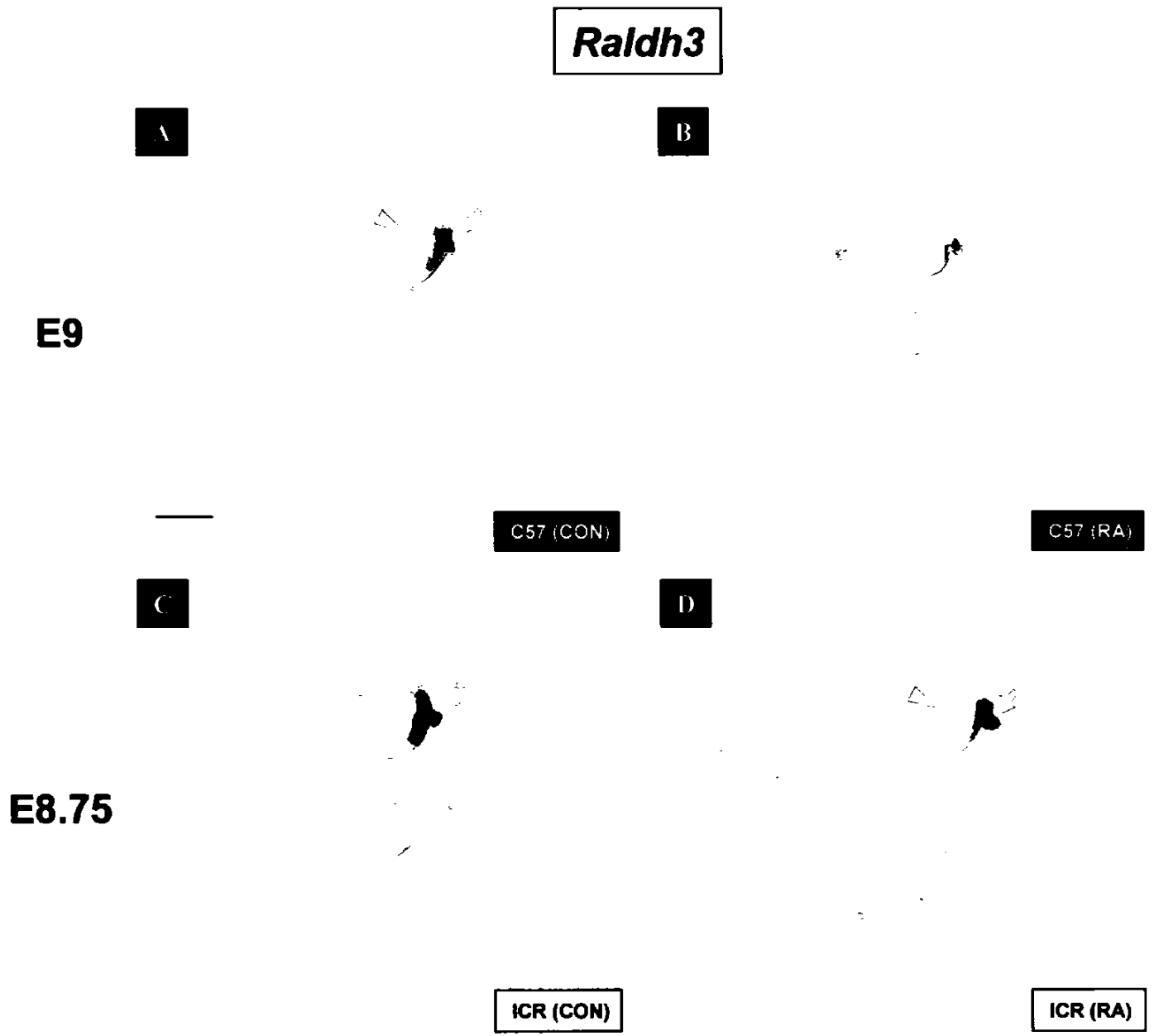
Raldh3
A
B
E9
C57 (CON)
C57 (RA)
C
D
E8.75
ICR (CON)
ICR (RA)

Figure 5-8 Whole mount *in situ* hybridization patterns of *Raldh3* in C57 and ICR embryos at E9.5 and E9.25 respectively with or without RA treatment.

A. At E9.5, in control (CON) C57 embryos, *Raldh3* expression was detected in a broad area: the surface ectoderm overlying the optic vesicle (arrowhead) and in the maxillary primordium of the first brachial arch (arrow).

B. At 9.5, in RA-treated (RA) C57 embryos, the expression level of *Raldh3* was reduced in comparison to C57 (CON) embryos.

C. At E9.25, in control ICR embryos, *Raldh3* expression was detected in the surface ectoderm overlying the optic vesicle, but was more eccentric to the optic vesicle when compared with that in C57 (CON) embryos at equivalent developmental stage (E9.5).

D. At E9.25, in RA-treated ICR embryos, expression of *Raldh3* in the surface ectoderm became restricted to the area just overlying the surface ectoderm.

Labels: Arrow, maxillary primordium of the first brachial arch
Arrowhead, optic vesicle

Scale bar: A to D, 1.4 mm

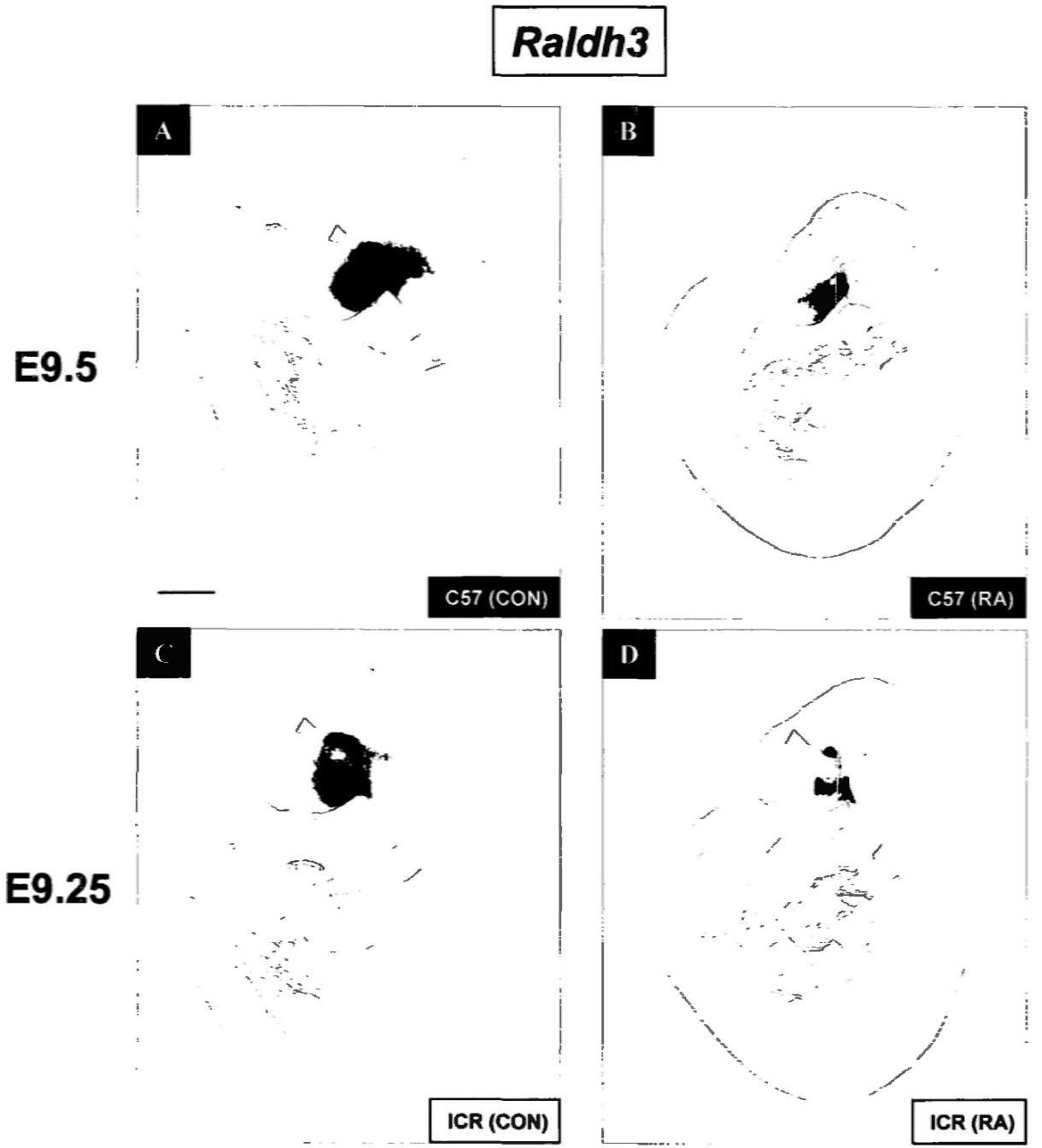
Raldh3
E9.5
E9.25
A
B
C
D
C57 (CON)
C57 (RA)
ICR (CON)
ICR (RA)

Figure 5-9 Whole mount *in situ* hybridization patterns of *Cyp26a1* in C57 and ICR embryos at E8.5 and E8.25 respectively with or without RA treatment.

A. At E8.5, in control (CON) C57 embryos, *Cyp26a1* expressed very strongly in the caudal end. Expression was also found in the second rhombomere (r2) and in the region underlying the optic pit (arrowhead).

B. At E8.5, in RA-treated (RA) C57 embryos, while being strongly expressed in the caudal end of the embryo, there was reduced *Cyp26a1* expression in the cranial domains.

C. At E8.25, in control ICR embryos, *Cyp26a1* expression was detected in the same expression domains as C57 (CON) embryos at equivalent developmental stage (E8.5).

D. At E8.25, in RA-treated ICR embryos, reduced expression of *Cyp26a1* was observed in the cranial domains.

Labels: Arrowhead, region underlying the optic pit
r2, second rhombomere

Scale bar: A to D, 0.05 mm

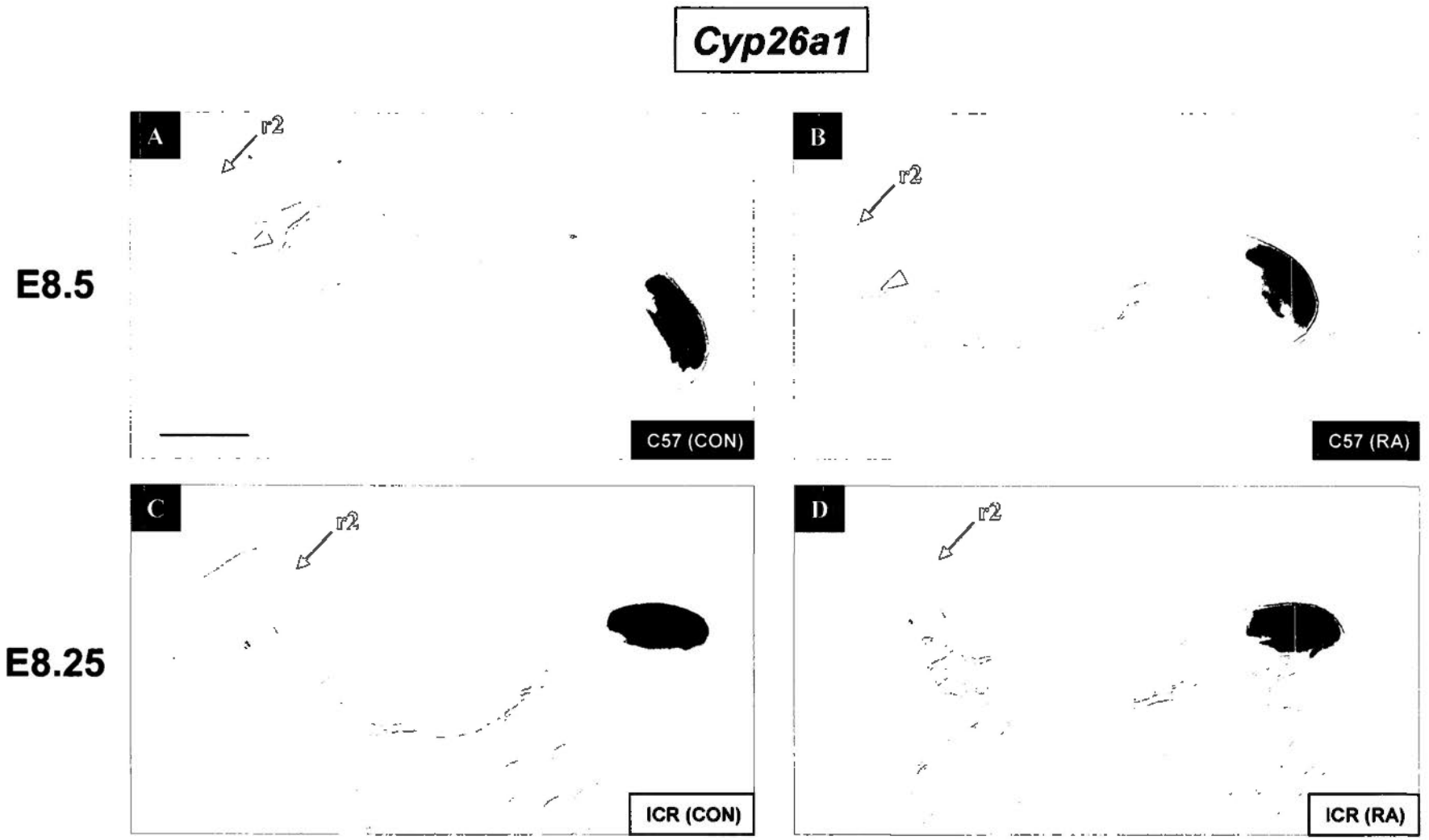
Cyp26a1
E8.5
E8.25
A
r2
C57 (CON)
B
r2
C57 (RA)
C
r2
ICR (CON)
D
r2
ICR (RA)

Figure 5-10 Whole mount *in situ* hybridization patterns of *Cyp26a1* in C57 and ICR embryos at E9 and E8.75 respectively with or without RA treatment.

A. At E9, in control (CON) C57 embryos, other than expressing at high levels in the caudal end, expression was upregulated in the cranial region and expression domains expanded to the ventral optic mesenchyme (arrowhead), the hindbrain (hb), areas around the first brachial arch and the otic vesicle (ot).

B. At E9, in RA-treated (RA) C57 embryos, there was reduced expression of *Cyp26a1* in the ventral optic region, in the first brachial arch and around the otic vesicle while expression in the caudal end remained strong.

C. At E8.75, in control ICR embryos, *Cyp26a1* expression was detected in domains similar to that in C57 (CON) embryos at equivalent developmental stage.

D. At E8.75, in RA-treated ICR embryos, there was slightly reduced expression of *Cyp26a1* in the ventral optic mesenchyme.

Labels: arrowhead, ventral optic mesenchyme
hb, hindbrain
ot, otic vesicle

Scale bar: A to D, 1.4 mm

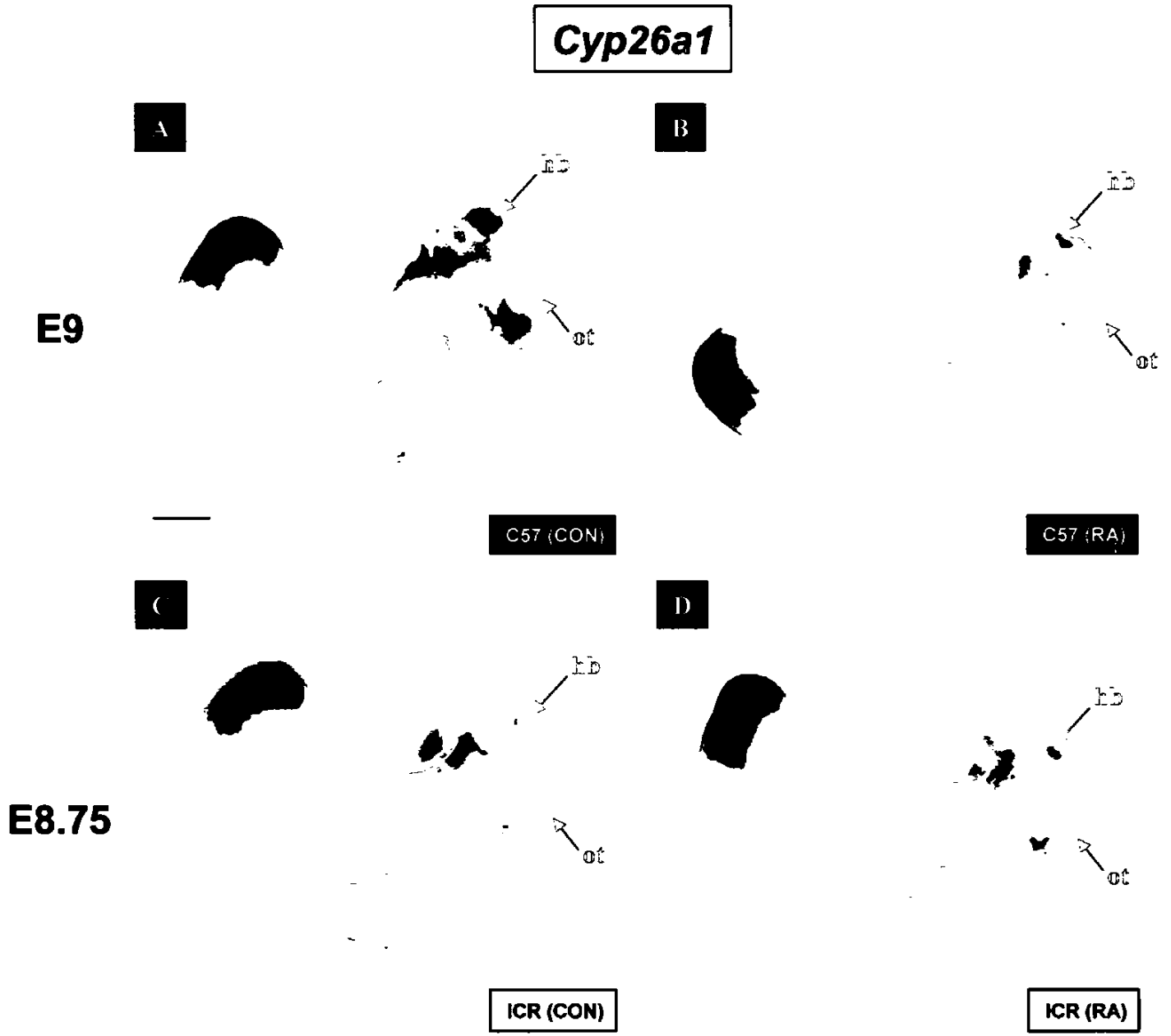
Cyp26a1
A
B
E9
hb
ot
C57 (CON)
C57 (RA)
C
D
E8.75
ICR (CON)
ICR (RA)

Figure 5-11 Whole mount *in situ* hybridization patterns of *Cyp26a1* in C57 and ICR embryos at E9.5 and E9.25 respectively with or without RA treatment.

A. At E9.5, in control (CON) C57 embryos, *Cyp26a1* expression was detected cranially in the hindbrain (hb), in a broad region around the facial mesenchyme and the first brachial arch, and in the otic vesicle (ot).

B. At E9.5, in RA-treated (RA) C57 embryos, there was reduced expression of *Cyp26a1* in the cranial expression domains, while expression in the caudal end remained strong.

C. At E9.25, in control ICR embryos, *Cyp26a1* expressed in domains similar to that in C57 (CON) embryos at equivalent developmental stage (E9.5).

D. At E9.25, in RA-treated ICR embryos, the expression level of *Cyp26a1* in the cranial domains was reduced in comparison to that in ICR (CON) embryos.

Labels: hb, hindbrain
ot, otic vesicle

Scale bar: A to D, 0.12 mm

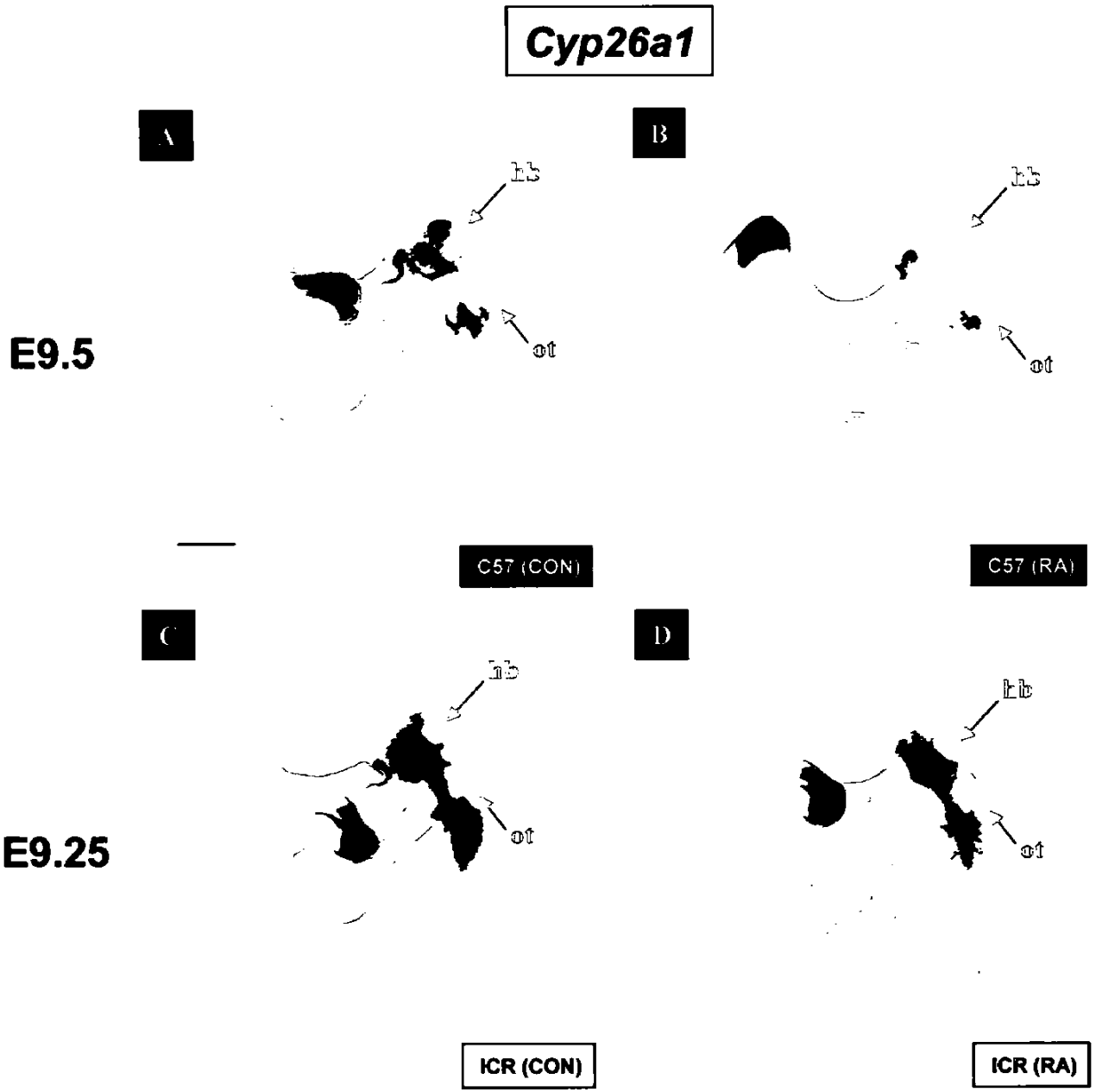
Cyp26a1
A
B
hb
ot
E9.5
C57 (CON)
C57 (RA)
C
D
hb
ot
E9.25
ICR (CON)
ICR (RA)

Figure 5-12 Whole mount *in situ* hybridization patterns of *Pax6* in C57 and ICR embryos at E8.5 and E8.25 respectively with or without RA treatment.

A. At E8.5, in control (CON) C57 embryos, *Pax6* was strongly expressed in the developing somites and in the future forebrain region.

B. At E8.5, in RA-treated (RA) C57 embryos, *Pax6* was strongly expressed in the somites as well as in the future forebrain region.

C. At E8.25, in control ICR embryos, expression of *Pax6* showed no observable differences from C57 (CON) embryos at equivalent developmental stage (E8.5).

D. At E8.25, in RA-treated ICR embryos, expression of *Pax6* remained strong in the future forebrain region in comparison to that in ICR (CON) embryos.

Scale bar: A to D, 0.05 mm

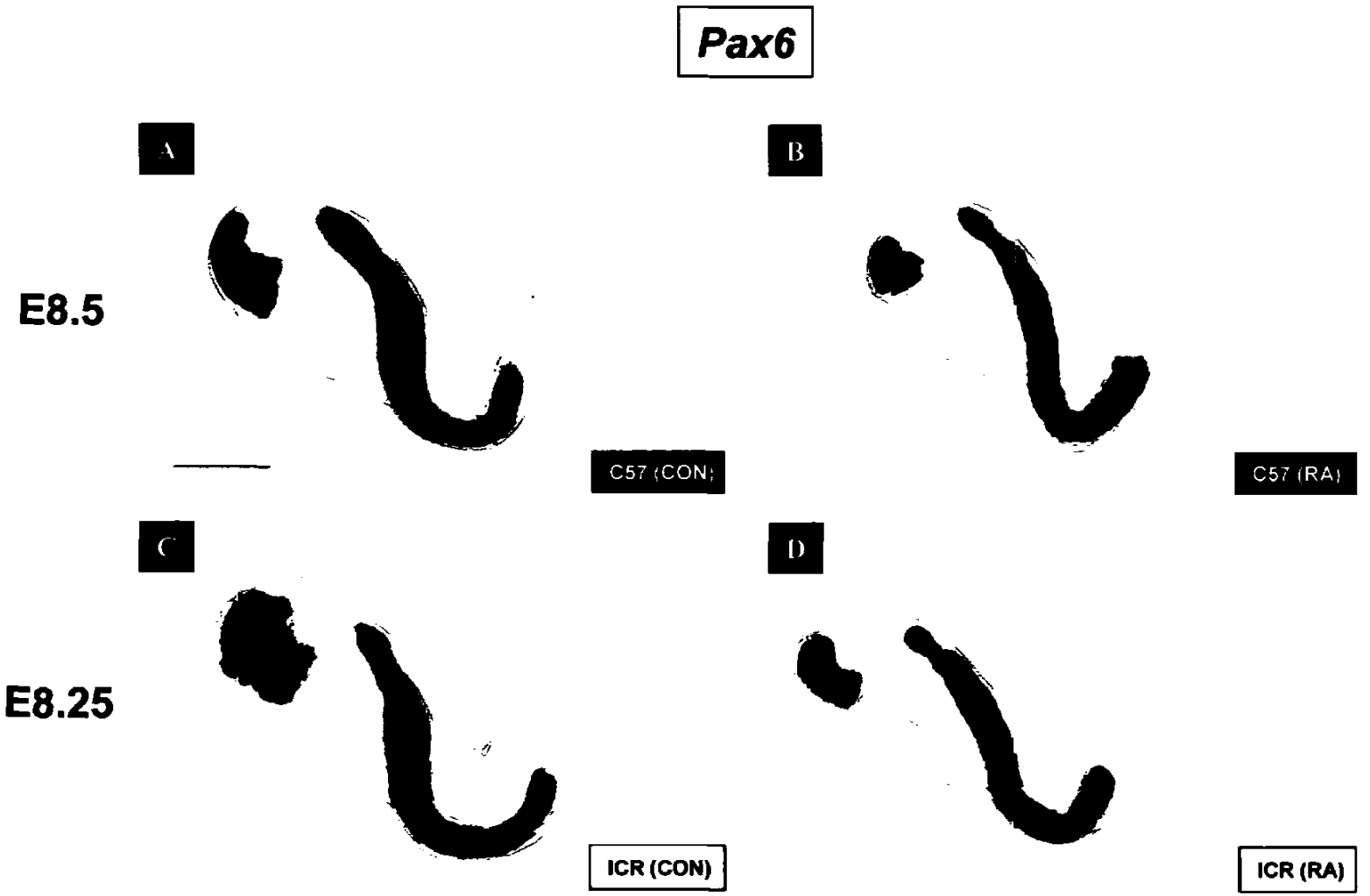
Pax6
A
B
E8.5
C57 (CON)
C57 (RA)
C
D
E8.25
ICR (CON)
ICR (RA)

Figure 5-13 Whole mount *in situ* hybridization patterns of *Hes1* in C57 and ICR embryos at E8.5 and E8.25 respectively with or without RA treatment.

A. At E8.5, in control (CON) C57 embryos, expression of *Hes1* was detectable in both the caudal region (arrow) and the cranial region including the optic pit (arrowhead).

B. At E8.5, in RA-treated (RA) C57 embryos, while expression of *Hes1* in the caudal end was similar to C57 (CON) embryos, there was marked reduction of *Hes1* expression in the cranial region.

C. At 8.25, in control ICR embryos, expression of *Hes1* was similar to that in C57 (CON) embryos at equivalent developmental stage (E9.25).

D. At E8.25, in RA-treated ICR embryos, there was no obvious difference in *Hes1* expression in comparison to that in ICR (CON) embryos.

Labels: Arrow, caudal end of the embryo
Arrowhead, optic pit

Scale bar: A to D, 0.05 mm

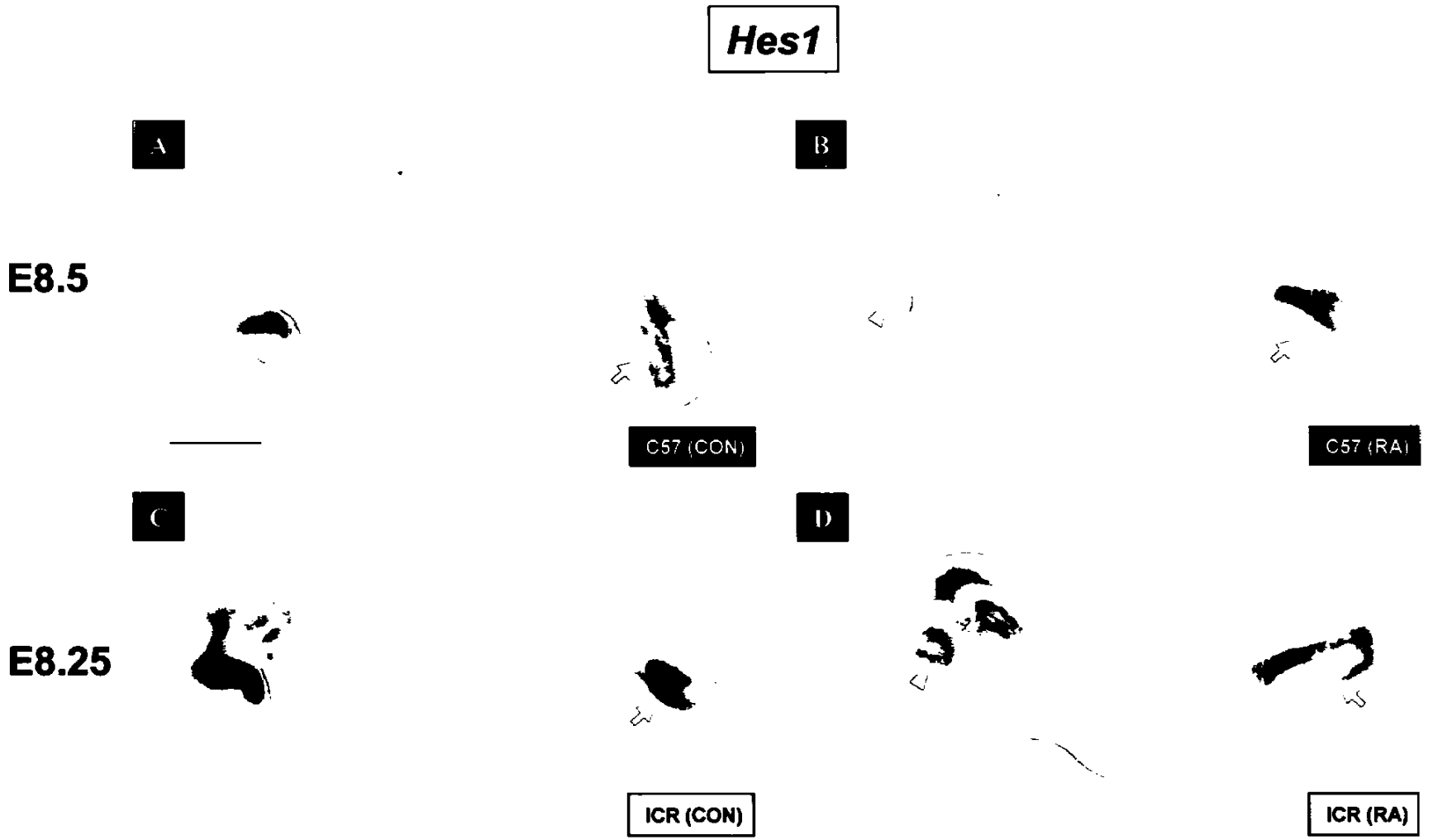
Hes1
A
B
E8.5
C57 (CON)
C57 (RA)
C
D
E8.25
ICR (CON)
ICR (RA)